Augmenting Plasticity and Recovery from Stroke by Modulating the Extracellular Matrix of the Central Nervous System

by

Anna Magdalena Wiersma

A thesis submitted in partial fulfillment of the requirements for the degree of

Doctor of Philosophy

Neuroscience
University of Alberta

Abstract

Recovery following stroke occurs almost entirely in the first weeks post injury. Moreover, the efficacy of rehabilitative training is limited beyond this narrow time frame. Sprouting of spared corticospinal tract axons in the spinal cord makes a significant contribution to sensorimotor recovery, but this structural plasticity is also limited to the first few weeks after stroke. Here, we first tested the hypothesis that inducing plasticity in the spinal cord during chronic stroke could stimulate a second wave of recovery from sensorimotor impairment. We potentiated spinal plasticity during chronic stroke, weeks after the initial ischemic injury, in rats via intraspinal injections of chondroitinase ABC, an enzyme which digests inhibitory extracellular matrix proteins (chondroitin sulfate proteoglycans). Our data show that chondroitinase injections into the grey matter of the cervical spinal cord administered 28 days after stroke induced drastic sprouting of corticospinal axons and reduced sensorimotor impairments. Importantly, this therapy dramatically potentiated the efficacy of rehabilitative training delivered during chronic stroke in a skilled forelimb reaching task.

To elucidate the mechanism by which chondroitinase ABC induced anatomical changes *in vivo,* we then investigated the direct regulation of neurite outgrowth by chondroitinase ABC cleavage byproducts in neurite cell cultures and assayed the release of the well-established anti-inflammatory molecules from isolated microglia and mixed glial cell cultures. Our data clearly demonstrates that one of the chondroitinase ABC generated cleavage stubs (C-4-S) directly promotes the outgrowth of neurites in a chondroitin sulfate proteoglycan dependent manner. We also demonstrate that the C-4-S cleavage stub induces the release of trophic and anti-inflammatory cytokines from microglia and mixed glia while attenuating the release of pro-inflammatory cytokines after biological activation of both isolated microglia and mixed glial

cultures.

Next, we examined the effects of exogenous administration of pleiotrophin, an endogenous growth promoting factor which binds growth inhibitory components of the extracellular matrix (chondroitin sulfate side chains), on neurite growth glial activation and glial release of immunomodulators *in vitro*. Our data suggests that pleiotrophin interacts with neurites in a chondroitin sulfate dependent manner to enhance outgrowth. In addition, we provide strong evidence that pleiotrophin modifies the cytokine expression profiles of microglia to favor the release of tropic factors and heightens the release of anti-inflammatory molecules following biological activation. Further, we found that pleiotrophin induced an anti-inflammatory cytokine release profile in mixed glial cell cultures when secondary inflammation was stimulated.

Since recovery following stroke is limited to the first few weeks after injury, enhancing plasticity during this time may reduce chronic deficits. To evaluate the efficacy of pleiotrophin as a therapeutic for stroke, we next tested the hypothesis that enhancing plasticity in the spinal cord in the subacute period following stroke via pleiotrophin injections could stimulate enhanced recovery of sensorimotor function. Our data show that pleiotrophin injections into the grey matter of the cervical spinal cord administered 7 days after stroke reduced sensorimotor impairments without inducing chronic pain. Anatomical studies revealed heightened expression of factors associated with plasticity in the stroke deinnervated cervical spinal cord of pleiotrophin treated rats. Further, our data suggests that pleiotrophin offers a protective effect to cervical spinal motor neurons left deinnervated by stroke and induces restoration of serotonergic fibers density in the cervical spinal grey matter. Combined, the data herein offers hope of improved quality of life via reduced sensorimotor impairment for the millions who live with long term disability as a direct result of stroke.

Preface

This thesis is an original work by Anna Magdalena Wiersma. All animal researched was conducted in accordance with Canadian Council on Animal Care guidelines. All animals use protocols were approved by the University of Alberta Animal Care and Use Committee, "Neuroprotection and neuroplasticity in the CNS, AUP361".

Research conducted for this thesis in chapter 2 and chapter 5 forms part of a research collaboration between Dr. I.R. Winship and Dr. K. Fouad both at the University of Alberta. Dr. K. Fouad, Dr. I.R. Winship and I collaborated on the experimental design and concept formation for chapter 2 and chapter 5. Data in Chapters 3 and 4 were acquired as part of a collaboration between Dr. I.R. Winship and Dr. K. Todd at the University of Alberta. Dr. K. Todd, Dr. I.R. Winship and I collaborated on the experimental design and concept formation for chapter 3 and chapter 4. All the data collection and analyses in these chapters are my original work including the literature review found in chapter 1.

Chapter 2 of this thesis has been submitted for publication as, Wiersma AW, Fouad K, Winship IR. Reopening the critical period for stroke recovery by augmenting spinal plasticity (2017). I was responsible for the data collection and analysis as well as the manuscript composition. K. Fouad contributed to experimental design, concept formation and manuscript edits. I.R. Winship was the supervisory author and was involved with experimental design, concept formation, manuscript composition and manuscript edits.

Acknowledgments

First and foremost, I want to thank my supervisor Dr. Ian R. Winship. His guidance, patience, knowledge and passion for research has made this thesis possible. Dr. Winship's continued faith and encouragement in this research over the past 5 years has been incredible. Thank you for your dedication to the work in this thesis, your ingenuity in designing these studies, your openness to new ideas and your incredible willingness to help. I am very blessed to have had such a wonderful supervisor.

I must also thank my co-supervisor Dr. Kathryn Todd whose love of neuroscience is a constant inspiration. Thank you Dr. Todd for exemplifying what it means to be a strong, successful and accomplished female scientist, you have been a tremendous role model. Dr. Karim Fouad has also played an essential role in my graduate studies as a member of my academic committee. It was a pleasure to learn surgical techniques from such a talented and prominent name in the spinal cord field.

All the member of the Neurochemical Research Unit at the University of Alberta have been a constant source of encouragement, support and friendship. Dr. Glen Baker is an indispensable member of the Neurochemical Research Unit who continues to leave a legacy of great kindness and even greater science. Thank you Dr. Mathew Churchward for all of your excellent guidance and wisdom, your expansive knowledge continues to amaze me. I am indebted to Gail Rauw who has worked tirelessly to help so many graduate students including myself. I must also thank Jocelyn Madeira and Patricia Kent for going far beyond the call of duty, your work is greatly appreciated. My fellow lab mates at the Neurochemical Research Unit including John W. Paylor, Mischa Bandet, Eszter Szepesvari, Junqiang Ma, Sam Joshva and Bernice Sist who have shared their idea, work and lives with me. Thank you for all the joy and

support you have provided over the course of my graduate studies.

This work was only possible because of funding support provided by Alberta Innovates Health Solutions, Heart and Stroke Foundation of Canada, Canadian Institutes of Health Research and the Natural Sciences and Engineering Research Council of Canada.

Finally, I would to thank and acknowledge my family for their unending love and encouragement. My parents Jake and Audrey Wiersma have supported me with love and understanding in every pursuit. Their faith in me and absolute dedication as parents is the sole reason I have achieved any of my goals. Thank you for being the best parents in the world. I also have to thank my brother Joshua Wiersma for being my best friend for the past 26 years. Your courage to be yourself and pursue your passions inspires me every day.

Table of Contents

Chapter 3:

In vitro cellular effects of chondroitinase ABC produced cleavage stubs..... 95

Chapter 4:

In vitro studies of pleiotrophin as a modulator of chondroitin sulfate proteoglycan mediated growth inhibition and neuroinflammation 138

Table of Figures

List of Abbreviations

ALK = anaplastic lymphoma kinase; AMPA = α-amino-3-hydroxy-5-methyl-4-isoxazolepropionic acid; ANOVA = analysis of variance; BDNF = brain derived neurotrophic factor; Brd2 = bromodomain-containing protein 2; BSA = bovine serum albumin (BSA); ChABC = chondroitinase ABC; ChAT = choline Acetyltransferase; CNS = central nervous system; CSPGs = chondroitin sulfate proteoglycans; CST = corticospinal tract; DMEM-F12 = dulbecco modified eagle medium/ham's F12; DMSO = dimethyl sulfoxide; DTI = diffusion tensor imaging; DTT = diffusion tensor tractography; FBS = fetal bovine serum; GAG = glycosaminoglycan; GAP-43 = growth associated protein 43; IBA-1 = ionized calcium-binding adapter molecule 1; ICC = immunocytochemistry; IGF-1 = insulin-like growth factor 1; iNOS = inducible nitric oxide synthase*;* LPS = lipopolysaccharide; mGlu = metabolic glutamate; MARCKS = myristoylated alanine-rich C-kinase substrate; MCA = middle cerebral artery; MN = motor neuron; MMP = matrix metalloproteases; MRI = magnetic resonance imaging; NAD+ = nicotinamide adenine dinucleotide; NMDA = N-methyl-D-aspartate; NO = nitric oxide; NOS = nitric oxide synthase (NOS); PARP-1 = poly(ADP-ribose)polymerase; PBS = phosphate buffered saline; Pen = penicillinase*;* PID = peri-infarct depolarization; PS = penicillin streptomycin; PTN = pleiotrophin; PTPσ = tyrosine phosphatase sigma; PWMT = paw with drawl mechanical threshold; ROS = reactive oxygen species; RPTP = transmembrane tyrosine phosphate receptor; SCG10 = superior cervical ganglia protein 1; SCLIP = SCG10 like protein; TNF-α = tumor necrosis factor-α; TLR = toll-like receptors; TSR-1 = thrombospondin type 1 repeat sequence; IL-1β = interleukin-1 beta; IL-6 = interleukin-6; IL-10 = interleukin-10; INF-γ = interferon gamma; WD = Wallerian degeneration.

Chapter 1:

An introduction to stroke, plasticity and modulators of plasticity, and a look beyond the peri-infarct cortex

The human brain is only 1250 cc in volume yet it defines every aspect of human experience, from cognition and memory to simple movement and basic biological function. When injury occurs to the brain it is devastating and can affect every aspect of human life. Stroke is the most common cause of neurological injury as an estimated 15 million people suffer a stroke each year (Feigin et al., 2010). Most stroke survivors are left with permanent brain injury, making it the largest cause of acquired adult sensory motor disability (Mozaffarian et al., 2015; Carmichael, 2016). Up to 94% of stroke survivors will experience sensory motor deficits after stroke, with diminished ability to perform motor tasks that require sensory information, even after rehabilitation (Carey et al., 1993; Carey, 1995; Julkunen et al., 2005). In Canada alone, 60,000 people suffer a stroke each year. Fortunately, 83% of stroke suffers will survive; however, most survivors are left with permanent brain damage. Currently in Canada, 400,000 stroke survivors are living with long term disability as a direct result of stroke (The Heart and Stroke Foundation of Canada). These chronic functional deficits persisting for years following stroke have devastating consequences on quality of life for stroke survivors. Despite the burden of this disability, currently there are very few clinical interventions which can improve the impairments during this chronic phase of stroke recovery. Research into new approaches to improve quality of life for those left with chronic sensory and motor deficits after cortical injuries such as stroke is necessary to address this unmet clinical need.

Stroke

Stroke is a neurological condition that results from disturbances of blood flow to the brain (Green, 2003; Doyle et al., 2008). This disruption may prevent blood flow to the whole brain during global stroke or only deprive blood flow to a localized area of the brain in focal stroke. In

addition, strokes can be classified as hemorrhage or ischemic. Hemorrhagic strokes are far less common than ischemic strokes and occur when an artery in the brain ruptures or leaks (Green, 2003). There are two types of hemorrhagic stroke. The most common type of hemorrhagic stroke is intracerebral hemorrhage, which occurs when an artery of the brain rupture and floods the surrounding brain tissue (intraparenchymal hemorrhage) and/or ventricles (intraventricular hemorrhage) with blood. Intracerebral hemorrhagic strokes are a type of intracranial bleed that can be caused by many conditions including: trauma, tumors, aneurysm and vascular abnormalities such as arteriovenous malformation (Mozaffarian et al., 2015). Less common is subarachnoid hemorrhagic stroke, which is caused by a bleed into the subarachnoid space between the arachnoid membrane and the pia mater that surrounds the brain. Subarachnoid hemorrhages are most often a result of cerebral aneurysm but can also occur following head trauma (Alberta Heart and Stroke Foundation).

Ischemic strokes are caused by vascular occlusion of cerebral arteries by a blood clot and account for about 87% of all stroke cases (Alberta Heart and Stroke Foundation, Mozaffarian et al., 2015). Ischemic injury results in the generation of several cortical microenvironments (Carmichael, 2006). The infarct core is formed where blood flow is most severely restricted, resulting in insufficient oxygen delivery to neural tissue that impairs oxidative phosphorylation and ATP generation, leading to depolarization and ultimately resulting in rapid irreversible necrotic cell death (Doyle et al., 2008). The infarct core is well defined only three hours after ischemic injury (Carmichael, 2006). Surrounding the core, there is a penumbra zone which lies between the evolving infarction and normally perfused tissues. The penumbra is functionally silent however it is often supplied with blood from collateral arteries anastomosing with branches of the occluded vasculature (Doyle et al., 2008). Cells in the penumbra are damaged

and begin to undergo apoptotic processes; however, much of the penumbra can be rescued if reperfusion is established in the first few hours following stroke. This rescue is time limited, as collateral arteries may not be able to sustain perfusion for extended periods (Doyle et al., 2008; Carmichael, 2006). Thus the penumbra can evolve into infarction in the hours and days after stroke, and preventing this evolution is a key target of pharmaceutical intervention early after ischemic injury. Unfortunately, few neuroprotective strategies have proven to be clinically beneficial, and only reperfusion has been shown to be clinically effective in reducing penumbra cell death (Carmichael, 2006; 2010). Diaschisis or remote changes in functional and structural connections between interconnected brain regions distant to the lesion also occurs following stroke, leading to wide spread dysfunction and degeneration in area distal to the stroke core (Carrera and Tononi, 2014). These changes can lead to further impairment after injury and continue to evolve in the weeks and months following stroke.

Mechanism of ischemic injury in the cortex

The lack blood flow following stroke induces an ischemic cascade that results in detrimental ionic imbalances, massive oxidative stress and primary inflammation. This reduction of blood flow results in insufficient oxygen delivery to neural tissue, thus impairing oxidative phosphorylation and ATP generation (Doyle et al., 2008). Up to 70% of the energy supplied to the brain is utilized by the Na+/K+ ATPase found on the plasma membrane of neurons that act to maintain membrane potential. Following ischemic insult, mitochondrial production of ATP is insufficient to sustain the energy requirements of these neuronal plasma membrane ATPases, leading to depolarization as Na+ rapidly enter neurons (Caplan, 2000; Brouns et al., 2009). The low intracellular calcium concentrations in cells is also maintained by a plasma membrane

ATPase and during ischemia intracellular calcium concentrations have been found to rise from 0.1-1μM to 50-100 μM (Edvinsson and Krause et al., 2002; Doyle et al., 2008). This dramatic rise in intracellular calcium concentration results in the mass activation of calcium dependent enzymes such as proteases, lipases and DNases. The activation of these enzymes contributes to the catabolism of essential cellular components, which cannot be restored due to a lack of ATP necessary for synthesis.

Depolarization of neuronal membranes and increased intracellular calcium levels during ischemia leads to the release of neurotransmitters from affected neurons. Glutamate is the major excitatory neurotransmitter in the brain, and a significant contributor to ischemic pathology. Increased intracellular sodium concentrations of oxygen deprived neurons cause the plasma membrane glutamate transporter to reverse leading to an efflux of glutamate down its concentration gradient into the synapse and increased intracellular calcium levels induce vesicular release of glutamate. Post-synaptic N-methyl-D-aspartate (NMDA) and 3-hydroxy-5-methy-4-isoxazolepropionic acid (AMPA) receptor activation causes further calcium flux into the cell and even greater calcium overload (Buchan et al., 1992). AMPA receptors under physiological conditions are calcium impermeable due to the GluR2 subunit; however, under ischemic conditions the subunit is down regulated, increasing AMPA permeability to calcium 18-fold (Bruno et al. 2001; Liu et al. 2006). Based on the contributions of these receptors to toxicity during stroke, it has been suggested that excitotoxic cell death can be delayed by blocking glutamate interaction with NMDA and AMPA receptors (Buchan et al., 1992). The loss of homeostatic regulation of ion gradients at the core of the ischemic infarct can lead to peri-infarct depolarization (PID). High levels of potassium and glutamate at the site of ischemic injury can induce repeated self-propagating waves of electrical activity throughout the penumbra

(Gonzales et al., 1992). Waves of PID are thought to cause further neural insult and secondary injury and have been found to occur in both animal models of stroke and human strokes.

Metabolic glutamate (mGlu) receptors also play a key role in ischemic excitotoxicity. Groups I metabotropic glutamate receptors increase calcium concentrations in the cytoplasm (mGluR1) and reduce intracellular potassium levels by opening ion channels (mGluR5) (Bruno et al., 2001). In addition, Group I mGlu receptors are excitatory, promoting NMDA activation (MGlu5) and suppressing the release the inhibitory neurotransmitter from GABAergic neurons (Berent-Spillson et al., 2006). Bruno et al. (2001) have demonstrated that antagonism of group I glutamate receptors is neuroprotective in animal models of cerebral ischemia, reducing excitotoxicity and intracellular ionic imbalances. Although group I metabolic glutamate (mGluR1,5) receptor activation after stroke leads to excitotoxicity and perpetuates neural injury, activation of group II (mGluR2,3) and groups III (mGluR4,5,6,7) receptors may reduce neuronal damage after injury. Group II receptors inhibit adenylyl cyclase, halting downstream cAMP-pathways thereby preventing activation of excitotoxic cAMP pathways (Berent-Spillson et al., 2006). Further, group II receptors are also thought to induce the production of neurotrophic factors (Bruno et al. 2001; Liu et al. 2006). Group III receptors play a key role in the activation of calcium channels and stimulation of group III restores intracellular calcium concentrations and vesicular release (Bruno et al. 2001). Agonists of group II and III glutamate receptors found at presynaptic terminals are neuroprotective, activating mGlu receptors which inhibit glutamate release into the synapse and reduce excitotoxicity (Bruno et al. 2001; Liu et al. 2006).

Ischemic conditions also promote the escape of electrons from the oxidative phosphorylation machinery, resulting in mitochondrial production of reactive oxygen species (ROS). Neural tissue is particularly susceptible to the deleterious actions of ROS as antioxidants

are in relatively low concentrations in the brain (Edvinsson and Krause et al., 2002; Doyle at al. 2008). Ischemic conditions promote the action of nitric oxide synthase (NOS), which produces nitric oxide (NO) gas. NO reacts with superoxide to produce the powerful oxidative agent peroxynitrite (Crack and Taylor, 2005). ATP depletion during ischemic insult is further perpetuated by the action of NO on poly(ADP-ribose)polymerase-1(PARP-1) (Doyle et al. 2008). NO up regulates PARP-1 activity, which results in depletion of adenosine dinucleotide (NAD+) (Gonzales et al., 1992). Processes dependent on NAD+ such as mitochondrial respiration are therefore impaired, leading to greater ATP deficits and ionic imbalances. ROS also activate matrix metalloproteases (MMP), which are known to increase blood brain barrier permeability and disrupt cerebral vasculature by degrading collagen and laminins of the basal lamina (Crack and Taylor, 2005).

Inflammation after stroke in the cortex

The inflammatory response following stroke has been associated with secondary neuronal injury, however aspects of the response can be neuroprotective. Doyle et al. (2008) divided the inflammatory response into three classes: the cellular response, the cytokine response and the toll-like receptors (TLR) response.

The cellular response

The cellular response is characterized by activation and accumulation of inflammatory cells such as blood-derived leukocytes, neutrophil and monocytes in the brain, which leads to additional inflammatory injury following the initial ischemic insult. Immediately following stroke (as early as 30 minutes after injury) there is an accumulation of monocytes and neutrophils at the site of

injury (Huang et al., 2006; Ross at al., 2007). In addition, ischemic injury induced an upregulation of integrins and immunoglobins, which mediate the adherence and activation of neutrophils to cerebral blood vessels. Adherence of neutrophils can disrupt and occlude microcirculation, preventing reperfusion and exasperating neural injury (Huang et al., 2006). Further, neutrophils release damaging enzymes and free radical oxygen species that contribute to neural damage. Huang et al. (2006) found that knocking out protein kinase C (which has a central role in neutrophil adhesion and oxygen radical production) in mice reduced the infarct volume when cerebral ischemia was experimentally induced. Although lymphocytes are not normally found in the nervous system, they can be detected in neural tissues 24 hours after initial ischemic insult (Doyle et al., 2008). The exact mechanism for lymphocyte entry into the brain remains unclear, however it is known that they play a role in neural damage following ischemic injury, and mice lacking B and T lymphocytes exhibit a 40% reduction in cortical infarct volumes (Hurn et al., 2007). Despite the initial effects of neutrophil and lymphocytes that may perpetuate neural damage, the action of these cells in long term process such as debris removal may be beneficial (Doyle et al. 2008).

The cytokine response

The cytokine response constitutes the upregulation of cytokines in the brain after stroke in infiltrating immune cells as well as resident glia and neurons (Sairanen et al., 2001). The most well characterized cytokines related to inflammation after ischemia are interleukin-1 (IL-1), tumor necrosis factor – alpha (TNF-α), interleukin-6 (IL-6), interleukin-10 (IL-10) and transforming growth factor-β (TGF-β) (Han et al. 2003). Of these cytokines, IL-1, IL-6 and TNF-α appear to aggravate ischemic injury; in contrast, IL-10 and TGF-β can be neuroprotective

(Allan and Rothwell, 2001). Following stroke there is a significant up regulation of cytokines IL-6 and IL-1 in neurons and microglia of the injured cortex (Tarkowski et al., 2006: Doyle et al. 2008). Increased IL-1 amplifies arachidonic acid release contributing to toxic acidosis, stimulates NMDA mediated excitotoxic effects, induces ROS release and enhances neutrophil infiltration (Huang et al. 2006). TNF-α mRNA, like IL-1 mRNA, is up regulated in the cortex within an hour of ischemic insult (Huang et al. 2006). Increased expression of TNF-α is associated with the accumulation of neutrophils, the induction of inflammatory mediators and a further break down of the blood brain barrier resulting in further expansion of the ischemic infarct (O'Neil et al., 2016). Although TNF-α upregulation is thought to have negative consequences on stroke pathophysiology it may have beneficial roles in plasticity and recovery by acting through Trk-independent mechanism (O'Neil et al., 2016).

Interestingly, IL-6 has been shown to be both pro-inflammatory and anti-inflammatory after ischemic injury. In animal studies IL-6 deficient mice have similar sized infarcts compared to wildtype suggesting that it does not enhance ischemic pathogenesis (Clark et al., 2000). In contrast, TGF-β is considered to be a neuroprotective cytokine after injury as it initiates neuroprotective pathways, aids in reduction of glutamate excitotoxicity, and enhances endothelial integrity in neural tissue (Huang et al., 2006). Similarly, IL-10 is an anti-inflammatory cytokine which is upregulated in the damaged cortex following stroke, where it inhibits pro-inflammatory cytokines IL-1 and TNF-α receptor expression/activation. Exogenous administration (Spera et al., 1998) or gene transfer of IL-10 (Ooboshi et al., 2005) in animal models of cortical stroke reduced ischemic infarct and improved functional outcomes. Cytokines therefore have a diverse role which a specific temporal distribution which can result in both detrimental and protective effects.

The toll-like receptors (TLR) response

TLR recognize invading pathogen-associated molecules including peptidoglycan (TLR2) and lipopolysaccharide (TLR4) which are components of bacterial cell walls. Upon activation TLRs induce cytokine and chemokine production, which initiate a local inflammatory response (Doyle et al., 2008). Following stroke there is an upregulation of endogenous factors that signal tissue damage and can serve as TLR ligands such as fibrinogen, host DNA and heat shock protein (in particular HSP 70). In addition, TLR2 mRNA is up-regulated in the brains of wild type mice following cerebral ischemia and is expressed by lesion-associated microglia.

In the central nervous system (CNS), TLRs are found on neurons, endothelial cells, microglia, astrocytes and oligodendrocytes (Edvinsson and Krause, 2002). When activated they induce a local immune cascade and further amplify cytokine and chemokine mediate inflammation, which is beneficial when invading pathogens are present but detrimental when triggered by ischemic damage. This dual role for TLR in stroke pathology is evident in the contradictory results of TLR knockout animal studies. Interestingly, mice lacing TLR2 or TLR4 have significantly reduced infarct sizes following ischemic injury when compared to wild type mice (Ziegler et al., 2007). However, microglial cultures studies have demonstrated that TLR4, and not TLR2, activation is responsible for apoptosis (Jung et al., 2005). Such conflicting experimental results are typical of the complex role that these receptors and the various cells that express them play in the post stroke inflammatory response.

Post stroke cortical plasticity

While injury at the stroke core is irreversible, tissue in the penumbra can be protected from death and partial recovery can occur through adaptive processes. Murphy and Corbett define recovery

as the re-establishment of the exact sensory-motor pathways that were present prior to the stroke (Murphy and Corbett, 2009). However, they recognize that this definition of recovery is rarely achieved after stroke and most measures of recovery only indicate changes in performance which may be compensatory in nature (Carmichael, 2003; Murphy and Corbett, 2009). Carmichael identifies three processes that contribute to recovery from stroke: resolution of tissue damage, behavioral compensation and neuronal plasticity (Carmichael, 2003; Winship and Murphy, 2009). Acute recovery in the initial hours and days following stroke is achieved by the resolution of tissue damage while later recovery, weeks to months after stroke, is mediated by compensatory plasticity (Carmichael, 2003; Murphy and Corbett, 2009; Winship and Murphy, 2009). Neuroplasticity in the post stroke brain allows physiological and anatomical changes in neural networks which facilitate functional recovery via the repair or restoration of damaged circuitry (Winship and Murphy, 2009). Functional recovery can be achieved by rewiring of surviving neurons to replace damaged networks and/or reinforces existing connections, thus allowing surviving regions of the cortex to take over the sensory motor functions of the damaged areas (Winship and Murphy, 2009).

Axonal sprouting after stroke

Axonal sprouting or the formation of new connections is one means by which anatomical change is achieved in the brain following stroke. Functional studies have shown that initially, subcortical stroke induced activation of the bilateral cortex in response to sensory or motor stimulation of impaired limbs (Butz et al., 2009). As recovery progresses bilateral activation is reduced and sensory motor activation of the stroke affected cortex or ipsilesional cortex increases along with activity in ipsilesional pre- and supplementary motor areas (Brown et al., 2010). The time scale

of the study suggests that the observed functional recovery may be a result of axonal sprouting.

Under physiological conditions, axonal sprouting is inhibited in the adult CNS by three broad classes of proteins: (1) Myelin-associated proteins such as Nogo A and myelin-associated glycoprotein; (2) extracellular matrix proteins such as tenascin and chondroitin sulphate proteoglycans; and (3) growth cone inhibitors such as ephrin and semaphorin (Li et al., 2004). These growth inhibitors are enhanced in the CNS after injury. For example, after spinal cord injury, protein expression of Nogo A, chondroitin sulphate, and semphorin IIIA is induced in the glial scar at the site of injury and in regions surrounding these scars (Kubo et al., 2008).

Nogo is a myelin-associated protein that has been identified as one of the chief inhibitors of axonal growth in the brain and spinal cord (Carmichael, 2010). Nogo is known to act through four receptors including Nogo receptor one (NgR1), a glycosyl-phosphoinositide linked protein (Carmichael, 2010). More recently PIRI, an immunoglobulin receptor, has been characterized as a functional receptor for Nogo (Atwal et al., 2008). NgR1 signal transduction occurs through TROY, p75 and Lingo-1, which are all members of the tumor necrosis factor (TNF) family (Liu et al., 2006). The Nogo signaling pathway provides many promising targets for pharmaceutical intervention of stroke and spinal cord injury. For example, antagonist peptides have been developed for Nogo, NgR1 and the downstream TNF Lingo-1 (Li et al., 2004; Lee et al., 2004, 2010).

Studies have demonstrated that mice lacking the Nogo receptor (NgR) recover complex motor function after stroke more completely than animals with intact with NgR (Lee et al., 2004). NgR deficient mice scored 2x higher than NgR intact mice on forepaw single pellet reaching tasks 30 days after photothrombotic of the somatosensory cortex (Lee et al., 2004). In addition, NgR deficient mice had greater numbers of axons (about 2x more than NgR intact

mice) radiating from the undamaged cortex cross the midline to innervate the ipsilateral cervical spinal cord, indicating that axonal plasticity after stroke is enhanced in NgR deficient mice (Lee et al., 2004).

In another study, rats were given a photothrombotic stroke that destroyed over 90% of the somatosensory cortex and treated with a function blocking antibody against Nogo-A delivered intrathecally for 2 weeks after stroke (Lindau et al., 2013). Rats which received the anti-Nogo-A-antibody regained 65% of baseline function on a single pellet skilled reaching task compared to only 20% in animals which did not receive a Nogo-A blockade. Bilateral retrograde tract tracing with two different tracers from the intact (ipsilesional) and the denervated (contralesional) side of the cervical spinal cord indicated that the intact corticospinal tract had extensively sprouted across the midline into the denervated spinal cord in the anti-Nogo-A-antibody treated mice only (Lindau et al., 2013). However, many of these fibers which re-crossed the midline were subsequently withdrawn, resulting in a 'side-switch' in the projection of a subpopulation of contralesional corticospinal tract axons (Lindau et al., 2013). These plastic changes occurred in parallel with somatotopic reorganization of the contralesional motor cortex of the anti-Nogo-A-antibody treated mice only (Lindau et al., 2013). Taken together these studies establish Nogo as a powerful inhibitor of axon sprouting that even prevents sprouting in areas distal to the injured cortex.

Although there is an upregulation of factors known to prevent or act as a barrier to plasticity following ischemic insult in the cortex, there is also an upregulation of factors that promote or are associated with plasticity and enhanced recovery. Factors that are associated with axonal growth such as growth associated protein 43 (GAP-43) and myristoylated alanine-rich C-kinase substrate (MARCKS) are upregulated after stroke. GAP-43 is a phosphoprotein that is

expressed in the growth cones of spouting axons. GAP-43 serves as an experimental marker of axonal spouting, and GAP-43 mRNA is found to be elevated for three days to one month following stroke, which has been correlated to an increased number of synapses at later time points (Stroemer et al., 1995). In the regions of the peri-infarct cortex which lie outside the glial scar, there is a pronounced up-regulation of axonal growth promoting proteins (Butz et al., 2009). This permissive environment for axonal growth in the brain, induced by stroke, results in a defined pattern of axonal sprouting (Carmichael 2010) and enhanced recovery.

Carmichael (2006, 2010) defines three biological time frames which occur after stroke and are associated with the expression of specific growth promoting genes. The first stage is axonal spouting, which occurs in the first three days after stroke. During this time rhythmic axonal discharge induces sprouting and early response gene expression is initiated. Genes for lipid raft proteins essential in growth cone production such as GAP-43 and MARCKS along with their transcription factor c-jun are expressed in this phase and continue to be expressed though out the lesion induced period of plasticity (Carmichael, 2006). The second phase of maintaining axonal spouting occurs seven to fourteen days after stroke. This phase is characterized by the expression of growth promoters such as cell adhesion molecule Li, embryonic tubulin Tal, and cyclin-dependent kinase inhibitor p21/wafl. This phase is also characterized by the induction of mRNA for inhibitor factors such as chondroitin sulfate proteoglycans, indicating that prior to this period growth inhibitory molecules have not yet been expressed (Butz et al., 2009) and that plasticity and neural tissue remodeling is temporally limited. Finally, 28 days after stroke marks the axonal maturation phase in which synapses developed during the earlier stages can now be anatomically detected. Expression of cytoskeleton remodeling genes superior cervical ganglia protein 10 (SCG10) and SCG10 like protein (SCLIP) define this phase of this phase (Hurn et al.,

2006; Carmichael, 2003).

Dendritic plasticity in the cortex

Most excitatory synapses in the cortex terminate onto dendritic extensions referred to as spines (Harris, 1999). These spines and their associated dendritic arbors have an essential role in functionally integrating synaptic inputs for multiple sources. In the adult brain, established dendritic spines are relatively constant; however, there is evidence that cortical injury such as stroke induces remolding of apical dendrites in the peri-infarct cortex and enhances dendritic spine turnover (Nudo and Milliken, 1996; Xerri et al, 1998; Winship and Murphy, 2009; Brown et al., 2007, 2010). Brown et al. (2007) demonstrated that only 0.14% of dendritic spines are gained and 0.19% are eliminated under physiological conditions in uninjured mice during a 6-hour imaging period. However, one week after induced cortical stroke spine formation significantly increased in the peri-infarct regions to 1.37 %, and dendritic spine formation remained elevated to 0.75% even six weeks after stroke (Brown et al., 2007). Interestingly, spine elimination although elevated was not significantly different in stroke animals when compared to uninjured control animals. Increased spine formation in the peri-infarct regions allowed a restoration of dendritic spine density from 1.81 spines/10 μm one week after stroke to 2.08 spines/10 μm 6 weeks after stroke (Brown et al., 2007). Additionally, the study noted that spine turnover rates farther from the infarct (at least 1.5 mm away from the infarct border) were not elevated compared to unlesioned animals, indicating that the peri-infarct zone is the focal point for dendritic plasticity following stroke. Additional studies by this group using three-dimensional reconstructions of chronically imaged dendritic arbors showed that dendrites grow preferentially away from the site of ischemic infarction and dendrites positioned toward the infarct core

progressively shorten (Brown et al., 2010). Further, stroke significantly increased the total length of dendrite that was remodeled per neuron from 94±11 mm pre-stroke versus 327±75 mm 2 weeks after stroke. However, the total dendritic length within individual neurons did not change significantly over time, even though there was a threefold increase in dendrite remodeling, leading Brown et al. (2010) to conclude that ischemic injury induces a balanced and branch-specific pattern of remodeling in a manner that conserves total dendritic length.

Neurogenesis in the cortex

The anatomical and structural changes which occur in the post stroke brain are in part due to new neuron incorporation into neural networks. In the adult brain, neurogensis occurs in two regions; the subgranular zone (SGZ) of the hippocampus and the subventricular zone (SVG) (Zhang et al., 2005; Ohab et al., 2008). Under physiological conditions, new neurons that develop in the SGZ are incorporated into the neural networks of the dentate gyrus, while neurons from the SVG migrate to the olfactory bulb (Zhang et al., 2001, 2005; Ohab et al., 2008; Tonchev, 2011). Increased cell proliferation has been discovered in the SGZ and SVG of rodent ischemic stroke models in the first two weeks after stroke, while increased cell proliferation has been reported in the SVG region of humans after stroke (Zhang et al., 2001, 2005). After proliferation in the SVG, immature neurons follow migrate to areas of ischemic injury in the striatum and cortex (Ohab et al., 2008). In the first weeks following stroke, tens of thousands of new immature neurons migrate on a mesh like network of astrocytes that extend processes linking ischemic injured tissue to the SVG (Ohab et al., 2008). Neuroblasts also migrate out of the SVG to the site of injury following an astrocytic vascular boarder which is rich in MMP, suggesting that neuroblasts may digest the extracellular matrix in a protease dependent fashion as they migrate

towards the site of injury (Ohab et al., 2008). The molecular guidance system that directs the movement of new neurons to the site of injury is yet to be determined, but there are many factors such as chondroitin sulfate proteoglycans that are known to inhibit and block migration, and few of these immature neurons survive to become mature neurons in the peri-infarct cortex (Zhang et al., 2001, 2005).

Glia and microglia in stroke

Stroke impacts the organization and function of glial cells in the CNS. Following ischemic insult glial cells undergo rapid changes in morphology, gene expression, and proliferation (Caleo, 2015). In the acute phase of stroke, astrocytes play both a deleterious and beneficial role in neuron survival. Astrocytes induce an inflammatory cytokine response which exacerbates the neuronal damage in the ischemic region, but some aspects of the inflammatory response have also been shown to limit lesion growth via anti-excitotoxicity effects (Sims et al., 2017). In addition, astrocytes release neurotrophic factors that promote cell survival and induce plasticity of spared neural networks (Lui et al., 2016). In studies where reactive gliosis was reduced by fluorocitrate, a specific astrocytic metabolic inhibitor (which is taken up by glial alone in the CNS, where it impairs carbon flux through the Krebs cycle and thereby inhibits glial metabolism), animals had worse behavioral outcomes after stroke, pointing to a potential protective role played by astrocytes early after injury in the CNS (Hayakawa et al., 2010). Although reactive astrocytes inhibit axonal spouting, they may have a fundamental role in stabilizing neural networks of CNS cutely (Hudson et al., 2015). In double knock out mice which did not produce GFAP, a cytoskeletal component (intermediate filament) of astrocytes or vimentin, a cytoskeletal component of neural mesenchyme cells, recovery of motor function

following cortical photothrombotic stroke was impaired. Interestingly, in these knock out mice where astrocytic reactivity is attenuated, CSPG expression was significantly increased in the lesion remote areas, but decreased in the ischemic lesion boundary zone at 3 days after stroke (Liu et al., 2014). There was reduced CST axonal remodeling in the deinnervated spinal cord, potentially due to increased CSPG expression that resulted from blocking astrocytic reactivity, indicating that active astrocytes may facilitate anatomical and behavioral recovery early after stroke (Liu et al., 2014).

Acutely, reactive astrocytes are neuroprotective and resolve tissue damage; however, glial scarring produced by active astrocytes can block axonal regrowth and drastically limit plasticity after resolution of the initial injury (Chen et al., 2014; Sims et al., 2017). For this reason, digesting CSPGs (a major component glial scars) after injury improves functional and anatomical outcomes (Chen et al., 2014). However, reactive astrocytes contribute to neurogenesis, synaptogenesis, axonal remodeling and angiogenesis, which are all essential to neurorepair in the later stages after injury (Liu and Chopp, 2016). Since the glial response to injury is both beneficial and detrimental at different time points after injury, modifying the glial response to ischemic insult may offer therapeutic potential, but greater characterization of the role of reactive astrocytes post stroke is needed (Sims and Yew, 2017).

Microglia have an equally paradoxical role in post stroke recovery as specific microenvironmental signals can induce microglia polarization into M1 or M2 phenotypes. In particular, stimulation of TLR ligands and INF-γ induces M1 polarization, while stimulation by IL-4/IL-13 supports the M2 polarization (Sica et al., 2012; David et al., 2013). Classically, M1 polarization is considered pro-inflammatory as M1 microglia release ROS and pro-inflammatory cytokines including interleukin-1β (Sica et al., 2012). The M1 phenotype is often associated with

phagocytosis as these microglia kill pathogens by iron restriction and phagosome acidification (Mantovani et al., 2004). Common M1 phenotype markers include CD16, CD32, CD86, MHC II, and iNOS (Fumagalli et al., 2014).

Microglia can also take on a classic M2 phenotype which is considered neuroprotective and promotes repair of the damaged CNS by scavenging cell debris and producing neurotrophic factors, such as insulin-like growth factor-1 (IGF-1). The M2 phenotype can be further subdivided into M2a, M2b and M2c where each phenotype is elicited by a different stimulus (Fumagalli et al., 2014). The M2a phenotype is stimulated by IL-4/IL-13, M2b is stimulated by immune complexes in combination with TLR or IL-1 receptor ligands, and finally the M2c phenotype is stimulated by IL-10 and glucocorticoids (Mantovani et al., 2002).

Each class of M2 polarized microglia is associated with a different aspect of the immune response. M2a microglia play an important role in mediating the Th2 immune response and are associated with increased IL-4 secretion (Martinez et al., 2008). These microglia also play a key role in parasitic encapsulation and have been identified as a possible source of type II sensitivity (Martinez et al., 2008; Fumagalli et al., 2014). The M2b phenotype has both pro- or anti-inflammatory functions and is thought to mediated the recruitment of regulatory T-cells and B-cell phenotypic switches, in addition to upregulating antigen presenting factors like MHCII and CD86 (Mantovani et al., 2002). M2b is also associated with changes in expression of cytokines, including upregulation of IL-10 and decreased expression of IL-12 (Martinez et al., 2008). The M2c phenotype has an essential function in scavenging debris after injury and is known to contribute to tissue remodel and the production of extracellular matrix components (Martinez et al., 2008). In addition, M2c macrophages are important for secretion of IL-10 and TGF-β (Mantovani et al., 2002). Recently another phenotype of microglia has been proposed, termed

M0, that represents a non-polarized microglia state with a novel microglia signature that is dependent on TGF-β signaling (Butovsky et al., 2014).

Although microglia are often defined as polarized to a discrete M1 or M2 state, the biological reality is that microglia are on a continuum between M1 and M2 where they produce a wide spectrum of factors. Ransohoff (2016) has criticized the microglia polarization model, emphasizing that this terminology was adapted to simplify scientific findings when the properties of microglia were largely uncharacterized and before the functional significance of microglia was fully understood. He argues that terminology suggesting microglia have discrete pathways of polarization obstructs research and should no longer be commonly accepted. Morganti et al. (2016) have demonstrated that after traumatic brain injury microglia simultaneously express phenotypic marker of both the M1 and M2 phenotypes. It is important to consider these findings especially when studying microglia in complex environments such as those after injury where it has been proven that microglia display a mixed phenotype and cannot be easily characterized into discrete categories.

Recent studies have demonstrated that the post stroke environment drives microglia function and phenotypes. Since microglia are ATP-dependent consumers of energy they are highly sensitive to hypoxia and changes in perfusion (Fumagalli et al., 2014). In addition, microglia express many surface receptors known as pattern recognition receptors (PRR), which allow then to sense damaged tissues as they bind danger-associated molecular patterns (DAMPs) that are released as a consequence of tissue damage (Fumagalli et al., 2014). After stroke, many DAMPs are present including hyaluronic acid generated by extracellular matrix degradation, fibronectin, high mobility group box 1 (HMGB1), nucleic acids, immune complexes, mannose residues and proteolytic enzymes (Kigerl et al., 2014). Microglia that express chemokine

receptors of the CC and the C-X-C family are rapidly recruited to the site of ischemic injury by chemokines released from host cells (Kigerl et al., 2014). Once recruited microglia interact with microenvironments including contact-dependent inhibitory signals and soluble molecules derived from injured neurons that drive polarization of microglia to different phenotypes. Ischemic conditions stimulate hypoxia-inducible factor-1α dependent pathways which promotes autophagic cell death in microglia cultures and the increased release of pro-inflammatory cytokines including IL-8 and TNF-α (Shi, 2009; Yang, 2014). Dynamic shifts in microglia phenotypes are associated with many neuro degenerative diseases and stroke induced polarization of microglia to the M1 phenotype may lead to irreversible loss of neurons (Tang and Le, 2016). Since microglia are so diverse in function and can rapidly adapt their expression profile based on the shifting microenvironments, it is difficult to define a single role for microglia in the post stroke CNS.

Changes that extend beyond the peri-infarct cortex

Most research and therapeutic interventions relating to post-stroke plasticity have focused on changes that occurs near the infarcted area. Plasticity and remapping of sensorimotor function in premotor, motor and somatosensory circuits of the cortex adjacent to the infarct (ipsilesional) are associated with better functional recovery after ischemic injury in human, primate and rodent models of stroke (Carmichael, 2003; Overman et al., 2012; Li et al., 2015). Plasticity after injury is not limited to the ipsilesional cortex as plastic changes are also observed in the hemisphere contralateral to the stroke where plasticity has been shown to both mediate and obstruct recovery (Carmichael, 2016). Interestingly, in small infarct cortical stroke, plasticity of cortical circuits in the spared hemisphere can result in the formation aberrant connections (Carmichael, 2016;

Carmichael et al., 2017) and over training of the uninjured limb (represented in the hemisphere contralateral to the stroke) can lead to reduced recovery of the stroke injured limb (Kim et al., 2015). However, in severe strokes with large cortical infarcts, blocking axonal spouting form the injured cortex into the intact cortex inhibits motor recovery (Carmichael, 2016).Thus contralesional plasticity is associated with improved recovery after large cortical strokes (Carmichael, 2016).

In large volume strokes, the contralesional CST may also sprout forming connections with spinal circuits left deinnervated by stroke making the cortical spinal tract a potential therapeutic targets. It is important to consider that over 90% of human stroke suffers will experience sensory deficits and motor difficulties on task requiring somatosensory information processing (Carey et al., 1995; 2002), indicating that the CST which transmits sensorimotor information between the cortex and spinal sensory motor circuits may offer a mechanism of sensory and motor recovery after stroke. Structural analysis demonstrates a critical correlation between focal ischemic damage to the corticospinal tract and functional sensory motor recovery after stroke (Wahl et al., 2014; Wahl and Schwab, 2014). This indicates that the corticospinal tract plays an integral role in functional recovery after stroke and serves as a good therapeutic target as networks in the spinal cord are still intact, but lack innervation by the stroke injured cortex (Soleman et al., 2012; Wahl et al., 2014).

CST changes after stroke – Wallerian degeneration

Wallerian degeneration (WD) as first reported in 1850 describes the anterograde degeneration of proximal axons or distal segments of nerves following insult to the cell body within the central and peripheral nervous system (Johnson et al., 1950; Jones et al., 2013). WD follows a well-

defined course beginning with the degradation of axonal structures in the first 2-7 days after injury (Iizuka et al., 1989). This degradation induces the infiltration of macrophages that promote the loss of myelin and astrocytic production of CSPG rich glial scars which become evident 2 weeks after injury (Lampert and Cressman, 1966). Finally, a pathological accumulation of extra cellular matrix proteins results in fibrosis and the eventual atrophy of the involved tract in the weeks and months following injury (Lexa et al., 19994; Thomalla et al., 2004; Taraschenko et al., 2015). Although the concept of WD has been in existence for over 150 years, it is not until the last few decades, with the refinement of magnetic resonance imaging (MRI) and more recently diffusion tensor imaging (DTI), that WD in the CST of humans could be detected following ischemic insult in the brain.

Early MRI studies investigating the pyramidal tracts of adult stroke patients revealed that CST integrity following stroke, as measured by proportional grid system analysis of proton weighted MRI images was associated with improved motor recovery as determined by a motor score test and recordings of magnetic evoked motor potentials (Binkofski et al., 1996). Other MRI studies demonstrated that the extent of brain stem WD correlated with the impairment of daily living activities in supratentorial hemorrhagic stroke patients (Fukui et al., 1994). Thus, WD occurs in the CST post stroke and that the extent of WD is correlated with poor motor outcomes. However, these preliminary studies were limited by the existing MRI technology that could only detect signal changes due to fibrosis in the CST, which does not appear until the chronic phase of stroke.

The recent development of DTI technology allows *in vivo* visualization of long descending white matter tracts from the brain to the CST. Signal changes or abnormality on DTI permit detection of demyelination, gliosis and parenchymal atrophy elucidating the early phases

of WD following injury (Taraschenko et al., 2015). DTI imaging has recently been used to detect WD in the pyramidal tracts within the first two weeks of stroke (Thomalla et al., 2004). For the first time, a correlation between the extent of WD in the pyramidal tracts at early time points after stroke and functional motor outcome after intracerebral hemorrhage has been established (Thomalla et al., 2004). Moreover, a case study of middle cerebral artery stroke showed evidence of WD though the right CST corona radiate extending to the upper cervical spinal cord (Liebeskind., 2004). Postmortem studies of the CST after stroke have confirmed a loss of myelin and axons, macrophages infiltration and tissue rarefaction as seen in DTI imaging (Matsusue et al., 2007).

CST changes after stroke – Inflammation

Primary inflammation immediately after ischemic injury and delayed secondary inflammation have been well studied in the cortex following ischemic injury, however less is known about the inflammatory processes which occur in the spinal cord following cortical injury and subsequent WD (Weishaupt et al., 2010; Jin et al., 2013). Animal studies have demonstrated that cortical ischemic injury induced in the forelimb motor cortex of rats causes degeneration of contralesional CST in the cervical spinal cord, with an increase in active microglia found at this level of the spinal cord 1 week after injury (Weishaupt et al., 2010). Notably, axonal degeneration extends to the thoracic spinal cord 4 weeks after injury, indicating that the spinal inflammation triggers secondary damage to axons passing through the site of primary inflammation. However, this secondary damage was not found to have any functional consequences on horizontal ladder testing of the hind limb and was not associated with persistent microglial activation (Weishaupt et al., 2010).

Dynamic secondary degeneration in spinal cord and ventral roots after focal cerebral infarction has recently been characterized at multiple levels of the spinal cord during extended time points after injury (Dang et al., 2016). The presence and degeneration of axons was established using a marker for neurofilament (mouse anti-neurofilament), which is a major component of the neuronal cytoskeleton that provides structural support for the axon and regulates axon diameter (Yuan et al., 2012). At one-week post stroke (middle cerebral artery occlusion in hypertensive rats) there is pronounced degeneration of neurofilament (a marker of axonal density) on both the ipsilesional and contralesional side of the cervical (C5) and lumbar (L5) spinal cord (Dang et al., 2016). Interestingly, this loss of axonal density corresponds with the onset of elevated IBA-1 levels marking active microglia (Dang et al., 2016). In the cervical spinal cord (C5), neurofilament levels remain depressed on both the ipsilesional and contralesional sides even at 12 weeks post stroke, correlating with IBA-1 levels peaking in the spinal cord at 8 weeks post injury and remaining elevated for 12 weeks (Dang et al., 2016).

The inflammatory response in the spinal cord is not limited to microglia, and astrocytes might also play an important role in damage caused by secondary inflammation. In both the cervical and lumbar spinal cord there is an upregulation in GFAP (indicating the presence of active inflammatory astrocytes), which was restricted to the contralesional side. Contralesional GFAP was determined to be slightly elevated for the first 4 weeks after stroke followed by a sharply increases from 4-12 weeks post stroke (Dang et al., 2016). The absence of GFAP may explain the finding that by 12 weeks post stroke in the lumber spinal cord (L5) neurofilament return to sham levels on the ipsilesional side despite elevated IBA-1 (Dang et al., 2016). Conversely, the elevated levels of GFAP selective to the contralesional side may elucidate why neurofilament levels remain depressed despite a bilateral increase in IBA-1 (Dang et al., 2016).

When looking specifically at the ventral horn, which houses essential spinal motor circuits and large motor neurons that conduct motor signals to the periphery, Dang et al. (2016) found different trends in neurofilament density than rest of the spinal cord. In the ventral horn of C5 and L5 on the contralesional side, there were significant decreases in neurofilament at 1 week post stroke, which seemed to recover by 2-3 weeks and then again drop almost two fold by 12 weeks post stroke. This indicates that detrimental secondary inflammatory processes are occurring in the ventral horn (Dang et al., 2016). Remarkably, in the ventral horn at both C5 and L5 there was a twofold upregulation of IBA-1 positive cells at 1week post stroke, corresponding the onset of neurofilament loss, that returned to baseline levels at week 12. A delayed upregulation of GFAP correlated with the secondary loss of neurofilament (Dang et al., 2016). This study illuminates the potential roles of secondary inflammation mediated by active microglia and astrocytes on axonal recovery and secondary loss of spinal cord axons at extended time points after stroke.

Cytokines are key mediators of the post stroke inflammatory response, which play a key role in recruiting and activating both astrocytes and microglia. Studies of pro-inflammatory factors in the spinal cord after stroke reveal that TNF-α and IL-6 peak in the spinal cord during the first 14 days after injury and gradually return to baseline levels by 28 days posts stroke (Sist et al., 2014). The increased expression of the inflammatory cytokines TNF-α and IL-6 parallel the temporal profile of microglial activation in the cord following cortical injury and suggest a role for TNF-α and IL-6 initiating secondary damage (Sist et al., 2014; Dang et al., 2016). Notably, the temporal profile of these inflammatory cytokines also closely paralleled markers of spinal plasticity, as described in detail below.

CST changes after stroke – Spinal plasticity

With the striking correlation between WD in the CST and motor deficits after stroke, it is essential to focus not only on the brain but also the CST and spinal circuits when considering motor recovery mechanisms. Spinal plasticity after stroke includes axonal sprouting from the CST and local spinal projection, and results from changes in mediators that induce or guide axonal extension and promote the formation of functional connections with spinal sensory and motor circuits.

Stroke can induce 'reparative' axonal sprouting which follows a defined trajectory from the contralateral sensorimotor cortex to the stroke deinnervated cervical spinal cord (Chen et al., 2002, Zai et al., 2009; Benowitz and Carmichael, 2010). The term 'reparative' sprouting is used to define long distance axonal spouting that occurs after stroke and can be stimulated by blocking glial growth inhibitors or inducing a neuronal growth program, and in every case it is associated with behavioral recovery (Carmichael, 2016). This sprouting primarily occurs in areas where axonal degeneration of stroke affected projections induced reactive astrocytosis and microglial responses. Further, these sprouting axons contribute to the remapping of forelimb motor representations of the stroke impaired ipsilateral limb (Lindau et al., 2014). This particular pattern of long distance sprouting from the uninjured cortex into the deinnervated cervical spinal cord is more prevalent in larger strokes as they are associated with greater contralateral cortical axonal sprouting (Carmichael, 2016).

'Reparative' axonal sprouting can be induced with therapies that promote longer distance and more robust axonal sprouting than stroke alone (Carmichael, 2016). In the cervical spinal cord, Nogo antagonists or inosine treatments (Chen et al., 2002; Zai et al., 2009, 2011; Lindau et al., 2014) induced reparative axonal sprouting within motor laminae of the spinal cord, resulting

in enhanced recovery (Overman et al., 2012; Wahl et al., 2014; Wahl and Schwab, 2014; Li et al., 2015). Pharmacogenetic studies of rats have identified a particular subset of 'side-switching' corticospinal fibers which extend from the uninjured cortex to re-innervate the stroke affected spinal cord resulting in improved motor function in the stroke impaired limb (Wahl et al., 2014). Anti-Nogo treatment enhances the density of these side switching fibers two fold and improves performance on single pellet reaching tasks by over 50 % (Wahl et al., 2014). When rewiring of these CST fibers is temporally blocked by viral gene transfer to express engineered Gi/o-coupled DREADD (designer receptor exclusively activated by designer drug) receptors (designer receptor exclusively activated by designer drug) in C5 and C6, rats suffered a decline in single pellet grasping performance of more than 35% (Wahl et al., 2014). The importance of midline-crossing corticospinal fibers in relation to functional outcomes has been demonstrated in various stroke and spinal cord injury models (Wiessner et al., 2003; Maier et al., 2006; Garcia-Alias et al., 2009; DeVetten et al., 2010; Reitmeir et al., 2011; Starkey et al., 2012). There is also strong evidence from spinal cord injury studies that supports the role of neurite outgrowth from interneurons in the spinal cord as a mechanism of spinal plasticity (Bareyre et al., 2004). Stroke induced reparative axonal sprouting appears to be an endogenous repair strategy in the CNS that plays a role in anatomical remodeling and spontaneous recovery from stroke.

Considering the limited capacity of the adult brain to form substantial new connections under physiological conditions, the extent of axonal sprouting after stroke is remarkable. This process is mediated by local guidance cues; factors associated with plasticity, neuroprotection and neurite outgrowth, found in the post stroke cortex are also expressed in spinal regions left deinnervated by stroke during a specific temporal window. Transient increase in protein expression of the neurotrophic factor BDNF at 3 days after stroke in the cervical spinal cord may

contribute to initiating structural plasticity in the spinal cord (Sist et al., 2014). In addition, stroke induces the expression of neurotrophin 3 (NT-3, a well-established neurotrophic factors found in motor neurons of the spinal cord, where it acts as a chemoattractant to guide regenerating axons and supports the growth and differentiation of new and existing neurons after injury (Yang et al., 1998; Alto et al., 2009; Sist et al., 2014) in the cervical spinal cord was significantly correlated with the expression of GAP-43 (Sist et al., 2014). GAP-43 is a marker of plasticity as it is highly expressed in the neural growth cones during development and axonal regeneration, is highly correlated with periods of heighted neurite outgrowth, and is crucial for axonal extension (Benowitz et al., 2000; Frey et al., 2000). Interestingly, GAP-43 is upregulated in the spinal cord 7-14 days after stroke but returns to baseline by 28 days, suggesting a finite period of structural plasticity at the level of the spinal cord that ends within one month of stroke onset (Sist et al., 2014). In addition, the extent of stroke injury (complete or partial) impacts on the expression levels of GAP-43, with complete injury of the forelimb somatosensory inducing greater GAP-43 expression (in both the amount of GAP-43 expressed and its spatial distribution) than did partial injury (Sist et al., 2014). Increased expression of axonal growth markers in larger strokes is likely a reflection of greater contralateral cortical axonal sprouting in these strokes as discussed earlier (Carmichael et al., 2017). The profile of GAP-43 expression indicates that forelimb motor cortex stroke induces a window of spinal plasticity in the affected spinal cord regions that correlates with injury severity but that this plasticity is finite (limited primarily to the first two weeks after injury).

Rehabilitation and plasticity

Rehabilitation is a key clinical component of post stroke recovery that is defined by the world

health organization as ‘behavioral modifications to reach and maintain optimal functioning in physical, intellectual, psychological and/or social domains following injury’ (WHO; 2001). Despite being the most successful intervention to enhance functional recovery after stroke, rehabilitative training is only effective during the finite period of enhanced plasticity which immediate follows stroke (Wahl and Schwab, 2014). Even with extensive and sustained rehabilitative training, sensorimotor recovery peaks by four weeks (in rodents) and three months (in humans) after stroke (Steinberg and Augustine, 1997; Krakauer et al., 2012; Wahl and Schwab, 2014). In animal studies, rehabilitative training initiated 4-7 days after ischemic injury is most effective for restoring motor performance (Nudo et al., 2006), and when rehabilitative training is initiated 14-28 days after injury functional outcomes are only modestly improved and animals retrained extensive functional deficits (Biernaskie et al., 2004). Even in rats that receive rehabilitative training beginning 4 days after stroke, extending the training periods beyond 28 days post stroke offers no functional benefit on motor tasks (Biernaskie et al., 2004). From these studies it is evident that once motor recovery has plateaued little functional improvement is gain from further rehabilitative training.

Interestingly, when the window of plasticity is enhanced immediately after stroke using anti-Nogo-A immunotherapy treatment for 2 weeks, animals have improved recovery of forelimb function one month after stroke on the single pellet reaching task (Wahl et al., 2014). However, when the same plasticity enhancing treatment is followed by 2 weeks of intense rehabilitative forelimb training (100 reaches per day in the single pellet reaching apparatus), animals showed a 40% improvement on single pellet reaching compared to animals given growth-promoting therapy or rehabilitative training alone (Wahl et al., 2014). In addition, animals receiving plasticity enhancement with rehabilitative training scored over 20% higher on a novel (Montoya

staircase test) skilled forelimb test (Wahl et al., 2014). This study provides clear evidence that enhancing the therapeutic window of plasticity can improve functional outcomes, however rehabilitative training is necessary to drive the formation of functional new connections induced by enhanced plasticity. Although interesting, enhancing plasticity during the early post stroke period does not offer a clinical benefit to the many stroke suffers left with remaining chronic deficits in the months and years after cortical injuries. New therapies targeted at reopening the window of plasticity must be explored to offer hope of reducing chronic deficits resulting from stroke.

Chronic deficits after stroke

Following brain and spinal cord injury, endogenous repair mechanisms have been found to promote axonal growth and neuroanatomical rewiring to compensate for and replace damaged synaptic connections (Carmichael, 2003). Additionally, gene and protein expression of factors essential to neural branching, survival, development and axonal growth are found to be elevated for a finite period in the adult brain and spinal cord following injury and can be further enhanced with rehabilitative training (Carmichael, 2003). However, recovery following stroke is limited and 94% of stroke suffers are left with chronic sensory and motor deficits (Carey et al., 1993). As such, stroke is the leading cause of acquired adult disability in the United States (Mozaffarian et al., 2015), costing the United States economy over 50 billion dollars each year for medical care for stroke survivors left with permanent disability (Ovbiagele et al., 2013). Loss or impairment of somatosensory motor function is one of the most prevalent complaints of stroke survivors (Klinger et al. 2012). Motor impairments of the contralateral upper limb are the most common functional deficit following stroke, with over 80% of subjects experiencing this acutely

(Cramer et al., 1997) and 60% having chronic upper limb disability (Dobkin, 2004).

The incomplete recovery that does occur after stroke occurs almost exclusively in the first few weeks following the initial injury: In rodent models, recovery plateaus around four weeks (Sist et al., 2014; Wahl et al., 2014; Figure 2.1 A), while human stroke survivors complete most of their recovery within the first three months after stroke (Steinberg and Augustine, 1997; Green, 2003). In humans, recovery of exploratory sensory tasks such as stereognosis, weight discrimination, or size evaluation showed good recovery in the first three months following stroke (Julkunen et al., 2005). However, after this period there are few functional improvements and some modalities including graphesthesia impairment and movement detection may even deteriorate after initial recovery (Julkunen et al., 2005). Even with extensive rehabilitation, recovery from stroke induce disability is limited and the optimal period for restoration of function appears to be finite. After this window, recovery stagnates, further rehabilitation is ineffective and stroke survivors are left with permanent sensorimotor disability (Lowry, 2010; Dimyan and Cohen, 2011). This limited recovery even with rehabilitation may result from the finite period of heightened plasticity that follows stroke.

CSPG's as inhibitors of plasticity

The extent of plasticity and structural reorganization following stroke is limited by factors in the brain and spinal cord that actively inhibit axonal outgrowth. In particular, the chondroitin sulfate proteoglycans (CSPGs) are prominent growth inhibiting factors that have been shown to be up-regulated in the CNS following stroke and spinal cord injury (Davies et al., 1997; Soleman et al., 2012). Elevated CSPG's levels in the extracellular matrix (ECM) after injury have been shown to reduce plasticity and prevent neurite out growth in the CNS (Asher et al., 1995; Fawcett et al.,

1989). Many of the inhibitory effects observed as a result of CSPG's are related to its highly electronegative structure which is composed of a central protein, O-linked to serine residues of multiple glucuronic acid, galactosamine and glycosaminoglycans (GAGs) covalently coupled to a protein core (GAGs, unbranched sugar chains consisting of repeating disaccharide units) (Crespo et al., 2007). This structure allows CSPGs to interact with neuronal receptors (Snow et al., 1994; Sivasakaran et al., 2004). Shen et al. (2009) demonstrated that the GAG units can bind the immunoglobin like domain of Receptor Protein Tyrosine Phosphate σ (RPTPσ) resulting in growth cone collapse. Furthermore, CSPG's can physically occlude growth promoting sites on the Schwann cell basal lamina of injured neurites (Zuo et al., 1998; McKeon et al., 1995) and have also been found to sequester neurotrophins (Crespo et al., 2007).

CSPG's are highly enriched in the glial scar where they are thought to be the main inhibitory molecule of axonal growth (Faulkner et al., 2004; Kawano et al., 2005). Davies et al. (1999) showed that transplanted dorsal root ganglion neurons could regrow axons through undamaged white matter of the CNS. However, when these growing axons reached a CSPG rich glial scar their growth was terminated. Further, Kawano et al. (2005) demonstrated that CSPG digestion can prevent fibrotic scar formation in the nigrostriatal tract after it is severed. Anti-inflammatories administered to reduce GFAP scarring after stroke also promote serotonergic re-innervation of deinnervated CNS territory (Wang et al., 2010). Finally, blocking glial growth inhibitors stimulates longer distance axonal sprouting after stroke enhancing reparative axonal outgrowth from the intact CST into the deinnervated cervical spinal cord (Carmichael et al. 2016).

Modulating neuroplasticity by CSPG cleavage

Digestion of CSPG's with the bacterial enzyme chondroitinase ABC (ChABC) has been shown to promote functional recovery after CNS injury. However, the mechanisms by which CSPG digestion promotes and enhances recovery are still not fully understood (Deepa et al., 2002, 2004). ChABC is an enzyme of the lyases family which specifically catalyzes the eliminative degradation of polysaccharides containing (1-4)-β-D-hexosaminyl and (1-3)-β-D-glucuronosyl or (1-3)-α-L-iduronosyl linkages to disaccharides containing 4-deoxy-β-D-gluc-4-enuronosyl groups. Put more simply, ChABC liberates the CS-GAG chains from the CSPG core protein thereby preventing CSPG–matrix glycoprotein interactions (Yamagata et al., 1968). By cleaving GAG chains from the protein core, ChABC removes the barricade of inhibitory ECM proteins which prevent axonal spouting, collapse growth cones and sequester trophic factors. ChABC can therefore overcome post injury inhibitory environments by enhancing structural plasticity.

A number of studies in the central and peripheral nervous systems have shown that ChABC digestion of CSPGs results in improved functional recovery after injury, enhances neurite outgrowth and augments a state of plasticity that was limited by CSPGs (Moon et al., 2001; Bradbury et al., 2002; Massey et al., 2006; Garcia-Alias et al., 2009; Alilain et al., 2011). Interestingly, relatively few studies have looked at delayed administration of ChABC in chronic injury as a means to re-open a window of plasticity. Shinozaski et al. (2016) noted that there are 50 times more patients with chronic-phase spinal cord injury than there are acute patients, yet almost all research into spinal cord injury is directed at the acute phase intervention. Notably, ChABC delivered to mice with chronic spinal cord injury improved functional outcomes but only when paired with intensive treadmill training (Shinozaski et al., 2016). Thus, the therapeutic potential of ChABC in spinal injury is extensive as ChABC appears to reopening a window of

plasticity and allow for new anatomical connections even in chronic injury. However, this plasticity requires guidance to form meaningful functional connections, and rehabilitation appears to be an essential mediator of ChABC induced recovery (Tom et al., 2009, Carter et al., 2011, García-Alías and Fawcett, 2012; Zhao and Fawcett, 2013; Shinozaski et al., 2016).

CSPG cleavage and Glia

Recent findings suggest that ChABC may attenuate astrogliosis and inflammation around the site of CNS injury (Karimi-Abdolrezaee et al., 2012). Following compressive spinal cord injury, ChABC administration was found to reduce the generation of new astrocytes whilst promoting astrocytic differentiation into an oligodendroglial lineage (Karimi-Abdolrezaee et al., 2012). This may be favourable for recovery as oligodendrocytes are necessary for re-myelination and glial population shifts that result in a reduction of reactive scar producing astrocytes are beneficial. ChABC enzymatic digestion of CSPG rich glial scar results in the production of sulfated disaccharide stubs, which are highly immunogenic neo-epitopes that signal phagocytic cleanup and further reduction of the glial scar (Glant et al., 1998; Ebert et al., 2008).

Microglia are also impacted by ChABC digestion of glial scars, however, there are conflicting views on how microglia respond to ChABC and its cleavage products. Some studies have suggested that ChABC may act to reduce microglial infiltration at the injury site therefore reducing scar formation (Rolls et al., 2008; Karimi-Abdolrezaee et al., 2012). However, there is also strong evidence that ChABC treatment promotes microglia activation (Glant et al., 1998; Ebert et al., 2008). ChABC cleavage stubs have been found to stimulate activated microglia to take on a novel regulatory neuroprotective phenotype (Rolls et al., 2005, 2008), shifting microglia from the M1 to the M2 phenotype. Further *in vitro* studies have confirmed that

microglia activated by ChABC cleaved CSPG disaccharides possess an increased capacity for phagocytosis whilst lacking cytotoxic functional properties such as NO secretion (Ebert at al., 2008). Moreover, microglia treated with cleaved CSPG disaccharides may be neuroprotective as they do not induce apoptosis of cultured photoreceptor cells but rather rescued them from IFN-γ-induced apoptosis (Ebert at al., 2008). Thus, the effect of ChABC digestion of CSPGs on different glial populations is diverse and likely to differ over the course of recovery.

Modulation of CSPG inhibition – An alternative to digestion

Although it is well accepted that CSPG's are potent inhibitors of post injury plasticity, reducing axonal sprouting and neurite growth, they also play a fundamental role in modulating immune responses and proliferation of progenitor cells after injury (Karimi-Abdolrezaee et al., 2012). During development, CSPGs have been shown to play a fundamental role in encouraging neuronal structural plasticity and pathfinding (Balmer et al., 2009; Fongmoon et al., 2007; Kowok et al., 2012) and in the presentation of growth factors (Galtrey and Fawcett, 2007). It is well established that ChABC abolishes post injury CSPG inhibition of neurite outgrowth. However, ChABC may also diminish the beneficial roles of CSPGs in regulating immune responses, stabilizing developing synapses and providing structural support for extending axons (Rolls et al., 2008). Therefore, new therapeutic alternatives which seek to modify CSPG function and restrict their role in the neurite growth inhibition are being investigated (Pavelive et al., 2016). One promising candidate molecule is pleiotrophin (PTN), an 18 KD secreted molecule with a wide range of biological functions. Originally identified in 1989 as a heparin binding molecule found in the bovine uterus (Milner et al., 1989), PTN is also referred to in the literature as heparin-affinity regulatory peptide (HARP), heparin binding- growth associated molecule

(HB-GAM), Heparin binding growth factor 8 (HBGF-8), osteoblast specific protein-1 and p18 (Jin et al., 2009).

Pleiotrophin structure & signaling

The structure of PTN is essential to the diversity of biological roles it plays throughout development and in injured perinatal tissue. PTN secretion is highly regulated both spatially and temporally, as only specific cell types in each microenvironment produce PTN at very specific time points in both development and following injury (Deuel et al., 2002). PTN is composed of 168 amino acids, with the functional protein consisting of 136 amino acids and 32 terminal amino acids acting as a recognition signal for secretion. PTN contains two beta sheet domains, each composed of three anti-parallel beta strands, the sheets are connected by a flexible linker (Kilpelaeinen et al., 2000). Sequencing experiments have demonstrated that the beta sheets are homologous with thrombospondin type 1 repeat sequence (TSR-1), which is common in extracellular proteins as this domain mediates cell-to-cell and cell-to-extracellular matrix interactions. In the case of PTN, the TSR domain serves to allow specific binding to heparin sulfate proteoglycans of the extracellular matrix (Raulo et al., 2005). The TSR-1 repeat in the beta sheet is specific for heparin, while TSR-1 repeats found in the C-terminus (aa 65-97) also promote PTN binding of heparin it additionally regulates the mitogenic, tumorigenic, angiogenic and neurotrophic actives of PTN (Hamma-Kourbali et al., 2008). PTN is considered a proto-oncogene as amino acid residues 41-64 contain a domain essential for transformation of NIH 3T3 cells (Zhang et al., 2006).

Interestingly, PTN is inactive after secretion, and it is only once PTN has bound heparin sulfate proteoglycan in the ECM that it becomes active (Kinnunen et al., 1996). Once bound to

heparin, PTN can bind various transmembrane receptors to induce a diverse set in intercellular cascades leading to various biological effects. PTN is known to bind all members of the transmembrane tyrosine phosphate receptor (RPTP) family (Pariser et al., 2005a). PTN binding to the RPTPβ/ζ results in decreased binding affinity of beta-catenin for E-cadherin and therefore a disruption of the cytoskeleton. PTN further destabilizes the cytoskeleton as it acts through beta-adducin and Fyn (Pariser et al., 2005b). PTN disruption of the cytoskeleton via interaction with the RPTPβ/ζ is thought to account for the role of PTN in cell adhesion, proliferation and transformation.

PTN also acts on the anaplastic lymphoma kinase (ALK) receptor, a well-established transmembrane growth factor receptor. While ALK alone is pro-apoptotic, in the presence of the PTN ligand the kinase activity becomes intrinsically active and it promotes proliferation and is anti-apoptotic (Mourali et al., 2006). PTN has also been found to bind N-syndecan, which is thought to contribute to the effect of PTN on neurite outgrowth and guidance when PTN binds to N-syndecan on embryonic day 9 in the developing axonal tracts (Kinnunen et al., 1998). Neurite outgrowth induced by N-syndecan binding to PTN can only occur in the presence of heparin sulfate chain (Kinnunen et al., 1998). One other receptor has been identified to interact with PTN, Low-density lipoprotein receptor related protein-5, and although the exact mechanism is not understood this interaction may account for the angiogenic effect of PTN in tumor tissue (Jin et al., 2009).

Pleiotrophin in CNS development

PTN expression in the CNS peaks at 1-2 weeks after birth in the rat. During this time PTN is found primarily in radial glial processes in the developing rat cerebral cortex (Merenmies and

Rauvala, 1990). During development, PTN interacts with a varieties of factors to enhance neurite outgrowth and promoter synaptogenesis. Expression of neuroglycan C, a CSPG which is up regulated in the CNS around post-natal week 2-3 (Nakanishi et al., 2010) is associated with enhanced dendritic branching and increased complexity of dendritic spines. Neuroglycan C therefore is an important factor in normal CNS development of neurites and synapses. It has been well established that Neuroglycan C must bind with Midkine in order to be activated (Muramatsu, 2002). However, it has more recently been shown that PTN can also bind Neuroglycan C, inducing neuritogenesis and synaptogenesis (Nakanishi et al., 2010).

Bromodomain-containing protein 2 (Brd2) is a chromatin family adaptor that is essential in cell-cycle-stimulation and neuronal development (Garcia-Gutierrez et al., 2014). Recently, PTN has been characterized as antagonist of Brd2 (Garcia-Gutierrez et al., 2014). PTN destabilizes the interaction of Brd2 with chromatin, resulting in enhanced neuronal differentiation, which is thought to be particularly important for the spinal cord neurogenesis and neural crest migration (Garcia-Gutierrez et al., 2014). PTN has also been found to act through both ALK and RPTPβ/ζ pathway to induce an upregulation of GAP-43 in the developing mouse at embryonic day 14.5 (Yanagisawa et al., 2010).

Pleiotrophin after peripheral nerve injury

PTN is found in the developing peripheral nervous system, however the role of PTN in the mature system is unclear (Mitsiadis et al., 1995). There is now strong evidence that PTN plays a key role in the repair of peripheral nerves after injury. Following nerve injury, PTN is not upregulated in the injured axons themselves, but rather in the Schwann cells, epithelial cells and macrophages surrounding the site of injury (Blondet et al., 2005). *In vitro* experiments suggest

that PTN may improve recovery from peripheral never injury, since PTN incubation improves outgrowth of injured nerves and promotes the formation of neuromuscular junctions in cell culture models (Szabat and Rauvala, 1996). However, one *in vivo* study suggested that PTN may impair the reinnervation of muscle by crushed nerves, as PTN treatment decreased Schwann cell density and impaired macrophage activity, resulting in a failure of the gastrocnemius muscle to recover contractile strength (Blondet et al., 2006). Other studies have found contrasting results, as adult sciatic nerve grafts treated *in vivo* with cells producing high levels of PTN survived much better than nerve grafts not treated with PTN producing cells (Jin et al., 2009). PTN was found to induce a dramatic increase in the number of regenerating myelinated axons (10x greater) at sites even 12 mm distal to the grafts, and there was a 33% greater restoration of compound motor action potentials in the sciatic nerve-innervated foot muscles in animals treated with PTN generating cells compared to animals treated with a control (Mi et al., 2007). It appears as though the mechanism for this recovery comes via the ALK receptor interaction, as blocking the ALK receptor causes a loss of the neurotrophic effect that was not seen other known PTN transmembrane receptors were blocked (Mi et al., 2007).

Pleiotrophin in neurological injury and degeneration

In the perinatal brain, PTN is expressed in both glial cells and neural cells. Following chemically induced seizure (pentylenetetrazole) in rat, PTN is upregulated in the neurons of the hippocampus, piriform cortex and parietal cortex (Wanaka et al., 1993). PTN expression was first discovered in the hippocampus during these seizure studies (González-Castillo et al., 2014) and lead to studies which determined that high frequency stimulation, which induced long term potentiation (LTP) in CA1 region of the hippocampus also induced PTN

upregulation (Amet et al., 2001). These studies indicated a possible role for PTN in LTP (Amet et al., 2001). Later studies demonstrated that hippocampal slices from PTN deficient mice exhibit a lowered threshold for induction of LTP (Amet et al., 2001) and that LTP was diminished in mice that overexpressed PTN (Pavlov et al., 2002) possibly by enhanced GABAergic inhibition in CA1 (Pavlov et al., 2006). PTN is a now being studied in Alzheimer disease patients, as changes in PTN expression may play a role in the pathophysiology of neurodegenerative diseases (Xu et al., 2014). Since many early studies of PTN focused on defining its role and expression in the hippocampus, the first studies looking at changes in PTN in response to ischemic cortical injury were conducted in the hippocampus as well. Takeda et al. (1995) were the first to look at ischemia induced changes in PTN regulation following transient forebrain ischemia. They found a 2-fold increases in PTN expression in the CA1 subfield where selective neuronal losses were detected following ischemic injury and determined (based on immunochemistry studies) that most of the PTN expressing cells were reactive astrocytes (Takeda et al., 1995).

Later studies of PTN expression after stroke expanded on the work of Takeda et al., (1995) to look at changes in PTN expression beyond the hippocampus (Yeh et al., 1998). Yeh et al., (1998) induced focal ischemic stroke in rats using the MCA ligation technique and found that 3 days after injury, PTN gene expression was significantly increased in activated macrophages, astrocytes, and endothelial cells, but this was limited to in areas of developing neovasculature. In contrast, they found that PTN gene expression was significantly decreased in cortical neurons 6 and 24 hours after injury and was completely undetectable in degenerating neurons 3 days post stroke (Yeh et al., 1998). More recent studies have focused on the role of PTN in mediating post stroke plasticity. The neuropeptide cocaine-and amphetamine-regulated transcript (CART) has

been found to play a significant neuroprotective role after cortical ischemic injury and the reperfusion injury which follows (Wang et al. 2014). In culture, CART reduces oxygen and glucose deprivation injury, resulting in less neural apoptosis and offers further neural protection by increasing expression of GAP-43, therefore promoting neurite outgrowth (Wang et al. 2014). Interestingly, the neuroprotective effect of CART is entirely dependent on PTN, when PTN is knocked down CART is completely ineffective indicating that the neuroprotective effects of some neuropeptides are mediated through a PTN pathway (Wang et al., 2014).

In vitro PTN offers selective neuroprotective to dopaminergic neurons (Hida et al., 2003). More recently, overexpression of PTN *in vivo* using viral vectors has demonstrate that PTN provides neuroprotection for tyrosine hydrolase or dopaminergic neurons in both the striatonigral and nigrostriatal pathways following 6-hydroxydopamine toxic insult (to mimic the dopaminergic loss in Parkinson's disease pathology) (Gombash et al., 2014). Not only does overexpression of PTN have a neurotrophic effect, it reverses functional deficits in forepaw use as a result of nigrostriatal system loss, suggesting a role for PTN in Parkinson's diseases treatment (Gombash et al., 2014). Using a prick injury model in the cerebral cortex, Paveliev et al. (2016) recently demonstrated that the injection of PTN into the site of cortical injury induced a robust regenerative response injured cortical neurons. In particular, they found PTN injection improved density of dendritic tufts and the number apical dendrite per neuron (cortical layer 5) 2-3 weeks post injury, with these effects limited to the injured area. Thus, PTN plays an important role in mediating neuroprotection following neurological injury and may offer protection against neurodegeneration.

Pleiotrophin in spinal cord injury

PTN expression in the uninjured perinatal spinal cord is thought to be exclusively from neural cells and not from cells of glial origins as seen in the brain (Wang et al., 2004). However, after spinal cord injury, PTN production is evident in reactive astrocytes and oligodendrocytes, as the spinal cord reverts to a state of glial PTN production which mimics the development stage (Wang et al., 2004). It should be noted the PTN is also produced by injured neurons in the spinal cord, indicating a possible innate mechanism for neural repair following injury (Wang et al., 2004). Cell culture experiments reveal that PTN induces neurite outgrowth when plated on CSPGs (Paveliev et al., 2016), while *in vivo* studies demonstrated that PTN increases axonal regeneration in the lesioned spinal cord (Mi et al., 2007). Interestingly, PTN upregulation in the spinal cord is associated with reduced chronic pain following peripheral nerve injury (Ezquerra et al., 2008). This result is specific to PTN, as upregulation in the spinal cord and dorsal root ganglia of midkine, a fellow growth promoting heparin binding molecule, does not induce a reduction in chronic pain in after peripheral never injury (Ezquerra et al., 2008).

In spinal cord explant cultures, PTN greatly increase motor neuron outgrowth and axons growing towards a PTN source from mini-ventral rootlets (Mi et al., 2007). Further, when these explant cultures are treated with glutamate transport inhibitors to induce glutamate toxicity, PTN is neuroprotective against excitotoxic motor neuron death (Mi et al., 2007). It is thought that the protective role of PTN in the spinal cord is mediated through the ALK receptor, as blocking this receptor leads to not only a loss of the PTN protective effect on glutamate toxicity but also to a reduction in the length of motor neurons and primary spinal motor neurite outgrowth (Mi et al., 2007). Other mechanism for PTN's protective effect in the spinal cord after injury may result from interacts with growth inhibiting CSPGs. CSPGs are highly upregulated following CNS

injury and create a structural barrier to regeneration. However, PTN binding of CSPGs facilities PTN activation of glypican-2 cell surface receptors which promote neurite outgrowth through downstream pathways (Paveliev et al., 2016). In addition, PTN inhibits the binding of CSPG to the growth inhibitory PTPRG (Paveliev et al., 2016). In a dorso-lateral spinal transection injury model where PTN is administered at the time of injury, PTN improved the number of number of axons entering the injury site for the caudal side and the number of axons traversing the injury site (Paveliev et al., 2016). Not only did PTN improve the number of axons traversing the injury site but multiple imaging session revealed that PTN treated axons grew significantly faster than untreated counter parts. The effects of PTN became evident 7 days after injection and PTN induced axon sprouting remained evident at 28 days post injury. Paveliev et al. (2016) hypothesized that PTN may play a crucial role in interactions between regenerating axons and pioneer axons which have already transversed the spinal cord lesion, which may account for the sustained effects of PTN. Thus, PTN is secreted by a multitude of cells types and interacts with many receptors and extracellular matrix components. Importantly, PTN expression in the spinal cord appears to be neuroprotective and growth promoting following nervous system injury.

Pleiotrophin in microglia and cytokine regulation

Following ischemia/reperfusion injury, expression of PTN is induced by injured microglia (Miao et al., 2012). Increased expression of PTN promotes microglia proliferation as PTN increases the phosphorylation of extracellular signal-regulated kinase ERK 1/2, leading to enhanced G1 to S phase transition in microglia cells. Interestingly, when ERK 1/2 phosphorylation is blocked with the inhibitor U0126, the action of PTN in propagating microglia proliferation is lost (Miao et al., 2012). The action of PTN is not limited to microglia proliferation, as it has also been

shown to induces changes in microglia cytokine expression. PTN has been shown to induce the microglial release of growth promoting factors including BDNF, ciliary neurotrophic factor (CNTF) and nerve growth factor (NGF) (Miao et al., 2012). PTN stimulated release of growth factors may account for some of the pro-plasticity role it plays after injury in the CNS. Interestingly, PTN has not been shown to induce microglia expression of pro-inflammatory factors in from microglia such as TNF-α, IL-1β and iNOS, despite the fact that it has been demonstrated to induce the expression of inflammatory cytokines such as TNF-α, IL-1β and IL-6 in quiescent human peripheral blood mononuclear cells (Achour et al., 2008). More studies are need to determine the effect of PTN on microglia cytokine expression and these studies should be expanded to include the role of PTN in cytokine expression of mixed glial populations.

Thesis outline and aims

Chapter 2: Reopening the critical period for stroke recovery by augmenting spinal plasticity

Recovery following stroke occurs almost entirely in the first weeks post injury. Moreover, the efficacy of rehabilitative training is limited beyond this narrow time frame. Sprouting of spared corticospinal tract axons in the spinal cord makes a significant contribution to sensorimotor recovery, but this structural plasticity is also limited to the first few weeks after stroke, suggesting that the closure of this window for spinal plasticity may regulate functional recovery.

Here, we tested the hypothesis that inducing plasticity in the spinal cord during chronic stroke could induce a second wave of recovery from sensorimotor impairment. We potentiated spinal plasticity during chronic stroke, weeks after the initial ischemic injury, in rats via microinjections of chondroitinase ABC into the grey matter of the cervical spinal cord

administered 28 days after photothrombotic stroke lesioning the forelimb sensorimotor cortex. The efficacy of spinal therapy to improve recovery from stroke was assessed using a battery of sensorimotor tests (including assessment of skilled reaching, forelimb use preference, and mechanical sensitivity) to determine if ChABC treatment at the level of the spinal cord could improve chronic sensory motor deficits after recovery had plateaued. We included measures of mechanical sensitivity to determine if our spinal treatment would induce aberrant rewiring of spinal circuits, which is associated with chronic pain.

To assess anatomical changes of the corticospinal tract originating in peri-infarct cortex anterograde neuronal tract tracers injected slightly medial to the infarct were used. Counting the number of tracer labeled spared fibers in tissue slice of cervical spinal cord (C4/C5) allowed CST integrity to be assessed and compared between chronic stroke animals with and without ChABC treatment. To determine if ChABC treatment promoted axonal sprouting measurements of the length and number of spared fibers branching into the deinnervated grey matter of the spinal cord normalized to the number of labelled fibers in the CST were compared between stroke animals which received ChABC or control treatment.

To model moderate and intense rehabilitative training and determine whether ChABC could make limited training more effective and/or remove plateaus that occur with continuous training. Rats were divided into groups that received either moderate task specific rehabilitative training (100 reaching attempts twice per day in the single pellet reaching apparatus) or high intensity training (1000 continuous reaches reaching attempts over 45 minutes twice per day) starting one day after injection with ChABC or control (29 days post-stroke) and extending to 56 days post stroke. Another experimental paradigm was designed to model permanent disability due to stroke even after extensive rehabilitation. Ideally, rehabilitative motor training is initiated

early after stroke, as early training has been shown to far exceed the benefits of delayed therapy in restoring behavioral performance Murphy and Corbett, 2009; Langhorne et al., 2010; Krakauer et al., 2012; Tennant, 2014). Even when rehabilitative training is continued for extended periods after injury into chronic stroke, it loses efficacy with time and most patients remain disabled. To model this scenario, we delivered moderate task specific training at 3 days post stroke which continued for 56 days.

The efficacy of spinal therapy to improve recovery from stroke when combined with different rehabilitation paradigms was assessed using a battery of sensorimotor tests (including assessment of skilled reaching, forelimb use preference, and mechanical sensitivity) to determine which rehabilitative strategy paired with ChABC treatment could most improve chronic sensory motor deficits after recovery had plateaued. We again included measures of mechanical sensitivity to determine if our spinal treatment when paired with various rehabilitation paradigms would induce aberrant rewiring of spinal circuits, which is associated with chronic pain.

We also assess anatomical changes of the corticospinal tract originating in peri-infarct cortex using anterograde neuronal tract tracers in each rehabilitative training group. Quantification of tracers from tissue slice of cervical spinal cord (C4/C5) allowed CST integrity to be assessed and compared between ChABC treated animals of differing rehabilitative paradigms. The length of spared fibers branching into the deinnervated grey matter of the spinal cord were compared between stroke animals which received ChABC or control treatment. This revealed which rehabilitative strategy in combination with ChABC treatment induced the greatest axonal sprouting.

Since the serotonergic system has been reported to be involved in compensatory mechanisms and recovery that follows spinal injury, and because serotonin has a crucial role in

regulating the excitability of spinal motor neurons (Hounsgaard et al., 1988) we evaluated changes in serotonergic fiber distribution in the grey matter of the cervical spinal cord at the C4 level 68 days after injury. Measures of serotonergic fiber density compared between ChABC treated animal, ChABC treated animals in different experimental paradigms and Sham animals help to elucidate changes in spinal serotonergic innervation under different treatment paradigms.

This study was designed to determine if removal of growth inhibitory CSPGs in the spinal cord of rats during chronic stroke combined with various rehabilitative training paradigms could induce a second wave of structural plasticity as measured by anatomical and functional outcomes. This study will provide value insight into treatment therapy and optimal rehabilitation strategies for the millions of individuals living permeant disability as a result of stroke.

Chapter 3: *In vitro* cellular effects of chondroitinase ABC produced cleavage stubs

Digestion of CSPGs with the bacterial enzyme chondroitinase ABC (ChABC) has been shown to promote functional recovery after CNS injury (Moon et al., 2001; Soleman et al. 2012). Moreover, ChABC treatment provides neuroprotection against both primary and secondary brain injury after stroke enhancing neural survival, augmenting axonal growth, enriching synaptic plasticity and thereby promoting improved neurological function (Chen at al. 2014). Despite many studies on ChABC treatment after CNS injury it is still unclear how CSPG digestion promotes and enhances recovery (Deepa et al., 2002, 2004).

In this study, we first sought to investigate the direct regulation of neurite outgrowth by CSPG cleavage stubs, which are sulfated disaccharide chains produced by ChABC enzymatic digestion of CSPGs. Specifically, we used a human neuroblastoma cell line (SH-SY5Y) plated on growth inhibitory CSPG or growth permissive laminin matrices and directly applied digestion

product ‘stubs’ (C-0-S, C-4-S or C-6-S) to the cell culture media and assessed neurite growth. In addition, we repeated the study but we incorporated the stubs into the matrices on which SH-SY5Y cells were growing and again looked for augmentation in neurite outgrowth. This experimental design was chosen as it allowed us to assess the effect of free and bound CSPGs on neurite outgrowth and to determine if these effects are CSPG dependent.

Second, we investigated the role of CSPG cleavage stubs in modulating the microglial immune response. To determine this, we exposed microglia to cleavage stubs, then we harvested the immune factors produced by the treated microglia and introduced them to SH-SY5Y neuronal cultures plated on CSPG or laminin to determine if microglia release factors which induce neurite outgrowth in the presence or absence of CSPGs. We repeated these experiments with microglia activated with a biological activator (IFN-γ) to determine if activated microglia produce different factors which alter neurite outgrowth and if that effect was CSPG dependent.

In addition, we assayed the release of the well-established anti-inflammatory molecules including interleukin-10 (IL-10) and BDNF and pro-inflammatory molecules including nitric oxide (NO), Tumor necrosis factor-α (TNF-α), cytokines interleukin-6 (IL-6) and interleukin-1β (IL-1β) by CSPG stub treated microglia which were left unstimulated or biologically activated (IFN-γ). This allowed us to elucidate changes in cytokine profiles on activated and unstimulated microglia in response to CSPG cleavage stubs.

Third, we expanded our study to establish the effect of CSPG cleavage stubs on mixed glial population that consist of not only microglia but astrocytes and oligodendrocytes as well (de Vellis and Cole, 2012). We used different combinations of biological activation to mimic primary injury in the CNS following by secondary inflammatory injury and again assayed for different inflammatory and anti-inflammatory factors. This study allowed us to determine the

effect of CSPG cleavage stubs on the cytokine release profile of mixed glial populations at different stages of biological activation to mimic primary and secondary inflammation. This study was designed to identify the effects of CSPG cleavage stubs on the outgrowth of neurites and the cytokine release profiles of isolated microglia and mixed glial populations.

Chapter 4: *In vitro* studies of pleiotrophin as a modulator of chondroitin sulfate proteoglycan mediated growth inhibition and neuroinflammation

In CNS injury, such as ischemic stroke, inhibitory extracellular matrix compounds chondroitin sulphate proteoglycans (CSPGs) are released by glial cells surrounding the injury (Fawcett and Asher, 1999). The deposition of CSPGs has been shown to decrease axonal growth and impair recovery (Fawcett and Asher, 1999). Pleiotrophin (PTN) is a growth factor and cytokine that is upregulated in the central nervous system (CNS) during periods of development and injury (Gonzales-Castillo et al., 2015), PTN has been shown to bind to CSPGs and promote neuritogenesis (Miller et al., 2015). However, the interaction between PTN and many cells in the CNS is not fully understood and little is known about the effect of PTN on expression profiles of cytokines from glia and microglia. This study investigated the effects of exogenous PTN on both neurite growth and glial responses *in vitro*.

In this study, we first sought to investigate the direct regulation of neurite outgrowth by PTN at various concentrations. Specifically, we used a human neuroblastoma cell line (SH-SY5Y) plated on growth inhibitory CSPG or growth permissive laminin matrices and directly applied PTN at various concentrations to the cell culture media and assessed neurite growth. This allowed us to establish if PTN alone could improve neurite outgrowth in human neuroblastoma cells lines and if the effect of PTN on neurite outgrowth is dependent on CSPGs. In addition, we

repeated the study on B35 rat neuroblastoma cells and compared the results those found in SH-SY5Y human neuroblastoma cells to determine if the effects of PTN were cell line or species specific.

Second we investigated the role of PTN in modulating the microglial immune response. We exposed microglia to PTN, then harevested the immune factors produced by the treated microglia and introduced them to SH-SY5Y neuronal cultures to determine if microglia release factors which induce neurite outgrowth following PTN treatment. This experiment was repeated with biologically activated microglia to determine if PTN induced the release of factors which improved neurite outgrowth from inflammatory microglia. In addition, the experiment was repeated in B35 cells to ensure the effects of PTN were not cell line specific. These experiments allowed us to determine if PTN induced the release of factors from stimulated or unstimulated microglia which improved neurite outgrowth in the presence or absence of CSPGs. We also assayed the release of the well-established anti-inflammatory molecules including IL-10 and BDNF and pro-inflammatory molecules including NO, TNF-α, IL-6 and IL-1β from PTN treated microglia which were left unstimulated or biologically activated (IFN-γ). This allowed us to elucidate changes in cytokine profiles on activated and unstimulated microglia in response to PTN.

Third, we expanded our study to establish the effect of PTN on mixed glial population that consist of not only microglia but astrocytes and oligodendrocytes as well (de Vellis and Cole, 2012). We used different combinations of biological activation to mimic primary injury in the CNS following by secondary inflammatory injury and again assayed for different inflammatory and anti-inflammatory factors. This study was designed to identify the effects of PTN on the outgrowth of neurites and the cytokine release profiles of isolated microglia and

mixed glial populations. Our data allowed us to determine the effect of PTN on the cytokine release profile of mixed glial populations at different stages of biological activation which mimic primary and secondary inflammation.

This study was designed to identify the effects of PTN on the outgrowth of neurites and the cytokine release profiles of isolated microglia and mixed glial populations in different states of biological activation.

Chapter 5: Augmenting spinal plasticity and recovery from stroke with intraspinal pleiotrophin *in vivo*

During development, PTN is an important axonal guidance molecule for CST axons originating in the motor cortex (Rauvala and Peng, 1998; Yanagisawa et al., 2010). Degeneration of these CST projections follow stroke, and this degeneration as well as secondary damage that follows at the level of the spinal cord contribute to the sensorimotor impairment after stroke (Weishaupt et al., 2013). Inducing plasticity using PTN in damaged sensorimotor spinal circuits may therefore facilitate the formation of new sensorimotor circuits or repair of spared CST projections and thereby promote recovery (Moon et al., 2001; Soleman et al., 2012). Here, we are the first to investigate if PTN administration into the spinal cord deinnervated by cortical stroke can improve functional recovery.

First, we induced a photothrombotic lesion in the forelimb sensorimotor cortex of rats to establish sensorimotor impairment in the forelimb. PTN microinjection into the deinnervated cervical spinal cord (C4/C5) was performed 7 days post injury to potentiate regenerative processes in injured sensorimotor spinal circuits. Skilled reaching, forelimb use asymmetry and mechanical sensitivity were measured following stroke and treatment to determine if PTN

injection had functional consequences on stroke sensory motor recovery. We included measures of mechanical sensitivity to determine if our spinal treatment would induce aberrant rewiring of spinal circuits, which is associated with chronic pain.

Second, we wanted to assess changes in axonal outgrowth since recent studies have identified PTN as a potent growth promoter in the CNS and PTN has been shown to increase neurite out growth in culture studies (Paveliev et al., 2016). We used GAP-43 to measure active axonal growth and determine if PTN could induce increased axonal outgrowth following cortical injury in the spinal cord (Seo et al., 2017).

Third, we wanted to evaluate changes in serotonergic fiber distribution in the grey matter of the cervical spinal cord. Standard immunochemical protocols were used to fluorescently label serotoninergic fibers in the cervical spinal cord which allowed us to determine if PTN treatment promotes alterations in serotonergic density in the spinal cord after cortical stroke.

Finally, tissue culture and explant studies have shown PTN to be particular important in motor neuron survival and demonstrated that PTN can protect motor neurons when they lose target derived growth factors (Mi et al., 2007). Strokes which damage the motor cortex disrupt the CST input to motor neurons which may result in a loss of motor neuron density as seen in other CNS injury models (Wu et al., 2016). Thus, we wanted to test if PTN could prevent a loss of motor neurons in C4/C5 which are typically deinnervated after cortical stroke focused on the forelimb somatosensory motor cortex. We confirmed the presence of motor neurons by labeling for choline acetyltransferase (ChAT) and counted all ChAT positive cells in the ipsilesional ventral horns. To further determine the effect of stroke and PTN treatment on motor neuron populations in the cervical spinal cord, we examined the morphology of the motor neurons in the ventral horn. There is evidence that motor neurons have a reduced sized when injured (Wu et al.,

2016) and counts of motor neurons do not detect these changes in motor neurons morphology. The average area of the motor neurons were evaluated for each animal on both the ipsilesional and contralesional sides of the spinal cord.

This study aimed to identify anatomical and functional changes induced by spinal PTN treatment 7 days after stroke. We investigated the role of PTN in promoting axonal outgrowth, restoring serotonergic fiber in the deinnervated spinal cord and sustaining motor neuron density and morphology in the stroke effected grey matter of ventral horn.

Chapter 2:

Reopening the critical period for stroke recovery by augmenting spinal plasticity

Introduction

Stroke is a leading cause of permanent adult disability worldwide. While the central nervous system (CNS) possesses endogenous mechanisms for plasticity within spared circuits that enable partial recovery of function lost to brain damage (Murphy and Corbett, 2009; Winship and Murphy, 2009; Overman and Carmichael, 2014), functional recovery after stroke is limited. Over 60% of stroke survivors (Dobkin, 2008) are left with persistent disability including partial paralysis, muscle weakness and impaired speech that drastically reduce quality of life by limiting independence and social participation (Kessner et al., 2016). The incomplete recovery that does occur after stroke occurs almost exclusively in the first few weeks following the initial injury: In rodent models, recovery plateaus around four weeks (Sist et al., 2014; Wahl and Schwab, 2014; Figure 2.1 A), while human stroke survivors complete most of their recovery within the first three months after stroke (Steinberg and Augustine, 1997; Green, 2003). In stroke patients and animal models, the type and timing of rehabilitative training is a principal determinant of the degree of recovery (Krakauer et al., 2012; Wahl and Schwab, 2014). However, even with extensive rehabilitation, recovery from stroke induce disability is limited. Optimal paradigms for rehabilitation are not well defined for patients and the most efficacious strategies are often not available to patients or patients are unable to fully perform these paradigms in the days and weeks following the stroke (Lowry, 2010). Thus, the optimal period for restoration of function appears to be finite and after this window recovery stagnates, further rehabilitation is ineffective and stroke survivors are left with permanent sensorimotor disability (Dimyan and Cohen, 2011).

As plasticity of the CNS underlies recovery from stroke, extending or augmenting the plasticity of spared neural circuits can reduce stroke-induced sensorimotor impairment. Experimental plasticity-enhancing treatments are most effective in driving recovery when

delivered early after injury and accompanied by rehabilitative training (Van den Brand et al., 2012; Hara, 2015; Jones and Adkins, 2015). Notably, plasticity of the corticospinal tract (CST) in the spinal cord makes a significant contribution to recovery from stroke-induced sensorimotor impairment (Ueno et al., 2012; Wahl et al., 2014; Wahl and Schwab, 2014; Van den Brand et al., 2012; Silasi and Murphy, 2014). However, the spinal plasticity elicited by cortical stroke has a limited temporal window that correlates with periods of sensorimotor recovery (Sist et al., 2014; Kessner et al., 2016; Figure 2.1 A and B). Augmenting plasticity in the spinal cord during this temporal window can potentiate recovery from cortical stroke by promoting the formation of compensatory connections from spared cortical neurons to spinal motor networks (Soleman et al., 2012).

One approach to augment plasticity is to degrade chondroitin sulfate proteoglycans (CSPGs) in the extracellular matrix. These molecules are potent inhibitors of neurite growth, physically occluding growth cones to induce their collapse, sterically hindering dendritic rearrangement, and physically blocking the action of growth promoting adhesion molecules (Silver and Miller, 2004; Afshari et al., 2010). In addition to creating a structural barrier to neurite growth (Cua et al., 2013), CSPG's also interact with tyrosine phosphate (Shen et al., 2009) and related leukocyte common antigen related phosphatase receptors (Xu et al., 2015) to induce growth inhibitory signaling. Deletion of CSPGs and their growth inhibitory receptors and blockade of downstream pathways (Monnier et al., 2003; Fisher et al., 2011; Sharma et al., 2012) therefore results in increased regeneration of CST fibers, sprouting of serotonergic axons, and improved functional recovery after spinal cord injury (Van den Brand et al., 2012; Silasi and Murphy, 2014). Digestion of CSPG's with the bacterial enzyme chondroitinase ABC (ChABC) can create permissive environment for the growth of axons (Moon et al., 2001; Houle et al.,

2006; Burnside and Bradbury, 2014), dendritic rearrangement and reestablishment of serotonergic fibers (Maier and Schwab, 2006). Notably, ChABC injection into the spinal cord during the period of heightened spinal plasticity that follows cortical stroke significantly improves sensorimotor recovery (Soleman et al., 2012). However, it is not known whether such spinal therapies can be used after the stroke-induced period for spinal plasticity to reopen the window of opportunity and make the injured CNS once again receptive to rehabilitative efforts. Given the limited ability of stroke patients to perform optimal rehabilitation soon after stroke, treatments that can extend or reopen a window for effective rehabilitative training could drastically reduce permanent disability in stroke survivors.

Here, we tested the efficacy with which spinal delivery of ChABC during chronic stroke could reopen the therapeutic window for CST plasticity and potentiate task-specific rehabilitative training (Figure 2.1 C). We found that ChABC stimulated potent plasticity of the CST but only modest sensorimotor recovery when administered during chronic stroke without sensorimotor rehabilitation. However, while task specific rehabilitative training delivered during chronic stroke was not effective in control animals, the combination of intraspinal ChABC with training induced drastic improvements in skilled reaching performance. Our findings demonstrate that removing inhibition of axonal growth by CSPGs in the spinal cord reopens the window for structural plasticity following stroke. Strikingly, this second wave of post-stroke plasticity can be harnessed to improve the efficacy of effective rehabilitation during chronic stroke, a potentially transformative finding for millions of stroke survivors currently living with permanent, intractable disability.

Materials and Methods

Animals

All experimental procedures were performed on male Sprague Dawley rats (400-550 g, Charles River). Animals were housed in pairs (2 per cage) under standard laboratory conditions of 12:12 hour light: dark cycles with controlled temperatures (22°C). Water and standard laboratory rat chow were available *ad libitum*, except during the training period when feeding was reduced to 50 g daily to maintain 85-90% ad libitum feeding body weight. All animal protocols were approved by the University of Alberta Animal Care and Use Committee in accordance with Canadian Council on Animal Care guidelines.

Experimental groups and design

Our aim was to assess if spinal delivery of chondroitinase ABC (ChABC) after behavioral recovery from stroke had plateaued could reopen the therapeutic window of spinal plasticity to promote further recovery. Anterograde tracers injected medial to the cortical ischemic lesion were utilized to quantify spared corticospinal tract innervation of the grey matter in the cervical spinal cord (Figure 2.1).

The first cohort of rats (n = 40) were divided into four experimental groups: Animals received photothrombotic stroke with a delayed spinal cord injection of ChABC enzyme (n = 11) or the control enzyme penicillinase (Pen, n = 11), while sham-stroke operated animals were given injections of ChABC (n = 9) or Pen (n = 9).

A second cohort of rats (n = 24) was given cortical photothrombotic strokes and divided into two groups, one receiving injection of ChABC (n = 12) and the other receiving injections of Pen (n = 12). Animals in four treatment groups received either delayed high intensity

rehabilitative training in a forelimb reaching task (n = 6 per group) or delayed moderate intensity training (n=6 per group) following spinal injection on day 28 after stroke.

Finally, a third cohort of rats received photothrombotic stroke (n = 16) and moderate reaching training starting 3 days after stroke that was continued until spinal injections of ChABC (n = 8) or Pen (n = 8) on day 28. Following injection, training recommenced for an additional 28 days.

Surgical procedures

Surgical procedures were performed in animals deeply anesthetized with 2-2.5% isoflurane (in 70% nitrous oxide and 30% oxygen) at a flow rate of 1 L/min. Body temperature was maintained at 37°C with a rectal temperature probe and heating pad.

Photothrombotic stroke

Rats were mounted in a stereotaxic frame and the forelimb somatosensory cortex corresponding to the preferred limb in skilled reaching tasks was located using stereotaxic coordinates (1-4 mm lateral; -1 to +3 mm anterior of bregma). A thin window was created over the 3 mm x 4 mm rectangular area, this was followed by a tail vein injection of Rose Bengal (a photosensitive dye) solution (30 mg/kg in 0.01 M sterile phosphate buffered saline; Sigma). The thinned skull over the somatosensory cortex was illuminated using a collimated beam of green laser light (532 nm, 17 mW; ~ 4.0 mm in diameter) for 10 minutes to photoactivate the Rose Bengal, occluding all illuminated cortical vasculature and inducing a focal ischemic lesion. This model was chosen for its ability target a defined area of the cortex and its high reproducibility. Sham surgical controls were treated in the same manner however illumination of the laser was eliminated.

Spinal administration of ChABC

28 days after recovering from photothrombosis of the somatosensory motor cortex, ChABC was delivered unilaterally to the cervical spinal cord contralateral to the stroke. Briefly, a partial laminectomy of C4 and C5 was performed to expose the contralesional spinal cord. Using a 10 µl Hamilton syringe mounted on a stereotaxic arm and fitted with a pulled glass tip, a 1.0 µl injection of either chondroitinase ABC (10 U/ml; Sigma) or Pen (same weight (µg) per volume (ml) as chondroitinase ABC; Sigma) was administered at both C4 and C5. Injections were positioned to 1 mm lateral of the midline at a depth of 1 – 1.5 mm and administered at a rate of 0.2 ul/min at both sites. The pipette was left *in situ* for 1 minute after injection to avoid backflow. Subsets of rats were euthanized 7 days after injection to ensure proper injection location and activity of the enzyme.

Anterograde anatomical tracing of the corticospinal tract

28 days after spinal cord injection of ChABC or Pen (56 days after stroke), Alexa-488 tagged dextran tracers were injected into peri-infarct motor cortex areas to investigate corticospinal tract axons in the grey matter of the cervical spinal cord. Briefly, two burr holes were made 1mm medial to the ischemic lesion. Using a Hamilton syringe fitted with a pulled glass microtubule tip, 1 µl of Dextran, Alexa Fluor® 488; 10,000 MW (of 1 mg/µL, Life Technologies, D-22910) was injected over 5 minutes at a rate of 0.2 µL/min at to a depth of 1.5 mm.

Transcardial perfusion and tissue preparation

At 68 days post stroke rats were perfused with 250 ml of saline heparin solution (0.02%) (37°C) followed by 250 ml of 4% formalin solution (4°C) administered at flow rate of 25 ml/min.

Immediately following perfusion brains and spinal cords were removed and submerged in 4% liquid formalin overnight at (4°C), then transferred to 30% sucrose solution (4°C) until the brains and spinal cords lost buoyance, then tissue was flash frozen.

Stroke volume analysis

Brain tissue was cryosectioned in 20 μm coronal slices and all the slices spanning the stroke were collected. For each slice the infarct was traced to determine the surface area, which was then multiplied by the depth of slice (20 μm) to determine the lesion volume. The infarct volumes for every slice spanning the lesion were summed to determine the total stroke volume. Animals from the stroke group which had incomplete lesions (stroke volume less than 2 mm^3) or lesions which did not fall in the targeted the somatosensory motor area where removed from the study.

Neuroanatomical tracer quantification

Spinal cord tissue from C3-C7 was cryosectioned in 35 μm transverse slices and mounted on Superfrost® Plus Gold slides (Fisher Scientific) with fluoromount-G (southern biotech) mounting medium to preserve fluorescence. Tissue was analyzed on a Leica SP5 Confocal microscope using a Leica HCX PL APO L 20 x 1.0NA water emersion objective lens and Leica LAS AF Software. Images were collected as 30 μm z-stacks composed of 10 x 0.3 μm steps taken at 600 Hz over a 736x736 μm section of tissue. Tile scans across the tissue allowed the grey matter across both the ventral and dorsal horns as well as the CST to be analyzed.
The number of labeled fibers in the CST of each animal in the most rostral section of C4 were counted by a blind observer using WCIF- ImageJ. Next the blind observer counted the number of

projections into the grey matter on both the contralesional and ipsilesional side of the spinal cord; these counts were repeated on 20 spinal cord sections between C4 and C5 and the average number of axon segments on each side of the grey matter was determined. The observer also measured the length of each axon segment greater than 1 μm. The total length of axon collaterals was summed and divided by the number of axons counted in the CST at C4 to reduce variability due to inter-animal differences in tracer efficacy or uptake (repeated on 20 sections and an average normalized length was determined for each animal).

Stereological quantification of fiber density was performed using a 50 x 50 grid fitted over the grey matter. Dorsal to ventral lines were positioned from the tip of lamina 1 to the border of ventral horn grey mater, and medial to lateral lines where positioned from the midline the lateral grey matter border. This grid was custom fit over the grey matter to ensure that variation in tissue shrinkage, orientation and deformation would not affect the total fiber counts. To achieve the heat plots (Figure 2.3 J,K) the grid was applied to the contralesional and ipsilesional side, the number of fibers over 5 μm in each grid section was counted.
Fiber overlay images (Figure 2.3 H,I) were obtained by tracing the fibers on raw immunofluorescent images between C4-C6. Images for each animal in a treatment group were then overlaid to create a summary figure for each experimental group.

Serotonin immunohistochemistry and densitometric quantification

Standard immunochemical protocols were used to fluorescently label serotoninergic fibers in the cervical spinal cord. Briefly, slides were dehydrated for 30 minutes at 37°C and then placed in universal blocker (DAKO, Cat.No. 0909) with 0.2% triton X-100 for 1 hour. Tissues were incubated over night with primary rabbit anti-serotonin antibody in (Sigma, Cat no. 5545; 1:500)

in 1% normal goat serum (NGS)/tris buffer saline (TBS). After washing in TBS the tissue was treated with goat anti-rabbit Texas Red (Vector Laboratories, Cat no. TT-1000; 1: 500) in 1% NGS/TBS and incubate in dark for 1hr. Finally, slides were mounted with vectashield fluorescent mounting medium containing DAPI (Vector laboratories, Cat No. H-1500) and glass coverslips. Densitometric quantification of serotonergic axon density was performed on regions of interest in the ventral horn on both the contralesional and ipsilesional side of a single tissue slice (see Figure 2.7). Confocal images were acquired with a 20 x dry objective lens on a Leica DMI6000B inverted microscope coupled to a Leica EL6000 compact light source for fluorescent excitation and captured on the Leica DFC365FX monochrome digital camera and analyzed using (LAS-AF 2.60 software. we defined a standard image size of 1024 × 1024 pixels and analyzed 5 tissue slices from C4 of each animal. Images were collected at the same gain voltage based pixel intensity to ensure optimal signal-to-noise ratio. ImageJ software was used to correct for background and quantify optical density. The average optical density of sham animals was set to 1.0 on both contralesional and ipsilesional side.

Behavioral training and testing

On skilled reaching tasks, rats (see below) were trained twice per day on 28 consecutive days and baseline values of performance were measured three days prior to stroke. Behavioral tasks were tested using the timelines shown in Figures 2.2, 2.4 and 2.5. Testing consisted of two test sessions, 4 hours apart and the average scores for the two tests were reported.

Montoya staircase task

In this task animals are placed in a clear Plexiglas box with a central platform and a thin staircase

on either side. Each stair has a small indent that can only be reached by the forelimb. Three food pellets (Test Diet, 45 mg banana flavor sucrose pellets) were placed in each of the indents on the seven stairs (21 pellets per side of the animal). Training consisted of 15 minutes uninterrupted in the Montoya staircase Plexiglas box and the number of pellets which rats successfully reached and consumed was recorded. To establish forelimb preference both the left and right staircase were filled with pellets during the first 14 training sessions. Once a dominant forepaw was established, the staircase on only the dominant forelimb side of the animal was loaded with pellets to reinforce reaching in the dominant forelimb for the remaining 14 sessions. Those animals which did not meet the minimum criteria of successfully retrieving 9 out of 21 pellets with either forelimb were eliminated from the study. Testing consisted of two 15 minute sessions conducted 4 hours apart and the average number of pellets reached in the two sessions was recorded as the reaching score for that day.

The single pellet-reaching task

Animals that received rehabilitative training were tested on a more stringent fine motor reaching task, the single pellet reaching task. Briefly, animals were placed in a clear Plexiglas box (39.5 cm x 12.5 cm x 47.5 cm) with a 1 cm wide slit in the front wall running floor to ceiling with a shelf (4 cm x 4 cm) mounted 6 cm above the mesh floor of the box. 45 mg rodent pellets in banana flavor (TestDiet) were placed 1.5 cm from the interior wall on the shelf contralateral to the limb the rat was to reach with. When a rat successfully retrieved a pellet off the shelf it was trained to then walk to the back of the apparatus to ensure that the rat was leaving the opening and repositioning itself for the next food pellet. Training consisted of 15 minute sessions two times each day with a 4-hour delay between sessions. Animals were allowed to reach for a

maximum of 100 pellets and those animals unable to reach 10 pellets after 15 days of training were eliminated from the study. After the first 15 sessions, a preferred limb was established; in all subsequent training sessions pellets were only loaded on the side of the platform that required reaching of the preferred limb. Testing consisted of two 15 minutes sessions in which a maximum of 20 pellets were presented to the preferred limb. Reaching performed was measured by two parameters (i) The number of attempts the rat made to reach by placing its arm through the opening towards the shelf with the pellets and (ii) the number of successful reaches (the rat successfully grasped the pellet). The reaching score was calculated as (Number of successful reaches)/(Number of attempted reaches) x 100. The final test scores reported were an average of both test scores achieved on the testing day. All figures report the reaching success rate normalized to baseline prior to stroke. The success rate for each group is reported as Mean ± Standard error to the mean (SEM).

Spontaneous forelimb use

The cylinder test was used to assess spontaneous forelimb use of animals when exploring vertical surfaces. In this test rats are placed in a clear Plexiglas cylinder (44 cm height x 35 cm diameter) with an open top. In each test rats were video recorded in the cylinder for 10 minutes and the first 20 rearing motions during exploration were analyzed and scored. We defined forelimb contact as placement of the fore paw against the wall of the cylinder with the whole palm to support the body weight of the animal. Thus, if an animal touches the wall with a single forelimb it was scored as an independent placement of the ‘left’ or ‘right’ forelimb. However, if the animals initially touched the vertical surface with one paw and subsequently planted the second paw on the wall to maintain balance and support the body weight, the touch was scored as ‘both’. In

addition, if the animal planted both paws simultaneously during a rear against the vertical surface, the touch is again scored as 'both'. The number of contacts with the impaired limb and unimpaired limb can be calculated as a percent of the total number of contacts.

Mechanical sensitivity testing

Mechanical sensitivity was assessed in the rat forepaw mid-plantar region using von Frey monofilaments. The procedure was modified for the forepaw from procedures previously described by Bradmen et al., (2015). The testing was done following the staircase method with removal of monofilaments 9 (4.17) and 13 (4.93) as suggested by Bradmen et al 2015. Testing was started at a midrange target force (4.08) to (6.1) 100g-target force using filaments 1-18 on a standard filament set. The filament application was standardized to 2 seconds on all trial with 10 applications. Animals were either scored as (i) responding or (ii) non-responding for each filament application, when a 50% withdrawal response was achieved, the target force of the filament was recorded as the paw withdrawal mechanical threshold (PWMT). We ensured a consistent blind operator for every experiment and analysis was done using log stimulant values to avoid bias across the range. The PWMT was determined by averaging two separate trials per test day conducted 4 hours apart.

Rehabilitative training

Rehabilitative motor training was conducted in the single pellet-reaching chamber. Two training intensities were provided: moderate and high intensity. In the moderate intensity group animals were allowed to reach for 15 minutes, two times each day for a maximum of 100 pellets per session. In the high intensity group, animals were allowed to reach for 1000 pellets or a

maximum of 2 hours, twice per day. During these training sessions animals were allowed to reach in place and did not have to return to the back of the cage before receiving the next pellet as in the test phase. Training was also classified as either early or delayed. In early rehabilitative training groups animals started training 3 days after stroke and received training every day for 53 consecutive days with a one-day break at 28 days for spinal injection surgery. In the delayed training group, animals received no training prior to receiving the spinal injection at 28 days. The delayed training animals began rehabilitation regiments at 29 days post stroke, one day after spinal injection, and continued daily until cortical tracers were injected at 56 days post stroke for a total of 27 days of rehabilitation training (Table 2).

Statistical analysis

Statistical analysis was performed using GraphPad Prism (Version7, GraphPad software, 2016). Statistical analysis of stroke size was performed using unpaired, two-tailed Students t-tests. Statistical analysis of behavioral performance on all tests was performed by two-way ANOVA. Holm-Sidak multiple comparison testing was performed between groups when a significant main effect of treatment or a significant interaction of time x treatment was found. When there was a significant main effect of time but no significant main effect of treatment or interaction we performed Holm-Sidak's *post hoc* testing to identify within group differences at different time points. Fiber count and length statistical analysis was performed by two-way ANOVA testing followed by *post hoc* Holm-Sidak's testing. Statistical evaluation of serotonergic fibers density was performed with one-way ANOVA, followed by Holm-Sidak's *post hoc*, to compare each treatment group to the un injured sham group.

Results

Intraspinal ChABC without training reduces sensorimotor deficits in an animal model of chronic stroke

The experimental timeline is illustrated in Figure 2.1 C. Photothrombotic stroke was used to induce consistent infarcts lesioning the entire forelimb somatosensory motor cortex (Figure 2.1 D-F). Spinal injections of ChABC or the inactive control enzyme Penicillinase (Pen) were administered 28 days following stroke. At this time point, endogenous promoters of plasticity that are upregulated early after stroke have returned to baseline, and spontaneous functional recovery (with or without rehabilitation) has plateaued (Sist et al., 2014; Kessner et al., 2016*;* Figure 2.1 A,B). Spinal injections were targeted to the deinnervated contralesional side of the spinal cord at cervical level 4 (C4), which represents a major termination point for CST axons originating in the forelimb sensorimotor cortex (Figure 2.1 G). Prior to photothrombotic stroke, animals were trained and tested on a battery of sensorimotor tasks (Montoya Staircase reaching, cylinder task, von Frey hair testing) to establish pre-stroke baseline (Figure 2.2 A). Animals were tested again 3, 7, 14, 28 days, 42 and 56 days post stroke to examine the time course of recovery before and after ChABC (or control) treatment (Figure 2.2 A).

Photothrombosis induced clear lesions of the forelimb sensorimotor cortex that were still apparent in both treatment groups 68 days after stroke (Figure 2.1 E,F). Major stroke-induced deficits in skilled reaching in the Montoya Staircase task were observed, with reaching performance reduced to 42.9 ± 7.1% and 43.2 ± 7.10% of pre stroke levels at 7 day after injury in ChABC-treated and control animals, respectively. Rats spontaneously recovered to 62.7 ± 4.9 and 61.6 ± 4.7% of pre stroke levels (ChABC and Control animals, respectively) by 28 days post stroke (prior to intraspinal injections). Multivariate analysis did not reveal a significant effect of

treatment group in stroke animals (Figure 2.2 C) or sham-stroke controls (Figure 2.2 D). However, a significant main effect of time ($F_{(5, 100)} = 25.52$, $P < 0.0001$) was observed. Notably, ChABC treated rats showed significant improvement in reaching performance between 28 (pre-ChABC) and 56 days post-stroke (Holm-Sidak, $P < 0.05$), whereas reaching performance in control rats did not improve between 28 and 56 days post stroke ($P > 0$ .05).

Stroke induced forelimb use asymmetry in the cylinder task showed partial recovery by 28 days post stroke then plateaued between 28-56 days (Figure 2.2 E). There was no effect of treatment on limb use preference ($P > .05$), however there was a significant main effect of time ($F_{(4, 80)} = 40.21$, $P < 0.0001$). Mechanical sensitivity was impaired by stroke with modest recovery to a plateau at 28 days in both treatment groups. There was a significant effect of time ($F_{(8,112)} = 12.86$, $P < 0.0001$) and a significant interaction of time and treatment group ($F_{(8,112)} = 2.38$, $P = 0.0249$), however there was no significant difference between groups at any time point using Holm-Sidak's multiple comparisons (Figure 2.2 G). There was no effect of treatment or time in ChABC-treated or control rats that did not receive stroke ($F_{(8,112)} = 0.9712$, $P = 0.4623$) (Figure 2.2 D,F,H).

ChABC induces axonal sprouting during chronic stroke

CST axons in the cervical spinal grey matter were labeled by injection of an anterograde tracer (Dextran, Alexa Fluor® 488; 10,000 MW) medial to the cortical ischemic infarct *5*6 days after injury (Figure 2.1 D-F). Axon fragments labeled by cortical injections were imaged in the cervical spinal cord (vertebrae C4 and C5) using confocal microscopy. To determine anatomical changes induced by ChABC digestion of CSPGs in the cervical spinal cord, the number and length (normalized to the total number of labeled fibers in the descending CST in the most rostral

section of C4) of labeled axon fragments derived from the CST found in the spinal grey matter was determined. In ChABC treated rats, extensive innervation of the cervical spinal grey matter by fibers emanating from the CST was apparent (Figure 2.3 A). In contrast, control animals had very limited innervation of the cervical grey matter by CST fibers originating in peri-infarct cortex (Figure 2.3 B). Significant main effects of treatment and hemisphere were observed for the average number (Two-way ANOVA, Treatment, $F_{(1,32)} = 17.42$, $P = 0.0002$; Hemisphere, $F_{(1,32)} = 12.32$, $P = 0.0014$; Interaction, $F_{(1,32)} = 9.378$, $P = 0.0044$) and mean length of axon fragments in the spinal grey matter (Treatment, $F_{(1,20)} = 11.04$, $P = 0.0034$; Hemisphere $F_{(1,20)} = 7.747$, $P = 0.0115$ Interaction, $F_{(1,20)} = 5.163$ $P = 0.0343$).

Post hoc comparisons revealed significantly more axon fragments (Mean difference of 58.6± 11.5 fibers between groups; Holm Sidak, $P < 0.0001$) and longer axon fragments (Mean difference of 29.1 ± 7.4 μm axon length between groups; $P = 0.0038$) in the contralesional grey matter (Figure 2.3 D-G). Moreover, CST fibers crossing over from the contralesional to the ipsilesional grey matter were observed in ChABC treated animals but not controls (Figure 2.3 D,E). A greater distribution of CST fibers throughout the cervical grey matter in ChABC treated rats is apparent in camera lucida diagrams (Figure 2.3 H,J). Fiber density heat plots illustrating the mean distribution of axon fragments confirmed that ChABC treatment promoted axonal sprouting throughout the cervical spinal grey matter with extensive innervation of lamina VII and lamina VI nearest to the CST (Figure 2.3 I). The density of fibers and distribution of fibers was limited in controls relative to the ChABC treated animals (Figure 2.3 I,K).

ChABC potentiates task specific rehabilitative training during chronic stroke

ChABC injection induced drastic axonal sprouting from the CST into the cervical grey matter,

but only a moderate (in comparison) functional improvement in measures of forelimb impairment. Rehabilitative training early after injury can reduce functional deficits but becomes ineffective during chronic stroke, potentially due to a closure of the critical period for heightened plasticity that follows in the weeks after stroke. Our anatomical data suggests that ChABC can recreate a window of heightened spinal plasticity in chronic stroke, which could in turn potentiate task specific training. The experimental timeline used to test this postulate is shown in Figure 2.4 A. Rats were trained on the single pellet reaching task prior to stroke and tested 3, 7, 14, 21, 28, 35, 42, 49 and 56 days post stroke. Three days after injection with ChABC or Pen control (28 days post-stroke), rats were divided into groups that received either moderate task specific rehabilitative training (100 reaching attempts twice per day in the single pellet reaching apparatus) or high intensity training (1000 reaching attempts twice per day) on days 29-56 post-stroke. These paradigms were chosen to model moderate and intense rehabilitative training and determine whether ChABC could make limited training more effective and/or remove plateaus that occur with continuous training.

Multivariate analyses revealed a significant interaction of time and treatment on reaching performance for both delayed moderate training ($F_{(8,80)} = 7.344$, $P < 0.0001$) and delayed high intensity training ($F_{(8,80)} = 2.682$, $P = 0.0115$) (Figure 2.4 C). In moderate training conditions, ChABC-treated rats exhibited significantly better reaching success (relative to controls) at 42 (Holm Sidak, $P < 0.01$), 49 ($P < 0.001$), and 56 ($P < 0.01$) days post-stroke. Notably, controls had only limited improvement from delayed training, while ChABC treated rats showed a dramatic improvement in testing on day 42. This delay between ChABC injection and sensorimotor improvement is consistent with ChABC enzyme kinetics and with previous work showing that the timing of spinal therapy relative to rehabilitation is crucial (Soleman et al.

2010) groups showed significant improvement in reaching performance during the high intensity training. However, ChABC injected rats exhibited superior performance at 49 ($P < 0.05$) and 56 days ($P < 0.01$) after stroke relative to controls.

Surprisingly, reaching performance at 56 days post stroke was improved relative to baseline performance in ChABC treated rats ($P < 0.05$). In both the moderate and high intensity training groups, ChABC did not alter performance on the cylinder or induce any changes to spontaneous forelimb use preference (Figure 2.4 E,F), nor did ChABC treatment induce aberrant mechanical sensitivity in von Frey test scoring (Figure 2.4 G,H). While a main effect of time was observed in both assays (Cylinder task, $F_{(1,80)} = 85.57$, $P < 0.0001$; von Frey test, $F_{(1,80)} = 207.5$, $P < 0.001$), there were no main effects of treatment or significant interactions or significant Holm-Sidak comparisons between time points after treatment.

Effects of delayed ChABC with early rehab

The final experimental paradigm was designed to model permanent disability due to stroke even after extensive rehabilitation. Ideally, rehabilitative motor training is initiated early after stroke, as early training has been shown to far exceed the benefits of delayed therapy in restoring behavioral performance Murphy and Corbett, 2009; Langhorne et al., 2010; Krakauer et al., 2012; Tennant, 2014). Rehabilitative training is continued into chronic stroke, though it loses efficacy with time and most patients remain disabled. To model this scenario, we delivered moderate task specific training starting 3 days post stroke and continuing for 56 days (Figure 2.5 A).

Early rehabilitative training induced marked improvement in skilled reaching and forelimb asymmetry in all animals by 28 days post stroke (from 3.4 ± 0.5% of baseline post

stroke to 74.2 ± 4.5% of baseline in controls prior to treatment and from 4.4 ± 0.5% to 65.2 ± 4.5% of baseline in ChABC groups prior to spinal injections). However, control animals showed minimal improvement in reaching score (16.8 ± 5.0% improvement) with additional training between 28 and 56 days post stroke, while ChABC injection on day 28 significantly potentiated the efficacy of rehabilitative training after treatment (52.4 ± 4.2% improvement). Multivariate ANOVA identified a significant interaction between treatment and time ($F_{(8,112)} = 10.84$, $P < 0.0001$) (Figure 2.5 B), and Holm-Sidak's multiple comparisons revealed that ChABC treated animals had significantly better reaching performance than control animals at 42 ($P < 0.01$), 49 ($P < 0.00001$) and 56 ($P < 0.00001$) days post stroke (despite an initial impairment relative to controls at 35 days post stroke ($P < 0.05$)) (Figure 2.5 B). There was no significant effect of treatment on cylinder reaching forelimb use scores; however, *posthoc* comparisons based on a significant main effect of time ($F_{(8,126)} = 48.128$, $P < 0.0001$) suggest that ChABC treated rats used their stroke affected limb significantly more on days 42 ($P < 0.001$), 49 ($P < 0.001$) 56 ($P < 0.0001$) than on day 28 (pre-treatment). The same effect was not observed in control rats (Figure 2.5 C). As in the case of the delayed training groups, there was a significant effect of time ($F_{(8,112)} = 19.71$, $P < 0.0001$) but no effect of ChABC injection on mechanical sensitivity or significant Holm-Sidak comparisons between time points after treatment (Figure 2.5 D).

Effects of combined therapy on CST and serotonergic innervation of the cervical cord

All animals that received rehabilitative training were injected with anterograde tracer into the peri-infarct cortex adjacent the stroke to investigate sprouting of spared fibers in the CST (as described earlier). Rats that received training paired with ChABC exhibited significantly higher fiber counts (contralesional grey matter, $F_{(1,54)} = 201.0$, $P < 0.0001$; ipsilesional, $F_{(1,54)} = 130.3$, P

< 0.0001) (Figure 2.6 G) and significantly greater fiber lengths ($F_{(1,54)} = 91.50$, $P < 0.0001$) (Figure 2.6 H) than rats that received training paired with Pen injection. High intensity training resulted in a greater number (but not length) of fibers on the contralesional side than the early ($P < 0.05$) or delayed moderate ($P < 0.001$) training groups (Figure 2.6 G,H). Notably, ChABC treated animals in the early rehabilitative training group exhibited a 20-fold increase in the number of fibers relative to controls, while animals in the delayed moderate and delayed high intensity training groups exhibited 5-fold and 16-fold increases in fiber number relative to controls.

Because the serotonergic system has been reported to be involved in compensatory mechanisms and recovery that follows spinal injury, and because serotonin has a crucial role in regulating the excitability of spinal motor neurons (Hounsgaard et al., 1988) we evaluated changes in serotonergic fiber distribution in the grey matter of the cervical spinal cord at the C4 level. A significant main effect of treatment paradigm on serotonergic fiber density in the spinal cord was observed (ANOVA, $F_{(8, 36)} = 7.428$, $P < 0.0001$). Serotonergic fiber density was reduced by stroke ($P < 0.05$ relative to sham-stroke controls), an effect that was not reversed by ChABC alone ($P < 0.05$ relative to shams). However, when ChABC was paired with moderate or intense delayed rehabilitative training (Figure 2.7 F,G), serotonergic innervation was not significantly different from sham-stroke controls. Pen controls still exhibited significantly reduced serotonergic fiber density relative to controls ($P < 0.01$). Notably, early rehabilitative training restored serotonergic axon density in controls and ChABC treated rats, though a trend toward synergistic effect remained. The effects of stroke, ChABC and training on serotonergic fiber density were restricted to the contralesional spinal hemisphere.

Discussion

Almost all recovery after stroke occurs in the first few weeks after the ischemic onset. Even with extensive and sustained rehabilitative training, sensorimotor recovery peaks by four weeks (in rodents) and three months (in humans) after stroke (Steinberg and Augustine, 1997; Krakauer et al., 2012; Wahl and Schwab, 2014). In this project, we sought to determine if pro-plasticity ChABC therapy delivered to the spinal cord during the chronic phase of stroke recovery could reopen the therapeutic window for recovery.

ChABC therapy requires rehabilitation for functional improvement

Despite drastic increases in the number, length, and distribution of CST axons in the cervical grey matter, there was only moderate functional benefit of ChABC alone (without rehabilitative training). This is not entirely surprising as previous studies in C4 spinal cord injury models indicated that ChABC only allowed for improvement in sensorimotor function when combined with rehabilitation (Garcia-Alias et al., 2009). Similar findings have been reported with other plasticity promoting treatments such as intracortical brain derived neurotrophic factor (Vavrek et al., 2006; Weishaupt et al., 2013).

To determine if this second window of plasticity could be harnessed to rekindle the effectiveness of task specific training, we paired ChABC with delayed reaching training in the single pellet task. Notably, rehabilitative training of moderate intensity was ineffective when paired with control injection, but ChABC paired with training induced significant improvement. Rats in both the ChABC and control groups that underwent intense forelimb reaching rehabilitative training starting after ChABC injection on day 28 showed significant improvement on the skilled forelimb reaching task. The ChABC treated animals again performed significantly

better than controls, with reaching success scores significantly better than baseline. These data suggest that ChABC can potentiate even rehabilitative training performed at maximum intensities and overcome potential ceiling effects of intense training. To model stroke patients who receive early rehabilitation that is continued through to chronic stroke, but who's recovery plateaus in the weeks following the initial injury, a cohort of rats received moderate rehabilitative training starting three days after stroke and continuing for eight weeks. Notably, while rehabilitative training efficacy plateaued by 28 days after stroke and was not significantly improved by control injection, rats exhibit a second wave of training-induced recovery after intraspinal ChABC injection.

ChABC opens a window of spinal plasticity

These data suggest that intraspinal ChABC can reopen or augment a window for training induced recovery during chronic stroke in a model approximating chronic stroke patients. A limited number of studies have identified similar patterns of task specific recovery during chronic stroke, including clinical investigations of constrained induced movement therapy starting 3 to 9 months after stroke that demonstrated that intense training can induce improvement in arm function for stroke patients even during chronic stroke (Wolf et al., 2006). Similarly, preclinical studies of chronic spinal cord injury have shown that ChABC can improve motor function outcomes (Garcia-Alias et al., 2009) even when administered in the chronic phase of recovery (Soleman et al., 2012) and the effects ChABC administered at time points early after CNS injury have been shown to be amplified with rehabilitation (Moon et al., 2001).

ChABC exhibited a potent pro-plasticity effect on CST axons in the spinal cord. Because nociceptive fibers can also sprout after injury or plasticity enhancing treatments, intraspinal

ChABC could potentiate mechanical sensitivity and induce hyperalgesia. However, von Frey hair testing did not indicate the development of pathological pain circuitry. While ChABC treated rats in some cases exhibited faster normalization of PWMTs to baseline (pre-stroke) levels, hyperalgesia (reduced PWMTs relative to baseline) was not observed in any treatment groups, suggesting that sprouting of nociceptive fibers did not occur to a level sufficient to alter pain sensitivity. Our data did suggest an interaction between ChABC treatment, rehabilitative training, and the density of serotonergic innervation of the cervical spinal cord. While ChABC alone did not induce an increase in serotonergic fiber density, ChABC paired with delayed training significantly increased serotonergic innervation. Following spinal cord injury, serotonergic input is lost to regions of the spinal cord distal to the site of injury (Fong et al., 2005).

ChABC therapy improves serotonergic innervation of the spinal cord after stroke

Interestingly, our data suggest that cortical stroke also significantly reduces serotonergic innervation of the spinal cord, despite the lack of overt injury to serotonergic fibers themselves. Direct application of serotonin to deinnervated spinal cord sites restores spinal excitability and can improve motor function (Fong et al., 2005) resulting from disruption of spinal circuits, indicating that restoration of serotonergic innervation is crucial for motor recovery after injury (Giménez et al., 1995; Leszczynska et al., 2015). Moreover, removal of growth inhibitory factors in the glial scar potentiates regrowth of serotonergic fibers and improves recovery after spinal cord injury (Giménez et al., 1995; Camand et al., 2004; Müllner et al., 2008). While some studies suggest that spontaneous regrowth of serotonergic fibers after spinal injury occurs over the first four weeks after spinal injury (Leszczynska et al., 2015), there is evidence that suggests serotonergic neurons have late intrinsic growth programs and long term studies show that

serotonergic fibers are continue to sprout over long periods (1-6 months) after injury (Li and Raisman, 1995; Hill et al., 2001; Filli et al., 2011). Increased serotonergic fiber density is one postulated mechanism of improved sensory motor recovery in ChABC treated and rehabilitated animals after spinal injury (Jacobs et al., 2002). Moreover, increases in the length of serotonergic fibers after injury correlate with improvement in both inter- and intra limb coordination (Leszczynska et al., 2015), which are crucial in skilled reaching tasks.

ChABC can induce a second wave of structural plasticity

In summary, our data conclusively shows that removal of growth inhibitory CSPGs in the spinal cord of rats during chronic stroke can induce a second wave of structural plasticity. This augmented plasticity potentiates delayed rehabilitative training and potentiates training efficacy that has plateaued after early rehabilitation. These data therefore suggest that permanent disability affecting millions of individuals living with the chronic effects of stroke may be treatable with spinal therapy and rehabilitation even months or years after the stroke. Our data emphasize that inducing a state of plasticity is not sufficient to induce recovery, and that combining such therapies with rehabilitative training is required for optimal recovery (Girgis et al., 2007). Moreover, our data suggest that recovery correlates with increased serotonergic input to spinal motor areas, and supports further study of spinal serotonergic manipulation as a tool to potentiate recovery and rehabilitation after stroke. Analysis of these serotonergic fibers again emphasized the importance of activity and rehabilitation after CNS injury, as removal of inhibitory CSPGs alone was insufficient to increase serotonergic density and maximal restoration of serotonergic fiber density in the spinal cord was only achieved when ChABC was combined with rehabilitative training.

Chapter 2: Figures

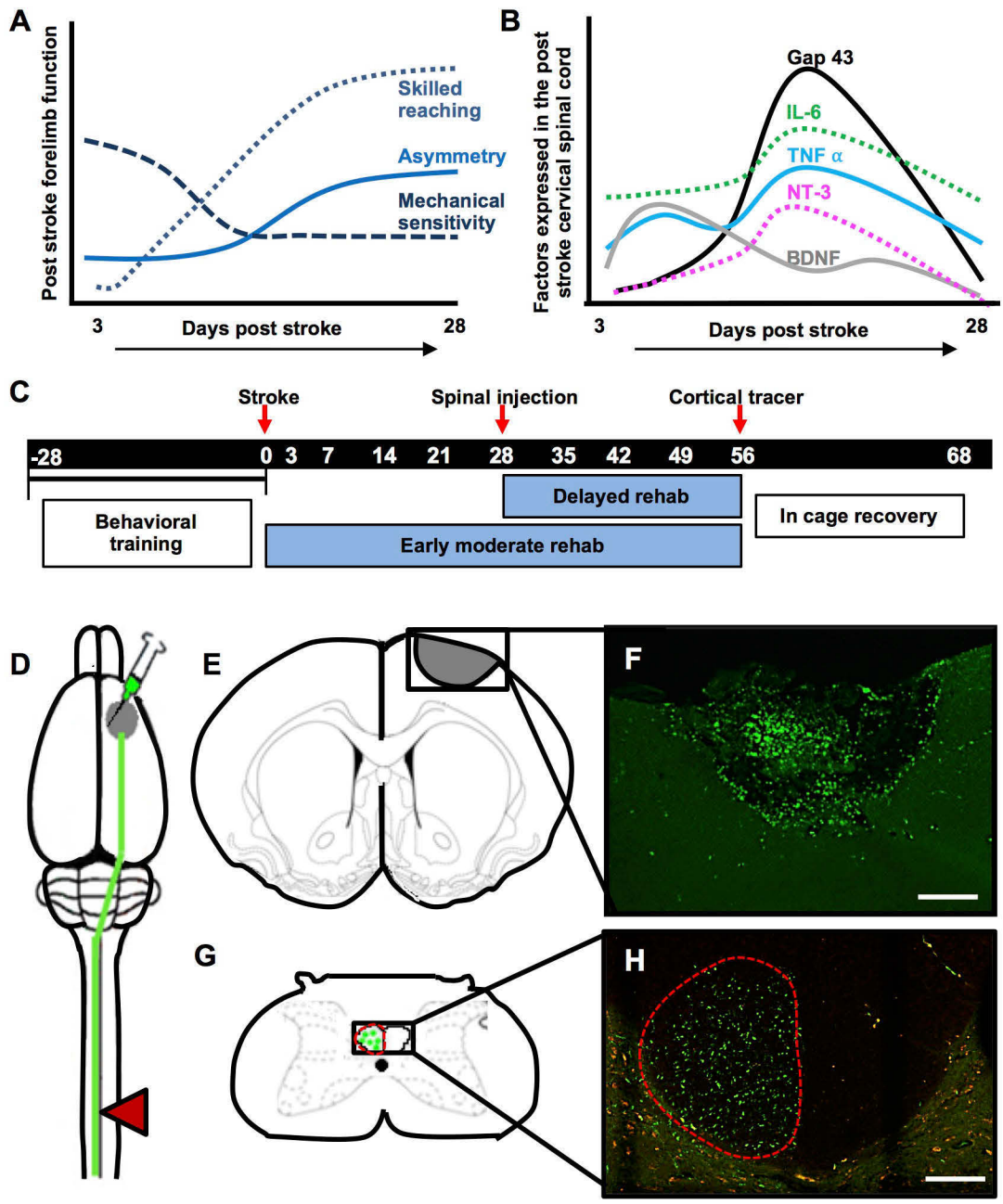

Figure 2.1. Experimental design. (A) Stroke induces sensorimotor impairment in rats that recover over the weeks following injury. Skilled reaching recovers over the first four weeks, but plateaus after this point. Spontaneous forelimb use preference shows a similar time course, with no further recovery after four weeks. If cortical lesions include the somatosensory cortex,

mechanical sensitivity is impaired and shows partial recovery by four weeks. (**B**) The time course of post stroke recovery corresponds with relative changes in cervical spinal cord protein expression associated with plasticity and nerve regrowth promotion. Periods of heightened sensorimotor recovery coincide with periods of peak expression of trophic (GAP-43, NT-3) and inflammatory (TNF-alpha, IL-6) cytokines in the spinal cord. Plateaued recovery coincides with a return to baseline levels of these cytokines (Sist et al., 2014). Our experiments were designed to test the hypothesis that spinal microinjection of ChABC can augment plasticity of the corticospinal tract and improve recovery even during chronic stroke, after this period of heightened plasticity has ended. (**C**) The experimental timeline of task specific training and testing relative to the performed surgical procedures to test this hypothesis. (**D**) Schematic illustrating targeted ischemic stroke over the forelimb sensorimotor cortex (grey circle), the location of anterograde tracer injection medial to the ischemic infarct to label axons descending in the corticospinal tract (green line), and the location of spinal injection of ChABC or Pen (control enzyme) at 28 days post stroke (red triangle). (**E**) Illustration of coronal section (+1.00 anterior of Bregma) demonstrating average size and stereotactic location of induced ischemic lesion. (**F**) Representative confocal image of infarct 68 days post injury. (**G**) Illustration of a transverse section at cervical vertebrae 5, with tracer labeled axons in contralesional CST. (**H**) Representative image of rat corticospinal tract, axons labeled with green fluorescent anterograde tracer injected adjacent the infarct.

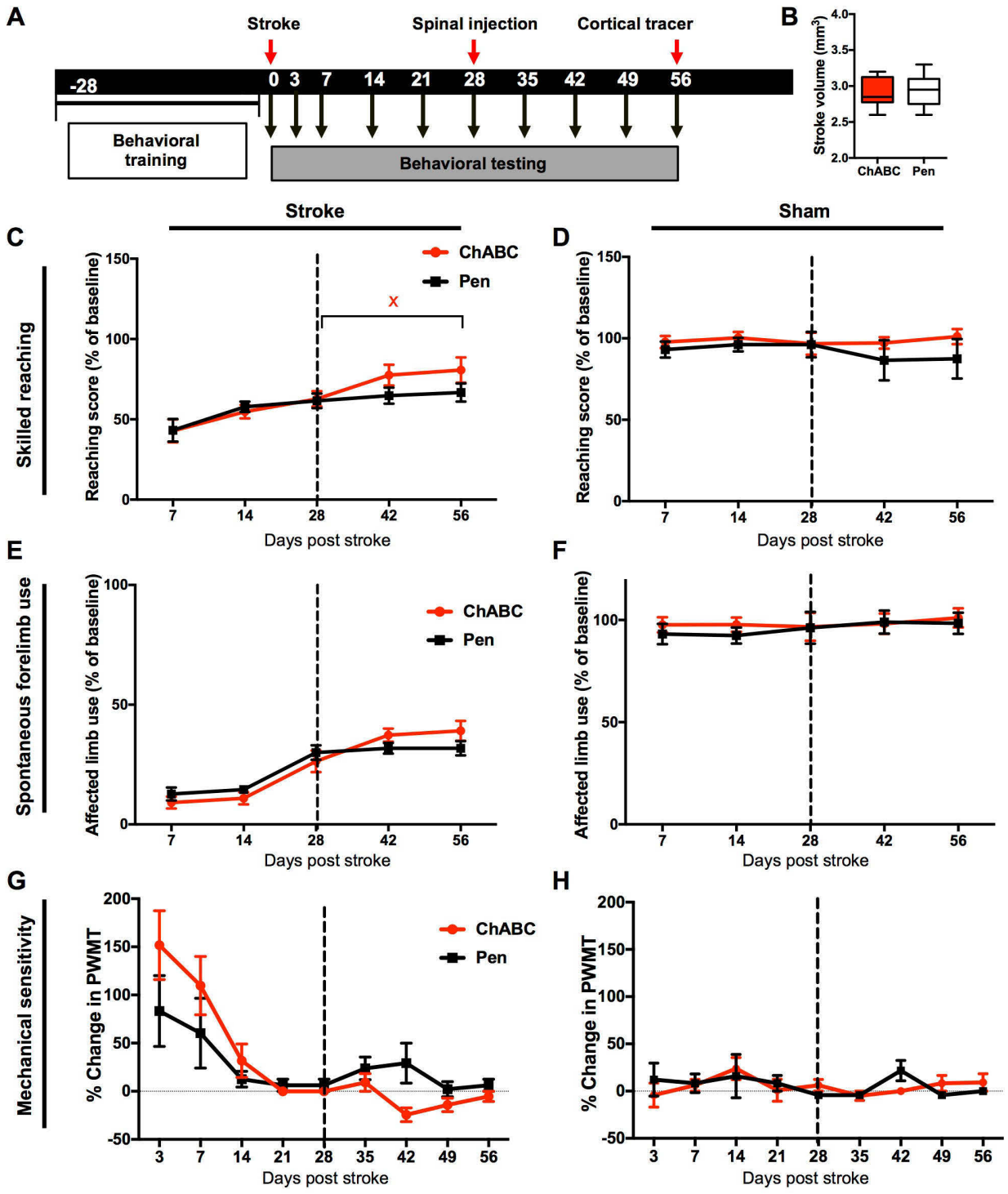

Figure 2.2. ChABC administered during chronic stroke without task-specific training moderately improves recovery. (**A**) Timeline showing behavioral testing and surgical procedures. (**B**) There were no significant difference in the stroke volumes between ChABC-

treated or Pen control groups (two tailed t-test; $P = 0.92$, t = 0.10, df =18). **(C)** Skilled reaching in the Montoya Staircase Task. There was no significant main effect of ChABC (relative to Pen controls) or time X treatment interaction ($P > 0.05$), however a significant effect of time was detected ($P < 0.0001$). Holm-Sidak post hoc comparisons within each treatment group (between time points) identified impaired reaching performance at post-stroke day 7 that improved by post-stroke day 42 and 56 ($P < .05$). However, only the ChABC group showed significant improvement after spinal injections, with improved performance at post-stroke day 56 (x, $P < 0.05$) relative to day 28. **(D)** There was no effect of time or treatment in sham-stroke controls (P > 0 .05). **(e)** There was no significant effect of treatment on spontaneous forelimb use measured in the cylinder task ($P > .05$), however there was a significant main effect of time ($P < 0.0001$). However, there were no significant differences in performance between 28 and 56 days in either group. **(F)** There was no effect of time or treatment in sham-stroke controls ($P >.05$). **(G)** A significant effect of time and interaction was detected in measures of mechanical sensitivity (time, $P < 0.0001$; interaction, $P = 0.0249$), but there were no significant differences between treatment groups at any time point after stroke. **(H)** There was no effect of time or treatment on mechanical sensitivity in sham-stroke animals.

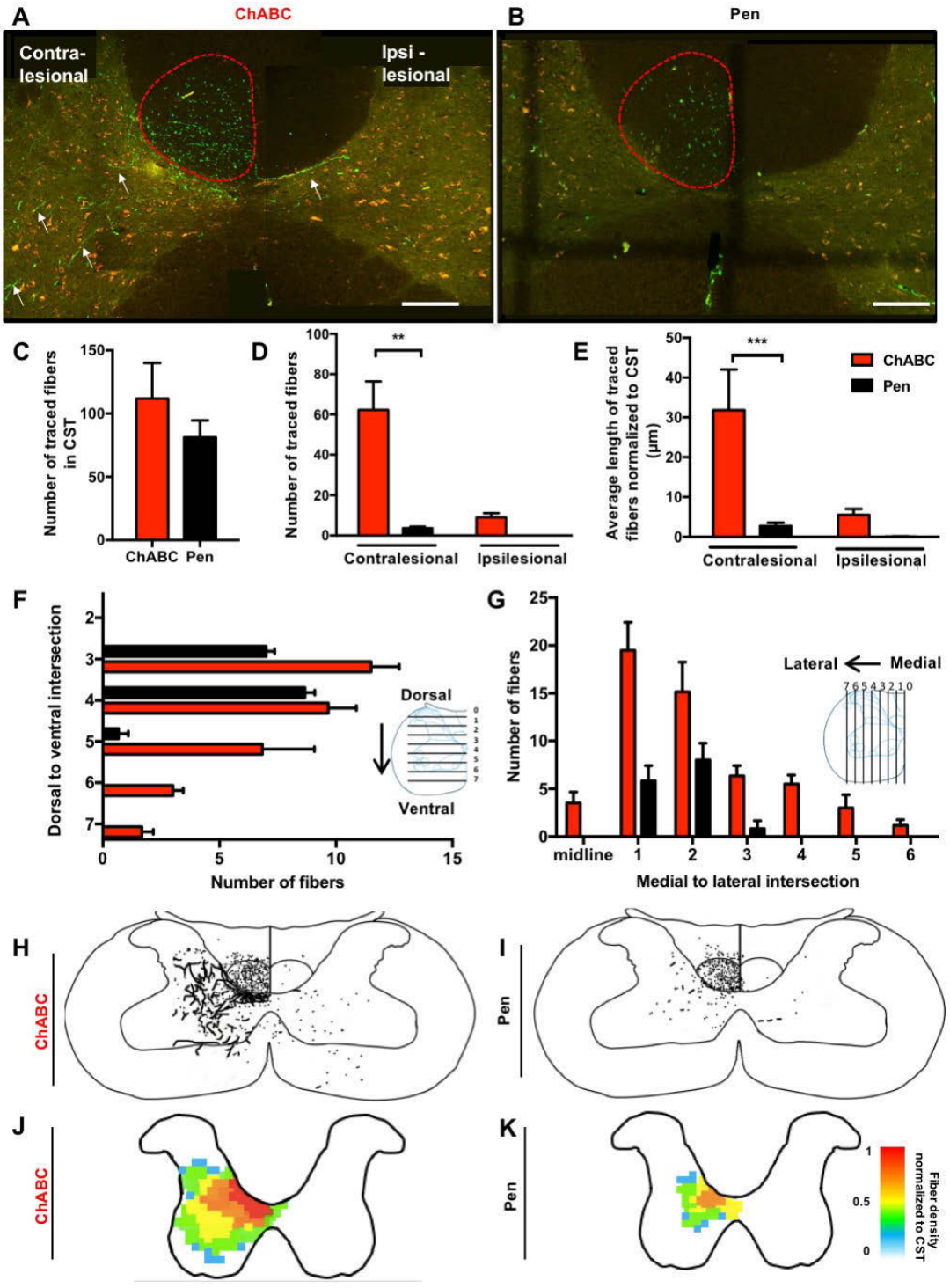

Figure 2.3. Delayed ChABC induces axonal spouting of stroke deinnervated axons. (**A**) Confocal microscopy of anterograde labeled axonal fragments and terminals (arrows) in the contralesional (stroke-denervated) CST (outlined in red) and the contralesional and ipsilesional

spinal cord grey matter in transverse sections spanning C4 and C5 of the cervical spinal cord of ChABC treated rat. (**B**) A transverse section through C4 in a Pen control rat. Note the reduced density of labeled axon fragments from the CST in the grey matter relative to the ChABC treated animal in **(A)**. Scale bars, 2 mm. (**C**) Following stroke there was no significant difference in the number of labeled fibers in the CST between treatment groups ($P = 0.38$; two-tailed $t = 0.91$, $df = 16$). (**D)** A significant main effect of treatment on the number of labeled axon fragments in the cervical grey matter was detected ($P = 0.0002$). Significantly more fibers were found in the spinal grey matter contralateral to the cortical infarct of ChABC treated animals (***, $P < 0.001$). (**E**) There was a significant effect treatment ($P = 0.0034$) on the average length of axon fragments in the spinal grey matter (normalized within animals to the total number of labeled fibers in the CST), with post hoc comparisons confirming greater axon length in the contralateral spinal grey matter of ChABC treated animals (**, $P < 0.01$). (**F**) ChABC increases dorsal to ventral and (**G**) medial to lateral distribution of fibers in the grey matter of the cervical spinal cord. (**H**) Camera lucida overlay tracings and density heat maps (**J, K**) showing drastically increased density and distribution of axon fragments after ChABC treatment relative to Pen controls.

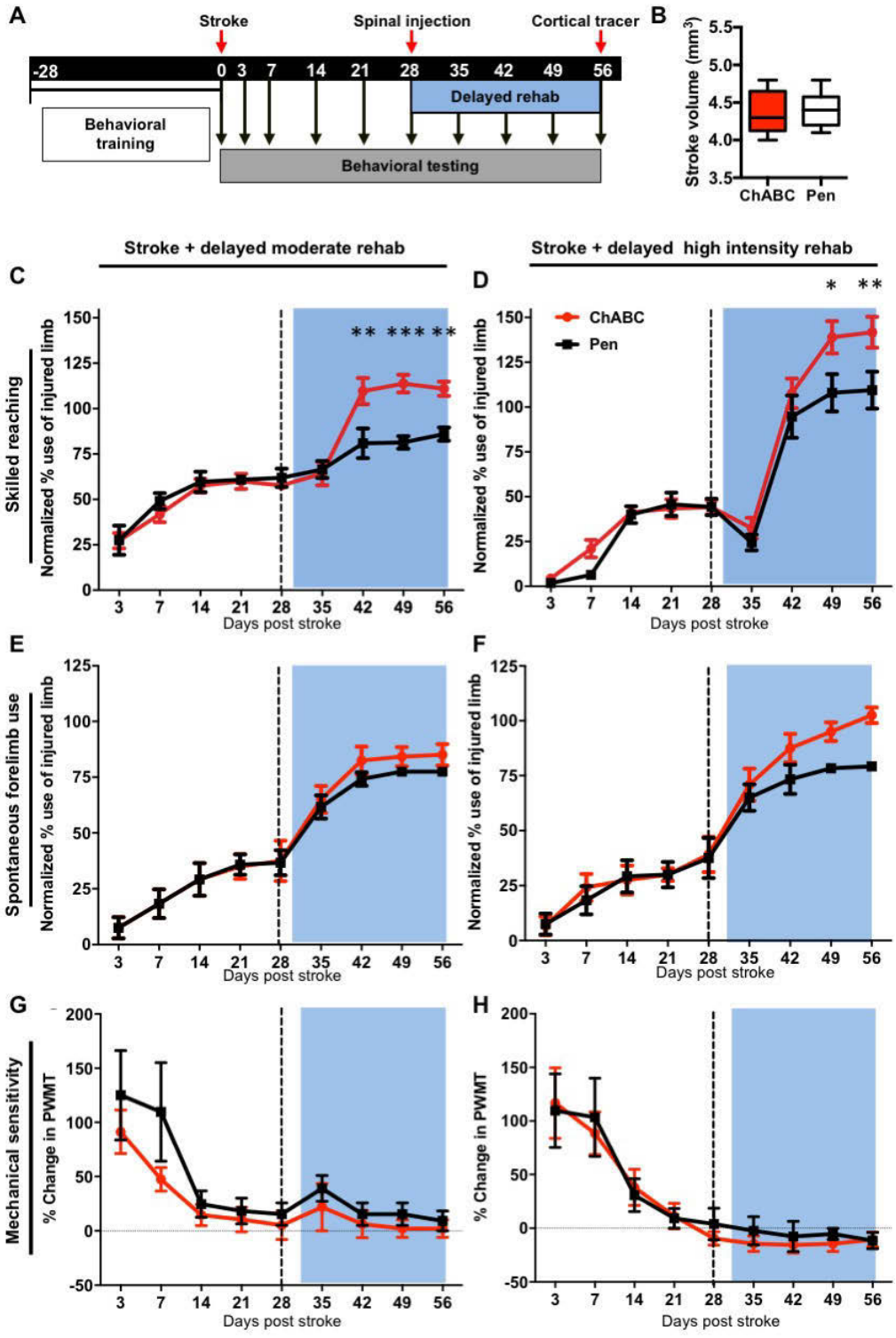

Figure 2.4. ChABC with delayed rehabilitative training of moderate or high intensity improves functional outcome. (**A**) Timeline showing delayed rehabilitative training starting 28

days post injury. (**B**) There was no significant difference in stroke volume between groups (P = 0.78, t = 0.28, df = 14). (**C**) Skilled reaching performance in the single pellet reaching task. There was a significant effect of time ($P < 0.0001$) and a significant time x treatment interaction ($P < 0.0001$). Holm-Sidak's multiple comparisons were used to compare the reaching performance of ChABC treated animals with Pen controls receiving the same training at each time point. ChABC treated animals performed significantly better than the Pen controls after treatment at 42 (**, $P < 0.01$), 49 (***, $P < 0.001$) and 56 (**, $P < 0.01$) days post stroke. There were no differences at time points prior to intraspinal injections. (**D**) ChABC rats and Pen controls that received high intensity training recovered to pre-stroke forelimb reaching performance. There was a significant interaction of time x treatment ($F_{(8,80)} = 2.682$, $P = 0.0115$) as well as a significant effect of time ($P < 0.0001$). ChABC treated animals performed significantly better than Pen controls at 49 (*, $P < 0.05$) and 56 (**, $P < 0.01$) days after stroke. (**E,F**) Animals receiving ChABC or Pen injections after injury combined with delayed rehabilitative training of moderate (**E**) or high intensity (**F**) exhibited no significant effect of treatment or interaction of time and treatment on the cylinder task to assess forelimb use preference. (**G, H**) Similarly, mechanical sensitivity was unaffected by ChABC or Pen treatment.

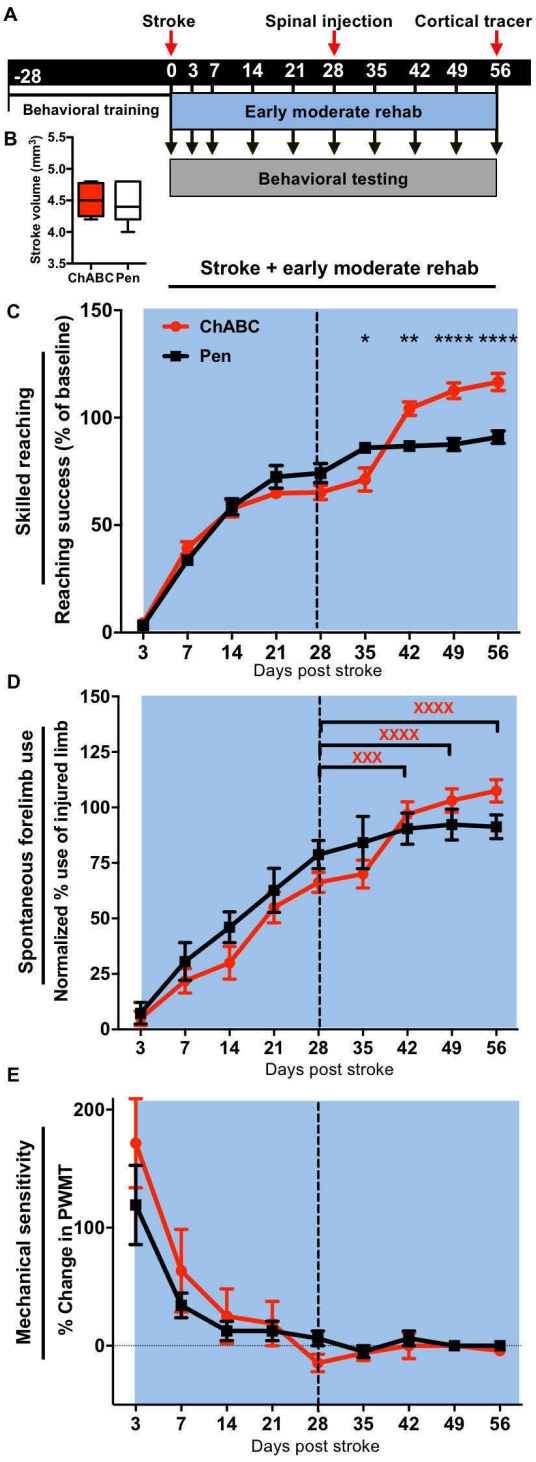

Figure 2.5. ChABC paired with early moderate rehabilitative training induced significant recovery of sensorimotor function (**A**). Timeline of testing, surgical procedures and training beginning 3 days post stroke. (**B**) There was no difference in stroke volume between groups (*P* =

0.67 t = 0.44 df=14). (**C**) There was a significant effect of time ($P < 0.0001$) and a significant interaction of treatment x time ($P < 0.0001$) in rats treated with moderate rehabilitative training early after stroke. Notably, ChABC treated animals had significantly better reaching performance than Pen controls at 42 (**, $P < 0.01$), 49 (****, $P < 0.00001$) and 56 (****, $P < 0.00001$) days post stroke (despite the fact that ChABC animals actually preformed significantly worse than Pen treated animals at 35 days post stroke (*, $P < 0.05$). (**D**) There was no significant effect of treatment in the cylinder task testing, however there was a significant effect of time ($P < 0.0001$). Within group post hoc comparisons revealed that only the ChABC treated animals significantly increased use of their affected limb on days 42, 49 and 56 post stroke when compared to day 28 limb use preference (^{xxx}, $P < 0.001$; ^{xxxx}, $P < 0.0001$). (**E**) There were no treatment effects or significant interactions on assays of mechanical sensitivity.

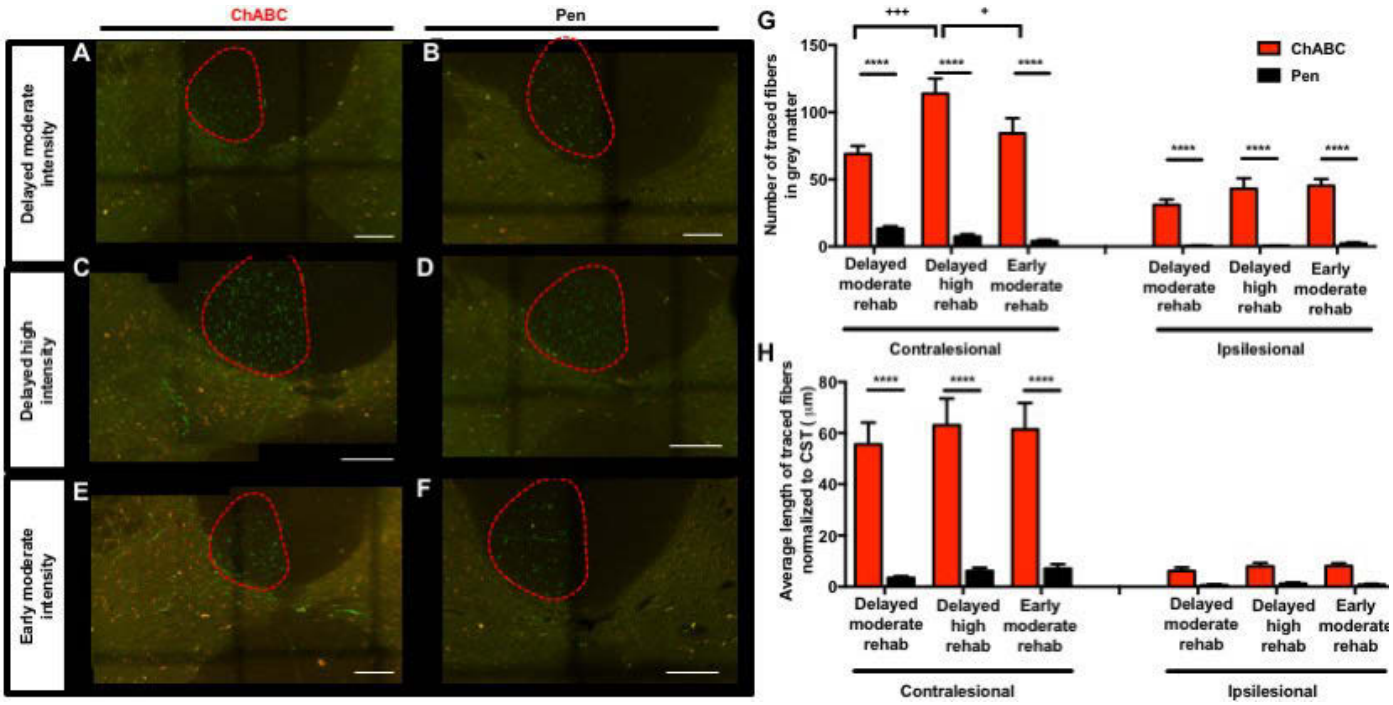

Figure 2.6. Histological analysis of anterograde tracer in animals receiving rehabilitative training. (**A-F**) Confocal microscopy of transverse sections through C4 showing CST fibers (Alexa-488 tagged dextran) originating from injections in the peri-infarct cortex. Representative sections are shown for animals receiving ChABC or Pen injection in the different rehabilitative training groups. Scale bars, 2mm. (**G**) Grey matter fiber counts showed a significant effect of treatment in both contralesional ($P < 0.0001$) and ipsilesional ($P < 0.0001$) grey matter. Significantly greater numbers of axon fragments were found in all ChABC treated groups relative to Pen controls receiving the same training (****, $P < 0.0001$). Notably, there was also a significant main effect of training on the contralesional side ($P = 0.0153$) and a significant interaction ($P = 0.027$), with delayed high intensity training significantly increased the number of labeled axon fragments in the grey matter in ChABC treated animals relative to ChABC treated animals receiving delayed ($^{+++}$, $P < 0.001$) or early ($^{+}$, $P < 0.05$) training at a moderate intensity.

(**H**) A significant main effect of treatment ($P < 0.0001$) was found on measures of average axon length in the spinal grey matter, with significantly greater axon length in ChABC treated animals (****, $P < 0.0001$) relative to Pen controls in every training group. There was no main effect of training group or significant interaction.

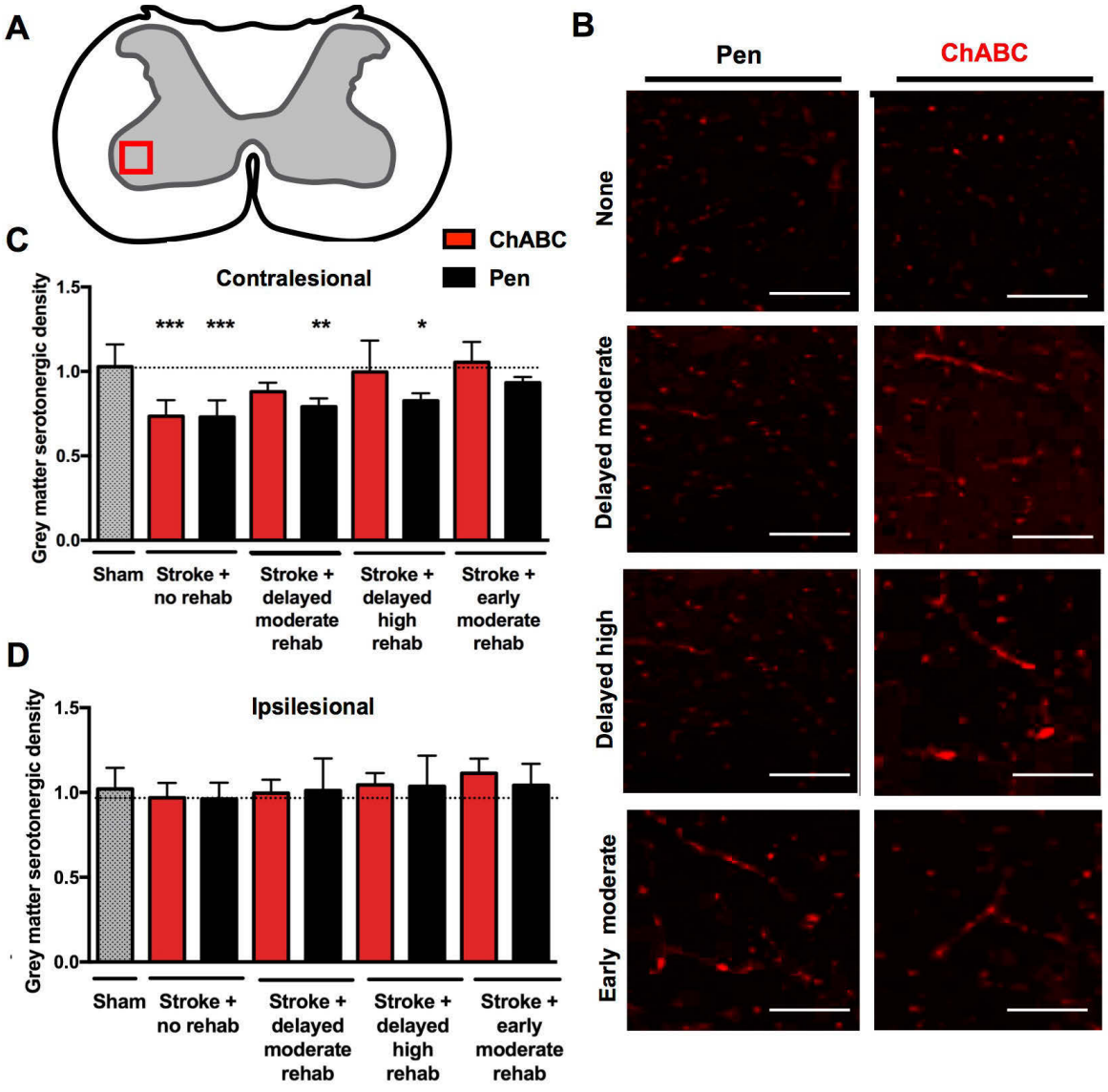

Figure 2.7. Changes in serotonergic fiber distribution in the cervical spinal cord (C4/5) grey matter. (**A**) Transverse spinal cord section, showing area of ventral horn grey matter selected for optical density quantification at C4. (**B**) ChAT labelled Serotonergic fibers (Texas red) from the area outlined in (**A**) of ChABC-treated rats or Pen controls under different training paradigms, Scale bar, 50 μm. (**C**) There was a significant main effect of treatment group on serotonergic density in the contralesional spinal grey matter (ANOVA, $P < 0.0001$). Notably, stroke significantly reduced contralesional serotonergic density relative to sham animals, and this

effect was not altered by ChABC treatment alone (without rehabilitative training; ***, $P < 0.001$). However, in ChABC treated animals receiving delayed training (both moderate and high intensity), there was no statically significant difference relative to shams. Pen controls receiving delayed training exhibited significantly reduced serotonergic density (**, $P < 0.01$; *, $P < 0.05$). Early rehabilitative training recovered serotonergic density, with no significant difference between ChABC-treated rats and Pen controls. (**D**) There was no main effect of treatment group on serotonergic density in the ipsilesional spinal grey matter ($P = 0.6960$).

Chapter 3:

In vitro cellular effects of chondroitinase ABC produced cleavage stubs

Introduction

Following central nervous system (CNS) injury such as stroke there is a marked upregulation of inhibitory chondroitin sulfate proteoglycans (CSPGs) (Sharma et al., 2012; Kwok et al., 2013; Burnside and Bradbury, 2014; Cua et al., 2013). Elevated CSPGs levels in the extracellular matrix (ECM) after injury have been shown to reduce plasticity and prevent neurite outgrowth in the CNS (Asher et al., 1995; Fawcett et al., 1989; Faulkner et al., 2004; Kawano et al., 2005). CSPGs are composed of a central protein O-linked to serine residues of multiple glycosaminoglycans (GAGs), which are unbranched sugar chains consisting of repeating disaccharide units with various sulfation patterns (Crespo et al., 2007). CSPG's inhibitory actions on neurite outgrowth may result from interaction with neuronal receptors (Snow et al., 1994; Sivasakaran et al., 2004), physical occlusion of growth promoting sites on the laminin (Zuo et al., 1998; McKeon et al., 1995), or high affinity sequestering of plasticity promoting factors (Crespo et al., 2007).

Digestion of CSPGs with the bacterial enzyme chondroitinase ABC (ChABC) has been shown to promote functional recovery after CNS injury (Moon et al., 2001; Soleman et al. 2012). Moreover, ChABC treatment provides neuroprotection against both primary and secondary inflammation after stroke enhancing neural survival, augmenting axonal growth, enriching synaptic plasticity and thereby promoting improved neurological function (Chen at al., 2014). Despite many studies on ChABC treatment after CNS injury it is still unclear how CSPG digestion promotes and enhances recovery (Deepa et al., 2002, 2004). It has been suggested that digestion products of ChABC (CSPG cleavage stubs) may play a crucial role in regulating plasticity.

Following ChABC digestion of proteoglycans, a number of unsaturated disaccharide

neoepitopes are generated at the non-reducing terminal of chondroitin sulfate glycosaminoglycan chains. ChABC digestion generates 3 main products: The C-0-S stub, which is an unsulfated chain produced by ChABC or CHACII enzymatic activity; the C-4-S stub, which is 4-sulfated and produced by ChABC digestion or after primary digestion by Chondroitinase B followed by subsequent digestion by Chondroitinase ACII or only dermatan sulfate glycosaminoglycan; and the C-6-S stub, which is 6 sulfated and generated via pre digestion with Chondroitinase ABC or Chondroitinase ACII (Hardingham et al., 1994). C-6-S is also found in undigested or 'native' chondroitin sulfate glycosaminoglycan chains consisting of a terminal glucuronic acid adjacent to 6-sulfatedN-acetyl-galactosamine (Hardingham et al., 1994; Del Rio et al., 2007). The chondroitinase-generated stub is commonly denoted as 3B3(+) for the 'native' terminal and as 3B3(-) for the digestion product epitope (we will use the term C-6-S to refer to the 3B3(-) epitope) (Maeda et al., 2010). These cleaved glycosaminoglycan side chains are thought to illicit an immune response and have been hypothesized to act as ligands at specific receptors based on sulfation patterns including the C-X-C ligand 12/C-X-C receptor 4 and leukocyte common antigen-related (LAR) family of receptors (Logun et al., 2016).

ChABC cleavage stubs are neoepitopes and are therefore highly immunogenic (Ekre et al., 1992; Glant et al., 1998), and many studies have focused on the interactions between ChABC cleavage byproducts and CNS immune cells including microglia, astrocytes and oligodendrocytes. After spinal cord injury, ChABC treatment has been found to reduce macrophage/microglia proliferation and induce a reduction in the number of newly generated astrocytes promoting their differentiation along an oligodendroglial lineage (Karimi-Abdolrezaee et al., 2012). Additional studies have demonstrated that ChABC treatment polarizes macrophages away from an inflammatory neurotoxic M1 phenotype (Kigeri et al., 2009) in favor of an anti-

inflammatory M2 phenotype, which promotes angiogenesis and tissue remodeling and limits secondary inflammatory-mediated injury (Bartus et al., 2014). Further studies have demonstrated that C-6-S treatment stimulates microglia to take on a novel regulatory neuroprotective phenotype marked by production of brain-derived neurotrophic (BDNF) and insulin-like growth factor 1 (IGF-1) (Rolls et al., 2005). In addition, microglia pre-incubated with C-6-S overcome the LPS-induced inhibition of IGF-1 expression, indicating microglia's cytokine response to biological activators is modified as a result of CSPG cleavage stubs (Rolls et al., 2005). Other studies have demonstrated that sulfated disaccharides derived from chondroitin sulfate proteoglycan protect against inflammation-associated neurodegeneration by modifying cytokine release profiles of invading immune cells (Rolls et al., 2006).

In this study, we first sought to investigate the direct regulation of neurite outgrowth by CSPG cleavage stubs. Specifically, we used a neuroblastoma cell line (SH-SY5Y) plated on growth inhibitory CSPG or growth permissive laminin matrices and directly applied digestion product 'stubs' (C-0-S, C-4-S or C-6-S) to the cell culture media and assessed neurite growth. In addition, we repeated this study incorporating the stubs into the matrices on which SH-SY5Y cells were grown, and again looked for augmentation of neurite outgrowth. Next, we investigated the role of CSPG cleavage stubs in modulating the microglial immune response. To determine this, we exposed isolated microglia in culture to cleavage stubs, then collected the media containing the immune factors released by the treated microglia. SH-SY5Y neuronal cultures were then incubated in this conditioned media to determine if microglia release factors which induce neurite outgrowth in a manner dependent on exposure to CSPG cleavage byproducts. We assayed the release of the well-established anti-inflammatory molecules including interleukin-10 (IL-10) and BDNF and pro-inflammatory molecules including nitric oxide (NO), tumor necrosis

factor-α (TNF-α), cytokines interleukin-6 (IL-6) and interleukin-1β (IL-1β) released by microglia that were left unstimulated or were biologically activated (with IFN-γ) after exposure to CSPG cleavage stubs. The effect of CSPG cleavage stubs on mixed glial populations, which consist not only microglia but astrocytes and oligodendrocytes as well (de Vellis and Cole, 2012), was also investigated. We used different combinations of biological activation to mimic primary injury in the CNS, with or without secondary inflammatory injury, and again assayed for different inflammatory and anti-inflammatory factors.

We found that both bound and free C-4-S cleavage stub directly promoted the outgrowth of neurites when cells were platted in inhibitory CSPG matrices but not on laminin, while C-6-S and C-0-S did not promote outgrowth of neurite in any plating condition. Further C-4-S cleavage stubs promote biologically activated microglia to release growth factor BDNF and anti-inflammatory molecule IL-10, while attenuating the release of pro-inflammatory factors NO and TNF-α, and media from activated microglia improved neurite outgrowth. Finally, we determined that C-4-S cleavage stubs induced mixed glial populations to release different factors during primary and secondary biological activation. After primary activation, C-4-S induced the release BDNF and attenuated the release of NO in mixed glial populations; however, after secondary inflammatory activation, C-4-S primed glial release of BDNF and the ant-inflammatory cytokine IL-10 while attenuating IL-1β and IL-6 release. Thus, this study identifies the trophic and anti-inflammatory effects of CSPG cleavage stubs and suggests potential of therapy with C-4-S stubs as a growth promoting and injury limiting therapy for stroke.

Materials and Methods

Reagents

The mouse anti-β-III tubulin antibody, anti-mouse Alexa 488 secondary antibody, Vectashield with 4′, 6-diamidino-2-phenylindole (DAPI), Retinoic Acid (RA), and the proteoglycan mixture were purchased from Cedarlane (Burlington, ON, CAN). Glycosaminoglycan (GAG) stubs (0S, 4S, 6S, or all the combined), chondroitinase ABC (ChABC), bovine serum albumin (BSA), dimethyl sulfoxide (DMSO), and Triton X-100 were purchased from Sigma Aldrich (Oakville, ON). All other reagents unless otherwise specified were purchased from ThermoFisher Scientific (Burlington, ON).

Cell culture – SH-SY5Y

The human SH-SY5Y neuroblastoma cell line was purchased from Cedarlane (Burlington, ON). Cells were maintained in DMEM-F12 supplemented with 10% FBS and antibiotics in a 37°C humidified 5% CO_2 incubator. Cells were differentiated with 10μM RA and grown in DMEM-F12 supplemented with 2.5% FBS for use in experiments.

GAG stubs and ChABC on neurite outgrowth of SH-SY5Y neuronal cells

Enhanced plasticity resulting in neurite outgrowth following ChABC treatment in the CNS may be mediated by a direct interaction of CSPG cleave stubs with receptors on neurite that augment and induce outgrowth. In this study, we sought to investigate the regulation of neurite outgrowth by specific CSPG cleavage byproducts. Specifically, we used a neuroblastoma cell line (SH-SY5Y) plated on growth inhibitory CSPG or growth permissive laminin matrices and introduced ChABC enzyme, individual digestion product ‘stubs’ (C-0-S, C-4-S or C-6-S), or a combination

of stubs to the culture media. We evaluated the effect of these treatments on the neurite outgrowth of SH-SY5Y cells plated on different matrices.

Before use in each assay, 24-well plates were coated with sterile mixtures of laminin (10μg/ml) or laminin (10μg/ml) plus proteoglycan mixture (5μg/ml) in phosphate buffered saline (PBS) and incubated for 1 h at 37°C. The plates were then rinsed with PBS before SH-SY5Y cells were seeded into each well at a concentration of 2 x 10^5 cells/ml in 0.4ml of DMEM-F12 containing 2.5% FBS. After seeding, cells were treated with 10 μM RA and incubated for 24 h in a 37°C humidified 5% CO_2 incubator. Following 24 h differentiation, cells were treated with 0.2U/mL ChABC, 5μg/ml GAG stubs, or PBS vehicle control and were placed back in the incubator. Following 72 h incubation, the cells were rinsed with PBS and used in immunocytochemistry experiments.

Effect of ChABC and GAG matrices on neurite outgrowth of SH-SY5Y neuronal cells

Before use in each assay, 24-well plates were coated with sterile mixtures of laminin (10 μg/ml), laminin (10 μg/ml) plus proteoglycan mixture (5 μg/ml), or laminin (10μg/ml), proteoglycan mixture (5 μg/ml), and GAG stub (5 μg/ml) or ChABC (0.2 U/ml) in phosphate buffered saline (PBS). Coated plates were then incubated for 1 h at 37°C. The plates were then rinsed with PBS before SH-SY5Y cells were seeded into each well at a concentration of 2 x 10^5 cells/ml in 0.4ml of DMEM-F12 containing 2.5% FBS. After seeding, cells were treated with 10μM RA and incubated for 96 h in a 37°C humidified 5% CO_2 incubator. Following incubation, the cells were rinsed with PBS and used in immunocytochemistry experiments.

Immunocytochemical assessment of neurite outgrowth in SH-SY5Y cultures

Cells were fixed in ice cold methanol for 0.5 h then blocked with 10% blocking solution (Dako) in 0.1% BSA for 1 h at room temperature. Wells were incubated with mouse anti-β-III tubulin in 0.1% BSA for 2 h at room temperature. For immunofluorescent visualization, culture plates were incubated with an anti-mouse Alexa 488 secondary antibody (1∶500) for 1 hour at room temperature. After three washes, Vectashield mounting media with DAPI was applied and a cover slip was mounted on top of cells. Negative controls without primary antibody were performed to rule out non-specific labeling by the secondary antibodies. Epifluorescent images were acquired using Leica DMI 6000B microscope mounted with Leica DFC365 FX monochrome camera at 40X. For neurite length calculations, four representative neurons in each well condition were traced and the measurement function in ImageJ was used to determine neurite length from the edge of the nucleus.

Neurite outgrowth of SH-SY5Y neuronal cells exposed to supernatants from ChABC stubs treated microglia

We sought to determine if ChABC or its cleavage products modulate the microglial immune response in the CNS leading to changes in neurite outgrowth. To determine this, we exposed microglia to ChABC or cleavage stubs, then we harvested the immune factors produced by the treated microglia and introduced them to SH-SY5Y neuronal cultures. Since CNS injury induces a state of microglial activation we repeated these experiments using microglia that had been activated with IFN-γ. It has been well established that cultured microglia activated by IFN-γ take on an similar secretory profile to those microglia injured by stroke in the CNS. This allowed us to assess changes in neurite outgrowth following exposure of neurites to factor expressed by

IFN-γ activated microglia treated with ChABC, cleavage stubs or vehicle solution. For use in transfer experiments, supernatant from previously plated microglia was aspirated and replaced with 1 ml of fresh DMEM-F12 containing 1% FBS. Microglia were treated with GAG stub (5μg/ml) or ChABC (0.2U/ml) in phosphate buffered saline (PBS), its vehicle solution (PBS) for 15 min before addition of 0.1 μg/ml IFN-γ or addition of equal volume of saline. After 72 h, 0.1 ml of supernatant was saved for future assays and 0.4 ml of cell-free supernatant was transferred to each well containing plated SH-SY5Y cells.

The human SH-SY5Y neuroblastoma cell line was purchased from Cedarlane (Burlington, ON). Cells were maintained in DMEM-F12 supplemented with 10% Fetal bovine serum (FBS) and antibiotics. Before use in each assay, 24-well plates were coated at 4°C with sterile mixtures of laminin (10 μg/ml) or laminin (10 μg/ml) plus proteoglycan mixture (5 μg/ml) in phosphate buffered saline (PBS). SH-SY5Y cells were seeded into each well at a concentration of 2 x 10^5 cells/ml and placed in a 37°C humidified 5% CO_2 incubator for 20mins. Then 0.4ml of DMEM-F12 containing 2.5% FBS was added to each well and cells were allowed to rest for 24 h. Overnight media was aspirated and SH-SY5Y cells were differentiated for 72 h with 10 μM RA. Differentiation media was aspirated and replaced with 0.4ml of cell-free supernatant from previously plated microglia and SH-SY5Y cells were incubated for 72h before being rinsed with PBS and used for immunocytochemistry.

Cell culture – Microglia

Since we found that C-4-S treatment of active microglia induced expression of factors which improved neurite outgrowth we wanted to study the expression profile of microglia treated with C-4-S at different time points before and after activation by IFN-γ. We looked for changes in

expression of well-established anti-inflammatory molecules such as IL-10 and the growth promoting neurotrophin BDNF. In Addition, we studied the release profile of pro-inflammatory molecules such as NO a marker of nitrate, TNF-α and cytokines IL-6 and interleukin-1β (IL-1β) which are known pro-inflammatory mediators.

Postnatal Day 1 rat microglia were isolated as previously described (Baskar Jesudasan et al., 2014). Briefly, mixed glia cultures were prepared from brain and spinal cord of post-natal Day 1 Sprague-Dawley rats. The meninges and blood vessels were removed from the brains and tissue was finely minced and dissociated enzymatically by 0.25% Trypsin-EDTA for 20 minutes at 37°C. Trypsin was inactivated with Dulbecco Modified Eagle Medium/Ham's F12 (DMEM-F12) containing 10% FBS and antibiotics (100 U/ml penicillin, 100 μg/ml streptomycin). The brain tissues were triturated mechanically in DMEM/F12 in 10% FBS with antibiotics and plated on poly-L-lysine coated T75 flasks.

After 14–21 days *in vitro* microglia were isolated by incubation with 150mM lidocaine. Briefly, 150mM of lidocaine in DMEM-F12 was added to mixed primary culture and incubated at 37°C in humidified 5% CO_2 incubator for 5 mins. Following incubation, flasks were agitated at 100 rpm at 37°C for 10 min then cells were collected and centrifuged at 2000 rpm for 2 minutes. Following centrifugation, supernatant was aspirated and DMEM-F12 was added to inactivate lidocaine, cells were centrifuged again for 8 minutes at 2000 rpm. Following centrifugation, cells were re-suspended, counted, and seeded into each well of a 24-well plate at a concentration of 1 x 10^5 cells/ml, in 0.4ml of DMEM-F12 containing 10% FBS and 0.4ml mixed glia conditioned media. Cells were then placed in a 37°C humidified 5% CO_2 incubator and allowed to rest overnight before use in experiments. Microglia were treated with GAG stub (25μg/ml) or ChABC (0.2U/ml) in phosphate buffered saline (PBS), its vehicle solution (PBS)

24 hours, 12 hours, 4 hours or 15 min before addition of 0.1 μg/ml IFN-γ or addition of equal volume of saline. After 72 h, 0.1 ml of supernatant was saved for future assays. In a second group Microglia were treated for 15 with GAG stub (25 μg/ml) or ChABC (0.2 U/ml) in phosphate buffered saline (PBS), its vehicle solution (PBS) 24 hours, 12 hours, 4 hours or 15 min after addition of 0.1 μg/ml IFN-γ or addition of equal volume of saline. After 72 h, 0.8 ml of supernatant was saved for future assays.

Cell culture - Primary mixed glia

In addition to its role in inflammation ChABC has been demonstrated to attenuate astrogliosis by reducing the generation of new astrocytes and promoting them to differentiate into an oligodendroglial lineage which is important for re-myelination after induced spinal cord injury (Karimi-Abdolrezaee et al., 2012). Thus we wanted to test the effects of the C-4-S cleavage stub on mixed glial cultures which consist of three main cell types: astrocytes, oligodendrocytes and microglia (de Vellis and Cole, 2012). In this study we used different combinations of biological activation to mimic primary injury in the CNS following by secondary inflammatory injury. Lipopolysaccharide (LPS) was used to induce primary injury following by C-4-S delivery, then a second inflammatory state was induced by IFN-γ. We used LPS for primary activation of glia as it induces a well characterized cytokine release profile in microglia (Nakamura et al., 1999; Baskar Jesudasan et al., 2014). Since LPS is a bacterial endotoxin, a secondary exposure may induce an adaptive immune response (Olson and Miller, 2004), therefore we used IFN-γ to induce an innate immune response and secondary inflammation. Using two biological activators is advantageous as there are many different populations of microglia with a distinct receptors resulting in different subsets of glia responding to LPS and IFN-γ (Pannell et al., 2014) by using

multiple methods of biological activation we prevent adaptive immune responses and ensure a more diverse subset of the microglia population are activated as multiple inflammatory activators are at work following CNS injury *in vivo*. We again assayed for pro and anti-inflammatory factors to see the influence of astrocytes, oligodendrocytes in combination with microglia on release of these factors. Briefly, mixed glia cultures were prepared from the brain of post-natal Day 1 Sprague-Dawley rats. The brains were placed in in Hank's balanced salt solution with 1 % penicillin-streptomycin (PS), the cortices and cerebellum were separated, and the meninges and blood vessels were removed. This tissue was finely minced and dissociated enzymatically by 0.25% Trypsin-EDTA for 20 minutes at 37°C. Trypsin was inactivated with Dulbecco Modified Eagle Medium/Ham's F12 (DMEM-F12) containing 10% FBS and antibiotics (1% PS). The brain tissues were triturated mechanically in DMEM/F12 in 10% FBS with 1% penicillin-streptomycin and plated on poly-L-lysine coated 12-well plates (1 ml 20 mg/ml PLL for 1 hour) with a ratio of 1 brain per plate at 1ml in each well. These plates were placed in a 37°C humidified 5% CO_2 incubator and allowed to rest for 2 weeks. DMEM/F12 (10% FBS, 1% PS), media was refreshed once per week. The cells were re-suspended with a 1 ml treatment of 0.09% Trypsin-EDTA for 20 minutes. Lifted cells were collected and centrifuged at 200 g, triturated in DMEM/F12 (10% FBS, 1% PS), and 1 ml per well was plated at a concentration of 1×10^5 cells/ml. Cells were then placed in a 37°C humidified 5% CO_2 incubator and allowed to rest for 3 days before use in experiments.

Direct effect of C-4-S on mixed glia & activated mixed glia

To study the direct effects of C-4-S on glial populations in a various states of biological activation we devised four biological conditions. First we tested the effects of 20 ng/ml of C-4-S

on glial cells which had not been exposed to a biological activator. Media was changed in mixed glial cells, 24 hours later 10 μl of PBS was added, cells were allowed to rest for 6 hours, then 20 ng/ml of C-4-S was added to the cultures which were allowed to rest for 18 hours before addition of another 10 μl of PBS after 24 hours the media was removed and assayed. In a second set of conditions (+LPS) we tested if C-4-S addition after a potent biological activation by LPS could alter the cytokine expression pattern of these activated glial. Again, media was changed in mixed glial cells, however this time after 24 hours 10 μl of LPS at 10 μg/ml was added, cells were allowed to rest for 6 hours, then 20 ng/ml of C-4-S was added to the cultures which were allowed to rest for 18 hours before addition of 10 μl of PBS after 24 hours the media was removed and assayed. In a third set of conditions (+IFN-γ) we sought to determine if pre-treatment for 18 hours with C-4-S would change cytokine expression 24 hours after activation with IFN-γ. Again media was changed in mixed glial cells, however this time 24 hours after media change 10 μl of PBS was added, cells were allowed to rest for 6 hours, then 20 ng/ml of C-4-S was added to the cultures which were allowed to rest for 18 hours before activation with of 10 μl of IFN-γ after 24 hours the media was removed and assayed. Finally, in a fourth set of activating conditions (+LPS, +IFN-γ) we wanted to test of C-4-S would affect the expression profile of mixed glia which had been activated by LPS and were in a 'primed' state before addition C-4-S, following C-4-S treatment glial were introduced to a secondary insult by +IFN-γ. Again media was changed in mixed glial cells, however this time 24 hours later 10 μl of LPS at 10 μg/ml was added, cells were allowed to rest for 6 hours, then 20 ng/ml of C-4-S was added to the cultures of these now 'primed' glia which were allowed to rest for 18 hours before addition of secondary activation in the form of 10 μl of IFN-γ at 10 μg/ml after 24 hours the media was removed and assayed. This study design allowed use to determine the effect of C-4-S on primed mixed glia

when exposed to a secondary insult mimicking the *in vivo* biological conditions in the CNS following stroke.

GRIESS assay

NO production was determined indirectly by measuring nitrite (NO_2) accumulation using the Griess reagent (Ding et al. 1988). Cell-free microglia culture media from experiments were collected and nitrite measurements were performed by mixing equal volumes (100 µl) of culture medium and Griess reagent (1% sulfanilamide, 0.2% N-1-naphthylethylenediamine in 3N HCl) followed by absorbance measurement at 570 nm on a spectrophotometer. Standard sodium nitrite solutions were used to calibrate absorbance readings.

ELISA (enzyme-linked immunosorbent assay)

The concentrations of growth factor BDNF, anti-inflammatory cytokine IL-10, and pro-inflammatory cytokines TNF-α, IL-6 and IL-1β in mixed glial culture media were measured by sandwich enzyme linked immunosorbent assay (ELISA). Briefly, 96 well plates were coated with goat anti-BDNF antibody (1:100, Santa Cruz Biotechnology, Dallas, TX) or anti-IL-10 antibody (1:100, Santa Cruz Biotechnology, Dallas, TX) or anti-TNF-α antibody (1:100, Santa Cruz Biotechnology, Dallas, TX) or anti-IL-6 antibody (1:100, Santa Cruz Biotechnology, Dallas, TX) or anti-IL-1β antibody (1:100, Santa Cruz Biotechnology, Dallas, TX) in 0.1M sodium bicarbonate buffer pH 9.6 and incubated overnight at 4°C. Following incubation, coating solution was removed and wells were blocked with 1% BSA/Skim milk powder for 2 h at room temperature. Following blocking, plates were rinsed in PBS-Tween 0.05% and either standards or samples were added to each well. Following incubation overnight at 4°C, plates were rinsed

with PBS-Tween and incubated with a biotin-conjugated anti-human secondary antibody (1:500, Peprotech, Rocky Hill, NJ) in PBS +1% BSA/Skim milk powder for 1 h, followed by Extravidin-alkaline phosphatase (1:10000 in PBS +1% BSA/ Skim milk powder) for 1 h. Fluorescence was developed by adding 0.2 mg/ml 4-MUP in diethanolamide (excitation 360nm and emission 440 nm) and fluorescent response was measured via microplate reader every 30 minutes until reaction end-point. Protein concentration was determined by linear regression.

Immunocytochemistry and confocal microscopy

To assess changes in glial populations we used immunochemistry following by florescent microscopy to differentiate between astrocytes, microglia and oligodendrocytes and quantified changes in cell populations. In addition, we looked for co-localization between specific glia cell types and inflammatory markers to asses which population of glia cells were responsible for the production of released factors. Finally scanning electron microscopy was performed to analyze mixed glial cell types and subtle anatomical changes in these cells induced by different combination of biological activation and C-4-S treatment.

At the end of treatment, cells were fixed in 5% PBS-buffered formalin (pH 7.4) for 10 minutes at room temperature. Each of the following sequential steps was preceded by washing 3x with PBS: fixed cells were blocked and permeabilized (PBS pH 7.4 supplemented with 1% HS and 0.1% Triton X-100 for 1 h), incubated with primary polyclonal rabbit Iba-1 (1:1000, Wako), monoclonal mouse iNOS (1:1000, abcam), and chicken polyclonal GFAP (1:5000, abcam) antibodies (PBS pH 7.4 with 0.1% HS, overnight at 4° C), incubated with secondary Alexafluor© 647 conjugated donkey-anti-mouse (1:500, Life Technologies), Alexafluor© 488 conjugated donkey-anti-rabbit (1:500, Life Technologies), and Alexafluor© 546 conjugated

goat-anti-chicken (1:500, abcam) antibodies (PBS with 0.1% HS, 2 h at room temperature), stained with Hoechst 33342, and mounted using Fluoromount-G (Southern Biotech). Confocal microscopy was performed on a Leica TCS-SPE inverted microscope. Post-processing was performed using ImageJ.

Statistical Analysis

Data are presented as means ± standard error of the mean (SEM). The effects of C-4-S *in vitro* with various activation patterns were evaluated statistically by the randomized block design analysis of variance (one-way or two-way ANOVA) followed by Tukey's Multiple Comparison *post hoc* test (n = 3, for each condition).

Results

Direct effect of soluble GAG stubs and ChABC on neurite outgrowth of SH-SY5Y neuronal cells

To determine the effect of directly treating neuronal cells with soluble GAG stubs or ChABC, differentiated SH-SY5Y cells were plated on either growth permissive laminin matrices or growth inhibiting CSPG matrices and then treated with GAG stubs C-0-S, C-4-S, C-6-S or all stubs combined at (5µg/ml), ChABC (0.2 U/ml) or vehicle control (PBS) and incubated for 72 h (Figure 3.1 A). Following incubation, neurite length was assessed via ICC images. There was a significant effect of treatment (ChABC or stubs) on cells plated with CSPG's (ANOVA; $F_{(5,12)} = 13.6$, $P = 0.0001$; Figure 3.1 B), whereas there was no effect of treatment with stubs or ChABC on cells plated on laminin (ANOVA; $F_{(5,18)} = 0.03123$; $P = 0.8991$; Figure 3.1 C). Treatment of SH-SY5Y neuroblastoma cells with C-4-S, but not C-0-S, C-6-S, combined stubs, or ChABC, significantly increased neurite length as determined by post hoc testing (Tukey's; $P = 0.0002$), but only when cells were plated on inhibitory CSPG matrices as shown in Figure 3.1. Figure 3.2 illustrates the morphology of SH-SY5Y cells grown a CSPG control (Figure 3.2 A) and SH-SY5Y cells grown a CSPG control after treatment with C-4-S (Figure 3.2 B).

Effect of GAG stub and ChABC matrices on neurite outgrowth of SH-SY5Y neuronal cells

To determine the effect of different matrices on neurite outgrowth, differentiated SH-SY5Y cells were plated on either growth permissive laminin matrices or growth inhibiting CSPG matrices with GAG stubs (5µg/ml), ChABC (0.2U/ml), or vehicle control integrated into the matrix (Figure 3.2 A). Cultures were incubated for 96 h, then neurite length was assessed via ICC images. Figure 3.2 illustrates the morphology of SH-SY5Y cells grown on a CSPG control

(Figure 3.2 A), SH-SY5Y cells grown on a CSPG matrices containing ChABC (Figure 3.2 C) and SH-SY5Y cells grown on a CSPG matrices containing stubs (Figure 3.2 D,E,F).

There was a main effect of treatment, and growth of SH-SY5Y neuroblastoma cells with C-4-S added to the plating matrix, but not C-0-S, C-6-S, combined stubs or ChABC, significantly increased neurite length when cells were plated with inhibitory CSPGs (ANOVA; $F_{(5,17)} = 2.847$, $P = 0.0480$) as shown in Figure 3.3 B. Post hoc testing confirmed that SH-SY5Y neuroblastoma cells on CSPG matrices with C-4-S had increased neurite length (Tukey's; $P = 0.048$) when compared to cells grown on CSPG matrices contain C-0-S, C-6-S, ChABC or control solution. However there was no effect of any stubs or ChABC on cells plated on laminin (ANOVA; $F_{(5,18)} = 0.8054$, $P = 0.5606$; Figure 3.3 C).

Neurite outgrowth of SH-SY5Y neuronal cells exposed to supernatants from C-0-S, C-4-S, C-6-S treated microglia

In these experiments, ChABC digestions stubs were tested for their ability to indirectly promote neurite outgrowth through induction of a trophic phenotype in microglia. Microglia were treated with C-0-S, C-4-S and C-6-S at a concentration of 25 ng/ml and results were compared to those obtained from samples treated with PBS vehicle solution only. Stubs or vehicle were added to microglia alone or microglia 15 min before stimulation with IFN-γ. Following 72 h incubation, cell free supernatants from the microglia cell cultures were transferred to SH-SY5Y cells to assess their neurite growth promoting activity (Figure 3.4 A). Following a 72 h incubation period, the neurite length was measured using ICC images.

When SH-SY5Y cells are plated on inhibitory CSPG matrices there is an effect of microglia supernatant. We found a significant effect of supernatant from microglial cultures

treated with ChABC generated stubs on neurite outgrowth of SH-SY5Y cells plated on CSPG (two-way ANOVA; $F_{(4, 30)} = 4.287$, $P = 0.007$; Figure 3.4 B). We also detected a significant effect of IFN-γ activated microglia on neurite outgrowth (two-way ANOVA; $F_{(1, 30)} = 32.96$, $P < 0.0001$). Only IFN-γ activated microglia treated with cleavage stubs produce factors which enhanced neurite outgrowth, and a significant interaction between IFN-γ and stub/vehicle treatment was identified (two-way ANOVA; $F_{(4, 30)} = 6.635$, $P = 0.0006$). Further post hoc analysis revealed a significant difference in neurite length of SH-SY5Y cells treated with supernatant from IFN-γ activated microglia treated with C-4-S compared to SH-SY5Y cells treated with supernatant from IFN-γ activated microglia treated with vehicle alone (Tukey's; P = 0.0025). C-4-S was the only stub which induced activated microglia to release factors which enhanced neurite growth on CSPG matrices and C-4-S only induced this effect when microglia were IFN-γ activated.

When SH-SY5Y cells are plated on permissive laminin matrices there is an effect of IFN-γ treatment but no effect of C-4-S treatment on the capacity of microglia supernatants to induce neurite outgrowth. We detected a significant effect of IFN-γ activation on microglia produced supernatant with respect to neurite outgrowth of SH-SY5Y cells when plated on CSPGs (two-way ANOVA; $F_{(1, 30)} = 31.10$, $P < 0.0001$; Figure 3.4 B). However we found no significant effect of ChABC generated stubs on the supernatant of microglia to induce neurite outgrowth of SH-SY5Y cells plated on laminin (two-way ANOVA; $F_{(4, 30)} = 0.9466$, $P = 0.4508$; Figure 3.4 C). There was also no significant interaction detected between C-4-S and IFN-γ ($F_{(4, 30)} = 1.122$, $P = 0.3647$) on microglia produced supernatant capacity to induce neurite outgrowth on laminin. In addition, post hoc testing revealed no significant effect of any stub on microglia supernatant added to laminin plated SH-SY5Y cells when compared to vehicle.

Exposing SH-SY5Y cells plated on laminin to supernatant from stub treated microglia (with or without IFN-γ activation), had no effect on neurite outgrowth (Figure 3.4 C) similar to SH-SY5Y cells plated on CSPG discussed earlier (Figure 3.4 B). Supernatant of unstimulated stub treated microglia did not induce any changes in neurite outgrowth on SH-SY5Y cells plated on CSPG's or laminin (Figure 3.4 B,C). Surprisingly, IFN-γ activated microglia treated with stubs released factors into supernatant that altered neurite outgrowth of SH-SY5Y plated on CSPG as discussed earlier, however this supernatant had no effect on SH-SY5Y cells when plated on laminin. In summary, our data suggest that supernatant of IFN-γ activated microglia treated with C-4-S induced neurite outgrowth of SH-SY5Y cells, but only when plated on CSPG matrices.

Effect of C-4-S on microglia viability and release of anti-inflammatory markers

To determine the effect of C-4-S on microglial cells directly, viability and cytokine release was measured. C-4-S was tested at concentration from 1 to 250 ng/ml and results were compared to those obtained from samples treated with PBS vehicle solution only. 25 ng/ml was found to be most effective concentrations of C-4-S in inducing cytokine release of growth factors and reducing inflammatory molecules, thus only data from 25 ng/ml concertation will be shown. C-4-S was added to microglia alone 24 hours, 12 hours, 4 hours or 15 minutes before stimulation with IFN-γ to determine if it would offer a protective effect (Figure 3.5 A). The same experiment was repeated except C-4-S was added 15 minutes, 4 hours, 12 hours or 24 hours after IFN- γ stimulation to determine the effect of C-4-S on already activated microglia (Figure 3.5 B). Following 72 h incubation, cell free supernatants from the microglia cell cultures were saved for GRIESS and ELISA assays and adherent microglia were assessed for viability via CVA.

CVA assays demonstrated that there was no significant effect of pretreatment at any time point with C-4-S on the viability of microglia alone (ANOVA; $F_{(3,20)} = 0.1055$, $P = 0.9959$) and there was also no effect C-4-S treatment following IFN-γ activation at any time point (ANOVA; $F_{(3,18)} = 2.44$, $P = 0.0974$; Figure 3.5 C).

To determine if the growth promoting effect of C-4-S detected earlier is in part mediated by factors expressed by microglia we looked at the release of BDNF, a known growth promoting trophic factors in the CNS. There was no significant effect of C-4-S on the release of BDNF in microglia pretreated with C-4-S before stimulated with IFN-γ (ANOVA; $F_{(4,17)} = 1.065.$, $P = 0.4038$). However, in microglia that were stimulated with IFN-γ and then treated with C-4-S, there was a significant effect of treatment (ANOVA; $F_{(4,15)} = 3.68$, $P = 0.0279$; Figure 3.5 D). Post hoc comparisons revealed that at C-4-S treatment of microglia 12 hours post IFN-γ activation is effective in significantly increasing BDNF production (Tukey's; $P = 0.0462$) when compared to vehicle treated microglia.

IL-10 is an established anti-inflammatory cytokine in the CNS. IL-10 concentrations were also quantified under the same treatment paradigms. There was no significant effect of treatment on the release of IL-10 in microglia when pretreated with C-4-S (ANOVA; $F_{(4,15)} = 0.3858$, $P = 0.8155$). However, IL-10 release was significantly affected by treatment with C-4-S after IFN-γ activation compared to vehicle treated control (ANOVA; $F_{(4,15)} = 7.176$, $P = 0.0019$; Figure 3.5 E). Post hoc testing revealed that C-4-S treatment significantly increased IL-10 release 12 hours (Tukey's; $P = 0.0202$) and 24 hours (Tukey's; $P = 0.0061$) after IFN-γ activation when compared to vehicle treated microglia.

Thus our data suggest that C-4-S at 25 ng/ml does not affect the viability of microglia cells. However, microglia cells treated with C-4-S 12-24 hours after IFN-γ activation have

enhanced release of growth and anti-inflammatory factors.

Effect of C-4-S on microglia release of pro-inflammatory markers

To further assess the immunomodulatory functions of C-4-S in microglia mediated inflammation, the effects of C-4-S on pro-inflammatory mediators release by microglia were also analyzed (Figure 3.5 A,B). Pretreatment of microglia with C-4-S before or following IFN-γ stimulation significantly affected the release of NO (ANOVA; $F_{(4,15)} = 3.465$, $P = 0.0340$ and $F_{(4,15)} = 4.609$, $P = 0.0126$, respectively; Figure 3.6 A). Post hoc testing revealed a significant reduction in NO release by microglia treated with C-4-S 15 minutes and 4 hours following stimulation with IFN-γ when compared to vehicle treated cells (Tukey's; $P = 0.00348$, $P = 0.0107$ respectively; Figure 3.6 A).

Similarly, TNF-α production was reduced in microglia given C-4-S treatment following IFN-γ (ANOVA; $F_{(4,15)} = 4.652$, $P = 0.0121$) however, pre-treatment with C-4-S had no significant effect on release of TNF-α (ANOVA; $F_{(4,15)} = 0.6671$, $P = 0.6247$; Figure 3.6 B). Post hoc comparisons identified a significant reduction in TNF-α release when C-4-S was administered 12 hours after IFN-γ activation (Tukey's; $P = 0.0347$) when compared to vehicle treated cells.

Interestingly, IL-1β production and release by microglia was significantly affected by C-4-S pre-treatment (ANOVA; $F_{(4,15)} = 5.934$ $P = 0.0045$; Figure 3.6 D) and post hoc testing revealed significant reductions in IL-1β (compared to vehicle control) at pretreatment time points of 4 hours (Tukey's; $P = 0.0342$) and 15 minutes (Tukey's; $P = 0.0058$). C-4-S administration at time points after IFN-γ stimulated also significantly affected IL-1β release (ANOVA; $F_{(4,15)} = 3.2$ $P = 0.0436$) but post hoc testing did not reveal any treatment time point at which IL-1β release

was significantly different than release from vehicle treated cells . IL-6 release was unaffected by C-4-S treatment at of microglia prior to activation (ANOVA; $F_{(4,15)} = 0.1546$, $P = 0.9579$) or following activation (ANOVA; $F_{(4,15)} = 0.179$, $P = 0.9457$) with IFN-γ, C-4-S did not have any effect on the release of pro-inflammatory molecules IL-6 from microglia (Figure 3.6 C).

Effect of C-4-S on mixed glial release of anti-inflammatory markers

While isolation of microglia permits mechanistic insight into the role of C-4-S in regulating their activation, *in vivo* environments included glial cells of multiple lineages that contribute to inflammation. To determine the effect of C-4-S on mixed glial cells in various conditions and different time points of biological activation, the release of well-established anti-inflammatory (BDNF, IL-10; Figure 3.7) and pro-inflammatory cytokines (NO, TNF-α, IL-6 and IL-1β; Figure 3.8) by mixed populations into cell culture media were assayed. To test the effect C-4-S on biologically activated glia, C-4-S (25 ng/ml) or vehicle (same volume as C-4-S) was introduced 6 hours after potent LPS activation (+LPS). In addition, the protective effect of C-4-S was studied and C-4-S or vehicle were added to mixed glia 12 hours prior to addition of biological activator IFN-γ (+IFN-γ). Finally, the effect of C-4-S or vehicle on 'primed' or activated glia exposed to a secondary insult were studied. In this case glia were again activated by LPS then treated with C-4-S or vehicle, however this time following C-4-S or vehicle treatment glial were exposed to a secondary insult by IFN-γ (+LPS, + IFN-γ) as this condition mimics primary biological insult following by secondary inflammatory insult common in injuries of the CNS (Figure 3.7 A).

Interestingly, C-4-S significantly increased BDNF release by mixed glia (two-way ANOVA; $F_{(1,64)}= 30.64$, $P<0.0001$; Figure 3.7 B). This effect was primarily observed in glial

cultures activated with LPS, and a significant effect of cell culture activation (two-way ANOVA; $F_{(3,64)} = 105.2$, P <0.0001; Figure 3.7 B) was detected along with a significant interaction of cell culture activation conditions and C-4-S treatment (two-way ANOVA; $F_{(3,64)} = 6.745$, $P = 0.0005$). Thus, C-4-S only induces BDNF release in activated glia and does not offer an effect on BDNF when added as a pretreatment before activation. Strikingly, post hoc analysis revealed a significant increase in BDNF production by C-4-S treated mixed glial cells activated with LPS or LPS + IFN-γ (Tukey's, $P = 0.0013$, $P < 0.0001$, respectively; Figure 3.7 B) when compared to the same cells treated with vehicle solution.

IL-10 an anti-inflammatory molecule in the CNS was nearly undetectable in mixed glial cultures alone and was increased after activation by LPS, IFN-γ or combined activation with LPS and IFN-γ. A significant effect of biologic activation in glial cultures was detected (two-way ANOVA; $F_{(3.64)} = 58.16$, $P < 0.0001$), as was a significant effect of C-4-S (two-way ANOVA; $F_{(1.64)} = 6.959$, $P = 0.0105$; Figure 3.7 C). A significant interaction of C-4-S treatment and activation conditions on IL-10 release was also detected (two-way ANOVA; $F_{(3.64)} = 16.78$, $P < 0.0001$). Post hoc analysis revealed that C-4-S treatment of LPS activated microglia with secondary activation via IFN-γ significantly increased IL-10 release when compared to mixed glial cultures under the same activation pattern but treated with vehicle (Tukey's; $P = 0.0166$).

Effect of C-4-S on mixed glial release of inflammatory markers

Since C-4-S drastically promotes the release of anti-inflammatory molecules in mixed glia populations, it is also important to study the role of C-4-S in the release of pro-inflammatory factors as well. NO is a potent marker of inflammation induced by glial cells and was measured using the GRIESS reaction.

C-4-S treatment was found to have a significant effect on NO release in mixed glial population (two-way ANOVA; $F_{(1,64)} = 14.8$, $P = 0.0003$). A significant effect of cell culture activation conditions was also detected (two-way ANOVA; $F_{(3,64)} = 3.465$ $P = 0.0212$; Figure 3.8 A). However no significant interaction between C-4-S treatment and activation conditions (two-way ANOVA; $F_{(3,64)} = 1.886$ $P = 0.1409$) was detected. Post hoc testing suggests that C-4-S only significantly altered NO release relative to vehicle in glial cultures that were activated with LPS prior to C-4-S administration (Tukey's; $P = 0.0051$).

TNF-α release was unaffected by C-4-S treatment (two-way ANOVA; $F_{(1,64)} = 2.531$, $P = 0.1164$), though cell culture activation did significantly impact mixed glial release of TNF-α (two-way ANOVA; $F_{(3,64)} = 5.361$ $P = 0.0023$; Figure 3.8 B). No significant interaction between C-4-S treatment and activation conditions was detected (two-way ANOVA; $F_{(3,64)} = 1.565$ $P = 0.2064$). Post hoc testing did not identify any condition in which C-4-S treated cells were significantly different form vehicle treated cells in terms of TNF-α release.

IL-6 was significantly affected by cell culture activation conditions (two-way ANOVA; $F_{(3,64)} = 114.3$ $P < 0.0001$) and C-4-S treatment (two-way ANOVA; $F_{(1,64)} = 56.09$ $P < 0.0001$; Figure 3.8 C), and a strong interaction between activation condition and C-4-S treatment was detected (two-way ANOVA; $F_{(3,64)} = 17.95$ $P < 0.0001$). IL-6 release was significantly different in C-4-S treated cells when compared to vehicle treated cells (Tukey's; $P < 0.001$) when C-4-S was administered to LPS activated glial before secondary IFN- γ activation.

In a very similar manner to IL-6, C-4-S treatment significantly affected the release or pro-inflammatory cytokine IL-1β (two-way ANOVA, Figure 3.8 D) as did glial activation conditions (two-way ANOVA; $F_{(1,64)} = 56.09$ $P < 0.0001$). There was also a strong interaction of treatment (C-4-S or vehicle) with activation conditions (two-way ANOVA; $F_{(3,64)} = 114.3$, $P <$

0.0001; Figure 3.8 D). Post hoc testing revealed that C-4-S significantly reduced IL-1β release by mixed glia exposed to dual activation by LPS and IFN-γ when compared to vehicle treated cells exposed to the same activation conditions in culture (Tukey's; $P = 0.0013$; Figure 3.8 D).

Thus, our data suggest that C-4-S restricts pro-inflammatory IL-1β and IL-6 cytokine release in activated mixed glial cultures exposed to a secondary biological inflammatory event and also reduces NO production after a primary inflammatory event.

Discussion

C-4-S directly promotes neurite outgrowth

In this study, we found that adding C-4-S stubs to SH-SY5Y cells increased neurite outgrowth, an effect that was limited to cells exposed to inhibitory CSPGs. Notably, the C-4-S stub was the only ChABC digestion product effective in improving outgrowth of neurites, and this effect was lost when C-4-S was administered in combination with C-0-S and C-6-S stubs. Treatment with the C-0-S stub alone reduced SH-SY5Y outgrowth when plated on growth permissive laminin, indicating that C-0-S maybe acting to prevent or restrict outgrowth. When CSPG stubs were incorporated into the matrices on which cells were grown, we again found that C-4-S improved neurite outgrowth. Under these condition, C-6-S reduced outgrowth relative to the control C-4-S administered in combination with C-0-S and C-6-S had no growth promoting effects.

There are several plausible reasons for the loss of C-4-S activity when in combination with other stubs. First, C-4-S may act at a specific receptor on the neurite which induces growth, C-4-S may have lower binding affinity for this site than C-0-S and C-6-S leading to it being out competed. Recent studies have provided evidence that CSPG's interact directly with cell surface receptors to induce growth inhibitory signaling in injured axons (Sharma et al., 2010). It possible that C-0-S or C-6-S stub interacts with these receptors to induce pathways which restrict growth, thereby nullifying the growth promoting effects of C-4-S. A second possibility is that C-0-S and or C-6-S act to reduce neurite outgrowth by promoting growth cone collapse, thus abolishing the trophic effect of C-4-S. Interestingly, in studies using synthetic polymers and biological enrichment of chondroitin sulfate which is di-sulfated (one sulfation at C-4 and one sulfation at C-6), the C-4,6-S motif was sufficient to induce growth cone collapse and inhibit neurite outgrowth in both CGN and DRG neurons (Brown et al., 2012; Shimbo et al., 2013; Glibert et

al., 2012). When the same tests were repeated using C-4-S and C-6-S, there was no growth inhibitory effect even at 100 times the concentration of that was need for C-4,6-S to induce inhibition (Brown et al., 2012). In similar studies, astrocytes which were lacking C-4,6-S were less inhibitory to cortical neuron outgrowth (Karumbaiah et al., 2011). Since it has been well established that sulfation patterns are important in rendering the biological activity of chondroitin sulfate proteoglycans, the varied responses of SH-SY5Y outgrowth to different chondroitin sulfate stubs is consistent with current literature.

C-4-S promotion of neurite outgrowth is CSPG dependent

Another key finding of this study is that C-4-S was only effective in promoting neurite outgrowth when added to cultures or incorporated into CSPG-matrices. There was no effect of C-4-S when given to SH-SY5Y cells grown on laminin or when incorporated into laminin matrices. Thus, the presence of CSPGs are necessary for C-4-S to induce detectable growth promotion above baseline. This is not entirely surprising as other growth factors have previously been shown to depend on binding to heparin sulfate (HS) chains of the neuron surface to induce their effect (Rauvala et al., 1994). The transmembrane tyrosine phosphatase gamma (PTPσ) regulates neurite outgrowth and plays key role in the interaction of proteoglycans and proteins. Recently, PTPσ was shown to mediate CSPG inhibition of neurite outgrowth by binding to the side chains of CSPG. Since C-4-S is a cleaved product of the side chain, it is possible that it can still interact with PTPσ thus reducing the CSPG inhibition (Shen et al., 2009; Coles et al., 2011). Chondroitin sulfates are also known to modulate intercellular signaling pathways and can localize soluble ligands to facilitate interaction of the ligand with cell surface receptors, thus the CSPG matrices may play an essential role facilitating the interaction of C-4-S with the receptors

on which it acts to promote neurite outgrowth. Studies have demonstrated that presentation of C-4,6-S ligand on the cell surface can enhance nerve growth factor signaling leading to improved neurite outgrowth (Pulsipher et al., 2014). In addition, CSPGs have been reported to interact with PTPσ, LAR phosphatase, NgR1 and NgR3 (Dickendesher et al., 2012; Fisher et al., 2011; Shen et al., 2009), to induce intercellular cascades with a variety of biological consequences. Thus, it is possible that C-4-S requires CSPG to facilitate interaction with the neurite cell surface in order to induce its growth promoting effects. Alternatively, these effects may only be detectable beyond baseline growth in the presence of inhibitory ECM components.

C-4-S induces microglia to release neurite outgrowth promoting factors

Our data also show that C-4-S treatment of IFN-γ activated microglia induced the release of factors that improved SH-SY5Y neurite outgrowth of cells plated on both CSPG and laminin matrices. This result lead us to examine the cytokine release profiles of microglia treated with C-4-S at various times before and after activation with IFN-γ. We found that C-4-S treatment hours after microglia activation induced release of BDNF and IL-10. The increased production of BDNF may explain the growth promoting effect of supernatant from activated microglia treated with C-4-S in SH-SY5Y cells, since this supernatant would contain high levels of growth factor. It is well established that BDNF interacts with TrkB receptors to induce neurite outgrowth (O'Neil et al., 2016; Sasi et al., 2017). While IL-10 has no established role in prompting neurite growth, it is known to reduce the production of TNF-α, IL-1β, IL-12 an IFN-γ. TNF-α is known to cause atrophy and reduction of synaptic markers (O'Neil et al., 2016) therefore reduction in these inflammatory factors by IL-10 may prevent degeneration of new neurite outgrowth. Furthermore, in monoculture studies of human neurons, addition of an inflammatory cytokine

mixture containing TNF-α and IL-1β restricted neurite growth and was neurotoxic under conditions of prolonged exposure (over 24 hours; Efremova et al., 2017). Thus a C-4-S mediated reduction in inflammatory cytokines may prevent growth inhibition and neurotoxicity particularly after injury when these inflammatory cytokines are up regulated.

C-4-S reduces release of pro-inflammatory cytokines from microglia

Not only did C-4-S did induce the production of anti-inflammatory molecules, it also reduced release of pro-inflammatory molecules. This reduction in inflammatory cytokine release is relevant to the secondary inflammatory damage that follows CNS injury and can perpetuate primary damage and further limit functional outcomes. Silencing the expression of full length CSPGs sulfated at carbon 4 in microglia cultures (using siRNA) prevents LPS induced mRNA expression of iNOS and cytokines including IL-1β, and TNF-α, indicating a key role of CSPG in inflammation (Gao et al., 2010). Interestingly only silencing expression of CSPGs that are sulfated at carbon 4 induces a reduction in the expression inflammatory cytokines from microglia. Therefore, it is likely that the cleave of full length pro-inflammatory CSPG into the C-4-S stub is essential to the mechanism of ChABC action *in vivo*.

Recent studies by biomaterial engineers have found that coating implant substances with chondroitin sulfate chains drastically reduces inflammatory responses. Biomaterials coated with polyelectrolyte multilayers (PEMs) composed of CSPG stubs or control chitosan were introduced to mixed glial cultures. Expression of IL-1β in response to implants was drastically reduced (over two fold) by CSPG stub coatings when compared to chitosan coating 24 hours after introduction of the biomaterials (Zhou et al., 2016). The CSPG sub coating also reduced macrophage adhesion, macrophage spreading morphology and foreign body giant cell formation

in response to the implanted biomaterial in culure (Zhou et al., 2016).

Chondroitin sulfates have also been shown to play an important role in mediating TNF-α expression. Treatment of obese mice with 1 g/kg/day of CSPG sulfate stubs (from bovine origin with a disaccharide sulfation profile of 63% of 4-sulfated, 31% of 6-sulfated and 6% of O-sulfated) administered by intraperitoneal injection reduced serum concentrations of IL-1β by 70% and TNF-α by over 80% after 6 days of treatment (Melgar-Lesman et al., 2016). Further, in culture studies of coronary endothelial cells and monocytes, stimulation with TNF-α induced a less pro-inflammatory cytokine response when cells were treated with chondroitin sulfates (C6S from shark cartilage and C4S from bovine trachea, mixed) (Tan and Tabatha, 2014). Of particular interest is the ability for chondroitin sulfates to reduce the activation of the TNF-α signaling pathway in endothelial cells by both the pERK and NFkB pathways (Melgar-Lesman et al., 2016; Tan and Tabatha, 2014). The binding of NF-κB to the promoter of target genes enhances the expression of pro-inflammatory cytokines including inducible nitric oxide synthase, thus treatment with C-4-S could act through a similar mechanism to reduce NO as observed out our study (Vallieres et al., 2008). In hippocampal slice models of glucose deprivation (OGD) followed by reoxygenation (OGD/Reox), chondroitin sulfates can modulate the local immune response to favor a reduction of inflammatory molecules including NO (Maetin-de-Saaverdra et al., 2011). Inducing OGD/Reoxygenation injury in hippocampal slices results in increased (1.5 fold) phosphorylation of p38 a promoter of cell death and inflammation (Xia et al. 1995) and enhanced expression (2.5 fold) of iNOS (an inducible enzyme which synthesizes NO) (Maetin-de-Saaverdra et al., 2011). However, when hippocampal slices were pretreated with chondroitin sulfate stubs (consists of a mixture of CS sulfated in position 4 (62%), 6 (32%) or unsulfated (6%) on the N-acetyl-D-galactosamine group) before OGD/Reoxygenation, injury induced

changes in p38 phosphorylation were inhibited and iNOS expression remained at basal levels (Maetin-de-Saaverdra et al., 2011). These studies demonstrate the complex role of chondroitin sulfate stubs in regulating intracellular pathways associated with expression of inflammatory factors.

C-4-S induces production of trophic factors in mixed glia

When we expanded our study to include mixed glial populations of microglia, astrocytes and oligodendrocytes, we found substantial increase (3 fold) in BDNF production by mixed glial compared to microglia alone following activation with LPS. The finding that LPS activated mixed glial cultures produce more BDNF than LPS activated microglia cultures alone is not entirely surprising as BDNF has been shown to be produced by astrocytes (Miyamoto et al., 2015) after cortical injury and oligodendrocytes (Segura-Ulate et al., 2017) in the cortex. Further after spinal cord injury BDNF is found to co-localized with all three glia subtypes in regions near the induced injury (Dougherty et al., 2000). Thus, the BDNF found in the supernatant of mixed glial is likely produced by all three glial subtypes and explains why more BDNF is observed in mixed glia when compared to microglia alone. In addition, when mixed glia were treated with C-4-S and activated with LPS followed by secondary activation with IFN-γ more BDNF was produced than in cultures activated with LPS or IFN-γ alone. It is likely that once glia are activated by LPS they are in a 'primed' state which allows them to rapidly respond to secondary perturbations and express programs associated with injury repair. This may explain why mixed glia produced substantially more BDNF in the condition of dual activation.

C-4-S reduces inflammatory factors released by mixed glia

When mixed glial cultures where activated with LPS or IFN-α alone, C-4-S treatment did not alter the expression of pro-inflammatory cytokines. However, when mixed glia were activated with LPS and IFN-α sequentially, C-4-S induced a 2 fold reduction in IL-1B release when compared to dual activated mixed glia treated with vehicle. This finding that C-4-S reduces IL-1B release after dual activation of microglia (LPS followed by IFN-α) and not by LPS alone was initially not expected. However, mixed glia may require a 'primed' or 'activated' state in order to induce their effects on IL-1B release. These finding are supported by evidence of similar mechanism in different immune cell types. In THP-1 macrophages, chondroitin sulfate treatment was ineffective after LPS and hyaluronic acid activation treatments alone and did not elicit ant-inflammatory response. However, primed with LPS, HA fragments produced large dose-dependent increases in IL-1β, this increase was attenuated by chondroitin sulfate treatment (Stabler et al., 2017). Similar to our study the ability of chondroitin sulfate to reduce expression of inflammatory IL-1B was only conferred in immune cells which were activated by LPS followed by a secondary inflammatory event.

Astrocytes play an important part in inflammation and their contribution to release factors in media collected form mixed glial cultures cannot be ignored. In studies of rat astrocyte cultures stimulated with LPS, chondroitin sulfate prevented translocation of p65 to the nucleus, reduced TNF-α mRNA and mitigated both cyclooxygenase 2 (COX-2) and inducible nitric oxide synthase (iNOS) induction by LPS (Canas et al., 2010). Therefore, C-4-S may could afford neuroimmunomodulatory actions under conditions of biological activation with LPS (Canas et al., 2010). In astrocytes, LPS mediated activation of toll-like receptor-4 (TLR-4) complex induces signaling pathways including the myeloid differentiation primary response protein-88

(MyD88) and the tumor necrosis factor receptor-associated factor-6 (TRAF-6). This activation results in downstream dysregulation of NF-κB leading to detrimental inflammatory response (Campo et al., 2009). Chondroitin-4-sulfate and chondroitin-6-sulfate act through a TLR 4 dependent pathway to significantly inhibited MyD88, TRAF-6 and downstream NF-κB activation, the inflammation cytokines, and inducible nitric oxide synthase (Campo et al., 2009). Our data suggests that CSPG cleavage byproducts, in particular the C-4-S stub, is a key mediator of neurite outgrowth and an important regulator of glial cytokine expression profiles.

Chapter 3: Figures

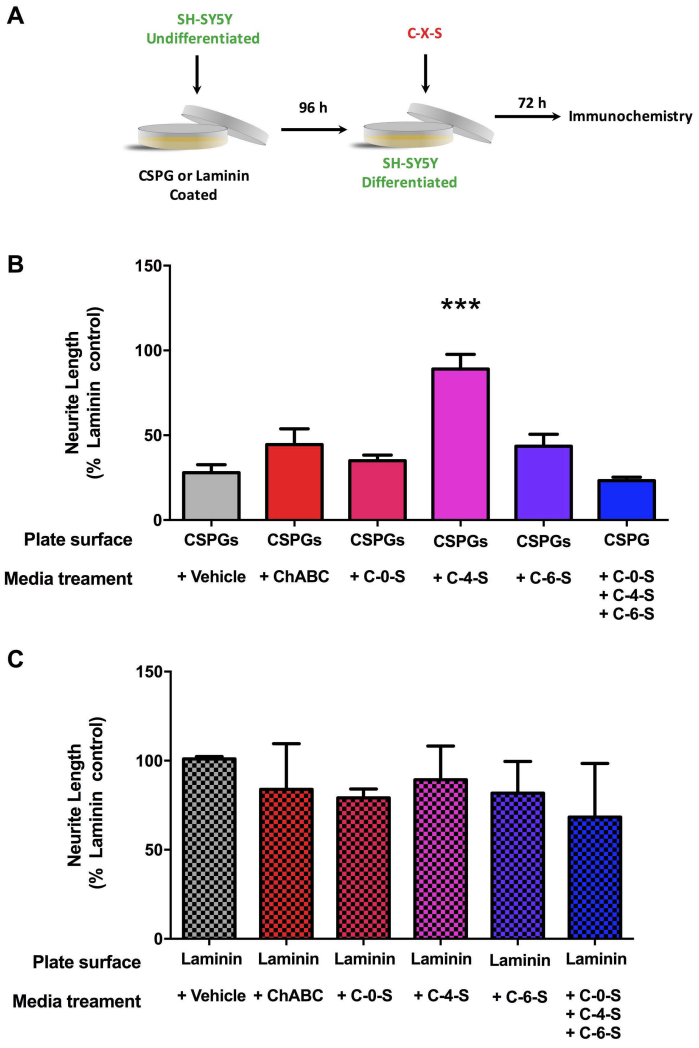

Figure 3.1. C-4-S increases neurite length in SH-SY5Y neuroblastoma cells. (**A**) Experimental design to determine the effects of stubs (C-X-S) or ChABC on the neurite length of SH-SY5Y neuronal cells grown on (**B**) CSPG matrices (5µg/ml) or (**C**) laminin and treated with 5 µg/ml stubs (C-0-S or C-4-S or C-6-S or all stubs combined) or 0.2 U/ml ChABC was examined. Data from 3 independent experiments are presented as a percentage of neurite length compared to control cells. The effects of treatment were assessed by the randomized block design ANOVA, followed by Tukey's multiple comparison post-hoc tests. *** $P < 0.001$, significantly different from all other treatments and cells treated with the vehicle solution only. Neurite length of SH-SY5Y cells on CSPG were significantly affected by treatment stubs or ChABC (ANOVA; $F_{(5,12)} = 13.6$, $P = 0.0001$) whereas cells plated on laminin matrices where not (ANOVA; $F_{(5,18)} = 0.03123$; $P = 0.8991$).

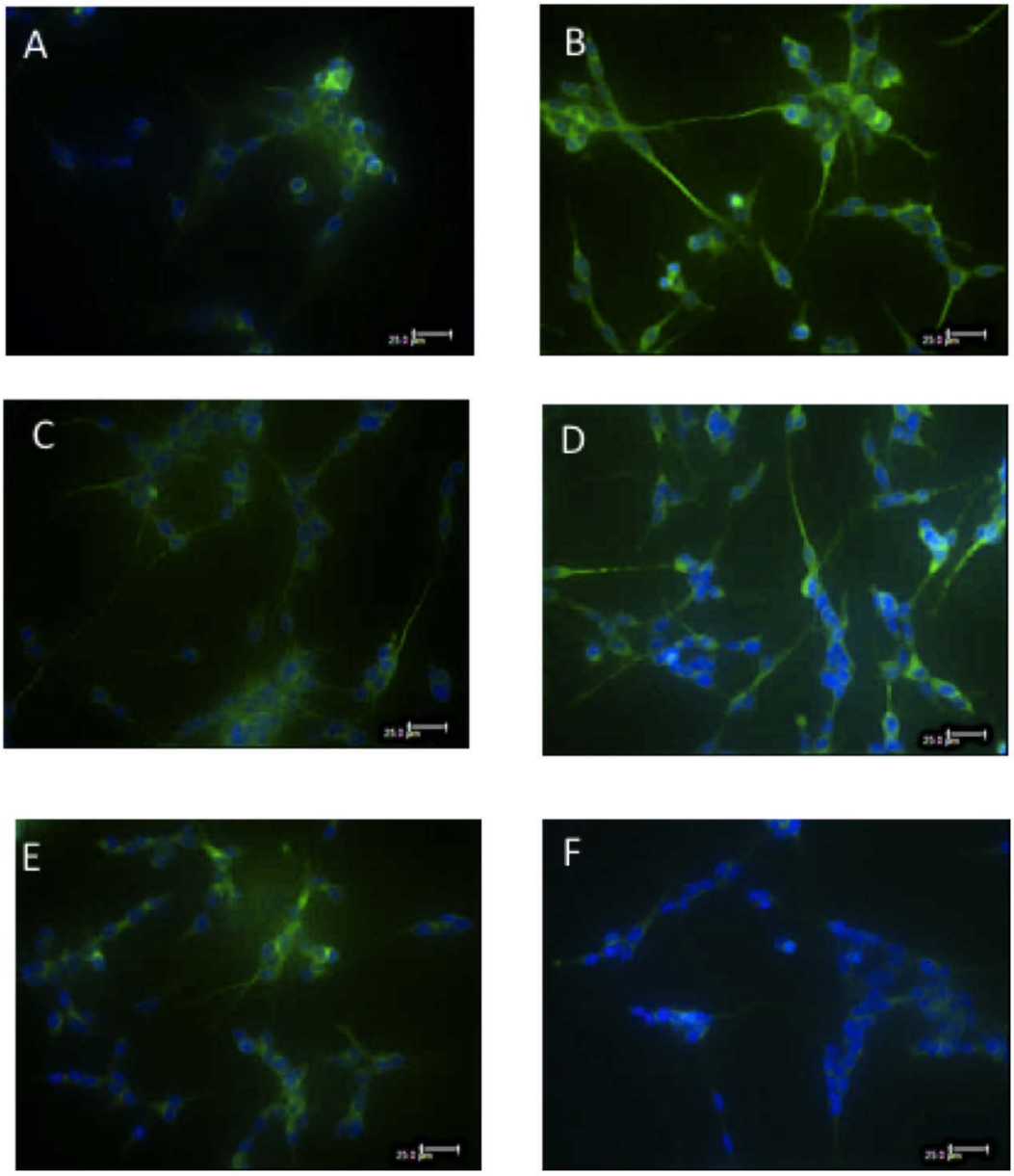

Figure 3.2. Immunofluorescence microscopy of SH-SY5Y cells. Epifluorescent images of SH-SY5Y cells cultures acquired at 40X, neurite processes identified in green with β-III tubulin (Alexa 488) and cell bodies labeled with nuclear stain DAPI (blue). (**A**) SH-SY5Y cells cultures grown a CSPG control. (**B**) SH-SY5Y cells grown on CSPG matrix and treated with C-4-S. (**C**) SH-SY5Y cells grown on CSPG matrices containing ChABC. (**D-F**) SH-SY5Y cells grown on CSPG matrices containing stubs: C-4-S (**D**) or C-6-S (E) or C-0-S (**F**). Photos are representative of 3-4 independent experiments. Scale bar = 25 μm.

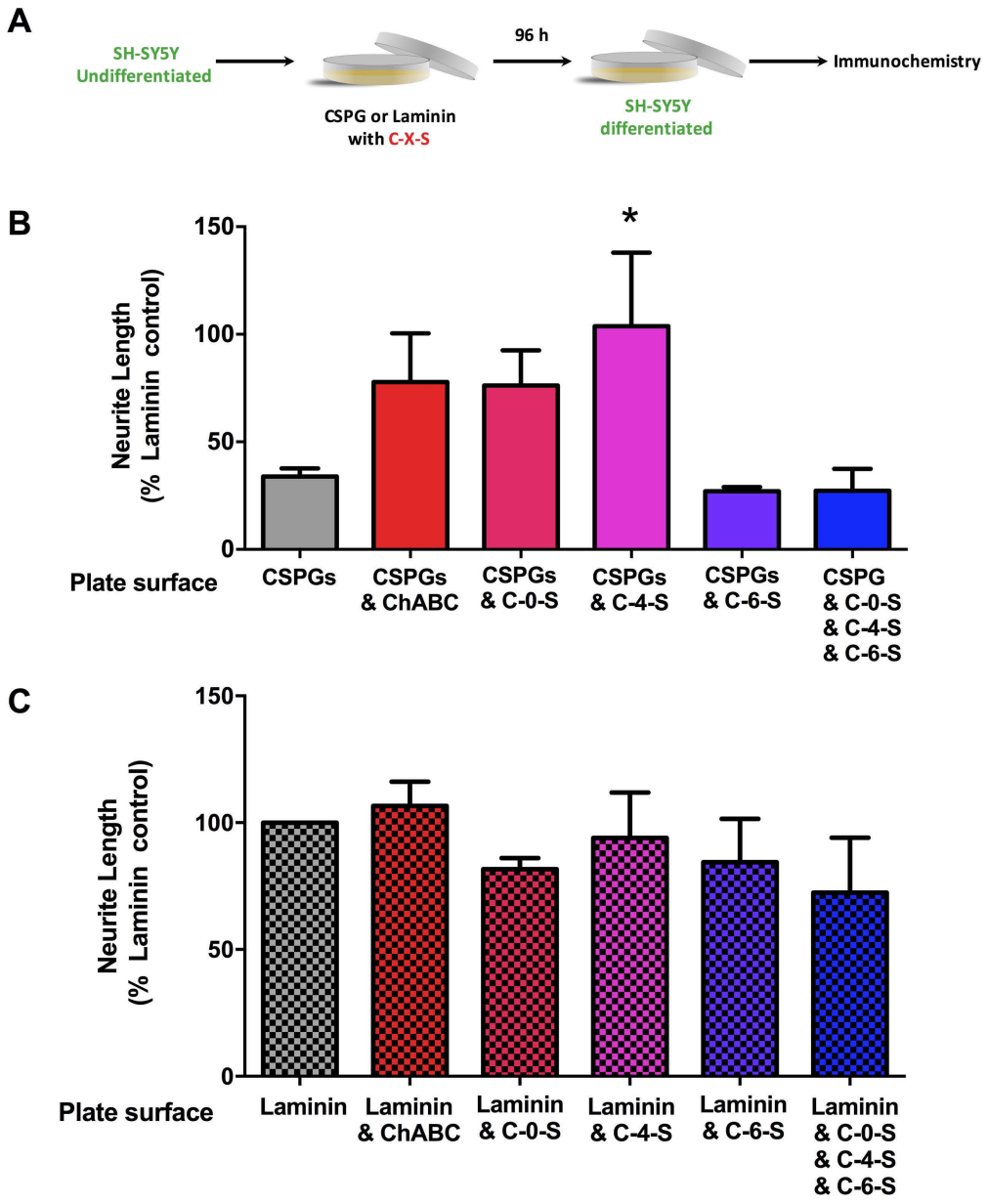

Figure 3.3. C-4-S added to CSPG matrices increases neurite length in SH-SY5Y neuroblastoma cells. (A) Experimental design to determine the effects of GAG stubs (C-X-S) or ChABC on the neurite length of SH-SY5Y neuronal cells grown on CSPG matrices (5µg/ml) in the presence (**B**) or absence (**C**) of 5 µg/ml GAG stubs or 0.2 U/ml ChABC was examined. Data from 3-4 independent experiments are presented as a percentage of neurite length compared to control cells. The effects of treatment were assessed by the randomized block design ANOVA, followed by Tukey's multiple comparison post-hoc tests. * $P < 0.05$, significantly different from all other treatments and cells grown with the vehicle solution only.

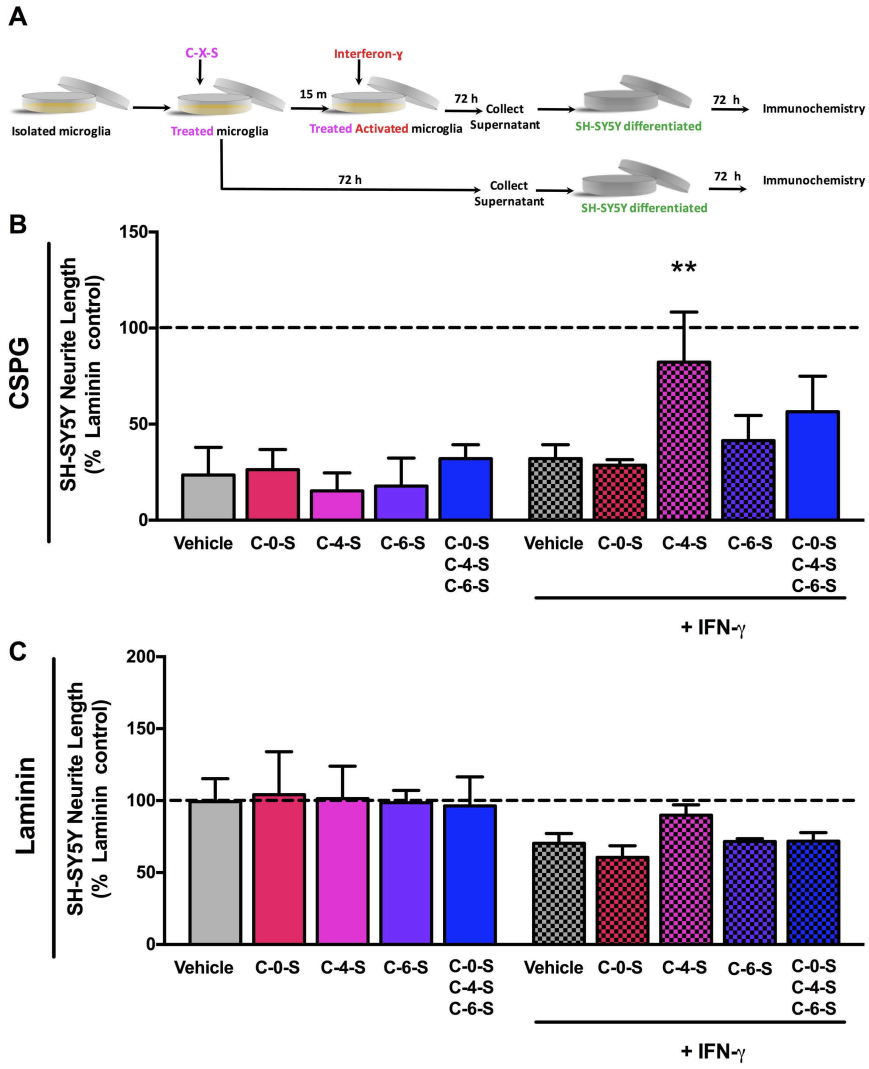

Figure 3.4. C-4-S restores CSPG inhibited SH-SY5Y neurite length after treatment with stimulated microglia cell supernatants only. (**A**) Experimental design to determine the effects of ChABC cleavage stubs (C-X-S) on the neurite length of SH-SY5H neuronal cells plated on (**B**) CSPGs or (**C**) Laminin, exposed to supernatants from primary rat microglia with or without stimulation by IFN-γ in the presence or absence of C-0-S, C-4-S, C-6-S or all stubs combined at 25 ng/ml was examined. Data from 4 independent experiments with cells obtained from four different microglial preparations are presented. The effects of ChABC stubs were assessed by the randomized block design two-way ANOVA, followed by Tukey's multiple comparison post-hoc test. ** $P < 0.01$, significantly different from stimulated samples treated with the vehicle solution only.

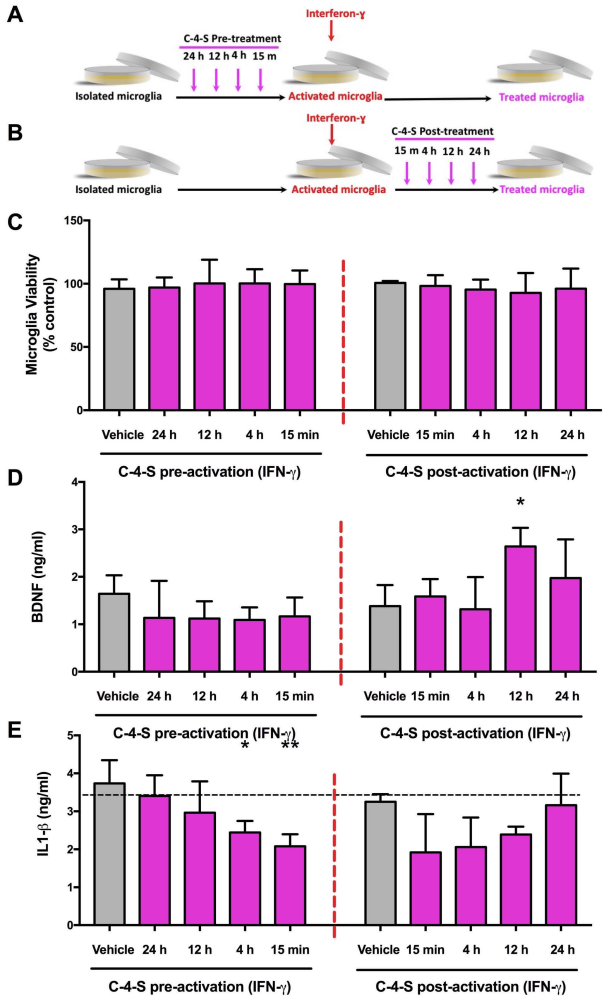

Figure 3.5. C-4-S does not affect microglia viability but improves the release BDNF and IL-10 when administered at specific time points after activation in rat microglia.

(**A**) Experimental design where Microglia were pre-treated at various time points with C-4-S (25 ng/ml) or its vehicle solution (PBS) before stimulation with IFN-γ (150 U/ml). (**B**) Experimental design in which Microglia were treated with C-4-S (25 ng/ml) or its vehicle solution (PBS) at various time points after stimulation with IFN-γ (150 U/ml). Following 72 h incubation, microglia viability was assessed by CVA (**C**) and concentrations of BDNF (**D**) and IL-10 (**E**) in cell-free supernatants were measured by ELISA. The horizontal dashed lines indicate the viability or concentration of mediators in supernatants from untreated microglia. Data from 3-7 independent experiments are presented. The effects of C-4-S were assessed by the randomized block design ANOVA, followed by Tukey's multiple comparison post-hoc test (**, $P < 0.01$ and *, $P < 0.05$).

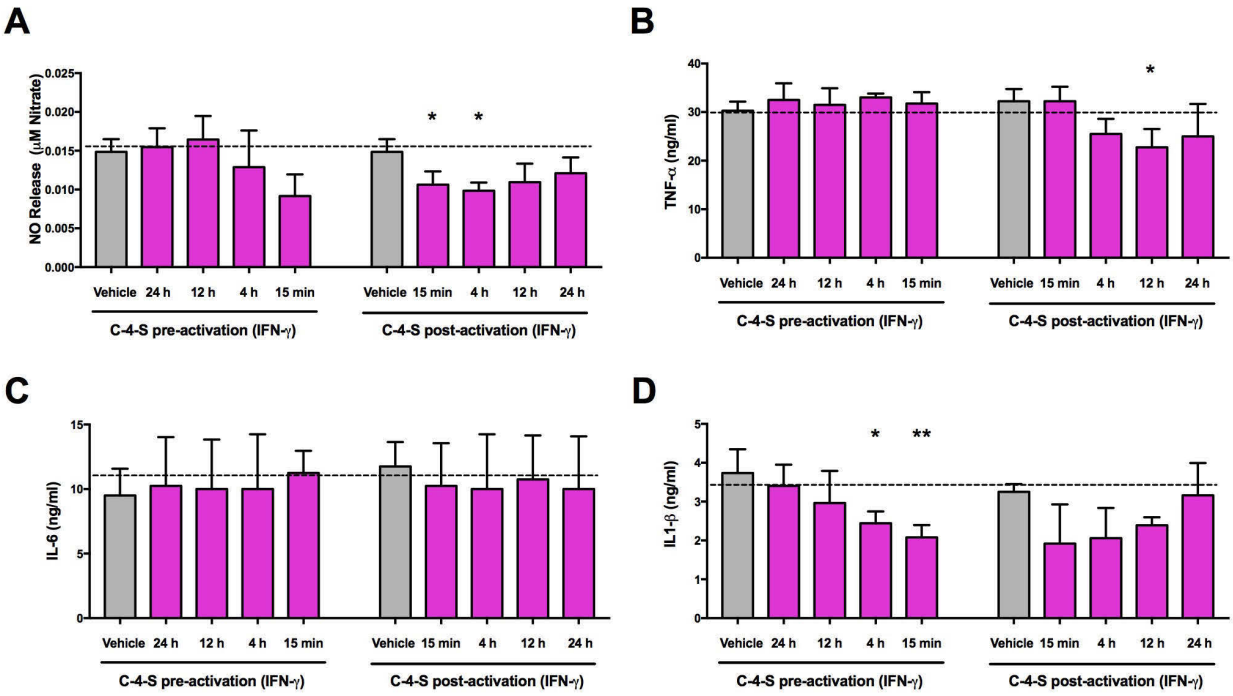

Figure 3.6. C-4-S reduces the release of NO, TNF-α and IL-1β from microglia cells stimulated with IFN-γ. C-4-S does not affect secretion of IL-6 by primary rat microglia cells. Microglia were treated with C-4-S at various time point before or after stimulation with IFN-γ (150 U/ml). After 72 h incubation and concentrations of NO (**A**) were measured by GRIESS; TNF-α (**B**), IL-6 (**C**) and IL-1β (**D**) in cell-free supernatants were measured by ELISA. The horizontal dashed lines indicate concentration of mediators in supernatants from untreated microglia. Data from 3-7 independent experiments are presented. The effects of C-4-S were assessed by the randomized block design ANOVA, followed by Tukey's multiple comparison post-hoc test (* $P < 0.05$; ** $P < 0.01$, significantly different from stimulated samples treated with the vehicle solution only).

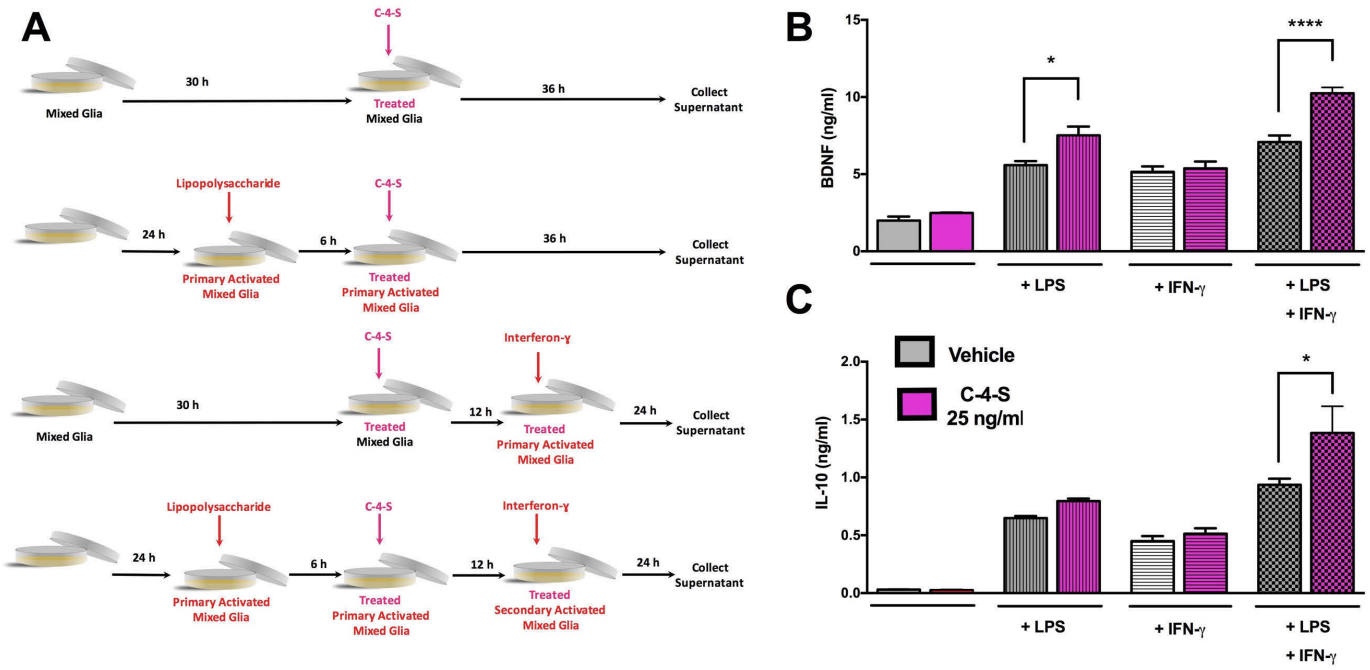

Figure 3.7. C-4-S increases the release of BDNF from mixed glia population when stimulated with LPS and increases release of both BDNF and IL-10 in cells stimulated with LPS followed by IFN-γ. (A) Experimental design in which mixed glial cell populations were treated with C-4-S (25ng/ml) or vehicle under 4 conditions: no stimulation, LPS stimulation followed by C-4-S or vehicle treatment, pre-treatment with C-4-S or vehicle followed by IFN-γ stimulation or dual activation where cells were stimulated with LPS followed by C-4-S or vehicle treatment which was followed by a second activation of these already primed glia via IFN-γ. (**B**) There was a significant effect of C-4-S on BDNF release by mixed glia (two-way ANOVA; $F_{(1,64)}= 30.64$, $P < 0.0001$) and a significant difference in post hos testing of BDNF release between C-4-S and vehicle treatment in the LPS activation and dual activation (LPS and IFN-γ) conditions (*, $P = 0.0013$; ****, $P < 0.0001$), respectively). (**C**) There was a significant effect of C-4-S in IL-10 release (two-way ANOVA; $F_{(1.64)} = 6.959$, $P = 0.0105$) and a significant difference in post hos testing of BDNF release between C-4-S and vehicle treatment in the LPS activation and dual activation (LPS and IFN-γ) conditions (*, $P = 0.0131$)The effects of C-4-S were assessed by the randomized block design two-way ANOVA, followed by Tukey's multiple comparison.

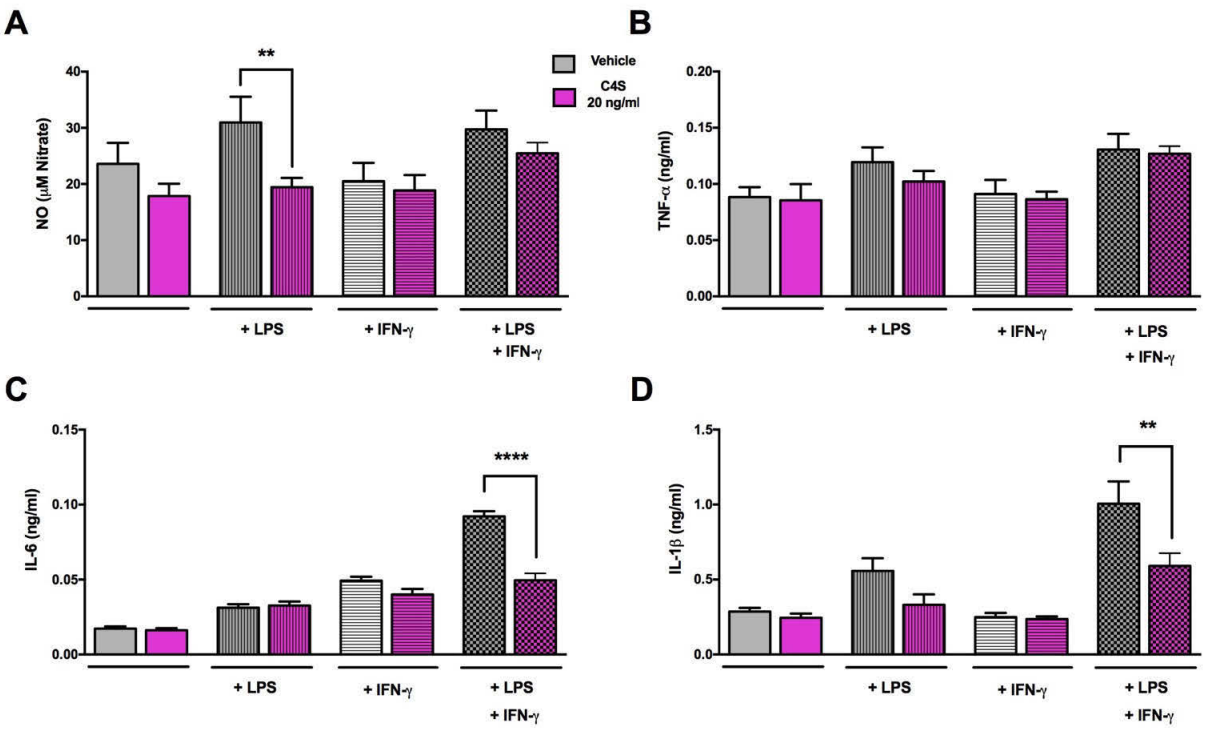

Figure 3.8. C-4-S decreases the release NO in glial stimulated in LPS alone IL-1β and IL-6 release from mixed glia population when stimulated with LPS and IFN-γ. Mixed glial cell populations were treated with C-4-S or vehicle under 4 conditions: no stimulation, LPS stimulation followed by C-4-S (25 ng/ml) or vehicle treatment, pre-treatment with C-4-S or vehicle followed by IFN-γ stimulation or dual activation where cells were stimulated with LPS followed by C-4-S or vehicle treatment which was followed by a second activation of these already primed glia via IFN-γ. (**A**) There was a significant effect of C-4-S on the release of NO (two-way ANOVA; $F_{(1,64)}$= 14.8, P = 0.0003; Tukey's *** P = 0.0051). (**B**)There was a no significant effect of C-4-S on TNF-α release (two-way ANOVA; $F_{(1,64)}$= 0.07865, P = 0.3785) (**C**) There was a significant effect of C-4-S on the release of L-6 (two-way ANOVA; $F_{(1,64)}$= 56.09: Tukey's **** P <0.0001). (**D**) There was also significant effect of C-4-S on IL-1β release (two-way ANOVA; $F_{(1,64)}$ = 56.09 P < 0.0001) and post hoc testing revealed significant reduction in IL-1β release in the presence of C-4-S treatment when compared to vehicle (**, P = 0.0013) in mixed glial cultures activated by both LPS and IFN-γ. The effects of C-4-S were assessed by the randomized block design two-way ANOVA, followed by Tukey's multiple comparison post-hoc test (** P < 0.001, significantly different from stimulated samples treated with the vehicle solution only).

Chapter 4:

In vitro studies of pleiotrophin as a modulator of chondroitin sulfate proteoglycan mediated growth inhibition and neuroinflammation

Introduction

During ischemic stroke, neural tissue in regions of severe ischemia (the stroke "core") is irreversibly damaged; however, injury in regions of less severe ischemia and in distal anatomically connected regions evolves over the hours and days following stroke (Dirnagl et al., 1999; Hossmann, 2006). Concomitant with this period of delayed degeneration, adaptive processes ("plasticity") act to repair and replace neural connections lost to stroke. While this plasticity underlies recovery from stroke, it is often incomplete and disability persists in stroke survivors. Information on endogenous molecules that regulate plasticity and neuronal repair after the ischemic attack may therefore facilitate the development of new targets for therapeutic intervention. In CNS injury, including ischemic stroke, inhibitory extracellular matrix compounds including the chondroitin sulphate proteoglycans (CSPGs) are released by glial cells surrounding the injury (Fawcett and Asher, 1999). The deposition of CSPGs has been shown to decrease axonal growth and impair recovery (Fawcett and Asher, 1999). Many of the inhibitory effects observed as a result of CSPG's are related to its highly electronegative structure, which allows interaction with neuronal receptors (Snow et al., 1994; Sivasakaran et al., 2004) including the immunoglobin like domain of receptor protein tyrosine phosphate σ (RPTPσ) to induce growth cone collapse (Shen et al., 2009).

CSPG inhibition and receptor interactions are modulated by a number of endogenous molecules. One potential modulator of CSPG growth inhibition is pleiotrophin (PTN), a growth factor and cytokine that is upregulated in the central nervous system (CNS) during periods of development and following injury (Gonzales-Castillo et al., 2015). PTN has been shown to bind to many receptors including receptor protein tyrosine phosphatases and PTN promotes cell proliferation, migration, and neuronal differentiation (Maeda et al., 1996, 1999; Menget al.,

2000). More recently, PTN has been shown to bind to CSPGs including neuroglycan-C and N-syndecan to promote neuritogenesis (Miller et al., 2015). In the CNS, PTN must bind chondroitin sulfate side chains in order to promote neurite outgrowth via the cell surface receptor proteoglycan glypican-2 and prevent the activity of growth inhibitory RPTPσ (Paveliev et al., 2016). In addition, PTN is known to upregulate the production of growth factors and inflammatory molecules in the CNS following insult (Fernandez-calle et al., 2017). However, the cell specific consequences of PTN on neuronal and glial cells in the CNS are not well defined.

Here, we examined the effects of exogenous PTN on neurite growth, glial activation and glial release of immunomodulators *in vitro*. Consistent with previous literature (Kinnunen et al., 1996; Hida et al., 2003), directly treating neuronal cell lines with PTN increased neurite outgrowth on inhibitory CSPG matrices only and had no effect on neurite outgrowth when cells were plated on laminin surfaces. Perhaps more interestingly, supernatant from activated microglia (via the activator interferon gamma (IFN)-γ) treated with PTN induced an increase in the length of neuronal cells plated on CSPGs to a greater extent than supernatants from microglia treated with IFN-γ or PTN alone. Assays of microglia supernatant revealed that PTN stimulates microglia to release BDNF a trophic factor and PTN induces a reduction in release of the inflammatory molecule IL-1B from biologically activated microglia. In mixed glial population PTN increases the release of BDNF and decreases the release of IL-1β following stimulation of the cultures with LPS and IFN-γ sequentially.

Materials and Methods

All animal protocols were conducted in accordance with Canadian Council on Animal Care Guidelines and approved by the Animal Care and Use Committee: Health Sciences for the University of Alberta.

Reagents

The mouse anti-β-III tubulin antibody, anti-mouse Alexa 488 secondary antibody, Vectashield with 4′, 6-diamidino-2-phenylindole (DAPI), Retinoic Acid (RA), pleiotrophin (PTN), and the proteoglycan mixture were purchased from Cedarlane (Burlington, ON, CAN). 4-Methylumbelliferyl phosphate (4-MUP), bovine serum albumin (BSA), dimethyl sulfoxide (DMSO), Extravidin-alkaline phosphatase, lidocaine, lipopolysaccharide (LPS), mouse anti-MAP-2 antibody and Triton X-100 were purchased from Sigma Aldrich (Oakville, ON). All other reagents unless otherwise specified were purchased from ThermoFisher Scientific (Burlington, ON).

Direct effect of PTN on neurite outgrowth of SH-SY5Y neuronal cells

The human SH-SY5Y neuroblastoma cell line was purchased from Cedarlane (Burlington, ON). Cells were maintained in DMEM-F12 supplemented with 10% FBS and antibiotics. SH-SY5Y cells were differentiated with RA. Before use in each assay, 24-well plates were coated with sterile mixtures of laminin (10μg/ml) or laminin (10 μg/ml) plus proteoglycan mixture (5μg/ml) in phosphate buffered saline (PBS). The plates were rinsed with PBS before SH-SY5Y cells were seeded into each well at a concentration of 2 x 10^5 cells/ml in 0.4ml of DMEM-F12 containing 2.5% FBS. After seeding, cells were incubated for 24 h in a 37°C humidified 5% CO_2

incubator before being treated with 10 μM RA. Following 72 h differentiation, media was aspirated and replaced with 0.4ml of DMEM-F12 containing 2.5% FBS. Immediately after addition of fresh media SH-SY5Y cells were treated with PTN (20, 10, or 5 ng/ml) or its vehicle solution (PBS). Following 72 h incubation, the cells were rinsed with PBS and used in immunocytochemistry experiments.

Direct effect of PTN on neurite outgrowth of B35 neuronal cells

The rat B35 neuroblastoma cell line was purchased from Cedarlane (Burlington, ON). Cells were maintained in DMEM-F12 supplemented with 10% FBS and antibiotics. B35 cells were used without differentiation. Before use in each assay, 24-well plates were coated with sterile mixtures of laminin (10 μg/ml) or laminin (10 μg/ml) plus proteoglycan mixture (5 μg/ml) in phosphate buffered saline (PBS). The plates were rinsed with PBS before B35 cells were seeded into each well at a concentration of 1 x 10^5 cells/ml in 0.4ml of DMEM-F12 containing 2.5% FBS. After seeding, B35 cells were incubated for 24 h in a 37°C humidified 5% CO_2 incubator before use in assays. All neuronal experiments were performed on cells grown on either laminin or laminin/proteoglycan mixtures.

After 24 h, media was aspirated and 0.4 ml of fresh DMEM-F12 containing 2.5% FBS was added to each well. Immediately after addition of fresh media B35 cells were treated with PTN (20, 10, or 5 ng/ml) or its vehicle solution (PBS). Following 72 h incubation, the cells were rinsed with PBS and used in immunocytochemistry experiments.

Neurite outgrowth of B35 neuronal cells exposed to supernatants from PTN treated microglia for use in transfer experiments, supernatant from previously plated microglia was aspirated and replaced with 0.9 ml of DMEM-F12 containing 3% FBS. Following 15 min

incubation, microglia were treated with PTN (20, 10, or 5 ng/ml), its vehicle solution (PBS), or 0.5 μg/ml LPS. After 72 h, 0.1 ml of supernatant was saved for future assays, 0.4 ml of cell-free supernatant was transferred to each well containing previously plated B35 cells, and microglial viability was assessed by the crystal violet assay. Following 72 h incubation with microglia supernatant, neuronal cells were rinsed in PBS and used in immunocytochemistry.

Microglia cell culture

Postnatal Day 1 rat microglia were isolated as previously described (Baskar Jesudasan et al., 2014). Briefly, mixed glia cultures were prepared from brain and spinal cord of post-natal Day 1 Sprague-Dawley rats. The meninges and blood vessels were removed from the brains and tissue was finely minced and dissociated enzymatically by 0.25% Trypsin-EDTA for 20 minutes at 37°C. Trypsin was inactivated with Dulbecco Modified Eagle Medium/Ham's F12 (DMEM-F12) containing 10% FBS and antibiotics (100 U/ml penicillin, 100 μg/ml streptomycin). The brain tissues were triturated mechanically in DMEM/F12 in 10% FBS with antibiotics and plated on poly-L-lysine coated T75 flasks.

After 14–21 days *in vitro* microglia were isolated by incubation with 150mM lidocaine. Briefly, 150mM of lidocaine in DMEM-F12 was added to mixed primary culture and incubated at 37°C in humidified 5% CO_2 incubator for 5 mins. Following incubation, flasks were agitated at 100 rpm at 37°C for 10 min then cells were collected and centrifuged at 2000 rpm for 2 minutes. Following centrifugation, supernatant was aspirated and DMEM-F12 was added to inactivate lidocaine, cells were centrifuged again for 8 minutes at 2000 rpm. Following centrifugation, cells were re-suspended, counted, and seeded into each well of a 24-well plate at a concentration of 1 x 10^5 cells/ml, in 0.4ml of DMEM-F12 containing 10% FBS and 0.4ml

mixed glia conditioned media. Cells were then placed in a 37°C humidified 5% CO_2 incubator and allowed to rest overnight before use in experiments. Microglia were treated with PTN (5- 20 μg/ml) in (PBS) or its vehicle solution (PBS) 15 min before addition of 0.1 μg/ml IFN-γ or addition of equal volume of saline. After 72 h, 0.1 ml of supernatant was saved for future assays.

Neurite outgrowth of SH-SY5Y neuronal cells exposed to supernatants from PTN treated microglia

PTN was tested for its ability to indirectly promote neurite outgrowth through induction of a protective phenotype of microglia. PTN was tested at concentrations ranging from 5 - 20 ng/ml and results were compared to those obtained from samples treated with PBS vehicle solution only. PTN was added to microglia alone or 15 min before stimulation with IFN-γ. Following 72 h incubation, cell free supernatants from the microglia cell cultures were transferred to B35 neuroblastoma cells to assess their neurite promoting activity. Following a 72 h incubation period, the neurite length was measured using ICC images.

For use in transfer experiments, supernatant from previously plated microglia was aspirated and replaced with 1 ml of fresh DMEM-F12 containing 1% FBS. Microglia were treated with PTN (20, 10, or 5 ng/ml), its vehicle solution (PBS) for 15 min before addition of 0.1 μg/ml IFN-γ. After 72 h, 0.1 ml of supernatant was saved for future assays and 0.4 ml of cell-free supernatant was transferred to each well containing plated SH-SY5Y cells.

The human SH-SY5Y neuroblastoma cell line was purchased from Cedarlane (Burlington, ON). Cells were maintained in DMEM-F12 supplemented with 10% FBS and antibiotics. Before use in each assay, 24-well plates were coated at 4°C with sterile mixtures of laminin (10μg/ml) or laminin (10μg/ml) plus proteoglycan mixture (5μg/ml) in phosphate

buffered saline (PBS). SH-SY5Y cells were seeded into each well at a concentration of 2 x 10^5 cells/ml and placed in a 37°C humidified 5% CO_2 incubator for 20mins. Then 0.4ml of DMEM-F12 containing 2.5% FBS was added to each well and cells were allowed to rest for 24 h. Overnight media was aspirated and SH-SY5Y cells were differentiated for 72 h with 10 μM RA. Differentiation media was aspirated and replaced with 0.4ml of cell-free supernatant from previously plated microglia and SH-SY5Y cells were incubated for 72h before being rinsed with PBS and used for immunocytochemistry.

Cell culture – Microglia cytokine release profile

Since we found that PTN treatment of active microglia induced expression of factors which improved neurite outgrowth we wanted to study the expression profile of microglia treated with PTN at different time points before and after activation by IFN-γ. We looked for changes in expression of well-established anti-inflammatory molecules such as interleukin-10 (IL-10) and the growth promoting neurotrophin brain derived neurotrophic factor (BDNF). In Addition, we studied the release profile of pro-inflammatory molecules such as NO a marker of nitrate, Tumor necrosis factor-α (TNF-α) and cytokines interleukin-6 (IL-6) and interleukin-1β (IL-1β) which are known pro-inflammatory mediators.

To determine the effect of PTN on microglial cells directly, viability and cytokine release was measured. PTN was tested at concentrations ranging from 5 - 20 ng/ml and results were compared to those obtained from samples treated with PBS vehicle solution only. PTN was added to microglia alone or 15 min before stimulation with IFN-γ. Following 72 h incubation, cell free supernatants from the microglia cell cultures were saved for GRIESS and ELISA assays and adherent microglia were assessed for viability via CVA.

Cell culture - Primary mixed glia

Briefly, mixed glia cultures were prepared from the brain of post-natal Day 1 Sprague-Dawley rats. The brains were placed in in Hank's balanced salt solution with 1 % penicillin-streptomycin (PS), the cortices and cerebellum were separated, and the meninges and blood vessels were removed. This tissue was finely minced and dissociated enzymatically by 0.25% Trypsin-EDTA for 20 minutes at 37°C. Trypsin was inactivated with Dulbecco Modified Eagle Medium/Ham's F12 (DMEM-F12) containing 10% FBS and antibiotics (1% PS). The brain tissues were triturated mechanically in DMEM/F12 in 10% FBS with 1% penicillin-streptomycin and plated on poly-L-lysine coated 12-well plates (1 ml at 20 mg/ml PLL for 1 hour) with a ratio of 1 brain per plate at 1ml in each well. These plates were placed in a 37°C humidified 5% CO_2 incubator and allowed to rest for 2 weeks. DMEM/F12 (10% FBS, 1% PS), media was refreshed once per week. The cells were re-suspended with a 1 ml treatment of 0.09% Trypsin-EDTA for 20 minutes. Lifted cells were collected and centrifuged at 200 g, triturated in DMEM/F12 (10% FBS, 1% PS), and 1 ml per well was plated at a concentration of 1 x 10^5 cells/ml. Cells were then placed in a 37°C humidified 5% CO_2 incubator and allowed to rest for 3 days before use in experiments.

Direct effects of PTN on mixed glial cultures

We wanted to determine the effect of PTN on mixed glial cultures which consist of three main cell types: astrocytes, oligodendrocytes and microglia (de Vellis and Cole, 2012) in various conditions and time points of biological activation, the release of well-established anti-inflammatory (BDNF, IL-10; Figure 4.6) and pro-inflammatory cytokines (NO, TNF-α, IL-6 and IL-1β; Figure 4.7) by mixed populations into cell culture media were assayed. To test the effect

PTN on biologically activated glia, PTN (20 ng/ml) or vehicle (same volume as PTN) was introduced 6 hours after potent LPS activation (+LPS). In addition the protective effect of PTN was studied where PTN or vehicle was added to mixed glia 12 hours prior to addition of biological activator INF-γ. Finally, the effect of PTN or vehicle on 'primed' or activated glia exposed to a secondary insult were studied. In this case glia were again activated by LPS then treated with PTN or vehicle, however this time following PTN or vehicle treatment glial were exposed to a secondary insult by IFN-γ (+LPS, + IFN-γ) as this condition mimics primary biological insult following by secondary inflammatory insult common in injuries of the CNS.

To study the direct effects of PTN on glial populations in a various states of biological activation we devised four biological conditions (Figure 4.6 A). First we tested the effects of 20 ng/ml of PTN on glial cells which had not been exposed to a biological activator. Media was changed in mixed glial cells, 24 hours later 10 μl of PBS was added, cells were allowed to rest for 6 hours, then 20 ng/ml of PTN was added to the cultures which were allowed to rest for 18 hours before addition of another 10 μl of PBS after 24 hours the media was removed and assayed. In a second set of conditions (+LPS) we tested if PTN addition after a potent biological activation by LPS could alter the cytokine expression pattern of these activated glial. Again, media was changed in mixed glial cells, however this time after 24 hours 10 μl of LPS at 10 μg/ml was added, cells were allowed to rest for 6 hours, then 20 ng/ml of PTN was added to the cultures which were allowed to rest for 18 hours before addition of 10 μl of PBS after 24 hours the media was removed and assayed. In a third set of conditions (+IFN-γ) we sought to determine if pre-treatment for 18 hours with PTN would change cytokine expression 24 hours after activation with IFN-γ. Again media was changed in mixed glial cells, however this time 24 hours after media change 10 μl of PBS was added, cells were allowed to rest for 6 hours, then 20

ng/ml of PTN was added to the cultures which were allowed to rest for 18 hours before activation with of 10 μl of IFN-γ after 24 hours the media was removed and assayed. Finally, in a fourth set of activating conditions (+LPS, +IFN-γ) we wanted to test of PTN would affect the expression profile of mixed glia which had been activated by LPS and were in a 'primed' state before addition PTN, following PTN treatment glial were introduced to a secondary insult by +IFN-γ. Again media was changed in mixed glial cells, however this time 24 hours later 10 μl of LPS at 10 μg/ml was added, cells were allowed to rest for 6 hours, then 20 ng/ml of PTN was added to the cultures of these now 'primed' glia which were allowed to rest for 18 hours before addition of secondary activation in the form of 10 μl of IFN-γ at 10 μg/ml after 24 hours the media was removed and assayed. This study design allowed use to determine the effect of PTN on primed mixed glia when exposed to a secondary insult mimicking the *in vivo* biological conditions in the CNS following stroke.

In this study we used different combinations of biological activation to mimic primary injury in the CNS following by secondary inflammatory injury. Lipopolysaccharide (LPS) was used to induce primary injury followed by PTN delivery, then a second inflammatory state was induced by IFN-γ. We used LPS for primary activation of glia as it induces a well characterized cytokine release profile which mimics CNS injury in microglia (Nakamura et al., 1999; Baskar Jesudasan et al., 2014). Since LPS is a bacterial endotoxin a secondary exposure may induce an adaptive immune response (Olson and Miller, 2004), therefore we used IFN-γ to induce an innate immune response and secondary inflammation. Using two biological activators is advantageous as there are many different populations of microglia with distinct receptor resulting in different subsets of glia responding to LPS and IFN-γ (Pannell et al., 2014). By using multiple methods of biological activation we prevent adaptive immune responses and ensure a more diverse subset of

the microglia population are activated as multiple inflammatory activators are at work following CNS injury *in vivo*. We again assayed for pro-inflammatory (BDNF, IL-10; Figure 4.6) and anti-inflammatory (NO, TNF-α, IL-6 and IL-1β; Figure 4.7) factors to see the influence of astrocytes, oligodendrocytes in combination with microglia on release of these factors.

Immunocytochemistry – Neurite length measurement

For immunocytochemical assessment of neurite outgrowth, B35 cells were fixed in 5% formalin and permeabilized with 0.1% Triton-x 100. Cells were treated with a 10% blocking solution (Dako) in 0.1% BSA for 1 h at room temperature to prevent non-specific binding of antibodies (blocking). MAP-2, a marker of neurite processes, and Palladin, a marker of axons, were used to identify neurite outgrowth. B35 cells were incubated with mouse anti- MAP-2 (1:200) in 0.1% BSA and rabbit anti- palladin (1:500) in 0.1% BSA overnight at 4°C.

For assessment of neurite outgrowth in SH-SY5Y cultures, cells were fixed in ice cold methanol for 0.5 h then blocked with 10% blocking solution in 0.1% BSA for 1 h at room temperature. B-III tubulin, a marker of neurite processes, was used to identify neurite outgrowth. SH-SY5Y cells were incubated with mouse anti-β-III tubulin in 0.1% BSA for 2 h at room temperature. After primary antibody incubation, the same visualization protocol was followed for each cell type.

For immunofluorescent visualization, culture plates were incubated with an anti-mouse Alexa 488 secondary antibody (1∶500) and an anti-rabbit Alexa 647 secondary antibody (1∶500) for 1 hour at room temperature. After three washes, Vectashield mounting media with DAPI was applied and a cover slip was mounted on top of cells. Negative controls without primary antibody were performed to rule out non-specific labeling by the secondary antibodies.

Epifluorescent images were acquired using Leica DMI 6000B microscope mounted with Leica DFC365 FX monochrome camera at 40X. For neurite length calculations, three representative neurons in each well condition were traced and the measurement function in ImageJ was used to determine neurite length from the edge of the nucleus.

For assessment of indirect effects of PTN on SH-SY5Y B-III tubulin, was used to identify neurite outgrowth via immunocytochemical assessment. SH-SY5Y cells were fixed in 5% formalin for 10 min at room temperature and then blocked and permeabilized in PBS containing 10% normal horse serum (NHS) and 0.1% Triton-X100 for 1 h at room temperature. Cells were incubated with mouse anti-β-III tubulin (1:500) in 0.1% NHS and 0.1% Triton-X100 overnight at 4°C. For immunofluorescent visualization, culture plates were incubated with an anti-mouse Alexa 488 secondary antibody (1∶500) and Hoechst (1:1000) for 1 h at room temperature. Cells were washed three times with PBS before Fluoromount-G mounting media was applied and a cover slip was mounted on top of cells. Epifluorescent images were acquired using Leica DMI 6000B microscope mounted with Leica DFC365 FX monochrome camera at 40X. For neurite length calculations, three representative neurons in each well condition were traced and the measurement function in ImageJ was used to determine neurite length from the edge of the nucleus.

CVA Assay

The crystal violet assay (CVA) was performed as previously described by Martin and Clynes (1992). This assay is based on the ability of viable, but not dead, cells to adhere to culture plates and absorb crystal violet dye. After removal of culture media, cells were rinsed with PBS and 400 µL of 0.25% aqueous crystal violet was added to each well. Following 10 min incubation,

the crystal violet solution was aspirated and the wells were rinsed 4 times with deionized H_20. The plates were then dried for 1-2 h at room temperature and the dark crystals which had formed were dissolved by adding 200µL 10% sodium dodecyl sulphate to each well. The plates were then incubated for 15 min on an orbital shaker to allow crystals to dissolve further. Optical densities were measured at 570 nm using a microplate reader (Molecular Devices SpectraMax M5) after transferring 0.1 ml aliquots to 96-well plates. The viable cell value was calculated as a percent of the value obtained from cells incubated with fresh medium only.

GRIESS Assay

NO production was determined indirectly by measuring nitrite (NO_2^-) accumulation using the Griess reagent (Ding et al., 1988). Cell-free microglia culture media from experiments were collected and nitrite measurements were performed by mixing equal volumes (50 µL) of culture medium and Griess reagent (1% sulfanilamide, 0.2% N-1-naphthylethylenediamine in 3 M HCl) followed by absorbance measurement at 570 nm on a spectrophotometer. Standard sodium nitrite solutions were used to calibrate absorbance readings.

BDNF ELISA

The concentration of BDNF (ng/ml) in microglia culture media was measured by sandwich enzyme linked immunosorbent assay (ELISA). Briefly, 96 well plates were coated with goat anti-BDNF antibody (1:100, Santa Cruz Biotechnology, Dallas, TX) in 0.1M sodium bicarbonate buffer pH 9.6 and incubated overnight at 4°C. Following incubation, coating solution was removed and wells were blocked with 1% BSA/Skim milk powder for 2 h at room temperature. Following blocking, plates were rinsed in PBS-Tween 0.05% and either standards or samples

were added to each well. Following incubation overnight at 4°C, plates were rinsed with PBS-Tween and incubated with a biotin-conjugated anti-human secondary antibody (1:500, Peprotech, Rocky Hill, NJ) in PBS +1% BSA/Skim milk powder for 1 h, followed by Extravidin-alkaline phosphatase (1:10000 in PBS + 1% BSA/ Skim milk powder) for 1 h. Fluorescence was developed by adding 0.2 mg/ml 4-MUP in diethanolamide (excitation 360nm and emission 440nm) and fluorescent response was measured via microplate reader every 30 minutes until reaction end-point. Protein concentration was determined by linear regression.

Statistical analysis

Data are presented as means ± standard error of the mean (SEM). The concentration-dependent effects of PTN *in vitro* were evaluated statistically by the randomized block design one-way or two-way analysis of variance (ANOVA) followed by Tukey's Multiple Comparison *post hoc* test.

Results

Direct effect of PTN on neurite outgrowth of SH-SY5Y and B35 neuronal cells

To determine the effect of directly treating neuronal cells with PTN, B35 and differentiated SH-SY5Y cells were plated on either growth permissive laminin matrices or growth inhibiting CSPG matrices and were then treated with various concentrations of PTN or vehicle control (PBS) for 72 h (Figure 4.1 A). Following incubation, neurite length was assessed via ICC images (Figure 4.1 D-F). A significant main effect of PTN treatment was observed in both SH-SY5Y and B35 cells plated in CSPGs (ANOVA; $F_{(3,16)} = 5.342$, $P = 0.0097$ and $F_{(3,12)} = 3.877$, $P = 0.0377$, respectively; Figure 4.1 B,C) and Tukey's *post hoc* comparisons revealed significant neurite outgrowth when CSPG plated cells were treated with 10 ng/ml PTN compared to vehicle treated cells ($P = 0.0065$ in SH-SY5Y and $P = 0.0328$ for B35 cells). There was no effect of PTN on cells plated on laminin at any of the concentrations tested (data not shown).

Neurite outgrowth of B35 neuronal cells exposed to supernatants from PTN treated microglia

Microglia (with or without stimulation with IFN-γ) were incubated with PTN at concentrations ranging from 5 - 20 ng/ml to determine PTN's ability to indirectly promote neurite outgrowth of B35 cells on CSPG or laminin surfaces via soluble mediators released into the media by the microglia. Results were compared to those obtained from samples treated with PBS vehicle solution only. PTN or vehicle were added to microglia alone or microglia 15 min before stimulation with IFN-γ. Following 72 h incubation, cell free supernatants from the microglia cell cultures were transferred to B35 cells to assess their neurite growth promoting activity (Figure 4.2 A). Following a 72 h incubation period, the neurite length was measured using ICC. We

found a significant effect of supernatant from microglial cultures treated with PTN on neurite outgrowth of B35 cells plated on CSPG (two-way ANOVA; $F_{(3, 24)} = 7.007$, $P = 0.00015$; Figure 4.2 B). However, we did not detected a significant effect of IFN-γ treatment of microglia on neurite outgrowth (two-way ANOVA; $F_{(1, 24)} = 0.1315$, $P = 0.7200$) and no significant interaction between IFN-γ and PTN/vehicle treatment was identified (two-way ANOVA; $F_{(3, 24)} = 0.4273$, $P = 0.7352$). Only IFN-γ activated microglia treated with PTN at 20 ng/ml produce factors which enhanced neurite outgrowth on CSPGs. Further post hoc analysis revealed a significant difference in neurite length of B35 cells exposed to supernatant from IFN-γ activated microglia treated with PTN at 20 ng/ml compared to B35 cells treated with supernatant from IFN-γ activated microglia treated with vehicle alone (Tukey's; P = 0.0310; Figure 4.2 B). PTN at 20 ng/ml was the only concertation of PTN that induced activated microglia to release factors which significantly enhanced neurite growth on CSPG matrices and PTN at 20 ng/ml.

Treating B35 cells plated on laminin with supernatant from microglia exposed to PTN also had an effect on neurite outgrowth. We found a significant effect of supernatant from microglial cultures treated with PTN on neurite outgrowth of B35 cells plated on CSPG (two-way ANOVA; $F_{(3, 24)} = 4.834$, $P = 0.0090$; Figure 4.2 C). We also detected a significant effect of IFN-γ activated microglia on neurite outgrowth (two-way ANOVA; $F_{(1, 24)} = 15.6$, $P < 0.0006$). Only microglia without IFN-γ activation treated with PTN at 20 ng/ml produce factors which enhanced neurite outgrowth, however no significant interaction between IFN-γ and PTN/vehicle treatment was identified (two-way ANOVA; $F_{(3, 24)} = 0.7121$, $P = 0.5543$). Further post hoc analysis revealed a significant difference in neurite length of B35 cells exposed to supernatant from microglia (without IFN-γ activation) treated with PTN at 20 ng/ml compared to B35 cells treated with supernatant from microglia treated with vehicle alone (Tukey's; P = 0.0244). 20

ng/ml was the only concertation of PTN that induced microglia to release factors which significantly altered neurite growth on laminin matrices and PTN.

Interestingly, treating IFN-γ activated microglia with PTN at 20 ng/ml induced release of factors which improved neurite outgrowth on CSPG but not laminin surfaces and treated microglia which are not activated by IFN-γ with PTN at 20 ng/ml induced release of factors which improved neurite outgrowth on laminin but not CSPG surfaces.

Neurite outgrowth of SH-SY5Y neuronal cells exposed to supernatants from PTN treated microglia

Microglia (with or without stimulation with IFN-γ) were incubated with PTN at concentrations ranging from 5 - 20 ng/ml to determine PTN's ability to indirectly promote neurite outgrowth of SH-SY5Y cells on CSPG or laminin surfaces via soluble mediators released into the media by the microglia (Figure 4.3 A). When SH-SY5Y cells are plated on inhibitory CSPG matrices there is an effect of microglia supernatant. We found a significant effect of supernatant from microglial cultures treated with PTN on neurite outgrowth of SH-SY5Y cells plated on CSPGs (two-way ANOVA; $F_{(4, 30)} = 4.287$, $P = 0.007$; Figure 4.3 B). We also detected a significant effect of IFN-γ activated microglia on neurite outgrowth (two-way ANOVA; $F_{(1, 30)} = 32.96$, $P < 0.0001$). Only IFN-γ activated microglia treated with PTN at 20 ng/ml produce factors which enhanced neurite outgrowth, however no significant interaction between IFN-γ and PTN/vehicle treatment was identified (two-way ANOVA; $F_{(4, 30)} = 6.635$, $P = 0.0006$). Further post hoc analysis revealed a significant difference in neurite length of SH-SY5Y cells exposed to supernatant from IFN-γ activated microglia treated with PTN at 20 ng/ml compared to SH-SY5Y cells treated with supernatant from IFN-γ activated microglia treated with vehicle alone

(Tukey's; P = 0.0060). PTN at 20 ng/ml was the only concertation of PTN that induced activated microglia to release factors which enhanced neurite growth on CSPG matrices and PTN at 20 ng/ml only induced this effect when microglia were IFN-γ activated.

Treating SH-SY5Y cells plated on laminin with supernatant from microglia exposed to PTN also had an effect on neurite outgrowth. We found a significant effect of supernatant from microglial cultures treated with PTN on neurite outgrowth of SH-SY5Y cells plated on laminin (two-way ANOVA; $F_{3, 33)} = 4.781$, $P = 0.0068$; Figure 4.3 C). However, we did not detected a significant effect of IFN-γ activated microglia on neurite outgrowth (two-way ANOVA; $F_{(1, 22)} = 0.06221$, $P = 0.8053$) and no significant interaction between IFN-γ and PTN/vehicle treatment was identified (two-way ANOVA; $F_{(3, 22)} = 0.8923$, $P = 0.4607$). Only microglia without IFN-γ activation treated with PTN at 20 ng/ml produce factors which enhanced neurite outgrowth. Further post hoc analysis revealed a significant difference in neurite length of SH-SY5Y cells exposed to supernatant from microglia (without IFN-γ activation) treated with PTN at 20 ng/ml compared to B35 cells treated with supernatant from microglia treated with vehicle alone (Tukey's; P = 0.0025, Figure 4.3 C). PTN at 20 ng/ml was the only concertation of PTN that induced microglia to release factors which enhanced neurite growth on laminin matrices and PTN, this result is consistent between B35 and SH-SY5Y cells, however PTN has no effect of SH-SY5Y cells plated on CSPG as was seen in B35 cells.

Effect of PTN on microglia viability and the release of anti-inflammatory markers

To determine the effect of PTN on microglial cells directly, viability and cytokine release was measured after PTN (5 - 20 ng/ml) was added to microglia alone or 15 min before stimulation with IFN-γ (Figure 4.4 A). CVA assays demonstrated that there was no significant effects of

PTN treatment on the viability of microglia alone (ANOVA; $F_{(3,20)} = 0.1055$, $P = 0.9959$) or microglia with IFN-γ activation (ANOVA; $F_{(3,18)} = 2.44$, $P = 0.0974$; Figure 4.4 B).

To determine if the growth promoting effect of PTN is in part mediated by released factors from microglia we looked at the release of BDNF, a known growth promoting trophic factors in the CNS. There was as significant effect of PTN on the release of BDNF in microglia alone (ANOVA; $F_{(3, 20)} = 4.7323$., $P = 0.0118$) and a strong statistical trend towards increased release in PTN treated microglia also stimulated with IFN-γ (ANOVA; $F_{(3,20)} = 3.985$, $P = 0.0523$; Figure 4.4 C). Post hoc analysis revealed a significant difference in BDNF release between vehicle and PTN 20 ng/ml (Tukey's; $P = 0.048$). Release of IL-10, a known anti-inflammatory molecule in the CNS, was also quantified (Fig. 4.4 D). There was no significant main effect of PTN on the release of IL-10 in non-stimulated microglia (ANOVA; $F_{(3,20)} = 1.382$., $P = 02772$) or microglia stimulated with IFN-γ (ANOVA; $F_{(3,20)} = 0.3781$, $P = 0.7698$; Figure 4.4 D) (though IL-10 release was higher in all treatment groups after activation).

Effect of PTN on release of pro-inflammatory markers

To determine the role of PTN in microglia-mediated inflammation, a number of inflammatory molecules were assayed after treatment with or without microglial activation (Figure 4.4 A). In assays of NO release, there was no significant effect of PTN on production of NO in non-stimulated microglia (ANOVA; $F_{(3,9)} = 0.6626$, $P = 0.5956$) or in microglia stimulated with IFN-γ (ANOVA; $F_{(3,16)} = 0.547$, $P = 0.6573$; Figure 4.5 A). Similarly, PTN treatment of microglia did not have any effect on the release of pro-inflammatory molecules TNF-α (ANOVA; $F_{(3,16)} = 3.502$, $P = 0.0400$: Figure 4.5 B) or IL-6 (ANOVA; $F_{(3,20)} = 0.1849$., $P = 0.9054$; Figure 4.5 C). The addition of IFN-γ to microglia cultures induced an upregulation in the production of TNF-α

and IL-6; however, again PTN treatment had no main effect on TNF-α (ANOVA; $F_{(3,16)} = 0.547$, $P = 0.6573$; Figure 4.5 B) or IL-6 (ANOVA; $F_{(3,20)} = 0.1849.$, $P = 0.9054$; Figure 4.5 C) release.

Similarly IL-1β production and release by non-stimulated microglia was not effected by PTN treatment (ANOVA; $F_{(3,24)} = 1.316.$, $P = 0.2924$; Figure 4.5 D). However, when microglia were activated with IFN- γ, PTN treatment had a significant effect on IL-1β release (ANOVA; $F_{(3,24)} = 11.56$, $P < 0.0001$). Post hoc analysis showed that IL-1β production was significantly reduced in IFN-γ stimulated microglia treated with PTN at 10 ng/ml ($P < 0.0001$) and 20 ng/ml ($P < 0.0001$) compared to IFN-γ stimulated microglia treated with vehicle alone (Figure 4.5 D).

Effect of PTN on mixed glial release of anti-inflammatory markers

Using mixed glial cell cultures, we investigated the role of PTN in mediating inflammation in mixed glial populations consisting of microglia, astrocytes and oligodendrocytes under various conditions of biological activation (Figure 4.6 A). Interestingly, there was a significant effect of PTN on BDNF release by mixed glia (two-way ANOVA; $F_{(1,64)}= 31.53$, $P<0.0001$), a significant effect of cell culture activation conditions ($F_{(3,64)} = 146.1$, $P<0.0001$) and a strong interaction of cell culture activation conditions and PTN treatment ($F_{(3,64)} = 8.783$, $P<0.000$, Figure 4.6 B). Post hoc analysis reveals a striking significant increase in BDNF production in LPS and LPS plus IFN-γ activated mixed glial cells treated with PTN at 20 ng/ml when compared the same cells treated with vehicle solution (Tukey's; $P < 0.001$, $P < 0.0001$ respectively; Figure 4.6 B).

IL-10 was nearly undetectable in media from baseline mixed glial cultures and after activation by IFN-γ alone, however after activation by LPS and IFN-γ in combination with LPS there was significant increase in production of IL-10. A significant main effect of cell culture conditions ($F_{(3.64)} = 82.37$, $P < 0.0001$; Figure 4.6 C) as well as a significant interaction of cell

culture activation conditions with treatment ($F_{(3.64)} = 3.489$, $P = 0.0206$). A trend towards a main effect of treatment was observed ($F_{(1.64)} = 3.486$, $P = 0.0665$, Figure 4.6 B,C).

Effect of PTN on mixed glial release of anti-inflammatory markers

NO in mixed culture media was measured via the GRIESS reaction. Neither PTN treatment or activation conditions had a significant main effect on NO release in mixed glial population ($F_{(1,64)} = 3.292$, P = 0.0662 and $F_{(3,64)} = 1.159$ $P = 0.3322$, respectively; Figure 4.7 A). TNF-α release was also unaffected by PTN treatment ($F_{(1,64)} = 0.07865$, $P = 0.3785$) or cell culture activation regime ($F_{(3,64)} = 2.038$ $P = 0.1174$; Figure 4.7 B). In contrast, IL-6 release was significantly affected by cell culture activation conditions (two-way ANOVA; $F_{(3,64)} = 265.2$ $P < 0.0001$; Figure 4.7 C) but not PTN treatment ($F_{(1,64)} = 0.03861$ $P = 0.8448$; Figure 4.7 C) and there was no significant interaction between cell culture activation condition and PTN treatment ($F_{(3,64)} = 14.23$ $P < 0.9340$; Figure 4.7 C) . Interestingly, both PTN treatment and cell culture activation conditions significantly affected the release of the pro-inflammatory cytokine IL-1β ($F_{(1,64)} = 4.41$, 1 $P = 0.0397$ and $F_{(3,64)} = 9.71$, $P < 0.0001$, respectively; Figure 4.7 D) however there was no significant interaction between PTN treatment and cell culture activation conditions ($F_{(3,64)} = 1.68$ $P = 0.1789$) . Post hoc testing revealed that PTN significantly reduced IL-1β release by mixed glia exposed to dual activation (LPS and IFN-γ) when compared to vehicle treated cells exposed to the same activation conditions ($P = 0.0013$; Figure 4.7 D). In conditions of dual activation where 'primed' mixed glia are exposed to a secondary biological activation PTN reduces the release of IL-1β and increases the release of BDNF, providing support for both neurotrophic and neuroprotective effects of PTN that are mediated in part by glial cells.

Discussion

Following CNS injury, the accumulation of CSPG's prevent neurite outgrowth and are a major barrier to post injury plasticity (Davies et al., 1997; Moon et al., 2002; Galtrey et al., 2007; Kowk et al., 2011; Soleman et al., 2012; Zhao et al., 2013). Although enzymatic digestion of CSPG's improves plasticity and functional recovery after stroke and spinal cord injury (Burnside and Bradbury, 2014), CSPGs also play important regulatory roles which are lost after digestion (Rolls et al., 2008; Paveliev et al., 2016). Thus, molecules which block the inhibitory action of CSPGs while allowing essential CSPG structures to remain in act are favorable candidates for post CNS injury treatment.

PTN improves neurite outgrowth in a CSPG dependent manner

In both SH-SY5Y and B35 neural cells, direct application of PTN significantly improved neurite outgrowth when cells were plated on inhibitory CSPG matrices but not when plated on growth permissive laminin matrices. This result is consistent with a recent study which found that PTN required interaction with chondroitin sulfate side chains in order to induce a growth promoting effect, and that enzymatic degradation of these side chains result in a loss of efficacy of PTN as a growth promoting molecule (Paveliev et al., 2016). The same study also determined that PTN binds chondroitin sides chains with high affinity, therefore out competing transmembrane tyrosine phosphatase sigma (PTPσ) and preventing activation of the growth inhibitory downstream pathways of PTPσ (Paveliev et al. 2016). In addition to removing inhibition induced by PTPσ, when PTN binds CSPG's it forms a complex which interacts which cell surface receptor bound glypican-2 which induces growth promotion (Paveliev et al., 2016). In light of these receptor interactions which require PTN to bind chondroitin sulfate side chains it

is not surprising that the growth prompting effect of PTN was only seen in our study when neurites were plated on CSPG matrices.

PTN alters microglia release factors which enhance neurite outgrowth

While PTN directly interacts with neurites to induce outgrowth, it is also possible that PTN acts on microglia and other glial cells that release factors that also enhance or support neurite growth. Microglia play an essential role in regulating the biochemical microenvironment of the healthy and injured CNS and release numerous cytokines and inflammatory mediators with established effects on neuroplasticity (Nakamura et al., 1999; Olson et al., 2004; Gao et al., 2010; Wang et al., 2010; Lia et al., 2012). To examine these indirect effects, microglia with or without activation by INF-γ were treated with PTN. Supernatant from these isolated microglia cultures containing all the released factors was then added to SH-SY5Y or B35 neural cells plated on CSPG's or laminin. Interestingly, both SH-SY5Y and B35 cells on plated on laminin had improved outgrowth from the supernatant of microglia treated with PTN (20 ng/ml) which had not been biologically activated. This same supernatant did not have an effect when cells were plated on CSPG matrix. This finding has important implications, suggesting non-activated microglia release factors which improve neurite outgrowth on permissive surfaces in a manner not dependent on CSPGs. However, when PTN treated microglia were activated with INF-γ, their supernatant did not enhance the growth of either cell type on laminin surfaces. Supernatant from activated microglia treated with 20 ng/ml PTN did improve neurite outgrowth of B35 cells on CSPG inhibitory surfaces, suggesting that the activation state of the microglia and the receptor profiles of the neurons modulate the effects on neurite extension.

PTN induces release of a growth factor but not inflammatory cytokines from microglia

To provide mechanistic insight into these effects on neurite growth, the secretory profiles of microglia with and without activation were assessed after treatment with PTN at various concentrations. Importantly, we found that PTN did not compromise microglia viability. In addition, non-stimulated microglia treated with PTN at 20 ng/ml had a significant increase in the release of BDNF, and a similar trend was observed in microglia activated by INF-γ. The greater effect on BDNF release of PTN in non-stimulated microglia may explain the greater effects on neurite extension observed on laminin under these conditions. Moreover, the growth promoting effect of PTN treated microglia supernatant was not seen on CSPG plated cells, suggesting that BDNF trophic action can be reduced by CSPGs that induce growth cone collapse (Snow et al., 1996; Castro and Kuffler, 2006).

Our findings are consistent with work suggesting PTN improves release of BDNF from microglia (Maio et al. 2012); however, we are the first to show that this effect is greater in microglia which have not been activated by INF-γ. Notably, treatment with PTN did not induce the release of inflammatory factors including NO, TNF-α, IL-6 or IL-1β. This result is in agreement with studies that show no changes in mRNA regulation of TNF-α, IL-1β and iNOS in microglia treated with PTN (Maio et al., 2012). In recent studies of BV2 microglia lines, simultaneous incubated LPS and PTN significantly potentiated the production of NO compared to cells only treated with LPS (Fernandez-Calle et al., 2017). While our data with INF-γ activation did not reveal a statistically significant main effect of PTN treatment, a trend towards a concentration dependent increase of NO release after activation was apparent.

In vivo studies in the prefrontal cortex have identified PTN as a potential regulator of inflammation, as mice which over express PTN have significantly increased levels of TNF-α, IL-

6, and MCP-1 in response to LPS when compared to wild type mice (Fernandez-Calle et al., 2017). In our studies of isolated microglia cultures activated with IFN-γ this was not found to be true as PTN had no effect on TNF-α, IL-6 or while IL-β levels which were significantly decreased after PTN treatment in INF-γ activated microglia. Notably, the study finding that PTN enhances LPS induced upregulation of inflammatory factors was performed *in vivo*, whereas the data above examines only the contribution of one specific glial cell type to this effect.

PTN modulates glia release of pro- and anti-inflammatory cytokines

To provide a more comprehensive assessment of the role of PTN in regulating immunomodulatory actions of glial cells, PTN treatment was assessed in mixed glial cultures containing microglia, astrocytes and oligodendrocytes (de Vellis and Cole, 2012). Different combinations of biological activation were used mimic primary injury in the CNS following by secondary inflammatory injury. LPS was used to induce primary injury following by PTN delivery, then a second inflammatory state was induced by INF-γ. As in the case of isolated microglia, mixed glia activated with LPS or INF-γ did not have enhances levels of BDNF; however, when mixed glia were activated by LPS or LPS followed by INF-γ there was a significantly greater release of BDNF by PTN treated cells. In most CNS injuries, the primary insult induces an inflammatory event that is considered beneficial. However sustained inflammation or a secondary wave of inflammation after injury is considered detrimental to tissue health and to recovery (Carmichael, 2013). Our findings that PTN may alter glial responses to a second wave of inflammation by inducing release of a trophic factor is exciting and suggest a potential benefit of PTN administration after CNS injury. As the magnitude of the effect was reduced isolated cultures of isolated microglia, these data suggest that BDNF release

is not restricted to microglia and that astrocytes and oligodendrocytes also contribute to the protective phenotype of PTN after injury.

In mixed glial populations activated with LPS or INF-γ or LPS followed by INF-γ there was no effect of PTN treatment on the release of the inflammatory factors NO, TNF-α or IL-6. Moreover, PTN reduced the release of inflammatory factor IL-1β when mixed glia were subjected to dual activation with LPS and INF-γ. Thus, PTN may enhance neuroplasticity and offer neuroprotection via direct actions on neurons (in a CSPG dependent manner) and via indirect actions via the modulation of glial cell release of BDNF (increased) and IL-1β (reduced).

PTN offer therapeutic potential

The combined trophic and anti-inflammatory actions of PTN suggest PTN is an excellent candidate molecule to improve axonal outgrowth and reduce detrimental secondary inflammation in the CNS following injury. PTN improves neurite outgrowth in growth restricting CSPG rich environments which are established after CNS injury. In addition, PTN enhances the release of growth promoting factor BDNF in microglia which are not biologically activated and in mixed glial cultures which are subject to a secondary inflammatory event. PTN also induces a reduction in the release of inflammatory IL-β in isolated microglia and in mixed glia which are exposed to an inflammatory event. Considering the key role PTN plays in promoting neurite outgrowth and inducing neuroprotection in secondary inflammation it has excellent therapeutic potential in CNS injury.

Chapter 4: Figures

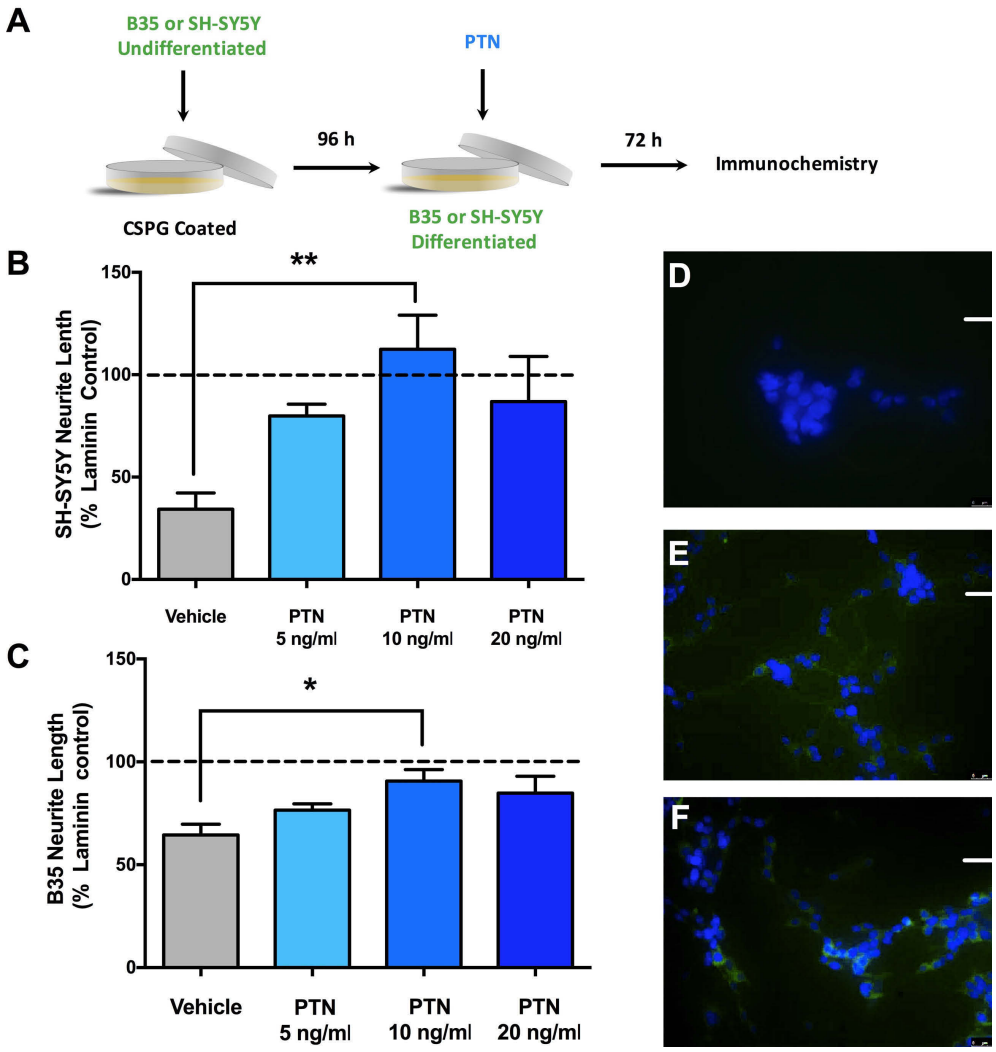

Figure 4.1. PTN increases neurite length in B35 and SH-SY5Y neuroblastoma cells. (A) Experimental design to determine the effects of PTN on the neurite length of SH-SY5Y (**B**) and B35 (**C**) neuronal cells grown on CSPG matrices (5 µg/ml) in the presence or absence of 5, 10, and 20 ng/ml PTN was examined. Data from 4-6 independent experiments are presented as a percentage of neurite length compared to control cells. The effects of PTN were assessed by the randomized block design ANOVA, followed by Tukey's multiple comparison post-hoc tests (* $P < 0.05$, ** $P < 0.005$, significantly different from samples treated with the vehicle solution only). (**D-F**) Epifluorescent images of SH-SY5Y cells cultures acquired at 40X, neurite processes identified in green with β-III tubulin (Alexa 488) and cell bodies labeled with nuclear stain DAPI (blue) cultures after incubation with vehicle control on CSPG matrix (**D**) on CSPG matrix with 10 ng/ml PTN (**E**) and laminin matrix with 10 ng/ml PTN (**F**). Photos are representative of 3 independent experiments. (**D-F**) Scale bar = 25 µm.

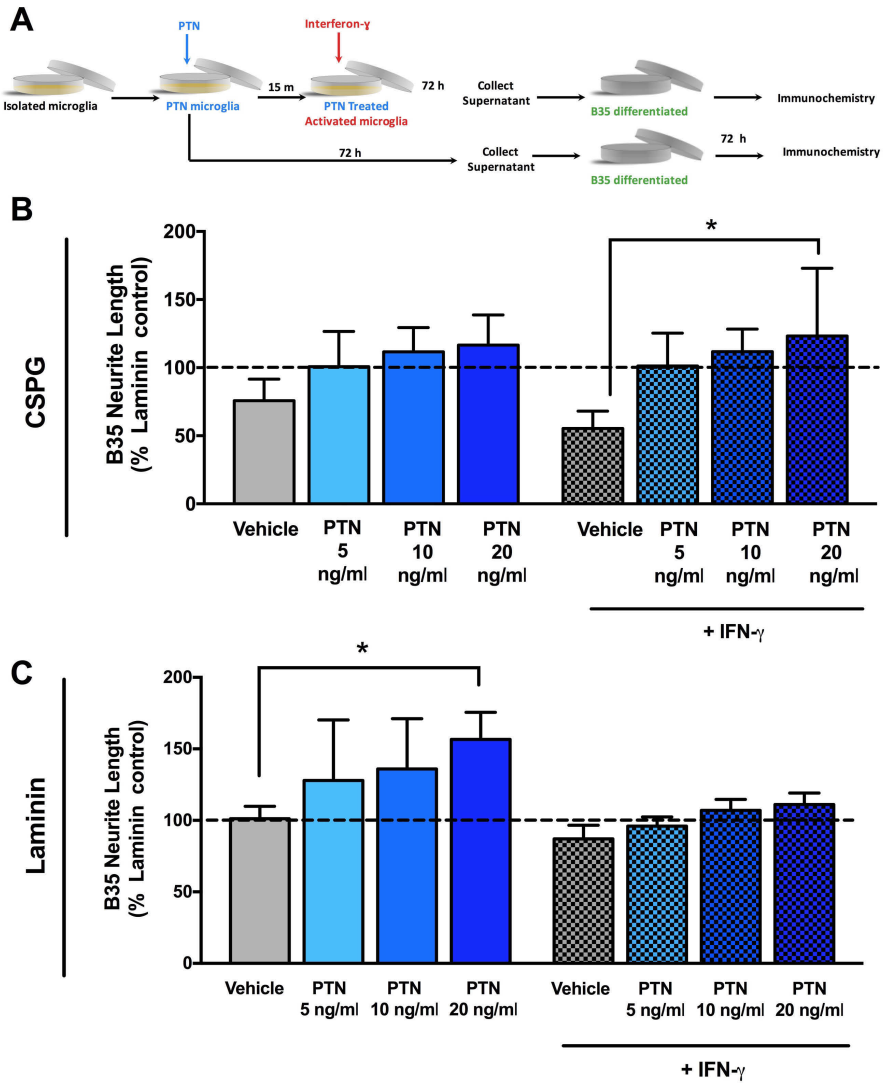

Figure. 4.2 – PTN treated stimulated microglia cell supernatants restores CSPG inhibited B35 neurite length and – PTN treated un-stimulated microglia cell supernatant promotes growth in permissive environments. (A) Experimental design to determine the effects of PTN on the neurite length of B35 neuronal cells plated on (**B**) CSPGs or (**C**) Laminin, exposed to supernatants from primary rat microglia with or without stimulation with IFN-γ in the presence or absence of 5, 10, or 20 ng/ml PTN was examined. Data from 4 independent experiments with cells obtained from four different microglial preparations are presented. The effects of PTN were assessed by the randomized block design ANOVA, followed by Tukey's multiple comparison post-hoc test (* $P < 0.05$, significantly different from stimulated samples treated with the vehicle solution only).

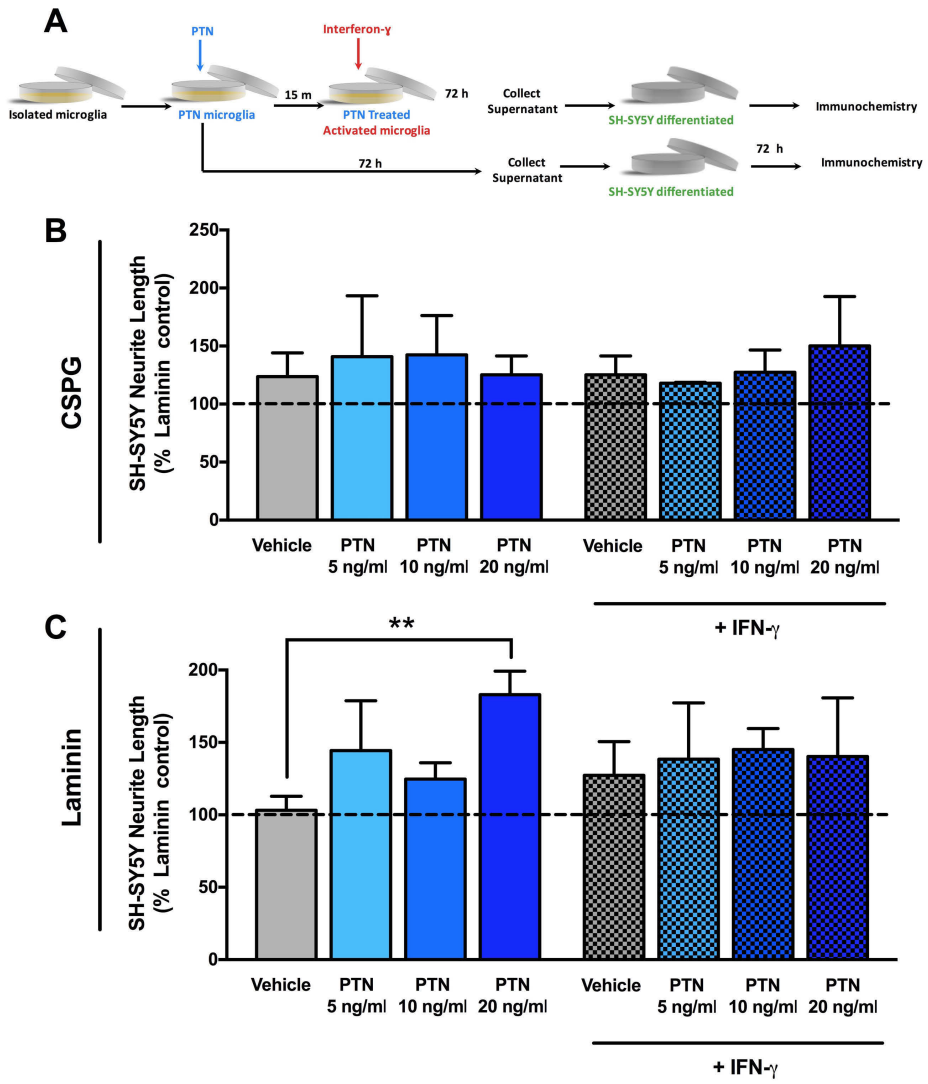

Figure. 4.3 – SH-SY5Y cells have improved neurite outgrowth when treated with supernatant from microglia cells exposed to PTN but only on laminin surface.

(**A**) Experimental design to determine the effects of PTN on the neurite length of SH-SY5Y neuronal cells plated on (**B**) CSPGs or (**C**) Laminin, exposed to supernatants from primary rat microglia with or without stimulation with IFN-γ in the presence or absence of 5, 10, or 20 ng/ml PTN was examined. Data from 4 independent experiments with cells obtained from four different microglial preparations are presented. The effects of PTN were assessed by the randomized block design ANOVA, no significant differences were found among any of the means. The effects of PTN were assessed by the randomized block design ANOVA, followed by Tukey's multiple comparison post-hoc test (** $P < 0.01$, significantly different from stimulated samples treated with the vehicle solution only).

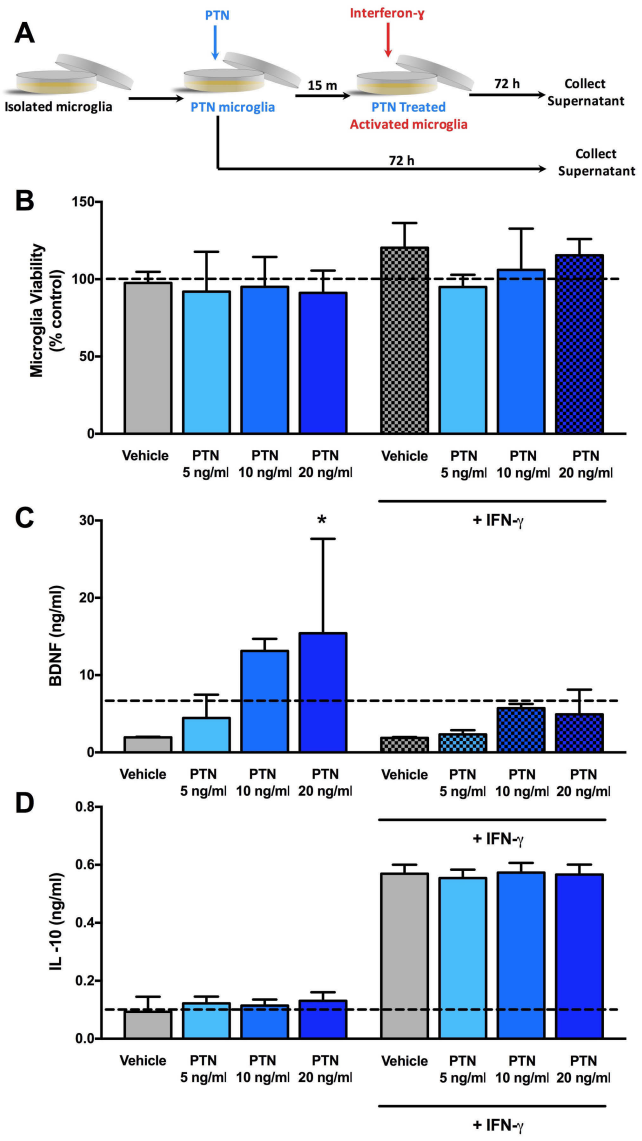

Figure. 4.4 – PTN increases the release of BDNF and does not affect microglia viability or release IL-10. PTN does not affect viability or secretion of anti-inflammatory IL-10 by primary rat microglia cells. (**A**) Experimental design where Microglia were pre-treated with various concentrations of PTN or its vehicle solution (PBS) for 15 min before stimulation with IFN-γ (150 U/ml). After 72 h incubation, microglia viability was assessed by CVA (**B**) and concentrations of BDNF (**C**) and IL-10 (**D**) in cell-free supernatants were measured by ELISA. The horizontal dashed lines indicate the viability or concentration of mediators in supernatants from untreated microglia. Data from 3-7 independent experiments are presented. The effects of PTN were assessed by the randomized block design ANOVA, followed by Tukey's multiple comparison post-hoc test (*, $P < 0.05$).

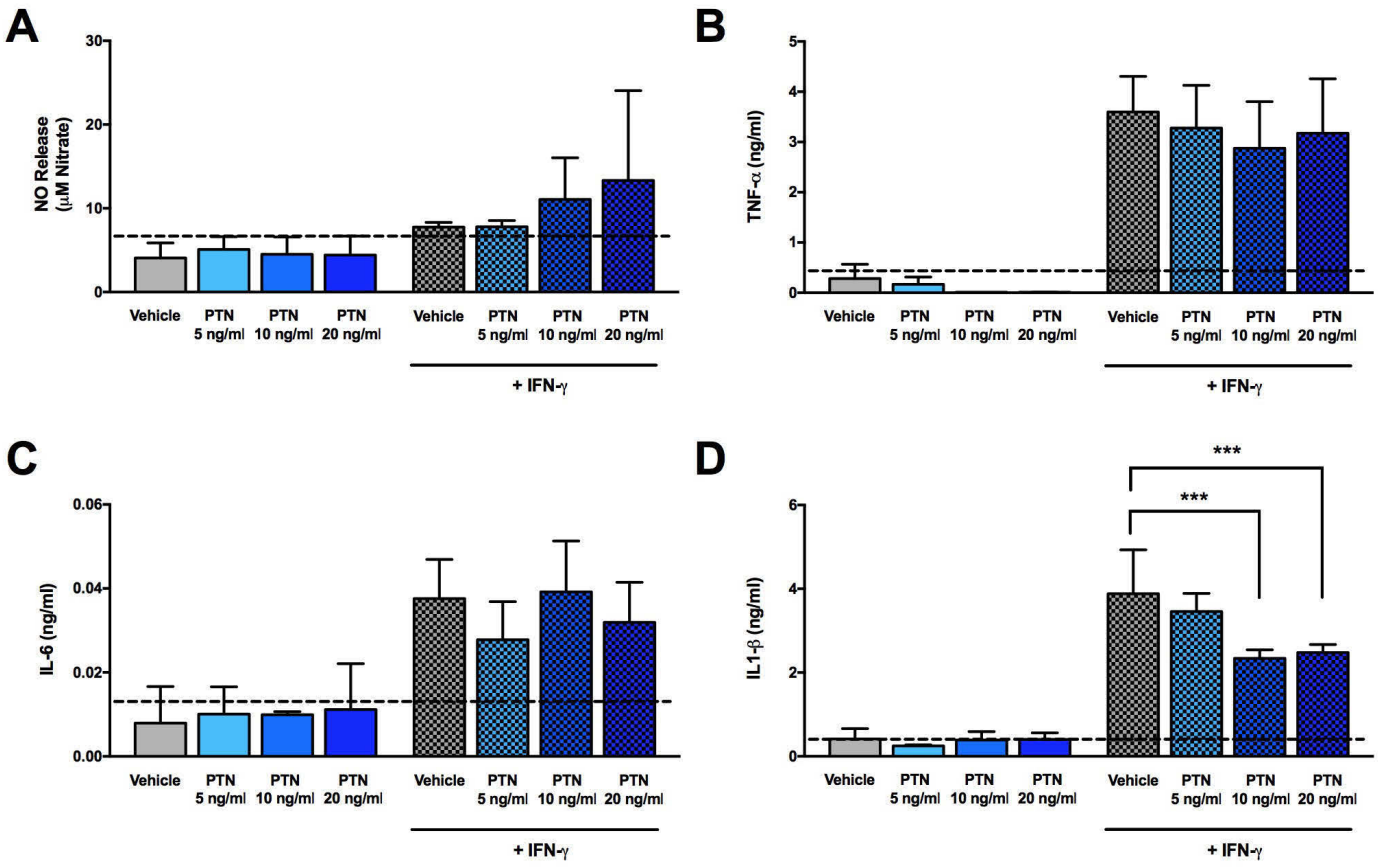

Figure. 4.5 – PTN increases the release of NO and decreases the release of IL-1β from microglia cells stimulated with IFN-γ. PTN does not affect secretion of inflammatory TNF-α and IL-6 by primary rat microglia cells. Microglia were pre-treated with various concentrations of PTN or its vehicle solution (PBS) for 15 min before stimulation with IFN-γ (150 U/ml). After 72 h incubation and concentrations of NO were measured by GRIESS (**A**) and TNF-α (**B**), IL-6 (**C**) and IL-1β (**D**) in cell-free supernatants were measured by ELISA. The horizontal dashed lines indicate the viability or concentration of mediators in supernatants from untreated microglia. Data from 3-7 independent experiments are presented. The effects of PTN were assessed by the randomized block design ANOVA, followed by Tukey's multiple comparison post-hoc test (*** $P < 0.001$, significantly different from stimulated samples treated with the vehicle solution only).

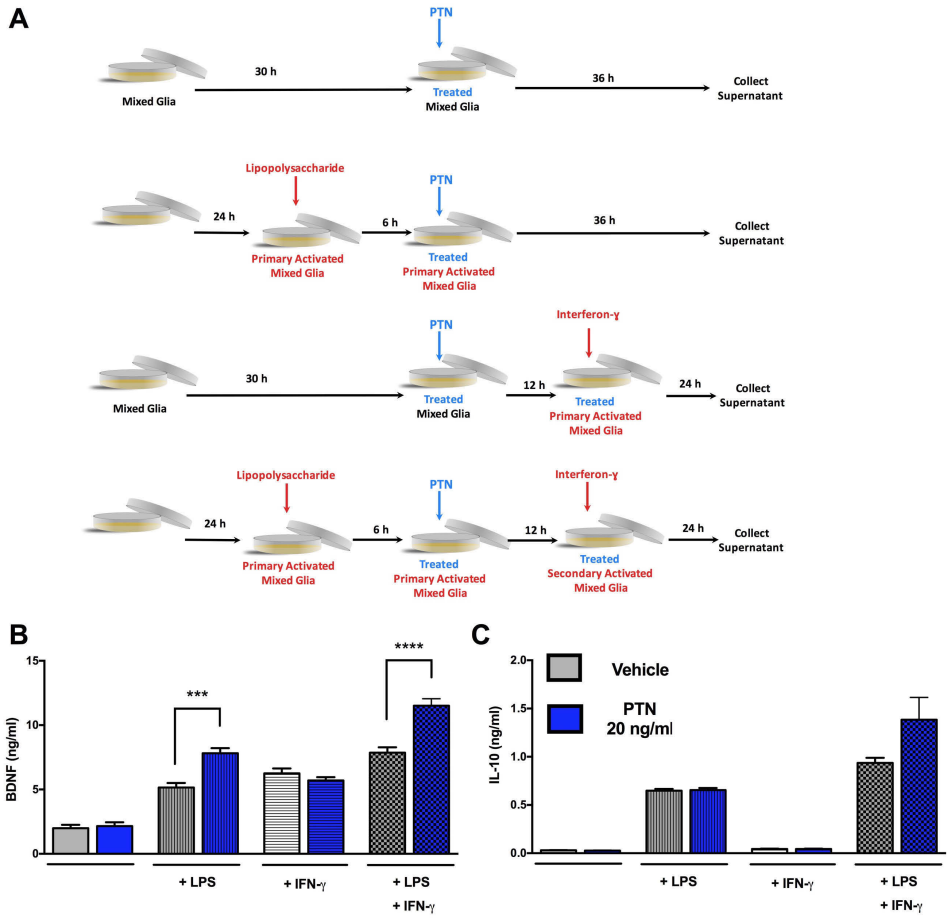

Figure. 4.6 – PTN increases the release of BDNF from mixed glia population when stimulated with LPS alone or LPS followed by IFN-γ. (**A**) Experimental design showing a summary of treatment conditions briefly, mixed glial cell populations were treated with PTN or vehicle under 4 conditions: no stimulation, LPS stimulation followed by PTN or vehicle treatment, pre-treatment with PTN or vehicle followed by IFN-γ stimulation or dual activation where cells were stimulated with LPS followed by PTN or vehicle treatment which was followed by a second activation of these already primed glia via IFN-γ. (**B**) There was a significant effect of PTN on BDNF release by mixed glia (two-way ANOVA; $F_{(1,64)} = 31.53$, $P < 0.0001$) and a significant difference in post hos testing of BDNF release between PTN and vehicle treatment only in the LPS alone dual activation condition (Tukey's; ***, $P < 0.001$, ****, $P < 0.0001$). (**C**) There was no significant effect of PTN in IL-10 release (two-way ANOVA; $F_{(1.64)} = 3.486$, $P = 0.0665$). The effects of PTN were assessed by the randomized block design two-way ANOVA, followed by Tukey's multiple comparison post-hoc test (*** $P < 0.0001$ and ****, $P < 0.0001$, significantly different from stimulated samples treated with the vehicle solution only).

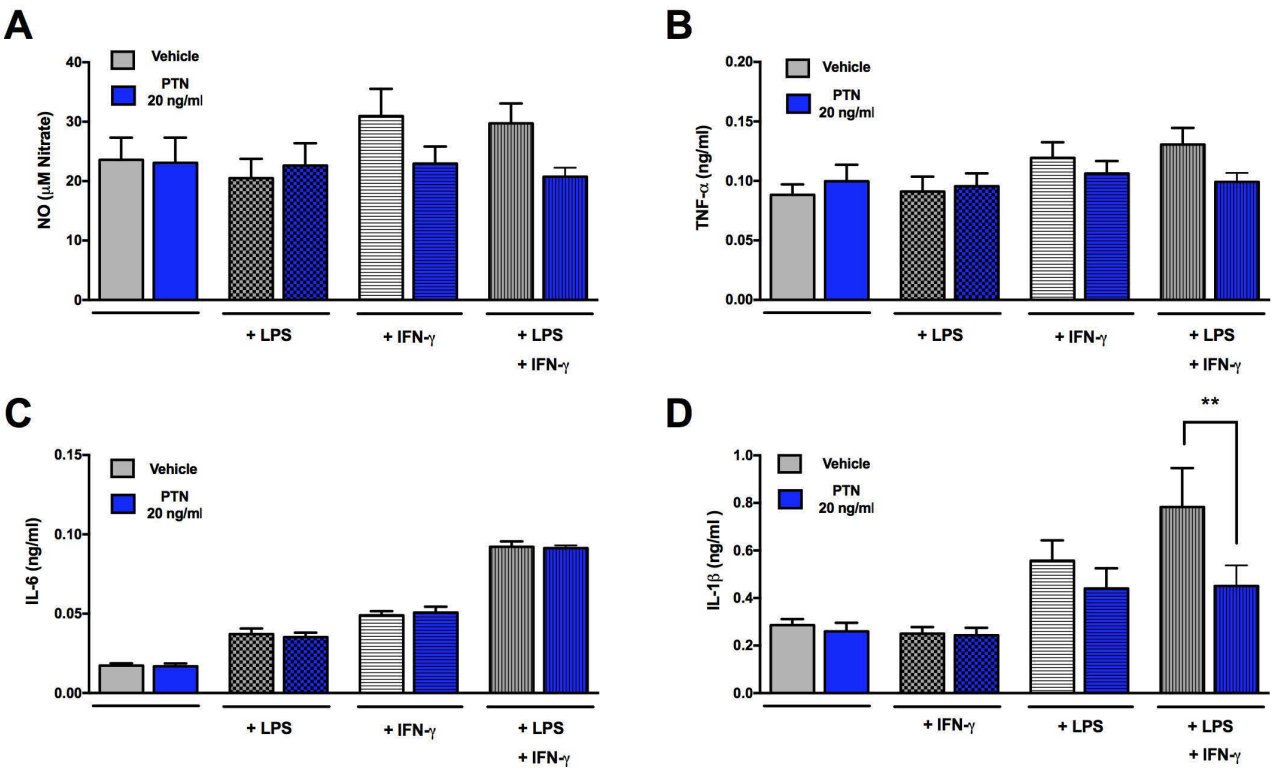

Figure 4.7 - PTN decreases the release of IL-1β from mixed glia population when stimulated with LPS and IFN-γ. Mixed glial cell populations were treated with PTN or vehicle under 4 conditions: no stimulation, LPS stimulation followed by PTN or vehicle treatment, pre-treatment with PTN or vehicle followed by IFN-γ stimulation or dual activation where cells were stimulated with LPS followed by PTN or vehicle treatment which was followed by a second activation of these already primed glia via IFN-γ. There was no significant effect of PTN on the release of (**A**) NO (two-way ANOVA; $F_{(1,64)} = 3.292$, $P = 0.0662$) (**B**) TNF-α (two-way ANOVA; $F_{(1,64)} = 0.07865$, $P = 0.3785$) or (**C**) IL-6 (two-way ANOVA; $F_{(1,64)} = 0.03861$ $P = 0.8448$). There was a significant effect of PTN on (**D**) IL-1β release (two-way ANOVA; $F_{(1,64)} = 4.411$ $P = 0.0397$) and post hoc testing revealed significant reduction in IL-1β release in the presence of PTN treatment when compared to vehicle ($P = 0.0013$) in mixed glial cultures activated by both LPS and IFN-γ. The effects of PTN were assessed by the randomized block design two-way ANOVA, followed by Tukey's multiple comparison post-hoc test (** $P < 0.001$, significantly different from stimulated samples treated with the vehicle solution only).

Chapter 5:

Augmenting spinal plasticity and recovery from stroke with intraspinal pleiotrophin *in vivo*

Introduction

Cerebral ischemia that damages the sensorimotor cortex leads to degeneration of descending axons in the cortical spinal tract (CST) that are left deinnervated by the cortical injury (Thomalla et al., 2004; Thomalla et al., 2005; Taraschenko et al., 2015). After cortical injury, there is an acute period of neuroplasticity in the cortex and the spinal cord marked by an up regulation of neurotropic and growth prompting factors (Overman et al., 2014; Sist et al., 2014; Kessner et al., 2016; Carmicheal et al., 2016). These factors facilitate axonal outgrowth and the anatomical rewiring of surviving circuits thought to underlie functional recovery (Van den Brand et al., 2012). However, anatomical plasticity is limited by inhibitory factors such as CSPGs that act as a barrier to repair and regeneration (Silver and Miller, 2004; Afshari et al., 2010; Cua et al., 2013). These inhibitory factors limit anatomical recovery after stroke leaving most stroke survivors with chronic sensory motor deficits (Carey et al., 1993; Dobkin 2008). Augmenting growth promoting pathways or antagonizing inhibitory pathways may therefore enhance or prolong the window for plasticity following cortical injury may improve chronic deficits and functional recovery (Soleman et al., 2012; Silasi and Murphy, 2014).

Pleiotrophin (PTN) is an endogenous growth promoting protein with potential to augment plasticity and improve recovery after stroke (Deuel et al., 2002). This 17 KD growth factor with a high affinity for heparin binding plays a critical role in signaling neural growth after injury, guiding and promoting axonal regeneration and protecting spinal neurons (Jin et al., 2009). PTN is minimally expressed in the embryonic and adult central nervous system (CNS), but is up-regulated during intermediate neonate development at a time when glia and neurons are rapidly differentiating and undergoing extensive outgrowth of cellular processes (Kinnunen et al., 1998; Mitsiadis et al., 1995; Merenmies and Rauvala, 1990). *In vitro*, PTN promotes outgrowth in glial

progenitor cells from both spinal cord and cortical primary cultures (Deule et al., 2002). Recent *in vitro* studies of CNS neurons and PC12 cells reveal that PTN reverses the inhibitory effect of chondroitin sulfate chains on neurite outgrowth: PTN binds glypican-2 at the neuron surface to enhance neuron growth and abolishes the growth inhibitory interaction of protein tyrosine phosphatase σ with CSPGs resulting in robust neuron growth (Paveliev et al., 2016).

Following cortical ischemic injury in rats, PTN is upregulated in the injured cortex with maximum expression 3 to 7 days post injury that gradually declines to baseline levels by 14 days post injury (Yeh et al., 1998). This window for PTN upregulation coincides with periods of heightened cortical plasticity and recovery after stroke (Sist et al., 2014). Notably, PTN is upregulated in vascular endothelial cells and activated macrophages and glia that surround the infarct (Wang et al., 2014). However, increased PTN expression is strictly localized to areas of new vessel formation, indicating an important angiogenenic role for PTN in the post stroke cortex (Wang et al., 2014). While PTN expression is not upregulated within neurons, exogenous PTN administered to the site of a focal cortical injury can induces growth of apical dendrites and dendritic tufts from neurons adjacent the injury (Paveliev et al., 2016).

Unlike cortical injury, spinal cord injury promotes upregulation of PTN in neurons, glia, astrocytes and oligodendrocytes with a preferentially distributed in regions closest to the injury site (Wang et al., 2004). Post injury spinal cord upregulation of PTN also peaks 3 to 7 days after injury, however it does not return to baseline for 28 days (Wang et al., 2004). This timeline matches the time course of spinal plasticity after stroke and functional recovery after cortical and spinal injury (Wang et al., 2004; Sist et al., 2014). Notably, exogenous PTN promotes injured axon regeneration, out growth, synaptogenesis and modification to glial environment in the spinal cord (Paveliev et al., 2016).

During development, PTN is an important axonal guidance molecule for CST axons originating in the motor cortex (Rauvala and Peng, 1998; Yanagisawa et al., 2010). Degeneration of these CST projections follow stroke, as well as the secondary damage that follows at the level of the spinal cord, contributes to the sensorimotor impairment after stroke (Weishaupt et al., 2013). Inducing plasticity in deinnervated sensorimotor spinal circuits may therefore facilitate the formation of new sensorimotor circuits or reinnervation of circuits by spared CST projections and thereby promote recovery (Moon et al., 2001; Soleman et al., 2012). Indeed, augmenting plasticity at the level of the spinal cord has established functional benefits after cortical stroke (Soleman et al., 2012; Kerzoncuf et al., 2016). Here, we are the first to investigate if PTN administration into the spinal cord deinnervated by cortical stroke can improve functional recovery. Photothrombosis lesioning the forelimb sensorimotor cortex was used to induce sensorimotor impairment in forelimb use in rats. PTN micro injection into the deinnervated cervical spinal cord (C4/C5) was performed 7 days post injury to potentiate regenerative processes in injured sensorimotor spinal circuits. Skilled reaching, forelimb use asymmetry and mechanical sensitivity was measured following stroke and treatment. In addition to functional changes we studied changes in microglial and astrocytic density in the spinal cord, the role of PTN in promoting axonal growth phenotypes, its effects on serotonergic fiber density in the grey matter of the cervical spinal cord, and effects on motor neuron density and morphology in the stroke effected grey matter of ventral horn.

Materials and Methods

Animals

All experimental procedures were performed on aged male Sprague Dawley rats (700-750 g, Charles River). Animals were housed in pairs (2 per cage) under standard laboratory conditions of 12:12 hour light: dark cycles with controlled temperatures (22°C). Rats were fed a diet of standard laboratory rat chow *ad libitum,* except during the training period when feeding was reduced to 25 g daily to maintain 85-90% *ad libitum* feeding body weight. Water was always available *ad libitum.* Animals were allowed to acclimatize to the facility for 1 week before commencing any experimental procedures. All animal use was approved by: The University of Alberta Animal Care and Use Committee and all animal protocols were conducted in accordance with Canadian Council on Animal Care Guidelines.

Experimental Groups and Design

Our aim was to assess if spinal delivery of PTN during functional recovery from stroke (7 days post injury) could extend the therapeutic window of spinal plasticity and promote enhanced recovery. We looked for PTN induced changes in somatosensory recovery following stroke as well as anatomical and biochemical changes in the spinal cord at 28 days post stroke.

Rats (n = 40) were divided into four experimental groups; animals received sham surgery (n = 10) or photothrombotic stroke (n = 30) with no intervention (n = 10), a spinal cord injection of PTN (n =1 0) or injection of a control (n = 10) at 7 days post stroke.

Behavioral training and testing

On skilled reaching tasks, rats were trained twice per day for 30 minutes on consecutive days for

6 weeks and baseline values of performance were measured three days prior to stroke. Behavioral tasks were tested using the timelines shown in Figure 5.1. Testing consisted of two test sessions, 4 hours apart and the average scores for the two tests were reported.

The single pellet-reaching task

This reaching task is widely used to assess deficits from injury and recovery after injury as this task required both fine motor function and sensory perception (Alaverdashvili and Whishaw, 2013). The skilled reaching task also offers the advantage of being able to distinguish between recovery and compensation (Alaverdashvili and Whishaw, 2013). In addition, this task is thought to closely mimic grasping in humans and recovery on the skilled reaching task greatly parallels human hand function recovery after stroke (Soleman et al., 2010).

Since the single pellet reaching task is difficult for animals to master rats were trained to reach for six weeks prior to stroke and baseline reaching scores were established in testing two days before photothrombosis. Animals which could not reach a pre-established minimum number of pellets were excluded from the study. Animals were again tested at 3, 7, 14, 21 and 28 days after stroke to assess deficits induced by stroke and subsequent recovery.

Briefly, animals were placed in a clear Plexiglas box (39.5 cm x 12.5 cm x 47.5 cm) with a 1 cm wide slit in the front wall running floor to ceiling with a shelf (4 cm x 4 cm) mounted 6 cm above the mesh floor of the box. 45 mg rodent pellets in banana flavor (TestDiet) were placed 1.5 cm from the interior wall on the shelf contralateral to the limb the rat was to reach with. When a rat successfully retrieved a pellet off the shelf it was trained to then walk to the back of the apparatus to ensure that the rat was leaving the opening and repositioning itself for the next food pellet. All animals received training consisting of 30 minute sessions two times

each day with a 4-hour delay between sessions. Animals were allowed to reach for a maximum of 100 pellets and those animals unable to reach 10 pellets after 15 days of training were eliminated from the study. After the first 15 sessions, a preferred limb was established; in all subsequent training sessions pellets were only loaded on the side of the platform that required reaching of the preferred limb.

Testing consisted of two 15 minute sessions in which a maximum of 20 pellets were presented to the preferred limb. Reaching performance was measured by two parameters (i) The number of attempts the rat made to reach by placing its arm through the opening towards the shelf with the pellets and (ii) the number of successful reaches (the rat successfully grasped the pellet). The success rate was calculated as (Number of successful reaches)/(Number of attempted reaches) x 100. The final test scores reported were an average of both test scores achieved on the testing day. All figures report the reaching success rate normalized to baseline prior to stroke. The success rate for each group is reported as Mean ± Standard error to the mean (SEM).

Spontaneous forelimb use

The cylinder test was used to assess spontaneous forelimb use of animals when exploring vertical surfaces (Schallert et al., 2000; Schallert et al., 1982). Prior to stroke animals tend to support their body weight with each paw equally or animals slightly favor a dominant paw when supporting body weight to explore a vertical surface (Schallert et al., 2000). However, after stroke animals tend to neglect the injured paw in weight support during vertical rearing. As animals recover they begin using the injured forepaw in weight support again. Asymmetry scores can be calculated based on which paw is used in bodyweight support when rearing to explore a vertical surface. Stroke induces an asymmetry in limb use as the injured paw is avoided in

rearing support, as animals recover asymmetry tends to be restored.

In this test rats are placed in a clear Plexiglas cylinder (44 cm height x 35 cm diameter) with an open top. In each test rats were video recorded in the cylinder for 10 minutes and the first 20 rearing motions during exploration were analyzed and scored. We defined forelimb contact as placement of the fore paw against the wall of the cylinder with the whole palm to support the body weight of the animal. Thus, if an animal touches the wall with a single forelimb it was scored as an independent placement of the 'left' or 'right' forelimb. However, if the animals initially touched the vertical surface with one paw and subsequently planted the second paw on the wall to maintain balance and support the body weight, the touch was scored as 'both'. In addition, if the animal planted both paws simultaneously during a rear against the vertical surface, the touch is again scored as 'both'. The number of contacts with the impaired limb and unimpaired limb can be calculated as a percent of the total number of contacts.

Mechanical sensitivity testing

Disruption of ascending sensory input circuits though the CST and damage to the sensory cortex following stroke can lead to loss of mechanical sensitivity in the forepaw (Dableh *et al*., 2011). Using von Frey monofilaments of various forces applied to the rat forepaw mid-plantar region we determined the filament force at which 50% paw withdrawal was achieved and this was recorded as the paw with drawl mechanical threshold (PWMT). All PWMT were normalized to pre stroke levels and pre stroke PWMT was set to zero. A PWMT of 100 means that rats did not respond to any filament indicating a complete lack of sensitivity, a PWMT of 0 indicates a return to pre stroke baseline mechanical sensitivity. Importantly, a PWMT score below zero indicates increased sensitivity relative to pre stroke levels, it is important to test animals given growth

promoting treatments such as PTN for increased mechanical sensitivity. These treatments may induce the formation of aberrant pain circuity leading to detrimental effects such as hyperalgesia. Although PTN may improve motor and sensory circuity, it is important to confirm that it does not also induce or perpetuate pain circuits leading to chronic pain.

The procedure was modified for the forepaw mid-plantar region from procedures previously described by Bradmen et al. (2015). The testing was done following the staircase method with removal of monofilaments 9 (4.17) and 13 (4.93) as suggested by Bradmen et al. (2015). Testing was started at a midrange target force (4.08) to (6.1) 100g-target force using filaments 1-18 on a standard filament set. The filament application was standardized to 2 seconds on all trial with 10 applications. Animals were either scored as (i) responding or (ii) non-responding for each filament application, when a 50% withdrawal response was achieved, the target force of the filament was recorded as the PWMT (Bradmen et al., 2015). We ensured a consistent blind operator for every experiment and analysis was done using log stimulant values to avoid bias across the range. The PWMT was determined by averaging two separate trials per test day conducted 4 hours apart.

Surgical procedures

Surgical procedures were performed in animals deeply anesthetized with 2-2.5% isoflurane (in 70% nitrous oxide and 30% oxygen) at a flow rate of 1 L/min. Body temperature was maintained at 37°C with a rectal temperature probe and heating pad.

Photothrombotic stroke

Rats were mounted in a stereotaxic frame and the forelimb somatosensory cortex corresponding

to the preferred limb in skilled reaching tasks was located using stereotaxic coordinates (1-4 mm lateral; -1 to +3 mm anterior of bregma). A thin window was created over the 3 mm x 4 mm rectangular area; this was followed by a tail vein injection of Rose Bengal (a photosensitive dye) solution (30 mg/kg in 0.01 M sterile phosphate buffered saline; Sigma). The thinned skull over the somatosensory cortex was illuminated using a collimated beam of green laser light (532 nm, 17 mW; ~ 4.0 mm in diameter) for 10 minutes to photoactivate the Rose Bengal, occluding all illuminated cortical vasculature and inducing a focal ischemic lesion. This model was chosen for its ability target a defined area of the cortex and its high reproducibility. Sham surgical controls were treated in the same manner however illumination of the laser was eliminated. The location and volume of stroke were confirmed postmortem and any animals which did not have an infarct volume between 5.0 and 6.0 mm^3 located over the somatosensory motor cortex (1-2 mm lateral; -1 to +1 mm anterior of bregma) as confirmed by stereotactic analysis were eliminated from the study.

Spinal administration of PTN

7 days after recovering from photothrombosis of the somatosensory motor cortex, PTN or an IgG control was delivered unilaterally to the cervical spinal cord contralateral to the stroke. Briefly, a partial laminectomy of C4 and C5 was performed to expose the contralesional spinal cord. Using a 10 µl Hamilton syringe mounted on a stereotaxic arm and fitted with a pulled glass tip, a 1.0 µl injection of either PTN (5 mg/ml) or IgG (5 mg/ml) was administered at both C4 and C5. Injections were positioned to 1 mm lateral of the midline at a depth of 1 – 1.5 mm and administered at a rate of 0.2 ul/min at both sites. The pipette was left *in situ* for 1 minute after injection to avoid backflow.

Transcardial perfusion and tissue preparation

At 68 days post stroke rats were perfused with 250 ml of saline heparin solution (0.02%) (37°C) followed by 250 ml of 4% formalin solution (4°C) administered at flow rate of 25 ml/min. Immediately following perfusion brains and spinal cords were removed and submerged in 4% liquid formalin overnight at (4°C), then transferred to 30% sucrose solution (4°C) until the brains and spinal cords lost buoyance, then tissue was flash frozen in isopentane (C_5H_{12}) at -65°C.

Stroke volume analysis

Brain tissue was cryosectioned in 20 μm coronal slices and all the slices spanning the stroke were collected. For each slice the infarct was traced to determine the surface area, which was then multiplied by the depth of slice (20 μm) to determine the lesion volume (Buchan et al., 1992).

The infarct volumes for every slice spanning the lesion were summed to determine the total stroke volume (Buchan et al., 1992). Animals from the stroke group which had incomplete lesions (stroke volume less than 2 mm^3) or lesions which did not fall in the targeted the somatosensory motor area where removed from the study (n = 1).

GFAP & IBA-1 immunochemistry

Since PTN has recently been shown to bind components of the glial scar (Miller *et al.*, 2015) we wanted to determine effect of PTN injection on astrocytes and astrocytic scar formation in the CNS. An antibody specific for glial fibrillary acidic protein (GFAP) was used as GFAP is highly expressed by astrocytes in the CNS after injury and is a major component of the glial scars

formed by astrogliosis (Carmichael, 2003; Lin et al., 2014).

Slides were warmed for 30 minutes at 37°C and then placed in universal blocker (DAKO, Cat.No. 0909) with 0.2% triton X-100 for 1 hour. Tissue was incubated over night with GFAP antibody produced in mouse (Sigma Aldrich, Cat No. G3893; 1:500) After washing in PBS the tissue was treated with Donkey anti-mouse Texas red (Invitrogen, Cat.No. A21206; 1:200) for 2 hours. Finally, vectashield fluorescent mounting medium containing DAPI (Vector laboratories, Cat No. H-1500) was spread over the tissue on the slides and a glass coverslip was overlaid.

PTN has been shown in cell culture to increase microglia proliferation (Miao et al., 2012). In order to study the role of PTN treatment in inflammation and microglia activation an Iba-1 (ionized calcium binding adaptor molecule 1) antibody was used. In the CNS IBA-1 is exclusively expressed in microglia and is found to be up-regulated when they are activated in response to injury and inflammation (Basker Jesudasan et al., 2014). IBA-1 can be used to differentiate between active and surveilling microglia of the CNS (Lai and Todd, 2008).

The above procedure was run in tandem using Wako, Anti -Iba-1 produced in rabbit (Invitrogen Cat no. 019-19741; 1:5000) as the primary antibody and Donkey anti-rabbit Alex 647 (Invitrogen, Cat No. A-31571; 1:200) as the secondary antibody.

Confocal images were acquired with 10 x and 20 x dry objective lenses on a Leica DMI6000B inverted microscope coupled to a Leica EL6000 compact light source for fluorescent excitation and captured on the Leica DFC365FX monochrome digital camera and analyzed using LAS-AF 2.60 software. ImageJ software was used to correct for background and quantify optical density and the average optical density of sham animals was set to 1.0 on both contralesional and ipsilesional side. 10 slices from the cervical spinal cord at level 4 were selected for each animal and an average density from the 10 slices was reported for each animal.

GAP-43 tyramine signal amplification immunochemistry

Recent studies have identified PTN as a potent growth promoter in the CNS and PTN has been shown to increase neurite out growth in culture studies (Paveliev et al., 2016). We used Growth Associated Protein -43 (GAP-43) markers to identify axonal growth cones and determine if PTN could induce increased axonal outgrowth following cortical injury in the spinal cord (Seo et al., 2017).

In order to confirm the presence of growth associated protein 43 (GAP-43) standard immunochemical protocols were followed in conjunction with tyramine signal amplification. Briefly, slides were baked at 37°C for 1 hour and incubated with the following (with 3 PBS washes in between each step): 0.3% hydrogen peroxide in phosphate buffer solution (20 minutes), rabbit polyclonal anti-GAP-43 (abcam, Cat.No. ab16053; 1:1000, overnight), Horse anti-rabbit biotin (Jackson ImmunoResearch; 1:400, 90 minutes), ABC reagents (VECTASTAIN® ABC Kit; 20µl soln. A and 20µl soln. B in 1mL PBS diluted 1:5, 30 mins), Biotinyltyramide in amplification diluents (Individual indirect tyramide reagent pack from NEN Life Science Products/PerkinElmer Life Sciences, Cat. No. SAT700; 1:75, 10minutes), Extra-Avidin FITC (Sigma; 1:500, 2 hours). Finally, vectashield fluorescent mounting medium containing DAPI (Vector laboratories, Cat No. H-1500) was spread over the tissue on the slides and a glass coverslip was overlaid. Confocal images were again acquired with a 20 x dry objective lens on a Leica DMI6000B inverted microscope coupled to a Leica EL6000 compact light source for fluorescent excitation and captured on the Leica DFC365FX monochrome digital camera and analyzed using LAS-AF 2.60 software. Images were collected at the same gain, exposer and voltage based pixel intensity to ensure consistency between images. ImageJ

software was used to correct for background and quantify optical density. The average optical density of sham animals was set to 1.0 on both contralesional and ipsilesional side. Ten slices from the cervical spinal cord at level 4 were selected for each animal and an average density from the 10 slices was reported for each animal

Serotonin immunohistochemistry and densitometric quantification

CNS injury which result in the disruption of CST axons can leave serotonergic fibers of the spinal grey matter deinnervated, leading to a pronounced loss of serotonergic fibers (Filli et al., 2011). Since the induced stroke encompassed the forelimb motor representation we wanted to evaluate changes in monoamine fiber distribution in the grey matter of the cervical spinal cord, at the corresponding C4 level. Standard immunochemical protocols were used to fluorescently label serotoninergic fibers in the cervical spinal cord.

Briefly, slides were dehydrated for 30 minutes at 37°C and then placed in universal blocker (DAKO, Cat.No. 0909) with 0.2% triton X-100 for 1 hour. Tissues were incubated over night with primary rabbit anti-serotonin antibody in (Sigma, Cat no. 5545; 1:500) in 1% normal goat serum (NGS)/tris buffer saline (TBS). After washing in TBS the tissue was treated with goat anti-rabbit Texas Red (Vector Laboratories, Cat no. TT-1000; 1: 500) in 1% NGS/TBS and incubate in dark for 1hr. Finally, slides were mounted with vectashield fluorescent mounting medium containing DAPI (Vector laboratories, Cat No. H-1500) and glass coverslips. Densitometric quantification of serotonergic axon density was performed on regions of interest in the ventral horn on both the contralesional and ipsilesional side of a single tissue slice. Confocal images were acquired with a 20 x dry objective lens on a Leica DMI6000B inverted microscope coupled to a Leica EL6000 compact light source for fluorescent excitation and

captured on the Leica DFC365FX monochrome digital camera and analyzed using LAS-AF 2.60 software. we defined a standard image size of 1024 × 1024 pixels and analyzed 5 tissue slices from C4 of each animal. Images were collected at the same gain voltage based pixel intensity to ensure optimal signal-to-noise ratio. ImageJ software was used to correct for background and quantify optical density. The average optical density of sham animals was set to 1.0 on both contralesional and ipsilesional side.

Motor neuron quantification and area calculation

In tissue culture and explant studies PTN has been shown to be particular important in motor neuron survival (Mi et al., 2007). Previous studies have shown that PTN can protect motor neurons when they lose target derived growth factors (Mi et al., 2007). Following stroke motor neurons lose input from the CST when the motor cortex in damage, thus we wanted to test if PTN could prevent a loss of motor neurons in C4/C5 which are left deinnervation from cortical stroke to the forelimb somatosensory motor cortex. We confirmed the presence of motor neurons by labeling for Choline Acetyltransferase (Chat) and counted all Chat positive cells in the ventral horns greater than 100 μm^2 as motor neurons. For each animals 10 tissue slices were analyzied and an average value was reported from theses slices for each animal.

Briefly, slides were dehydrated for 30 minutes at 37°C and then placed in universal blocker (DAKO, Cat.No. 0909) with 0.2% triton X-100 in phosphate buffer saline (PBS) for 1 hour. Tissues were incubated over night with primary rabbit anti-ChAT antibody in (abcam, Cat no. ab178850; 1:500) with 1% universal blocker/ PBS. After washing in PBS the tissue was treated with goat anti-rabbit Texas Red (Vector Laboratories, Cat no. TT-1000; 1: 500) in 1% NGS/PBS and incubate in dark for 1hr. Finally, slides were mounted with vectashield fluorescent

mounting medium containing DAPI (Vector laboratories, Cat No. H-1500) and glass coverslips. Confocal images were acquired with a 20 x dry objective lens on a Leica DMI6000B inverted microscope coupled to a Leica EL6000 compact light source for fluorescent excitation and captured on the Leica DFC365FX monochrome digital camera and analyzed using (LAS-AF 2.60 software.

ChAT positive cells in the ventral horns with areas greater than 300 μm^2 were counted as motor neurons. 10 spinal cord slices between C4 and C5 were selected for each animal and the motor neurons present in the ventral horns of both the contralesional and ipsilesional spinal cord were counted (Filli et al., 2011). An average number of motor neurons in contralesional and ipsilesional ventral horns were calculated for each animal from the 10 analyzed slices.
To further determine the effect of stroke and PTN treatment on spinal motor neuron population of the cervical spinal cord we looked at the morphology of the motor neurons in the ventral horn. There is evidence that motor neurons have a reduced area when injured (Wu et al., 2016) and counts of motor neurons do not detect these changes in motor neurons morphology. The average area of the motor neurons counted for each animal on each side of the spinal cord was also determined. ImageJ software was used to manually trace the cell body of each counted neuron, from the tracing ImageJ software calculated the area of the traced motor neuron. The average of area of motor neurons in both contralesional and ipsilesional ventral horns were calculated for each animal.

Statistical analysis

Statistical analysis was performed using GraphPad Prism (Version7, GraphPad software, 2016). All figures presented show the mean and error bars denote the standard error of the mean (SEM)

Statistical analysis of stroke size was performed using unpaired, two-tailed Students t-tests. Statistical analysis of behavioral performance on all tests was performed by two-way ANOVA. Holm-Sidak multiple comparison testing was performed between groups when a significant main effect of treatment or a significant interaction of time x treatment was found. When there was a significant main effect of time but no significant main effect of treatment or interaction we performed Holm-Sidak's post hoc testing to identify within group differences at different time points.

Statistical evaluation of GFAP, IBA-1, GAP-43, serotonergic fibers density, motor neuron number and area were performed with two-way ANOVA, followed by Holm-Sidak's post hoc, to compare each treatment group to the un injured sham group. In addition, One-way ANOVA was used when each side of the spinal cord (ipsilesional or contralesional) was looked at independently, Holm-Sidak's post hoc was used to compare each experimental group to all other groups on the same side of the spinal cord.

Results

Histological assessment of ischemic lesions

The photothrombotic stroke model was used to induced consistent infarcts of the dominant forepaw forelimb somatosensory motor cortex. Stroke location and volume was confirmed by histological volume and stereotactic analysis. At 28 days after stroke, the infarct volumes measured 5.47 ± 0.08 mm^3 in PTN-treated rats and 5.43± 0.09 mm^3 in controls animals (Figure 5.1 D). There was no significant difference in volume between groups (unpaired t-test P = 0.6842, t = 0.4133 df =18).

PTN enhances post-stroke recovery

To determine deficits in forelimb motor function induced by stroke and subsequent recovery, rats were tested on the single pellet skilled reaching task and cylinder task of forelimb use preference at 3, 7, 14, 21 and 28 days post stroke. In addition, to assess changes in forelimb sensory function von Frey filament tests (mechanical sensitivity) adapted to the fore paw were done at 3, 7, 14, 21 and 28 days post stroke. Baseline performance values were established from tests performed one day prior to stroke (Figure 5.1 A). Stroke lesioning the forelimb sensorimotor cortex resulted in deficits when using the contralateral forelimb across all animals. At three days post stroke animals only achieved 10.94 ±1.55% of pre stroke reaching score on the single pellet reaching task (Figure 5.2 A,B). Two-way ANOVA of single pellet reaching performance over 28 days after stroke identified a significant main effect of time ($F_{(4,72)}$ = 174, P < 0.001) and PTN intraspinal treatment ($F_{(1,18)}$ = 7.378, P = 0.0142). Post hoc Holms-Sidak's multiple comparison tests revealed that PTN treated animals performed significantly better than controls at 28 days post stroke (P = 0.0054) achieving 94 ± 1.8% of their reaching success rates at baseline relative

to control animals that recovered to 76.6 ± 2.0% of baseline. These success rates represented a significant improvement from day 21 to 28 in PTN treated rats ($P < 0.0001$) but not controls ($P = 0.0836$). Notably, two-way ANOVA restricted to pre-treatment time points (3 and 7 days reaching performance) did not reveal any significant group differences or interactions ($P > 0.05$) prior to spinal injections.

Photothrombosis of the forelimb sensorimotor cortex also significantly reduced the use of the injured forelimb for weight support during rearing motions in all rats. Cylinder testing showed that after stroke the use of the preferred forelimb for weight support in rearing motions was reduced from 54.6 ± 2.9 to only 15.2 ± 3.3% after stroke (Figure 5.2 C,D). Analysis of forelimb preference data identified a significant main effect of time (Two-way ANOVA; $F_{(4, 72)} = 168.6$, $P < 0.0001$) but not of treatment (Two-way ANOVA; $F_{(1, 18)} = 3.203$, $P = 0.0904$). Holms-Sidak post hoc multiple comparisons within groups identified no significant changes in forelimb use preference between 7 days and 14, 21 or 28 days post stroke ($P > 0.05$) in control treated animals. However, PTN treated animals improved significantly from 7 days post stroke (pre-treatment) compared to 14 days ($P = 0.0402$), 21 days ($P < 0.0001$) and 28 days ($P < 0.0001$) post stroke.

Changes in mechanical sensitivity after stroke were studied using standard von Frey filament testing modified to the forepaw. Analyses of PWMT identified a significant main effect of time (Two-way ANOVA; $F_{(4, 72)} = 207.5$, $P < 0.0001$) but no significant main effect of treatment on mechanical sensitivity (Two-way ANOVA $F_{(4, 72)} = 1.577$, $P = 0.2252$; Figure 5.2 E,F). Holms-Sidak post hoc multiple comparisons within groups identified significant changes in forelimb mechanical sensitivity comparing 14 ($P < 0.001$), 21 ($P < 0.0001$) and 28 ($P < 0.0001$) days post stroke to 7 days post stroke in both PTN and control treated animals. Notably, PTN

treated animals exhibited significantly improved sensitivity when comparing 14 and 21 days post stroke ($P = 0.0098$) and 14 and 28 days post stroke while control animals did not ($P > 0.05$). Both PTN treated rats and controls exhibited significant improvement when sensitivity at 14 and 28 days was compared ($P < 0.0001$ and $P = 0.048$, respectively). Animals in the both the PTN and control groups recovered mechanical sensitivity to pre stroke levels (Figure 5.2 E,F) but there was no indication of hyperalgesia.

PTN treatment does not alter astrocyte or microglial cell density in spinal cord

Following cortical injury, axons in the corticospinal tract deinnervated by the ischemic infarct undergo Wallerian degeneration, inducing astrogliosis and the expression of glial fibrillary acidic protein (GFAP), which is a major component of inhibitory scars in the spinal cord. There was a significant effect of treatment condition on spinal cord GFAP immunofluorescent labeling intensity (two-way ANOVA; $F_{(3,22)} = 0.2905$, $P = 0.8318$, Figure 5.3 A). The side of the spinal cord in relation to the ischemic lesion (contra or ipsilesional) also had a significant effect on GFAP labeling (two-way ANOVA; $F_{(1,22)} = 0.06221$, $P = 0.8053$) and there was a significant interaction between side of the spinal cord and treatment condition on GFAP immunofluorescent labeling intensity (two-way ANOVA; $F_{(3,22)} = 0.8923$, $P = 0.4607$).

Independent analysis of immune labeling for GFAP on the contralesional side of the C4 spinal cord revealed a significant effect of treatment group on the GFAP density (One-way ANOVA $F_{(3.36)} = 5.584$, $P = 0.0030$, Figure 5.3 A,C). Multiple comparison testing (Holm-Sidak) on the contralesional side revealed significant difference (elevations) in GFAP labeling in stroke animals ($P = 0.0205$), stroke animals with PTN treatment ($P = 0.0056$) and stroke animals with vehicle treatment ($P = 0.0102$) when compared to Sham animals. Post hoc testing (Holm-Sidak)

also showed that there were no significant differences between stroke animals in different treatment groups. GFAP labeling was not significantly different between stroke animals with no treatment and stroke animals with PTN treatment ($P = 0.8992$) or stroke animals with vehicle treatment group ($P = 0.9275$). There was no significant effect of stroke on the ipsilesional side (One-way ANOVA; $F_{(3.36)} = 0.6956$, $P = 0.5608$, Figure 5.3 A) when independently analyzed.

Similarly, analysis of Iba-1 labelling for active microglia showed that the side of the spinal cord in relation to the ischemic lesion (contra or ipsilesional) has significant effect on IBA-1 labeling (two-way ANOVA; $F_{(1,72)} = 18.71$, $P < 0.0001$, Figure 5.3 B). However, there was no significant effect of treatment condition on spinal cord IBA-1 immunofluorescent labeling intensity (two-way ANOVA; $F_{(3,72)} = 2.236$, $P = 0.0913$, Figure 5.3 B) or interaction between side of the spinal cord and treatment condition on IBA-1 immunofluorescent labeling intensity (two-way ANOVA; $F_{(3,72)} = 2.143$, $P = 0.1022$).

Independent analysis of immunofluorescent labeling for IBA-1 on the contralesional side of the C4 spinal cord revealed a significant effect of treatment group on the IBA-1 density ($F_{(4,36)} = 4.237$, $P = 0.0065$, Figure 5.3 B,C). Multiple comparison testing (Holm-Sidak) on the contralesional side revealed significant difference (elevations) in IBA-1 labeling in stroke animals ($P = 0.0258$), stroke animals with PTN treatment ($P = 0.0131$) and stroke animals with vehicle treatment ($P = 0.0025$) when compared to Sham animals. Post hoc testing (Holm-Sidak) also showed that there were no significant differences between stroke animals in different treatment groups. IBA-1 labeling was not significantly different between stroke animals with no treatment and stroke animals with PTN treatment ($P = 0.7623$) or stroke animals with vehicle treatment group ($P = 0.6887$). There was no significant effect of stroke on the ipsilesional side (One-way ANOVA; $F_{(3.36)} = 0.2431$, $P = 0.8657$, Figure 5.3 B) when independently analyzed.

PTN and axon outgrowth

PTN has been demonstrated as a potent growth promotor of axons (Paveliev et al., 2016). GAP-43 is a protein found in axonal growth cones and it is commonly used as a marker of active axonal outgrowth. GAP-43 immunolabelling was therefore used to determine if spinal administration of PTN could induce axonal outgrowth in the cervical spinal cord following cortical injury.

There was a significant effect of treatment condition on spinal cord GAP-43 immunofluorescent labeling intensity (two-way ANOVA; $F_{(3,72)} = 24.22$, $P < 0.0001$, Figure 5.4 A). The side of the spinal cord in relation to the ischemic lesion (contra or ipsilesional) also had a significant effect on GAP-43 labeling (two-way ANOVA; $F_{(1,72)} = 85.68$, $P < 0.0001$) and there was a significant interaction between side of the spinal cord and treatment condition on GAP-43 immunofluorescent labeling intensity (two-way ANOVA; $F_{(3,72)} = 23.36$, $P < 0.0001$). Independent analysis of the contralesional spinal cord revealed that treatment had a significant effect on GAP-43 immunofluorescent labeling intensity (one-way ANOVA; $F_{(3,36)}=3.36$, $P<0.0001$). Further, multiple comparison testing (Holm-Sidak) on the contralesional side revealed significant differences in GAP-43 labeling between stroke animals ($P = 0.0047$), stroke animals with PTN treatment ($P < 0.0001$) and stroke animals with vehicle treatment ($P = 0.0046$) when compared to sham animals. Post hoc testing (Holm-Sidak) also showed a significant difference between stroke animals with no treatment and stroke animals with PTN treatment ($P < 0.0001$), however no significant difference was found between stroke animals with no treatment and stroke animals with vehicle treatment ($P = 0.9647$). There was also a significant difference in GAP-43 detected between stroke animals receiving PTN and stroke animals receiving vehicle ($P < 0.0001$ Figure 5.4 A-E). Independent analysis of immune labeling for GAP-43 on the

ipsilesional side of the C4 spinal cord did not reveal any significant differences between treatment groups (One-way ANOVA; $F_{(3.36)} = 0.8182$, $P = 0.4923$, Figure 5.4 A). Heightened contralesional expression of GAP-43 21 days after spinal injection suggests that PTN induces long lasting increases in active axonal sprouting.

PTN and monoamines (serotonergic) fibers

Degradation of CST axons following stroke leaves serotonergic fibers of the contralesional grey matter deinnervated, potentially leading to changes in monoamine fiber density in the spinal cord (Figure 5.5 B, C-F). Analysis of immunofluorescent serotonergic fiber density showed that the side of the spinal cord in relation to the ischemic lesion (contra or ipsilesional) has significant effect on serotonergic fiber density (two-way ANOVA; $F_{(1,72)} = 9.183$, $P = 0.0034$, Figure 5.5 A, C-F) however, there was no significant effect of treatment condition on spinal cord serotonergic fiber density (two-way ANOVA; $F_{(3,72)} = 2.554$, $P = 0.0034$). There was a significant interaction detected between side of the spinal cord and treatment condition on serotonergic fiber density (two-way ANOVA; $F_{(3,72)} = 3.787$, $P = 0.0140$, Figure 5.5A).

Independent analysis of the contralesional spinal cord revealed a significant effect of treatment group on the density of immunolabelling for serotonin (ANOVA; $F_{(3.36)} = 7.824$, $P = 0.0004$, Figure 5.5 A). Stroke animals and stroke animals with control injections showed a significant reduction in serotonergic fibers density when compared to sham animals (Holms-Sidak; $P = 0.0027$, $P = 0.0021$; respectively). Interestingly, stroke animals treated with PTN did not exhibit a significant reduction in serotonergic density when compared to sham animals (Holms-Sidak; $P = 0.6386$). Furthermore, stroke animals treated with PTN showed significantly greater serotonergic density than stroke animals with control injection ($P = 0.0164$) or stroke

alone ($P = 0.0232$). There was no difference in grey matter serotonin density in the ipsilesional C4 grey matter (ANOVA; $F_{(3.36)} = 0.05454$, $P = 0.9830$, Figure 5.5 A) when independently analyzed. Thus, we found that stroke induced a reduction in serotonergic fiber density in the contralesional spinal grey matter that was restored by PTN administration.

Motor neuron survival & morphology

Following stroke in the motor cortex and degeneration of the CST, degeneration of spinal cord grey mater motor neurons has been reported (Dang et al., 2016). To test if intraspinal PTN can prevent or reverses this degeneration, analysis of motor neurons immune labeled with ChAT was performed in the spinal cord at levels C4/C5. There was a significant effect of treatment condition on motor neuron number (two-way ANOVA; $F_{(3,72)} = 3.317$, $P = 0.0246$, Figure 5.6 A,B,D). The side of the spinal cord in relation to the ischemic lesion (contra or ipsilesional) also had a significant effect on the number of motor neurons (two-way ANOVA; $F_{(1,72)} = 19.86$, $P < 0.0001$) and there was a significant interaction between side of the spinal cord and treatment condition with relation to motor neuron counts (two-way ANOVA; $F_{(3,72)} = 3.246$, $P = 0.0268$, Figure 5.6 B).

Notably, there was a significant effect of stroke and treatment on motor neuron density in the contralesional spinal cord (ANOVA; $F_{(3.36)} = 7.208$ $P = 0.0007$, Figure 5.6 B). Holm-Sidak's multiple comparisons identified a significant reduction in motor neuron numbers in the stroke alone group ($P = 0.0031$) and the stroke with control injection group ($P = 0.0031$) when compared to the non-stroke sham (Figure 5.6 A,B,D). The PTN treated group was not significantly different form the non-stroke sham group ($P = 0.3523$). There were no changes in motor neuron number on the ipsilesional spinal cord (ANOVA; $F_{(3.36)} = 0.05594$ $P = 0.9823$)

(Figure 5.6 B).

Because injured motor neurons tend to decrease in somatic area, morphology of motor neurons was also assessed. The side of the spinal cord in relation to the ischemic lesion (contra or ipsilesional) had a significant effect on the number of motor area (two-way ANOVA; $F_{(1,72)}$ = 10.79, P = 0.0016 Figure 5.6 C,B,D). However, there was no significant effect of treatment condition on motor neuron area (two-way ANOVA; $F_{(3,72)}$ = 0.5673, P = 0.6380, Figure 5.3 A) and there was also no significant interaction between side of the spinal cord and treatment condition with relation to motor neuron area (two-way ANOVA; $F_{(3,72)}$ = 0.5131, P = 0.6745, Figure 5.6 C).

When analyzing hemisphers individually, a significant effect of treatment was detected on the contralesional spinal cord (ANOVA; $F_{(3.36)}$ = 7.946 P = 0.0003) (Figure 5.6 C). Similar to the motor neuron counts, stroke animals that received PTN treatment did not significantly differ from sham animals in the area of their motor neurons (P = 14.25). However, stroke animals (P = 0.0018) and stroke animals with control injections (P = 0.0008) had significant decreases in motor neuron cell body areas when compared to sham animal motor neuron cell body areas (Figure 5.6 C,D). There were no changes in motor neuron area in the ipsilesional spinal cord (ANOVA; $F_{(3.36)}$ = 0.1205 P = 0.9474, Figure 5.6 C). These results indicate that PTN can exert a protective effect for motor neurons in the spinal cord left deinnervated by injury to cortical motor areas.

Discussion

In this project, we sought to determine if pro-plasticity therapy delivered to the spinal cord 7 days after stroke could improve functional and anatomical recovery. The spinal cord contains essential sensory and motor pathways that are deinnervated, by stroke, and this spinal dysfunction contributes to the disability experienced by over 60% of stroke survivors (Dobkin, 2008, Kessner et al., 2016). Here, we provide preliminary evidence suggesting that PTN, an established growth promoting molecule during CNS development, administered into the spinal cord can augment spinal plasticity, reduce spinal degeneration, and improve recovery from cortical stroke.

PTN improves sensorimotor functions after stroke

Photothrombotic stroke lesioning the forelimb sensorimotor cortex resulted in an impairment in rats' ability to perform forelimb sensory motor tasks. Strikingly, intraspinal PTN administered into the spinal cord 7 days after these photothrombotic lesions was associated with improved performance on measures of skilled reaching and forelimb use preference. PTN has support as a potential therapy to improve outcomes in neurodegenerative diseases such as Parkinson (Gombash et al., 2012) and after spinal cord injury (Wang et al., 2004, Mi et al., 2007), but this is the first data that demonstrate PTNs ability to improve sensory motor outcomes after stroke.

PTN does not induce aberrant mechanical sensitivity

Recent studies have demonstrated a potent pro-plasticity effect of PTN in the spinal cord (Paveliev et al., 2016). Because nociceptive fibers can also sprout after injury or following

plasticity enhancing treatments, intraspinal PTN could theoretically increase mechanical sensitivity to the point of inducing hyperalgesia or mechanical allodynia. However, von Frey hair testing did not indicate the development of pathological pain circuitry. PTN and control treated rats exhibited similar patterns in normalization of PWMTs to baseline (pre-stroke) levels, hyperalgesia (reduced PWMTs relative to baseline) was not observed in any treatment group, suggesting that sprouting of nociceptive fibers did not occur to a level sufficient to alter pain sensitivity. It has been demonstrated that PTN mRNA upregulation during chronic pain development is associated with more rapid recovery from mechanical allodynia, though this effect was exclusive to Fischer 344 rats and was not replicated in Lewis or Sprague-Dawley rats (the latter were used in this study) (Ezquerra et al., 2007). Thus, while it is important to consider that endogenous expression of PTN may be strain specific, exogenous PTN would not be expected to induce mechanical allodynia based on our findings and these previous data.

PTN does not induce pathological inflammation

In cell culture models of ischemia/reperfusion injury, PTN has been demonstrated to enhance G1 to S phase transition of microglia resulting in increased microglial proliferation and activation (Miao et al., 2012). In our study, we did not observe any effect of PTN in microglial activation, though this is not surprising as *in vitro* microglia activation peaked at 24 hours after PTN administration and our assessment occurred 21 days after PTN treatment (Ito et al., 2001). It is possible that PTN did induce microglia proliferation and activation early after injection that reduces to average post-stroke levels by 21 days after injection (28 days after stroke). Increased microglial activity, even if only acute following PTN, could result in the excess production of proinflammatory molecules and exasperate astrocytic gliosis and formation of GFAP rich scars.

However, our data provide no indication of increased GFAP density in PTN treated rats. Furthermore, PTN has been proven to down-regulated microglia production of proinflammatory cytokines such as TNF-α, IL-1β or NO (Ito et al., 2001; Wang et al., 2010). Since PTN has a temporally limited role in microglia activation and does not induce proinflammatory cytokines release, it is not surprising that our results at 21 days post injection indicate no increased activity of microglia or aberrant astrogliosis in PTN treated animals when compared to control treated animals.

PTN induces post stroke neurite outgrowth

PTN has been well established as a growth promoter through the CNS in both *in vivo* and *in vitro* experiments (Paveliev et al., 2016). In a dorso-lateral spinal transection injury model where PTN was administered at the time of injury, PTN improved not only the number of axons entering the injury site for the caudal side but also the number of axons traversing the injury site (Paveliev et al., 2016). In addition, multiple *in vivo* imaging session revealed that PTN treated axons grow significantly faster than untreated axons (Paveliev et al., 2016). In these studies, the effects of PTN become evident 7 days after injection and PTN induced axon sprouting remained evident at 28 days post injury (Paveliev et al., 2016). Paveliev et al. (2016) hypothesize that PTN may play a crucial role in interactions between regenerating axons and pioneer axons that have already transversed the spinal cord lesion, which may account for the prevalent effects of PTN evident long after injection.

During development, PTN plays a crucial role in upregulating GAP-43 mRNA (Yanagisawa et al., 2010). In light of these previous studies, it not unexpected that we found increased levels of GAP-43, a protein marker of extending axon projections, in PTN treated

animals even 21 days after injection. This provides conclusive evidence that PTN promoted periods of active neurite outgrowth. However, sole use of GAP-43 as a marker of plasticity is a limitation of the study. While increased GAP-43 levels indicate heightened plasticity, manipulations which enhance GAP-43 have also been shown to reduce survivability in the same cells (Overman et al., 2014; Carmichael, 2016). In the case of the spinal cord, over expression of GAP-43 prolongs and enhances axonal spouting but at the same time increasing susceptibility of adult motor neurons to death (Harding et al., 1999). Moreover, expression of GAP-43 does not explicitly translate to axonal spouting and it does not represent a 1:1 relationship with axonal sprouting or final formation of new functional synapses (Carmichael et al., 2017). Second, GAP-43 levels do not give any indication of which axons are sprouting or the trajectory of the sprouting processes (Carmichael et al., 2017). Thus, while GAP-43 is a useful indictor of axonal spouting and plastic processes, caution must be used when making assumptions from immunohistochemical data as presented here.

PTN improves serotonergic innervation in the spinal cord after stroke

Serotonergic fibers found in the ventral spinal cord originate in the raphe nuclei of the medulla oblongata. Both the raphe pallidus and the raphe obscurus project to the ventral horns of spinal grey matter where they synapse on both interneurons and motor neurons, playing a key role in activating motor circuits, transmitting somatosensory information and facilitating reflexes (Kosofsky and Molliver, 1987; Jacobs et al., 2002). Following SCI, serotonergic input is lost to regions of the spinal cord distal to the site of injury (Fong, 2005), resulting in a significant reduction in serotonergic fibers in the ventral horns (Filli et al., 2011). This loss of serotonergic fiber density is evident 4 days after spinal cord injury and is still prevalent at 28 days post injury,

even at sites distal to the induced injury (Filli et al., 2011). Despite the lack of spinal injury, in our study stroke lesioning the somatosensory motor cortex reduced serotonergic density in the ventral grey matter of the contralesional to the stroke. Remarkably, we showed that treatment at 7 days post stroke with PTN reversed the deficits in serotonergic fiber density. It is likely that PTN promoted the regrowth of serotonergic fibers post injury, and this may account for some of the functional benefits resultant from PTN treatment. Since direct application of serotonin to the deinnervated spinal cord sites can improve stepping function and other motor deficits resulting from disruption of spinal circuits (Li & Raisman, 1995; Hill et al., 2001), PTN induced restoration of serotonergic innervation may play a crucial role augmenting motor recovery after injury.

PTN improves motor neuron density and morphology in the spinal cord after stroke

Following stroke, Wallerian degeneration of the CST leads to a loss of motor inputs into the spinal cord resulting in degeneration of deinnervated motor neurons. In our study PTN administration significantly reduced motor neuron cell loss. These results are supported by explant culture studies of the spinal cord in which PTN successfully increase motor neuron and axon outgrowth and exhibited neuroprotective action against excitotoxic motor neuron death (Mi et al., 2007). It is thought that the protective role of PTN in the spinal cord is mediated through the anaplastic lymphoma kinase (ALK) receptor, as blocking this receptor leads to not only a loss of the PTN protective effect on glutamate toxicity but also to a reduction in the length of motor neurons and primary spinal motor neurite outgrowth (Mi et al., 2007). We are the first to show that PTN administration it the spinal cord following ischemic stroke can preserve motor neuron density and prevent motor neuron atrophy in the deinnervated spinal cord.

In summary, our data shows that PTN enhanced atomically plasticity after stroke, reduced the loss of serotonergic fibers and motor neurons, and promoted the expression of growth associated proteins in the spinal cord. In addition, PTN improved behavioral recovery after stroke without inducing spinal inflammation or inducing aberrant pain circuity. Thus, intraspinal PTN is an attractive therapeutic intervention after cortical injury such as stroke.

Chapter 5: Figures

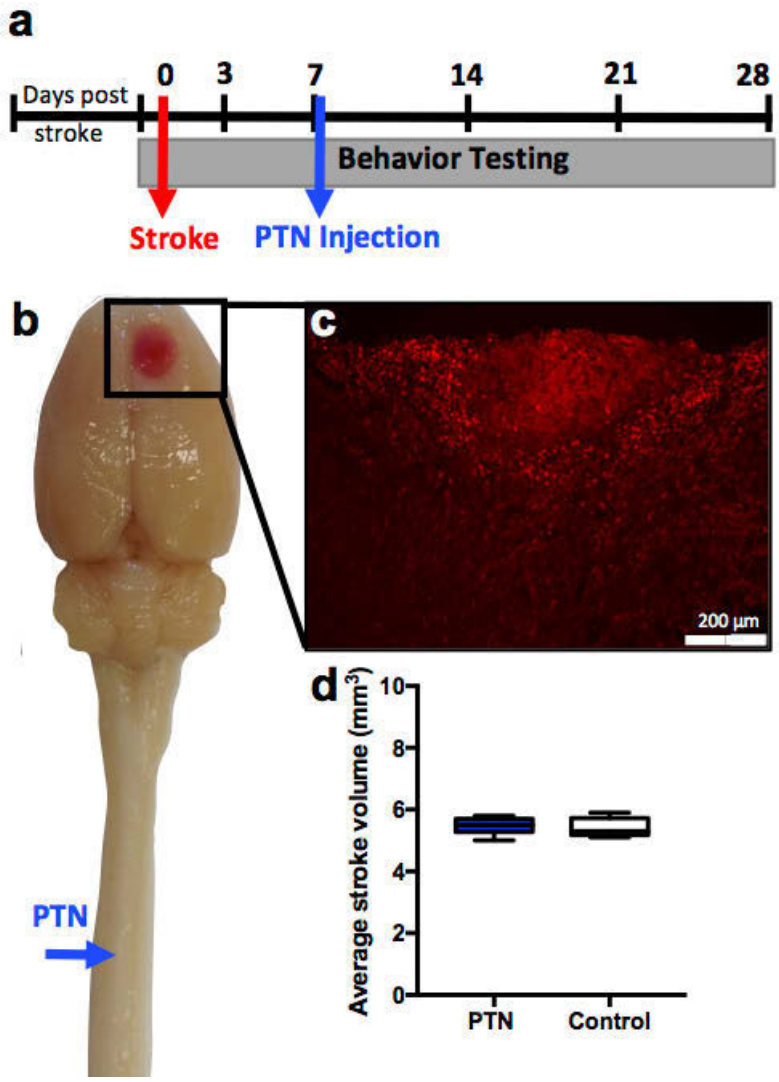

Figure 5.1. PTN spinal injection after induced photothrombotic stroke. (**A**) Time line of behavioral testing and surgical procedures. (**B**) Image of perfused rat brain demonstrating the location of induced stroke over the somatosensory motor cortex and location of PTN spinal injection at C4/C5. (**C**) GFAP (red) stain of stroke induced lesion at 7 days post stroke, showing infarct size and location, at the time of PTN injection, 10x confocal. (**D**) Average volume of induced stroke in PTN and Control treated animals, there was no significant difference in stroke sizes (two tailed unpaired t-test, $P = 0.68$).

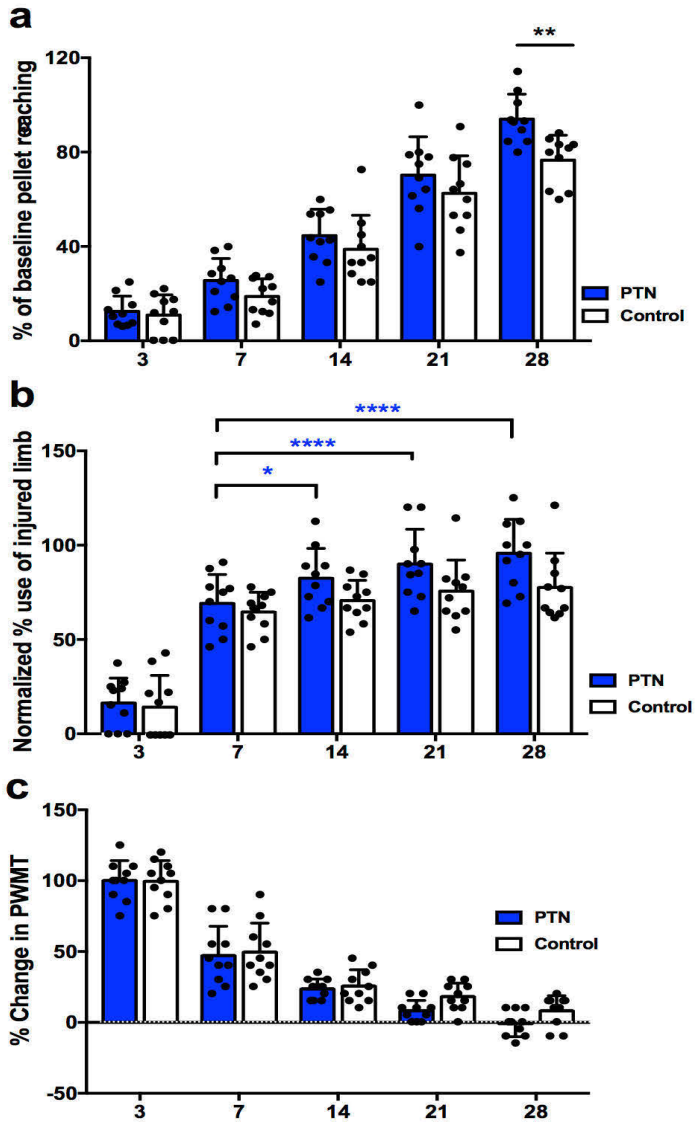

Figure 5.2. Effects of stroke on sensorimotor tasks. (**A**) Single pellet reaching score means as a percent of base scores established before stroke. Animals treated with PTN preformed significantly better than control treated animals at 28 days post stroke (Holms-Sidak; **, $P < 0.01$) overall there was a significant effect of PTN treatment (Two-way ANOVA; $F_{(1,18)} = 7.378$, $P = 0.0142$) and time (Two-way ANOVA; $F_{(4,72)} = 174$, $P < 0.001$). (**B**) The mean use of injured limb normalized to pre stroke use in the cylinder task for body weight support during rearing. Two-way ANOVA revealed a significant effect of time ($F_{(4, 72)} = 168.6$, $P < 0.000$) thus Holms-Sidak *post hoc* multiple comparisons were used to determine within group difference in

recovery. Use of the stroke injured paw was significantly improved in the PTN group between 7 days and 14, 21 and 28 days post stroke (*, $P < 0.05$; ***, $P < 0.001$; ****, $P < 0.001$). Whereas there was no improvement between 7 days (pre injection) and any post injection time points ($P > 0.05$) in the control injection group. (**C**) Changes in paw with drawl mechanical threshold (PWMT) compared to pre stroke using von Frey monofilaments testing of mechanical sensitivity there was no significant main effect of treatment on mechanical sensitivity (Two-way ANOVA; $F_{(4, 72)} = 1.577$, $P = 0.2252$), both PTN and control groups recovered to pre stroke sensitivity levels, indicating an absence or chronic pain.

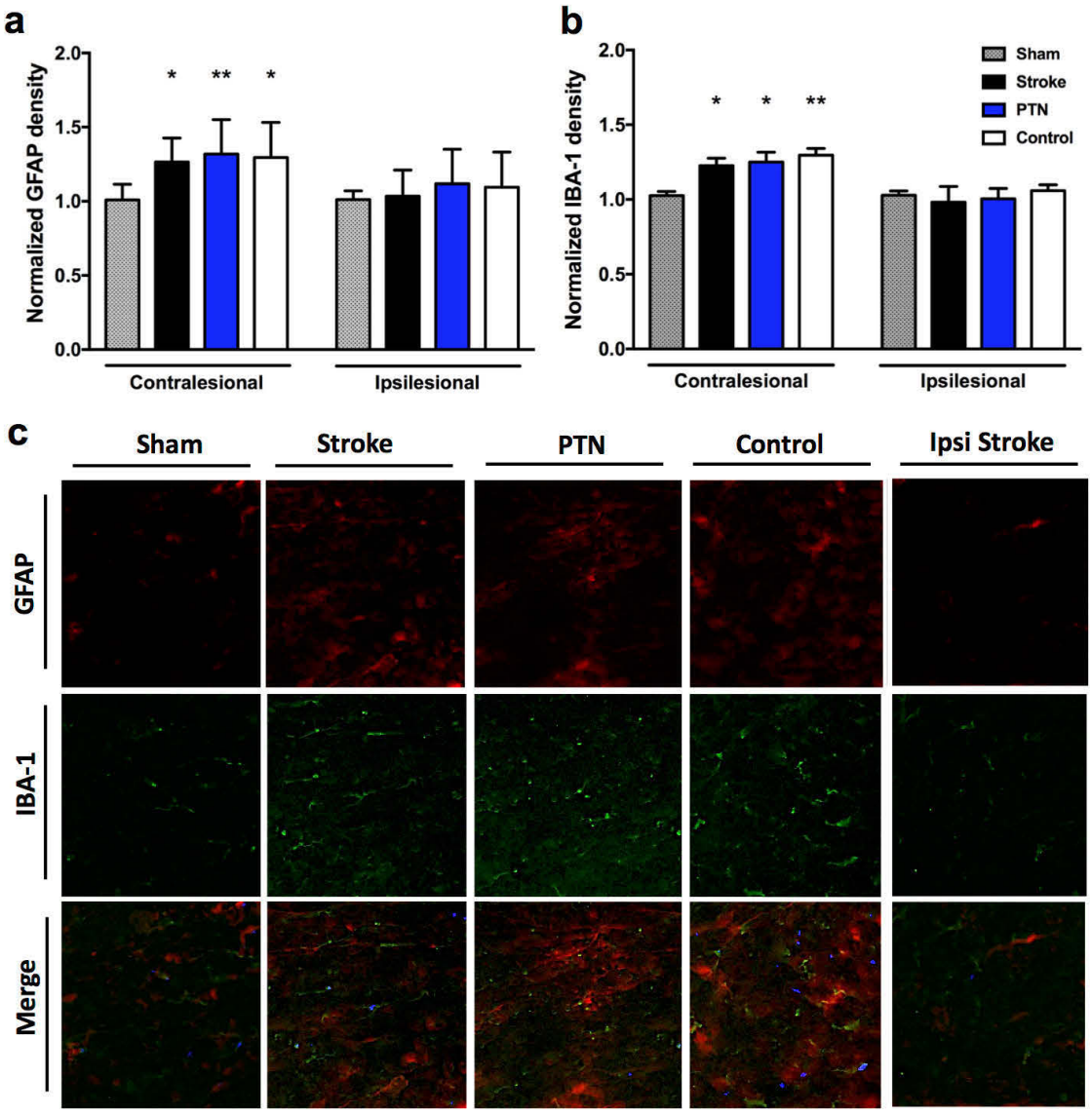

Figure 5.3. Post stroke changes in GFAP and IBA-1 density. (**A**) GFAP density normalized to sham, there was a significant effect of stroke on the contralesional side (One-way ANOVA $F_{(3.36)}$ =5.584, $P = 0.003$) with significant within differences between groups on the contralesional side when compared to sham (Holms-Sidak; **, $P < 0.01$; *, $P < 0.05$) (**B**) IBA-1 density normalized to sham there was a significant effect of stroke on the contralesional side (ANOVA; $F_{(3,36)}$ = 0.2745, $P = 0.7621$) with significant within differences between groups on the contralesional side when compared to sham (Holms-Sidak; **, $P < 0.01$; *, $P < 0.05$). (**C**) Fluorescent confocal images of GFAP in red (Texas Red) and IBA-1in green (Alexa 488) labelling in the ventral horn grey matter of the C4 spinal cord at 20x magnification (scale bar 100 µm).

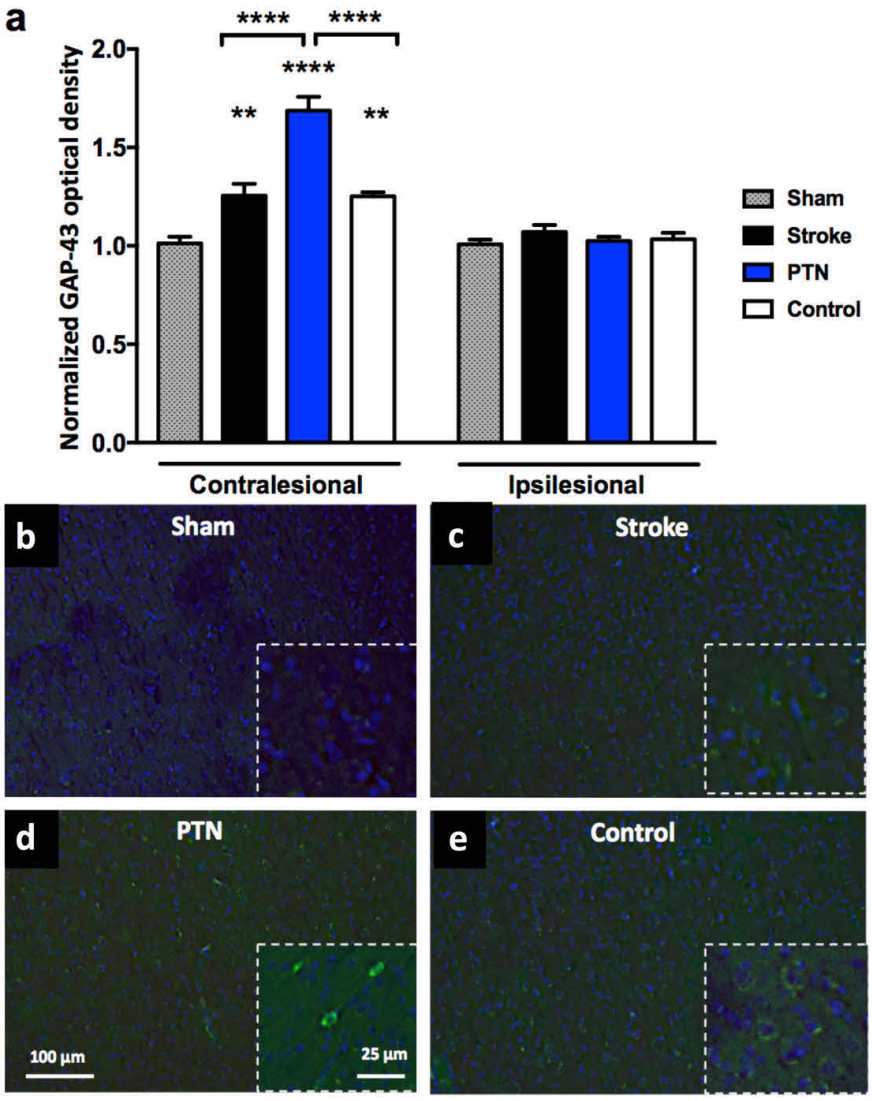

Figure 5.4. Normalized GAP-43 density. (**A**) Optical density of fluorescent GAP-43 labeling in the ventral horn of the C4 spinal grey matter with significant differences between groups on the contralesional sides (one-way ANOVA; $F_{(3,36)} = 3.36$, $P < 0.0001$). Significant elevation in contralesional GAP-43 levels when comparing PTN treated animals (Holms-Sidak; ***, $P < 0.001$), stroke and stroke with control injections (Holms-Sidak; **, $P < 0.01$) to sham animals. PTN treated animals had significantly elevated levels of GAP-43 when compared to stroke animals and stroke animals with control injections (Holms-Sidak; ****, $P < 0.0001$). (**B-E**) Confocal imaging (10x) on the contralesional side of the C4 spinal cord of GAP-43 (green, Alexa 488) and cell nuclei with DAPI (blue) fluorescent labeling in the ventral horn grey mater, with insets of 20x magnification (scale bars 100 µm and 25 µm respectively).

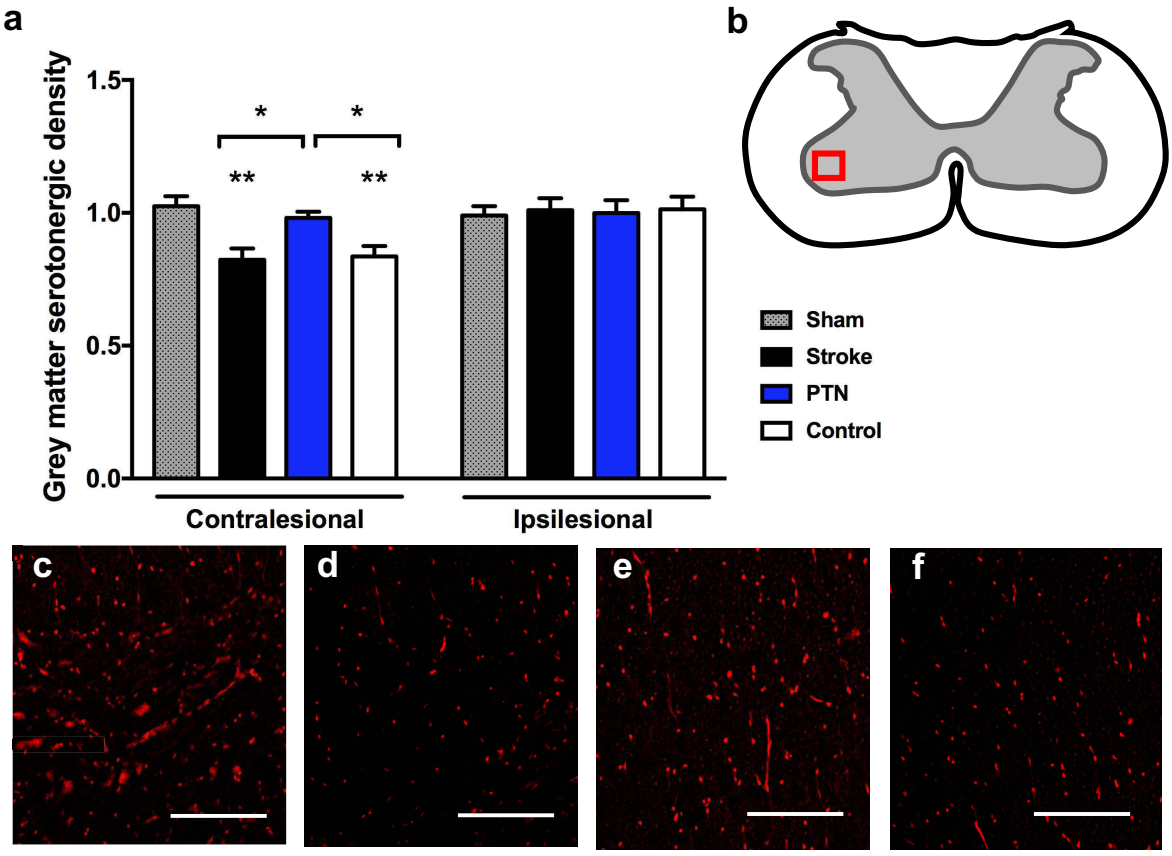

Figure 5.5. Changes in post stroke serotonergic density. (**A**) Stroke induces a significant reduction in serotonergic fibers density (ANOVA; $F_{(3.36)} = 7.824$ $P = 0.0004$) of the C4 ventral horn grey matter. Stroke animals not receiving PTN treatment had significant reduction in serotonergic fiber density compared to sham (Holms-Sidak; **, $P < 0.001$) and significant reduction when compared to PTN treated stroke animals (Holms-Sidak; *, $P = 0.0164$). (**B**) Schematic illustrating the location of C4 ventral horn grey matter analyzed for serotonergic fiber optical density. (**C-F**) Confocal imaging (10x) of serotonergic fibers fluorescent labeled (Texas red) in the ventral horn grey matter as outlined in (**B**). Images include (**C**) contralesional sham, (**D**) contralesional stroke, (**E**) contralesional stroke with PTN treatment and (**F**) contralesional stroke with vehicle treatment (scale bar 100 μm).

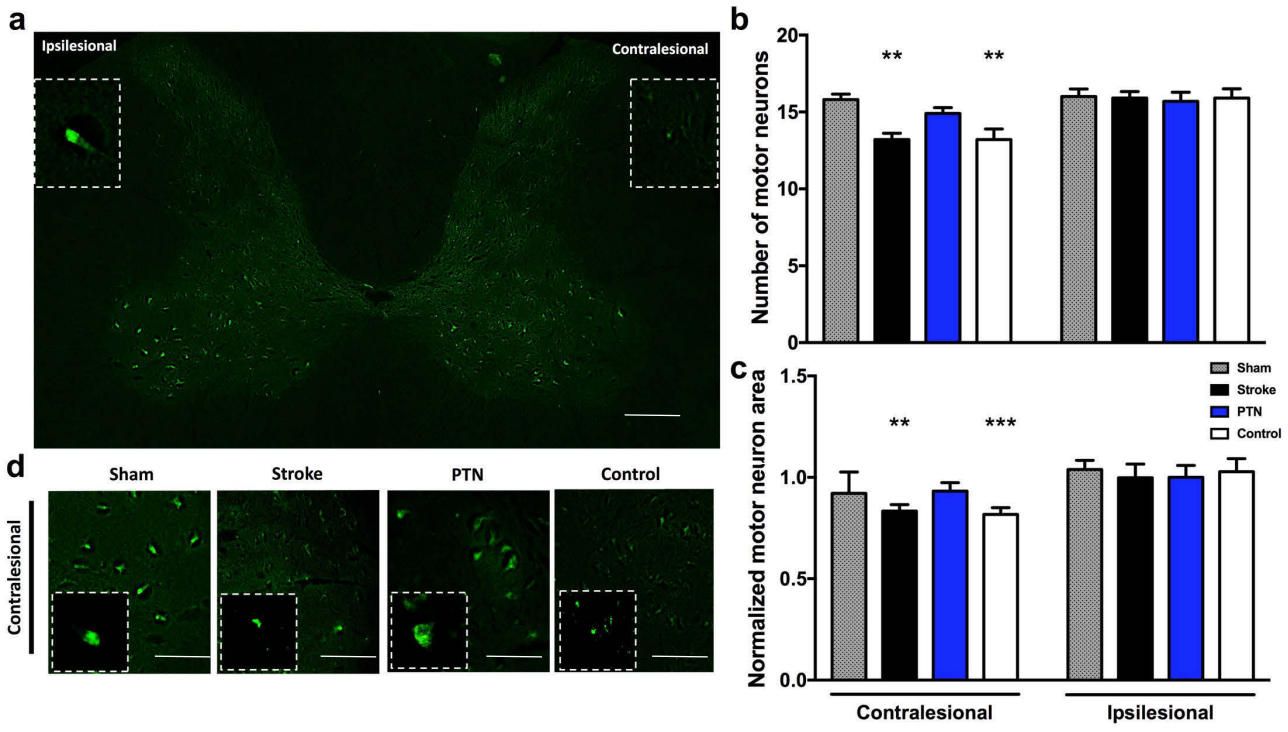

Figure 5.6. Post stroke changes in motor neuron density and morphology. (A) Confocal fluorescent microscopy (5x) showing depletion of motor neurons labelled with ChAT antibody in green (Alexa 488) in a cross section of the C4 spinal cord contralesional spinal cord (scale bar = 250 μm). (**B**) Average number motor neurons in of the C4 dorsal horn. There is a significant reduction in the number of motor neurons as a result of stroke (ANOVA; $F_{(3.36)} = 7.208$ $P = 0.0007$) when compared to sham animals (Holm-Sidak; **, $P = 0.0031$) which is recovered by PTN treatment. (**C**) Average area of motor neurons counted in (B) normalized to sham. Significant effect of stroke on the contralesional side (ANOVA; $F_{(3.36)} = 7.946$ $P = 0.0003$) where stroke and stroke control treated animals have significant reductions in moto neuron size compared to sham Holm-Sidak; **, $P < 0.01$, *** , $P < 0.001$). (**D**) Contralesional motor neurons of the ventral horn (10x) with inset image of (20x) motor neuron labelled with ChAT in green (Alexa 488; scale bar = 50 μm).

Chapter 6:

Conclusion

Stroke is a leading cause of permanent adult disability worldwide. Although some recovery occurs in the first few weeks after stroke (Wahl and Schwab, 2014; Wahl et al., 2014), over 90% of stroke survivors (Carey et al., 1993; Dobkin, 2008) are left with persistent disability ranging from partial paralysis to muscle weakness and impaired speech (Kessner et al., 2016). This thesis investigated pro-plasticity therapies that modulate growth inhibition in the spinal cord as avenues to reopen or augment the therapeutic window for recovery.

ChABC modulates plasticity in the spinal cord after stroke

In Chapter 2, the hypothesis that inducing plasticity in the spinal cord during chronic stroke could stimulate a second wave of recovery from sensorimotor impairment was tested. Although most traditional treatments for stroke are focused on the cortex, this study targeted the spinal cord. Notably, structural analyses in human patients has established a critical correlation between damage and degeneration in the corticospinal tract and functional sensory motor recovery after stroke (Lindenberg et al., 2010; Wahl et al., 2016). Our study expands on previous studies that have demonstrated that augmenting plasticity in the spinal cord with ChABC during the temporal window of stroke-induced plasticity (3 days post stroke) can potentiate recovery from cortical stroke by augmenting the formation of compensatory connections from spared cortical neurons to spinal motor networks (Soleman et al., 2012). Although promising, improving plasticity in early time points after stroke would not benefit chronic stroke suffers left with permanent disability even after rehabilitation. Therefore, in this study spinal plasticity was potentiated during chronic stroke, weeks after the initial ischemic injury. Rats were administered microinjections of chondroitinase ABC into the grey matter of the deinnervated cervical spinal cord 28 days after photothrombotic stroke lesioning of the forelimb sensorimotor cortex. The

efficacy of spinal therapy to improve recovery from stroke was assessed using a battery of sensorimotor tests (including assessment of skilled reaching, forelimb use preference, and mechanical sensitivity) and the plasticity of the corticospinal tract originating in peri-infarct cortex was assessed using anterograde neuronal tract tracers.

ChABC induces anatomical plasticity

Chondroitinase ABC digests chondroitin sulfate proteoglycans, potent inhibitors of neurite outgrowth found in the extracellular matrix, and our data show that these chondroitinase injections induced drastic sprouting of corticospinal axons in spinal grey matter. Although it has already been demonstrated that spinal injections of ChABC early after stroke promote cervical collateral sprouting of the uninjured CST (Soleman et al., 2012), no studies have assessed sprouting of the spared CST projections that arise from tissue adjacent the infarct. Therefore, this study focused on spared fibers of the injured CST which mediate connections between the stroke deinnervated spinal cord and the injured cortex by injecting retrograde tracers slightly medial to the cortical infarct. We demonstrate that ChABC induces extensive re-innervation of the cervical spinal grey matter by fibers emanating from the injured CST and an increase in CST fibers crossing over to the ipsilesional spinal grey matter. This is the first evidence that ChABC can induce sprouting of the injured CST during chronic stroke.

Although novel sprouting induced by ChABC from the injured CST was found in this study, the effect of delayed ChABC treatment on collateral sprouting of the uninjured CST was not assessed. In severe strokes with large cortical infarcts, there is axonal spouting from the injured cortex into the intact cortex and remapping of sensory motor connection to the uninjured CST, thus the uninjured CST is likely to be an important factor in our experimental model

(Carmicheal et al., 2016; Wahl et al., 2014). Wahl et al. (2014) suggested that the recovery of rat forelimb function after stroke after plasticity enhancing treatments originates from extensive and precise reinnervation of the stroke-denervated spinal hemicord by midline-crossing fibers from the intact motor cortex and CST. It would be interesting to determine if ChABC can elicit the same pattern of reinnervation when applied during chronic stroke, and determine the functional correlates of rewiring of the ipsi- and contra-lesional CST.

Tracers studies elegantly demonstrate the sprouting of spared fibers; however, this is only one component of plasticity. Changes in synaptic density in the cervical spinal cord of chronic stroke rats were not evaluated. Studies combining tracers and synaptophysin immunochemistry as a correlate of synapse number and location would provide greater insight into the role of spared and uninjured branching fibers in the CST. However, the formation of synapses does not prove the formation of meaningful, functional connections as it has been established that sprouting fibers are not always functionally connected to the surrounding neural networks (Tom et al., 2009). Although axonal sprouting is an important component of post stroke plasticity further studies are needed to expand on this work and explore additional aspects of plasticity including the formation of new synaptic connections.

ChABC therapy requires rehabilitation for functional improvement

Heightened anatomical spinal plasticity induced by ChABC was associated with significantly improved performance on skilled reaching tasks. However, despite drastic increases in the number, length, and distribution of CST axons in the cervical grey matter, there was only moderate functional benefit of ChABC alone (without rehabilitative training). Although disappointing, this result was not unexpected as previous studies in C4 spinal cord injury models

indicate that ChABC injection alone does not allow for improvements in sensorimotor function and it is only once ChABC is combined with rehabilitative training that functional benefits are achieved (Garcia-Alias et al., 2009). When task specific rehabilitative training was delivered during chronic stroke, ChABC dramatically potentiated the efficacy of training, leading to significant improvements in sensory motor function. Equivalent training in animals with control injections was significantly less effective. Similar findings have also been reported with other plasticity promoting treatments such as intracortical BDNF (Vavrek et al., 2006; Weishaupt et al., 2013) and the effects ChABC administered at time points early after CNS injury have been shown to be amplified with rehabilitative training (Moon et al., 2001).

Finally, to model patients who receive early rehabilitation but remain disabled during chronic stroke, a cohort of rats received rehabilitative training initiated early after stroke and sustained into the chronic phase of recovery. Animals receiving rehabilitative training starting 3 days after stroke recovered a greater degree of sensory motor function at 28 days post stroke than did animals receive no rehabilitative training; however, reaching performance did not significantly improve between 14-28 days despite sustained rehabilitative training (Figure 2.5). This result is in agreement with animal studies demonstrating that training initiated 4-7 days after ischemic injury is most effective for restoring behavioral performance (Nudo et al., 2006) and rehabilitative training initiated 14-28 days after injury only modestly improved functional outcomes as animals retained extensive functional deficits (Biernaskie et al., 2004). Although early rehabilitative training improved sensory motor recovery, animals still experienced a plateau in recovery 14-28 days after stroke and were left with chronic deficits despite ongoing training (Figure 2.5 C). This is in alignment with previous studies finding that extending the training periods beyond 28 days post stroke offers no functional benefit as most recovery is achieved in

the first 14 days after stroke regardless of extended periods of training (Biernaskie et al., 2004).

From these studies it is evident that once behavioral recovery has plateaued little functional improvement is gained from any further rehabilitative training. We are the first to demonstrate that after initial recovery from stroke (with or without training) spinal injection of ChABC can induce plasticity that allows functional recovery of chronic deficits. Although we found ChABC offers a reduction in functional deficits on task for which animals received rehabilitative training, this does not necessarily translate to global improvements across all sensory motor tasks.

ChABC offers task specific improvements

The results obtained in this our only indicate that ChABC improves performance on task for which specific rehabilitation training was assigned (Figure 2.2 C; Figure 2.4 C,D; Figure 2.5 A) . In light of an important scientific review cautioning 'be careful what you train for' (Tetzlaff et al., 2009), it is evident that other measures of forelimb function on tasks which were not part of the rehabilitative training could have been included in the study. Girgis et al. (2007) demonstrated that animals with cervical spinal cord injury that were given task specific training performed better on the trained task than animals given no rehabilitative training. However, animals which received task specific training were significantly worse on novel untrained tasks (horizontal ladder) when compared to animals receiving no rehabilitative training at all (Girgis et al., 2007). Future studies are needed to investigate if this finding carries over to the post stroke treatment paradigm used in this study. These studies should include the additional forelimb testing on untrained tasks such as ladder walking in order to determine if the forelimb functional improvement is task specific.

ChABC induces a defined temporal window of plasticity

Interestingly, our results show that ChABC opens a window of recovery that closely mimic that of the innate recovery (Figure 2.5 A). Animals achieved most functional improvements between 7-14 day after treatment and the functional improvements induced by ChABC plateau by 28 days post injection (Figure 2.5 A). The window of secondary plasticity is temporally limited by the enzyme kinematics of ChABC. Enzymatic studies showed the digestion of GAG chains is most elevated from 7 to10 days after injection (Lin et al. 2007), which is likely why functional improvements do not emerge until at least 7 days after injection. The reestablishment of peri-neural nets and GAG chain structures begins 14 days after injection are close to pre digestion levels at 4 weeks after injection (Lin et al., 2007). The restoration of CSPG matrices likely closes the window of plasticity induced by their digestion.

It is tempting to consider future studies in which ChABC injections are administered every 14 days for months to extend the induced period of plasticity, thereby preventing a plateau in functional recovery. Similarly, mammalian-compatible engineered ChABC delivered via lentiviral vector (LV-ChABC) can be induce large-scale CSPG digestion for spinal cord repair which may lead to drastic improvement in plasticity (Bartus et al., 2014). Although inducing an extended period of plasticity is attractive, it is important to consider that all plasticity is not functionally beneficial and extended periods of unregulated plasticity are unlikely to induce exponential improvements. Carmichael et al. (2016) identifies a form of maladaptive plasticity termed “unbound axonal sprouting”, which could occur in the spinal cord after prolonged plasticity enhancing treatments, leading to aberrant axonal sprouting into functionally unrelated parts of the cervical spinal cord. After stroke, when Nogo signaling in rats is blocked followed

by intense daily skilled reach training (sequential administration of plasticity enhancement followed by training) axonal sprouting and functional recovery are enhanced (Wahl et al., 2014). However, when Nogo is blocked at the same time as intense daily skilled reach training (simultaneous administration of plasticity enhancement and training) animals again have enhancing sprouting but functional outcomes are worse than control conditions. This may be the result of aberrant unbound spouting inducing maladaptive connectivity in the spinal cord that dampens recovery. Fortunately, in our study (Figure 2.5 A) combining rehabilitative training with the window of plasticity induced by ChABC did not worsen functional outcomes, but we administered our plasticity enhancing treatment after innate plasticity was extinguished, whereas the Nogo blockade (Wahl et al., 2014) was administered immediately after stroke when innate plasticity was still heightened. In human studies, stroke patients given high intensity rehabilitation immediately after stroke when innate plasticity is enhanced recovered less well than those patients beginning treatment later 4 to 7 days after stroke (Domerick et al., 2008). Considering these findings, prolonged ChABC expression to induce a long sustained period of plasticity could potentially induce aberrant unbounded axonal sprouting.

As an alternative to extending the window of plasticity into one long period of enhanced axonal sprouting, we might consider inducing sequential windows of plasticity allowing a plateau in recover before re-initiating plasticity. Although this strategy limits plasticity to a finite period, this may prevent unbounded axonal sprouting. Opening multiple windows of plasticity may offer a more viable solution than simply keeping the window of plasticity open for an extended period of time. This could be achieved with multiple injections or with an inducible expression system.

ChABC does not induce the formation of pain circuity

Nociceptive fibers can also sprout after injury or plasticity enhancing treatments, intraspinal ChABC could potentiate mechanical sensitivity and induce hyperalgesia. Therefore, in this study we incorporated testing for mechanical touch sensitivity using the von Frey hair test (Figure 2.2 G,H, Figure 2.4 G,H, Figure 2.5 E). Von Frey hair testing did not indicate the development of pathological pain circuitry. While ChABC treated rats in some cases exhibited faster normalization of PWMTs to baseline (pre-stroke) levels, hyperalgesia (reduced PWMTs relative to baseline) was not observed in any treatment groups, suggesting that sprouting of nociceptive fibers did not occur to a level sufficient to alter pain sensitivity. Von Frey hair testing only measures mechanical allodynia, so in future studies thermal hyperalgesia could also be incorporated. Spasticity is another potentially undesired side effect of plasticity enhancing treatments. Future studies should therefore asses the range of motion in the effected limb of the animal and the loss or selective shortening of soft tissue in the injured limb post modem (Iwasawa et al., 2016).

ChABC, rehabilitation and serotonergic density in the spinal cord

From this study a clear interaction between ChABC treatment, rehabilitative training, and the density of serotonergic innervation of the cervical spinal cord has emerged. Chronic stroke animals had a reduction in serotonergic fiber density on the deinnervated side of the spinal cord at C5 which was not improved by ChABC treatment alone; however, when ChABC was paired with rehabilitation serotonergic density was restored. We postulate that recovery of serotonergic fiber density is one mechanism by which sensory motor function is improved after ChABC treatment as spinal cord injury studies have demonstrated the importance of serotonergic fibers

regrowth in sensory motor function (Jacobs et al., 2002). Tom et al. (2009) found that ChABC treatment after spinal cord injury induces serotonergic fiber spouting, however despite the improved serotonergic density there were no detectable changes in the density of synaptic components or any functional improvements on behavioral tests assessing motor function (Tom et al., 2009). In future studies immunochemistry for synapsin 6 or synaptophysin should be employed to assess changes in synaptic density of the spinal grey matter and focus on colocalization of active synapse with serotonergic fibers (Tom et al., 2009). Future studies might also examine extended time points after ChABC treatment (3-6 months post injection) to determine if the enhanced serotonergic fibers density induced by ChABC and rehabilitative training is maintain or if these fibers diminish in the months after induced plasticity.

Overall, this study demonstrated for the first time that ChABC administered in the spinal cord of rats with chronic sensory motor deficits as a result of stroke can induce a second wave of post-stroke plasticity that can be harnessed to improve the efficacy of effective rehabilitative training, a potentially important finding for millions of stroke survivors currently living with permanent, intractable disability. The underlying mechanism by which ChABC promotes enhanced recovery are not fully understood, therefore *in vitro* experiments to further elucidate the effects of ChABC and its cleavage produces on different isolated neural cells types were performed.

C-4-S directly interacts with neurons to induce outgrowth

We first investigated the direct regulation of neurite outgrowth by CSPG cleavage stubs. Specifically, we used a human neuroblastoma cell line (SH-SY5Y) plated on growth inhibitory CSPG or growth permissive laminin matrices and directly applied ChABC digestion byproducts

('stubs', C-0-S, C-4-S or C-6-S) to the cell culture media and assessed neurite growth (Figure 3.1). In addition, we repeated the study but we incorporated the stubs into the matrices on which SH-SY5Y cells were growing and again looked for augmentation in neurite outgrowth (Figure 3.3). This experimental design was chosen as it allowed us to assess the effect of free and bound cleavage byproducts on neurite outgrowth and to determine if these effects are CSPG dependent. We found that both bound and free C-4-S cleavage stub directly promoted the outgrowth of neurites when cells were platted in inhibitory CSPG matrices but not on laminin, while C-6-S and C-0-S did not promote outgrowth of neurite in any plating condition. Thus, the presence of CSPGs are necessary for C-4-S to induce growth promotion. This is not entirely surprising as other growth factors have previously been shown to depend on binding to heparin sulfate (HS) chains of the neuron surface to induce their effect (Rauvala et al., 1994). In addition, PTPσ has recently been shown to mediate CSPG inhibition of neurite outgrowth by binding to the side chains of CSPG. Since C-4-S is a cleaved product of the side chain, it is possible that it can still interact with PTPσ thereby reducing the CSPG inhibition (Shen et al., 2009; Coles et al., 2011). Binding studies of PTPσ and the C-4-S cleavage stub should be conducted in the future to assess if the cleavage stub is acting on PTPσ specifically and determining binding affinity would also be useful. Understanding the direct interaction of the cleavage stubs with different growth receptors is an important future direction since we have shown that the C-4-S stubs alone induces neurite outgrowth and does so in a CSPG dependent manner. CSPG may be required to facilitate the interaction of C-4-S with the receptor at which it acts to induce outgrowth since chondroitin sulfates are also known to modulate intercellular signaling pathways and can localize soluble ligands to facilitate interaction of the ligand with cell surface receptors. Moreover, since ChABC cleavage produces stubs which are highly immunogenic neo-epitopes, they interact with a variety

of immune cells types in the CNS and their role in neurite outgrowth is not restrict to direct interaction with neurons (Glant et al., 1998; Ebert et al., 2008).

Effect of C-4-S stubs on microglia

There are conflicting views on how microglia respond to ChABC and its cleavage products. Some studies have suggested that ChABC may act to reduce microglial infiltration at the injury site therefore reducing scar formation (Rolls et al., 2008; Karimi-Abdolrezaee et al., 2012); however, there is strong evidence that ChABC treatment promotes microglia activation (Ebert et al., 2008). ChABC cleavage stubs have been found to stimulate activated microglia to take on a novel regulatory neuroprotective phenotype (Rolls et at., 2005, 2008), shifting microglia from the M1 to the M2 phenotype. In this study C-4-S cleavage stubs were found to promote biologically activated microglia to release the growth factor BDNF and the anti-inflammatory molecule IL-10 (Figure 3.5), while attenuating the release of pro-inflammatory factors NO and TNF-α (Figure 3.6), as a result media from C-4-S treated activated microglia to improved neurite outgrowth (Figure 3.4). Our data supports the finding of Rolls et al. (2005) that ChABC generated cleavage stubs induces a protective phenotype in microglia. Future studies should be designed to investigate changes in the expression of M1 (CD16, CD32, CD86, MHC II, and iNOS) and M2 (enzyme arginase 1) microglia markers after treatment with the C-4-S stub to elucidate if C-4-S is inducing a phenotypic shift. In addition, it would be interestingly to study in culture how these markers change after biological activation by an activator such as IFN-γ or LPS and if the C-4-S stub can prevent a shift in phenotype following activation.

In vitro studies have confirmed that microglia activated by ChABC cleaved CSPG disaccharides possess an increased capacity for phagocytosis whilst lacking cytotoxic functional

properties such as NO secretion (Ebert at al., 2008). Although we did not perform assays for phagocytosis we did find that the C-4-S stub reduced NO in biologically activated microglia (Figure 3.6 A), confirming the finding of Ebert at al (2008) that CSPG cleavage stubs reduced microglia inflammatory profiles. In addition, we were able to isolate which cleavage stub was responsible for this effect in isolated microglia cultures.

All the microglia in this study were cultured from day 1-2 rat pups, which induces a possible source of error. Recent studies of microglia harvested from day 3 mouse pups by Crain et al. (2013) demonstrate that microglia at P3 have relatively high expression of iNOS, TNFα and arginase-I mRNA when compared to adult microglia (2-4 months) which are characterized by low proinflammatory cytokine expression. These age-dependent differences in gene expression indicate that microglia likely undergo phenotypic changes during ontogenesis and development. When comparing cultured P3 microglia to microglia *in vivo*, primary microglia prepared from P3 mice had considerably altered gene expression, with elevated levels of TNFα, CD11b and arginase-I, suggesting that culturing may significantly alter microglial properties (Crain et al., 2013). Although P3 cultured microglia are more inflammatory than healthy adult microglia *in vivo*, they may inadvertently mimic microglia near the ischemic injury in the stroke injured brain. It is important to consider that the way microglia behave *in vitro* is not a direct reflection of how they behave *in vivo*, however these reductionist models are important when attempting to determine the mechanism of action of any molecule at a cellular level. *In vivo*, microglia closely interact with astrocytes, especially after injury and during inflammatory processes, therefore we investigated the effect of the C-4-S stub on mixed glia cultures under various activation conditions.

Effect of C-4-S stubs on mixed glia

C-4-S cleavage stubs induce mixed glial populations to release different factors during primary and secondary biological activation. After primary activation, C-4-S induced the release BDNF and attenuated the release of NO in mixed glial populations; however, after secondary inflammatory activation, C-4-S primed glial release of BDNF and the anti-inflammatory cytokine IL-10 (Figure 3.7 B,C) while attenuating IL-1β and IL-6 release (Figure 3.8 C,D). The finding that LPS activated mixed glial cultures produce more BDNF than LPS activated microglia cultures alone is not entirely surprising as BDNF has been shown to be produced by astrocytes (Miyamoto et al., 2015) and oligodendrocytes (Segura-Ulate et al., 2017) in the cortex. Further, after spinal cord injury BDNF is found to co-localized with all three glia subtypes in regions near the induced injury (Dougherty et al., 2000). In THP-1 macrophages, chondroitin sulfate treatment after LPS or hyaluronic acid activation treatment alone did not elicit ant-inflammatory response. However, primed with LPS, HA fragments produced large dose-dependent decrease in IL-1β production by THP-1 macrophages (Stabler et al., 2017). Similar to our study the ability of chondroitin sulfate cleavage stubs to reduce expression of inflammatory IL-1B was only conferred in immune cells which were activated by LPS followed by a secondary inflammatory event (Figure 3.8 D). This study identifies a trophic and anti-inflammatory effect of a CSPG cleavage stubs and suggests potential of therapeutic potential of the isolated C-4-S stub. CSPG inhibition and receptor interactions are modulated by a number of endogenous molecules and therapies which do not rely on the digestion of CSPG must also be considered.

PTN, an endogenous modulator of CSPG induced growth restriction

One potential modulator of CSPG growth inhibition is pleiotrophin (PTN), a growth factor and cytokine that is upregulated in the central nervous system (CNS) during periods of development and following injury (Gonzales-Castillo et al., 2015). In the CNS, PTN must bind chondroitin sulfate side chains in order to promote neurite outgrowth via the cell surface receptor proteoglycan glypican-2 and prevent the activity of growth inhibitory protein tyrosine phosphatase sigma receptors (Paveliev et al., 2016). In addition, PTN is known to upregulate the production of growth factors and inflammatory molecules in the CNS following insult (Fernandez-calle et al., 2017). However, the cell specific consequences of PTN on neuronal and glial cells in the CNS are not well defined.

Here, we examined the effects of exogenous PTN on neurite growth (Figure 4.1, 4.2), glial activation and glial release of immunomodulators (Figure 4.4, 4.5) *in vitro*. Consistent with previous literature (Kinnunen et al., 1996; Hida et al., 2003), directly treating neuronal cell lines with PTN increased neurite outgrowth on inhibitory CSPG matrices only and had no effect on neurite outgrowth when cells were plated on laminin surfaces (Figure 4.1). Our finding that PTN is only effective in improving neurite outgrowth on CSPG matrices is also supported by recent studies which determined that PTN binds chondroitin sides chains with high affinity, therefore out competing transmembrane tyrosine phosphatase sigma (PTPσ) and preventing activation of the growth inhibitory downstream pathways of PTPσ (Paveliev et al., 2016). In addition to removing inhibition induced by PTPσ, when PTN binds CSPG's it forms a complex which interacts which cell surface receptor bound glypican-2 which induces growth promotion (Paveliev et al., 2016). In light of these receptor interactions which require PTN to bind chondroitin sulfate side chains it is not surprising that the growth prompting effect of PTN was

only seen in our study when neurites were plated on CSPG matrices. However, PTN may also indirectly improve neurite outgrowth by modifying the release of cytokines from other neural cells types.

PTN modulates microglia cytokine release

PTN directly interacts with neurites to improve outgrowth (Figure 4.1) but supernatant from activated (IFN-γ) microglia treated with PTN also induced an increase in the length of neurites plated on CSPGs. Supernatant from activated (IFN-γ) microglia treated with PTN improved neurite outgrowth to a greater extent than supernatants from microglia treated with IFN-γ or PTN alone (Figure 4.2). Assays of microglia supernatant revealed that PTN stimulates microglia to release BDNF a trophic factor (Figure 4.4) and PTN induces a reduction in release of the inflammatory molecule IL-1B from biologically activated microglia (Figure 4.5). These findings are consistent with work suggesting that PTN improves release of BDNF from microglia (Maio et al., 2012); however, we are the first to show that this effect is greater in microglia which have been activated by INF-γ. In addition, the finding that PTN reduces the release of inflammatory molecules is supported by previous studies that show no changes in mRNA regulation of TNF-α, IL-1β and iNOS in microglia treated with PTN (Maio et al., 2012).

It is important to considered that our results may be specific to the cultures model chosen. We found PTN reduced the release of inflammatory molecules from microglia cultured from day 1-2 rat pups, however other studies using BV2 microglia lines found that simultaneous incubated LPS and PTN significantly potentiated the production of NO compared to cells only treated with LPS (Fernandez-Calle et al., 2017). It is possible that variation in microglia type and culture conditions account for the conflicting results between studies. *In vivo*, microglia are not isolated

but exist in complex microenvironments which are constantly in flux and microglia closely interact with other glial cells types.

PTN modulates mixed glial release of cytokines

To provide a more comprehensive assessment of the role of PTN in regulating immunomodulatory actions of glial cells, PTN treatment was assessed in mixed glial cultures containing microglia, astrocytes and oligodendrocytes (de Vellis and Cole, 2012). In mixed glial populations activated with LPS or INF-γ or LPS followed by INF-γ there was no effect of PTN treatment on the release of the inflammatory factors NO, TNF-α or IL-6. Moreover, PTN reduced the release of inflammatory factor IL-1β when mixed glia were subjected to dual activation with LPS and INF-γ. These novel results indicate that PTN may have a neuroprotective effect against secondary inflammation, we are the first to assess the effects of PTN on mixed glial cultures under various conditions of biological activation. These results must be taken with caution as *in vivo* studies in the prefrontal cortex have identified PTN as a potential regulator of inflammation, as mice which over express PTN have significantly increased levels of TNF-α, IL-6, and MCP-1 in response to LPS when compared to wild type mice (Fernandez-Calle et al., 2017). Therefore, more studies are needed to determine the effect of PTN *in vivo* as the results presented here may be altered in cell cultures.

In most CNS injuries, the primary insult induces an inflammatory event that is considered beneficial. However sustained inflammation or a secondary wave of inflammation after injury is considered detrimental to tissue health and to recovery (Carmichael, 2013). Our findings that PTN may alter glial responses to a second wave of inflammation by inducing release of a trophic factor is exciting and suggest a potential benefit of PTN administration after CNS injury. The

combined trophic and anti-inflammatory actions of PTN suggest PTN is an excellent candidate molecule to improve CNS recovery after injury.

PTN modulates plasticity in the spinal cord after stroke

We designed a study to determine if PTN administration into the spinal cord deinnervated by cortical stroke could improve functional recovery (Figure 5.1). Photothrombotic lesioning of the forelimb sensorimotor cortex was used to induce sensorimotor impairment in forelimb use in rats. PTN microinjection into the deinnervated cervical spinal cord (C4/C5) was performed 7 days post injury to potentiate regenerative processes in injured sensorimotor spinal circuits. Skilled reaching, forelimb use asymmetry and mechanical sensitivity was measured following stroke and treatment. Stroke lesioning of the forelimb sensorimotor cortex resulted in deficits when using the contralateral forelimb across all animals. Animals which received PTN treatment recovered substantially more sensorimotor function than did animals given a vehicle injection (Figure 5.2). PTN treated animals scored significantly higher than vehicle treated animals on both forelimb skilled reaching tasks and forelimb spontaneous asymmetry tests 28 days after stroke (Figure 5.2 A). Recent studies have demonstrated a potent pro-plasticity effect of PTN in the spinal cord (Paveliev et al., 2016) and PTN is promising as potential therapy to improve outcomes in neurodegenerative diseases such as Parkinson (Gombash et al., 2012) and after spinal cord injury (Wang et al., 2004, Mi et al., 2007). We are the first to demonstrate that PTN has the ability to improve sensory motor outcomes after stroke.

Although these results are interesting future studies are needed to determine the best time after injury at which to administer PTN. Here only one time point (7 days post stroke) was tested. Conducting studies of PTN during chronic stroke (months after injury) would be very

interesting as we have demonstrated that digesting CSPG in the spinal cords of stroke rats with chronic sensory motor deficits improves functional outcomes. Although it is well accepted that CSPG's are potent inhibitors of post injury plasticity, reducing axonal sprouting and neurite growth, they also play a fundamental role in modulating immune responses and proliferation of progenitor cells after injury (Karimi-Abdolrezaee et al., 2012), therefore treatments like PTN which modify CSPG's inhibitory properties may be advantageous. Future studies should include a component of rehabilitation to determine if pairing PTN with rehabilitative training has a synergistic effect.

Animals in both the PTN and control groups recovered mechanical sensitivity to pre stroke levels and there was no indication of hyperalgesia induced by PTN treatment (Figure 5.2 C). It has been demonstrated that PTN mRNA upregulation during chronic pain development is associated with more rapid recovery from mechanical allodynia, though this effect was exclusive to Fischer 344 rats and was not replicated in Lewis or Sprague-Dawley rats (used in this study) (Ezquerra et al., 2007). While it is important to consider that effect of PTN on mechanical sensitivity may be strain specific, the results of this study are supported by previous work showing that PTN does not induce mechanical allodynia in Sprague-Dawley rats (Ezquerra et al., 2007). To appreciate the mechanisms by which spinal injection of PTN improves functional recovery from stroke, cellular and anatomical changes in the spinal cord were considered next.

PTN does not alter glial density *in vivo*

In addition to functional changes, we studied changes in microglial and astrocytic density in the spinal cord. No evidence was found to suggest that PTN induces an inflammatory response, since PTN did not induce changes in microglia activation or accumulation in the spinal cord (Figure

5.3 B,C). In addition, we did not find any evidence of PTN induced reactive astrogliosis (Figure 5.3 A,C). Previous studies have indicated that PTN enhances G1 to S phase transition of microglia resulting in increased microglial proliferation and activation (Miao et al., 2012), but this effect was not detected in our immunoassay. However, the spinal cord was analyzed 21 days after injection and previous *in vitro* studies have shown that microglia activation peaked at 24 hours after PTN administration (Ito et al., 2001). Although PTN was not found to alter microglia populations, it was found to enhance factors associated with neurite outgrowth.

PTN induces expression of GAP-43

PTN treated animals were found to have increased levels of GAP-43 (Figure 5.4), a protein marker of extending axon projections, 21 days after injection, providing evidence that PTN injection promotes prolonged plasticity. During development PTN plays a crucial role in upregulating GAP-43 mRNA (Yanagisawa et al., 2010). This study is the first to provide evidence that exogenous PTN in the injured adult CNS induces GAP-43 expression. Although this is exciting is it important to consider that expression of GAP-43 does not explicitly translate to axonal spouting and it does not represent a 1:1 relationship with axonal sprouting or formation of new functional synapses (Carmichael et al., 2017). It is also important to consider that GAP-43 levels do not give any indication of the trajectory of axonal sprouting (Carmichael et al., 2017). Although GAP-43 is a useful indictor of axonal spouting and plastic processes, caution must be used when making assumptions from immunohistochemical data as presented here. Enhanced levels of GAP-43 are associated with plasticity, but GAP-43 can also reduce survivability of some cells types (Overman et al., 2014; Carmichael et al., 2016). In addition, following spinal cord injury increased GAP-43 prolongs and enhances axonal spouting but at the

same time increasing susceptibility of adult motor neurons to death (Harding et al., 1999). In this studies PTN improved functional outcomes and no reduction in motor neuron survival was detected in PTN treated animals. Considering the importance of the CST and its possible role reinnervating the stroke injured spinal cord after induced plasticity, further studies using neuronal tract tracing are need to directly determine the effect of PTN administration on axonal spouting from the CST.

PTN restores serotonergic density

Following some cases of SCI, serotonergic input can be lost in regions of the spinal cord distal to the site of injury (Fong, 2005). As a result significant reductions in serotonergic fibers can be detected in the ventral horns of spinal regions distal to the injury (Filli et al., 2011). This loss of serotonergic fiber density at sites distal to the induced injury is evident 4 days after spinal cord injury and is still prevalent at 28 days post injury (Filli et al., 2011). Following stroke in the somatosensory cortex a similar pattern of serotonergic fiber density loss was detected on the stroke deinnervated hemicord (C4-C5). Remarkably, treatment at 7 days post stroke with PTN reversed the deficits in serotonergic fiber density in the cervical spinal cord (C4-C5; Figure 5.5). This regrowth of serotonergic fibers post injury may account for some of the functional benefits resultant from PTN treatment (Li & Raisman, 1995; Hill et al., 2001). Few stroke studies have quantified serotonergic fiber density at sites distal to the cortex and this is the first study to show that PTN administration to the stroke deinnervated spinal cord restores serotonergic fiber density. As above, incorporating synaptic markers would strengthen the serotonin findings. It would also be valuable to assess the spinal cord at extend time points after PTN treatment (3-6 months post injection) to determine if the improved serotonergic density is maintained or if these

fibers fail to form meaningful connections and are eliminated.

PTN preserves motor neuron density and morphology

In addition to improving serotonergic fiber density, PTN administration significantly reduced motor neuron cell loss. This is the first study to demonstrate that PTN administration it the spinal cord following ischemic stroke can preserve motor neuron density (Figure 5.6 B) and prevent motor neuron atrophy (Figure 5.6 C) in the deinnervated spinal cord. Spinal cord explant culture studies support our findings as PTN successfully exhibited neuroprotective action against excitotoxic motor neuron death in these models (Mi et al., 2007). This is the first study to demonstrate a similar effect *in vivo*.

In summary, our data shows that PTN enhanced atomically plasticity after stroke, reduced the loss of serotonergic fibers and motor neurons, and promoted the expression of growth associated proteins in the spinal cord. In addition, PTN improved behavioral recovery after stroke without inducing spinal inflammation or inducing aberrant pain circuity. Thus, intraspinal PTN is an attractive therapeutic intervention after cortical injury such as stroke.

Conclusion

All of these studies taken together indicate that CSPG mediated inhibition of plasticity in the spinal cord can be overcome to enhance recovery and improve chronic deficits resulting from stroke. These studies offer hope of improved quality of life for the millions who live with long term disability as a direct result of stroke. Continued research into new approaches to improve quality of life for those left with chronic sensory and motor deficits after cortical injuries such as stroke is necessary to address this unmet clinical need.

References

Afshari FT, Kwok JC, White L, Fawcett JW. Schwann cell migration is integrin-dependent and inhibited by astrocyte-produced aggrecan. Glia 2010; 58: 857-69.

Alaverdashvili M, Whishaw IQ. A behavioral method for identifying recovery and compensation: Hand use in a preclinical stroke model using the single pellet reaching task. Neuroscience & Biobehavioral Reviews 2013; 37: 950-67.

Alia C, Spalletti C, Lai S, Panarese A, Chisari C, Lamola G, et al. Neuroplastic Changes Following Brain Ischemia and their Contribution to Stroke Recovery: Novel Approaches in Neurorehabilitation. Frontiers in Cellular Neuroscience 2017.

Alilain WJ, Horn KP, Hu H, Dick TE, Silver J. Functional regeneration of respiratory pathways after spinal cord injury. Nature Reviews Neuroscience 2011; 12.

Amet LEA, Lauri SE, Hienola A, Croll SD, Lu Y, Levorse JM, et al. Enhanced Hippocampal Long-Term Potentiation in Mice Lacking Heparin-Binding Growth-Associated Molecule. Molecular and Cellular Neuroscience 2001; 17: 1014-24.

Atwal JK, Pinkston-Gosse J, Syken J, Stawicki S, Wu Y, Shatz C, et al. PirB is a Functional Receptor for Myelin Inhibitors of Axonal Regeneration. Science 2008; 322: 967-70.

Bachmann LC, Lindau NT, Felder P, Schwab ME. Sprouting of brainstem-spinal tracts in response to unilateral motor cortex stroke in mice. The Journal of neuroscience: the official journal of the Society for Neuroscience 2014; 34: 3378-89.

Balmer TS, Carels VM, Frisch JL, Nick TA. Modulation of Perineuronal Nets and Parvalbumin with Developmental Song Learning. Journal of Neuroscience 2009; 29: 12878.

Bamford J, Sandercock P, Dennis M, Warlow C, Burn J. Classification and natural history of clinically identifiable subtypes of cerebral infarction. The Lancet 1991; 337: 1521-6.

Bartus K, James ND, Didangelos A, Bosch KD, Verhaagen J, Yáñez-Muñoz RJ, et al. Large-Scale Chondroitin Sulfate Proteoglycan Digestion with Chondroitinase Gene Therapy Leads to Reduced Pathology and Modulates Macrophage Phenotype following Spinal Cord Contusion Injury. J Neurosci 2014; 34: 4822-36.

Benakis C, Garcia-Bonilla L, Iadecola C, Anrather J. The role of microglia and myeloid immune cells in acute cerebral ischemia. Frontiers in Cellular Neuroscience 2015; 8.

Benowitz LI, Perrone-Bizzozero NI. The relationship of GAP-43 to the development and plasticity of synaptic connections. Annals of the New York Academy of Sciences 1991; 627: 58.

Benowitz LI, Carmichael ST. Promoting axonal rewiring to improve outcome after stroke. Neurobiology of Disease 2010; 37: 259-66.

Berent-Spillson AR. Metabotropic glutamate receptor-mediated protection from glucose-induced oxidative injury in sensory neurons. 2006.

Betty P Liu, William B.J Cafferty, Stephane O Budel, Stephen M Strittmatter. Extracellular regulators of axonal growth in the adult central nervous system. Philosophical Transactions of the Royal Society B: Biological Sciences 2006; 361: 1593-610.

Biernaskie J, Chernenko G, Corbett D. Efficacy of Rehabilitative Experience Declines with Time after Focal Ischemic Brain Injury. Journal of Neuroscience 2004; 24: 1245-54.

Binkofski F, Seitz RJ, Arnold S, Classen J, Benecke R, Freund H-. Thalamic metabolism and corticospinal tract integrity determine motor recovery in stroke. Annals of Neurology 1996; 39:

460-70.

Blondet B, Carpentier G, Ferry A, Courty J. Exogenous Pleiotrophin Applied to Lesioned Nerve Impairs Muscle Reinnervation. Neurochem Res 2006; 31: 907-13.

Blondet B, Carpentier G, Lafdil F, Courty J. Pleiotrophin Cellular Localization in Nerve Regeneration after Peripheral Nerve Injury. Journal of Histochemistry and Cytochemistry 2005; 53: 971-7.

Bradbury EJ, Carter LM. Manipulating the glial scar: Chondroitinase ABC as a therapy for spinal cord injury. Brain Research Bulletin 2011; 84: 306-16.

Bradman MJG, Ferrini F, Salio C, Merighi A. Practical mechanical threshold estimation in rodents using von Frey hairs/Semmes–Weinstein monofilaments: Towards a rational method. J Neurosci Methods 2015; 255: 92-103.

Brouns R, De Deyn PP. The complexity of neurobiological processes in acute ischemic stroke. Clinical Neurology and Neurosurgery 2009; 111: 483-95.

Brown CE, Boyd JD, Murphy TH. Longitudinal in vivo Imaging Reveals Balanced and Branch-Specific Remodeling of Mature Cortical Pyramidal Dendritic Arbors after Stroke. Journal of Cerebral Blood Flow & Metabolism 2010; 30: 783-91.

Brown CE, Li P, Boyd JD, Delaney KR, Murphy TH. Extensive Turnover of Dendritic Spines and Vascular Remodeling in Cortical Tissues Recovering from Stroke. The Journal of Neuroscience 2007; 27: 4101-9.

Brown JM, Xia J, Zhuang BQ, Cho KS, Rogers CJ, Cristal I. CI, et al. A sulfated carbohydrate epitope inhibits axon regeneration after injury. Proceedings of the National Academy of Sciences

of the United States of America 2012; 109: 4768-73.

Bruno V, Battaglia G, Copani A, D'Onofrio M, Di Iorio P, De Blasi A, et al. Metabotropic Glutamate Receptor Subtypes as Targets for Neuroprotective Drugs. Journal of Cerebral Blood Flow & Metabolism 2001; 21: 1013-33.

Buchan AM, Slivka A, Xue D. The effect of the NMDA receptor antagonist MK-801 on cerebral blood flow and infarct volume in experimental focal stroke. Brain Research 1992; 574: 171-7.

Burnside ER, Bradbury EJ. Review: Manipulating the extracellular matrix and its role in brain and spinal cord plasticity and repair. Neuropathol Appl Neurobiol 2014; 40: 26-59.

Busch SA, Silver J. The role of extracellular matrix in CNS regeneration. Curr Opin Neurobiol 2007; 17: 120-7.

Butovsky O, Jedrychowski MP, Moore CS, Cialic R, Lanser AJ, Gabriely G, et al. Identification of a unique TGF-β-dependent molecular and functional signature in microglia. Nature neuroscience 2014; 17: 131-43.

Butz M, Wogotter F, Van Ooyen M. Activity dependant structural plasticity. Brain Research Review 2009; 60: 287-305.

Cafferty WBJ, Bradbury EJ, Lidierth M, Jones M, Duffy PJ, Pezet S, et al. Chondroitinase ABC-Mediated Plasticity of Spinal Sensory Function. Journal of Neuroscience 2008; 28: 11998-2009.

Caleo M. Rehabilitation and plasticity following stroke: Insights from rodent models. Neuroscience 2015; 311: 180-94.

Camand E, Morel M, Faissner A, Sotelo C, Dusart I. Long-term changes in the molecular composition of the glial scar and progressive increase of serotoninergic fibre sprouting after

hemisection of the mouse spinal cord. Eur J Neurosci 2004; 20: 1161-76.

Campo GM, Campo S, Avenoso A, D'Ascola A, Nastasi G, Calatroni A. Molecular size hyaluronan differently modulates toll-like receptor-4 in LPS-induced inflammation in mouse chondrocytes. Biochimie 2010; 92: 204-15.

Cañas N, Gorina R, Planas AM, Vergés J, Montell E, García AG, et al. Chondroitin sulfate inhibits lipopolysaccharide-induced inflammation in rat astrocytes by preventing nuclear factor kappa B activation. Neuroscience 2010; 167: 872-9.

Caplan LR. Caplan's Stroke. Boston [u.a.]: Butterworth-Heinemann; 2000.

Carey LM. Somatosensory Loss after Stroke. CRP 1995; 7: 51-91.

Carey LM, Matyas TA, Oke LE. Sensory loss in stroke patients: effective training of tactile and proprioceptive discrimination. Archives of physical medicine and rehabilitation 1993; 74: 602-11.

Carey LM, Matyas TA, Oke LE. Evaluation of impaired fingertip texture discrimination and wrist position sense in patients affected by stroke: Comparison of clinical and new quantitative measures. Journal of Hand Therapy 2002; 15: 71-82.

Carmichael ST. Plasticity of Cortical Projections after Stroke. The Neuroscientist 2003; 9: 64-75.

Carmichael ST. Cellular and molecular mechanisms of neural repair after stroke: making waves. Annals of neurology 2006; 59: 735-42.

Carmichael ST. Targets for neural repair therapies after stroke. Stroke; a journal of cerebral circulation 2010; 41: S126.

Carmichael ST. Emergent properties of neural repair: elemental biology to therapeutic concepts. Annals of Neurology 2016; 79: 895-906.

Carmichael ST, Archibeque I, Luke L, Nolan T, Momiy J, Li S. Growth-associated gene expression after stroke: evidence for a growth-promoting region in peri-infarct cortex. Exp Neurol 2005; 193: 291-311.

Carmichael ST, Kathirvelu B, Schweppe CA, Nie EH. Molecular, cellular and functional events in axonal sprouting after stroke. Exp Neurol 2017; 287, Part 3: 384-94.

Carrera E, Tononi G. Diaschisis: past, present, future. Brain : a journal of neurology 2014; 137: 2408-22.

Carter LM, McMahon SB, Bradbury EJ. Delayed treatment with Chondroitinase ABC reverses chronic atrophy of rubrospinal neurons following spinal cord injury. Experimental Neurology 2011; 228: 149-56.

Castro C, Kuffler DP. Membrane-bound CSPG mediates growth cone outgrowth and substrate specificity by Schwann cell contact with the DRG neuron cell body and not via growth cone contact. Exp Neurol 2006; 200: 19-25.

Chen P, Goldberg DE, Kolb B, Lanser M, Benowitz LI. Inosine Induces Axonal Rewiring and Improves Behavioral Outcome after Stroke. Proceedings of the National Academy of Sciences of the United States of America 2002; 99: 9031-6.

Chen X, Liao S, Ye L, Gong Q, Ding Q, Zeng J, et al. Neuroprotective effect of chondroitinase ABC on primary and secondary brain injury after stroke in hypertensive rats. Brain Res 2014; 1543: 324-33.

Choudhury GR, Ding S. Reactive astrocytes and therapeutic potential in focal ischemic stroke. Neurobiology of disease 2016; 85: 234-44.

Clark WM, Rinker LG, Lessov NS, Hazel K, Hill JK, Stenzel-Poore M, et al. Lack of interleukin-6 expression is not protective against focal central nervous system ischemia. Stroke; a journal of cerebral circulation 2000; 31: 1715.

Crack P, Taylor J. Reactive oxygen species and the modulation of stroke. 2005.

Crain JM, Nikodemova M, Watters JJ. Microglia express distinct M1 and M2 phenotypic markers in the postnatal and adult central nervous system in male and female mice. J Neurosci Res 2013; 91: 1143-51.

Cua RC, Lau LW, Keough MB, Midha R, Apte SS, Yong VW. Overcoming neurite-inhibitory chondroitin sulfate proteoglycans in the astrocyte matrix. Glia 2013; 61: 972-84.

Dableh LJ, Yashpal K, Henry JL. Neuropathic pain as a process: reversal of chronification in an animal model. Journal of pain research 2011; 4: 315.

Dang G, Chen X, Chen Y, Zhao Y, Ouyang F, Zeng J. Dynamic secondary degeneration in the spinal cord and ventral root after a focal cerebral infarction among hypertensive rats. Scientific reports 2016; 6: 22655.

de Vellis J, Cole R. Preparation of mixed glial cultures from postnatal rat brain. Methods in molecular biology (Clifton, N.J.) 2012; 814: 49.

De Vetten G, Coutts SB, Hill MD, Goyal M, Eesa M, O'Brien B, et al. Acute corticospinal tract Wallerian degeneration is associated with stroke outcome. Stroke; a journal of cerebral

circulation 2010; 41: 751-6.

Deuel TF, Zhang N, Yeh H, Silos-Santiago I, Wang Z. Pleiotrophin: A Cytokine with Diverse Functions and a Novel Signaling Pathway. Archives of Biochemistry and Biophysics 2002; 397: 162-71.

Dimyan MA, Cohen LG. Neuroplasticity in the context of motor rehabilitation after stroke. Nat Rev Neurol 2011; 7: 76-85.

Djerbal L, Lortat-Jacob H, Kwok J. Chondroitin sulfates and their binding molecules in the central nervous system. 2017.

Dobkin BH. Training and exercise to drive poststroke recovery. Nat Clin Pract Neuro 2008; 4: 76-85.

Dougherty KD, Dreyfus CF, Black IB. Brain-Derived Neurotrophic Factor in Astrocytes, Oligodendrocytes, and Microglia/Macrophages after Spinal Cord Injury. Neurobiology of Disease 2000; 7: 574-85.

Doyle KP, Simon RP, Stenzel-Poore MP. Mechanisms of ischemic brain damage. Neuropharmacology 2008; 55: 310-8.

Dromerick AW, Lang CE, Birkenmeier RL, Wagner JM, Miller JP, Videen TO, Powers WJ, Wolf SL, Edwards DF. Very Early Constraint-Induced Movement during Stroke Rehabilitation (VECTORS): A single-center RCT. Neurology 2009; 73: 195-201.

Duncan PW, Goldstein LB, Horner RD, Landsman PB, Samsa GP, Matchar DB. Similar motor recovery of upper and lower extremities after stroke. Stroke 1994; 25: 1181-8

Dunja Frey, Thorsten Laux, Lan Xu, Corinna Schneider, Pico Caroni. Shared and Unique Roles

of CAP23 and GAP43 in Actin Regulation, Neurite Outgrowth, and Anatomical Plasticity. The Journal of Cell Biology 2000; 149: 1443-53.

Edvinsson, L Krause, D N. Cerebral Blood Flow and Metabolism.: Lippincott Williams and Wilkins; 2002.

Efremova L, Chovancova P, Adam M, Gutbier S, Schildknecht S, Leist M. Switching from astrocytic neuroprotection to neurodegeneration by cytokine stimulation. Arch Toxicol 2017; 91: 231-46.

Ekre HP, Naparstek Y, Lider O, Hydén P, Hägermark O, Nilsson T, et al. Anti-inflammatory effects of heparin and its derivatives: inhibition of complement and of lymphocyte migration. Advances in experimental medicine and biology 1992; 313: 329.

El Ali A, Kilic E, Hermann DM, Kilic U, Salani G, Reitmeir R, et al. Post-acute delivery of erythropoietin induces stroke recovery by promoting perilesional tissue remodelling and contralesional pyramidal tract plasticity. 2011.

Ezquerra L, Alguacil LF, Nguyen T, Deuel TF, Silos-Santiago I, Herradon G. Different pattern of pleiotrophin and midkine expression in neuropathic pain: Correlation between changes in pleiotrophin gene expression and rat strain differences in neuropathic pain. Growth Factors 2008; 26: 44-8.

Filli L, Zörner B, Weinmann O, Schwab ME. Motor deficits and recovery in rats with unilateral spinal cord hemisection mimic the Brown-Séquard syndrome. Brain 2011; 134: 2261-73.

Fisher D, Xing B, Dill J, Li H, Hoang HH, Zhao Z, et al. Leukocyte Common Antigen-Related Phosphatase Is a Functional Receptor for Chondroitin Sulfate Proteoglycan Axon Growth

Inhibitors. J Neurosci 2011; 31: 14051-66.

Fong AJ, Cai LL, Otoshi CK, Reinkensmeyer DJ, Burdick JW, Roy RR, et al. Spinal Cord-Transected Mice Learn to Step in Response to Quipazine Treatment and Robotic Training. J Neurosci 2005; 25: 11738-47.

Fongmoon D, Shetty AK, Basappa, Yamada S, Sugiura M, Kongtawelert P, et al. Chondroitinase-mediated Degradation of Rare 3-O-Sulfated Glucuronic Acid in Functional Oversulfated Chondroitin Sulfate K and E. Journal of Biological Chemistry 2007; 282: 36895-904.

Fukui K, Iguchi I, Kito A, Watanabe Y, Sugita K. Extent of pontine pyramidal tract Wallerian degeneration and outcome after supratentorial hemorrhagic stroke. Stroke 1994; 25: 1207-10.

Fumagalli S, Perego C, Pischiutta F, Zanier ER, De Simoni M. The ischemic environment drives microglia and macrophage function. Frontiers in neurology 2015; 6: 81.

Galtrey CM, Fawcett JW. The role of chondroitin sulfate proteoglycans in regeneration and plasticity in the central nervous system. Brain Research Reviews 2007; 54: 1-18.

Gao Q, Lu J, Huo Y, Baby N, Ling EA, Dheen ST. NG2, a member of chondroitin sulfate proteoglycans family mediates the inflammatory response of activated microglia. Neuroscience 2010; 165: 386-94.

Garcia-Alias G, Barkhuysen S, Buckle M, Fawcett JW. Chondroitinase ABC treatment opens a window of opportunity for task-specific rehabilitation. Nat Neurosci 2009; 12: 1145-51.

García-Alías G, Fawcett JW. Training and anti-CSPG combination therapy for spinal cord injury. Experimental Neurology 2012; 235: 26-32.

Garcia-Gutierrez P, Juarez-Vicente F, Wolgemuth DJ, Garcia-Dominguez M. Pleiotrophin antagonizes Brd2 during neuronal differentiation. Journal of cell science 2014; 127: 2554-64.

García-Pérez MA. Forced-choice staircases with fixed step sizes: asymptotic and small-sample properties. Vision Research 1998; 38: 1861-81.

Gilbert RJ, McKeon RJ, Darr A, Calabro A, Hascall VC, Bellamkonda RV. CS-4,6 is differentially upregulated in glial scar and is a potent inhibitor of neurite extension. Molecular and Cellular Neuroscience 2005; 29: 545-58.

Giménez Y, Ribotta M, Rajaofetra N, Morin-Richaud C, Alonso G, Bochelen D, Sandillon F, et al. Oxystdrol (7β-hydroxycholestesteryl-3-oleate) promotes serotonergic reinnervation in the lesioned rat spinal cord by reducing glial reaction. J Neurosci Res 1995; 41: 79-95.

Girgis J, Merrett D, Kirkland S, Metz GAS, Verge V, Fouad K. Reaching training in rats with spinal cord injury promotes plasticity and task specific recovery. Brain 2007; 130: 2993-3003.

Gleichman AJ, Carmichael ST. Astrocytic therapies for neuronal repair in stroke. Neurosci Lett 2014; 565: 47-52.

Go AS, Mozaffarian D, Roger VL, Benjamin EJ, Berry JD, Blaha MJ, et al. Heart disease and stroke statistics--2014 update: a report from the American Heart Association. Circulation 2014; 129: e28.

Gombash SE, Manfredsson FP, Mandel RJ, Collier TJ, Fischer DL, Kemp CJ, et al. Neuroprotective potential of pleiotrophin overexpression in the striatonigral pathway compared with overexpression in both the striatonigral and nigrostriatal pathways. Gene therapy 2014; 21: 682-93.

Gonzalez B, Leroux P, Lamacz M, Bodenant C, Balazs R, Vaudry H. Somatostatin Receptors are Expressed by Immature Cerebellar Granule Cells: Evidence for a Direct Inhibitory Effect of Somatostatin on Neuroblast Activity. Proceedings of the National Academy of Sciences of the United States of America 1992; 89: 9627-31.

González-Castillo C, Ortuño-Sahagún D, Guzmán-Brambila C, Pallàs M, Rojas-Mayorquín AE. Pleiotrophin as a central nervous system neuromodulator, evidences from the hippocampus. Frontiers in cellular neuroscience 2014; 8: 443.

Gordon S. Alternative activation of macrophages. Nature Reviews Immunology 2003; 3: 23-35.

Green JB. Brain Reorganization After Stroke. Topics in Stroke Rehabilitation 2003; 10: 1-20.

Hamma-Kourbali Y, Bernard-Pierrot I, Heroult M, Dalle S, Caruelle D, Milhiet PE, et al. Inhibition of the mitogenic, angiogenic and tumorigenic activities of pleiotrophin by a synthetic peptide corresponding to its C-thrombospondin repeat-I domain. Journal of Cellular Physiology 2008; 214: 250-9.

Hara Y. Brain Plasticity and Rehabilitation in Stroke Patients. Journal of Nippon Medical School 2015; 82: 4-13.

Harding DI, Greensmith L, Mason M, Anderson PN, Vrbová G. Overexpression of GAP-43 induces prolonged sprouting and causes death of adult motoneurons. The European journal of neuroscience 1999; 11: 2237-42.

Harris KM. Structure, development, and plasticity of dendritic spines. Current Opinion in Neurobiology 1999; 9: 343-8.

Hayakawa K, Nakano T, Irie K, Higuchi S, Fujioka M, Orito K, et al. Inhibition of reactive

astrocytes with fluorocitrate retards neurovascular remodeling and recovery after focal cerebral ischemia in mice. Journal of Cerebral Blood Flow & Metabolism 2010; 30: 871-82.

Heiss W. The Concept of the Penumbra: can it be Translated to Stroke Management? International Journal of Stroke 2010; 5: 290-5.

Hida H, Jung C, Wu C, Kim H, Kodama Y, Masuda T, et al. Pleiotrophin exhibits a trophic effect on survival of dopaminergic neurons in vitro. European Journal of Neuroscience 2003; 17: 2127-34.

Hill CE, Beattie MS, Bresnahan JC. Degeneration and Sprouting of Identified Descending Supraspinal Axons after Contusive Spinal Cord Injury in the Rat. Exp Neurol 2001; 171: 153-69.

Hill JJ, Jin K, Mao XO, Xie L, Greenberg DA. Intracerebral chondroitinase ABC and heparan sulfate proteoglycan glypican improve outcome from chronic stroke in rats. Proceedings of the National Academy of Sciences 2012; 109: 9155-60.

Honglian S. Hypoxia Inducible Factor 1 as a Therapeutic Target in Ischemic Stroke. Current Medicinal Chemistry 2009; 16: 4593-600.

Hosp JA, Luft AR. Cortical Plasticity during Motor Learning and Recovery after Ischemic Stroke. Neural Plasticity 2011; 2011: 1-9.

Houle JD, Tom VJ, Mayes D, Wagoner G, Phillips N, Silver J. Combining an Autologous Peripheral Nervous System "Bridge" and Matrix Modification by Chondroitinase Allows Robust, Functional Regeneration beyond a Hemisection Lesion of the Adult Rat Spinal Cord. Journal of Neuroscience 2006; 26: 7405-15.

Hounsgaard J, Hultborn H, Jespersen B, Kiehn O. Bistability of alpha-motoneurones in the

decerebrate cat and in the acute spinal cat after intravenous 5-hydroxytryptophan. J Physiol (Lond) 1988; 405: 345-67.

Hsu JE, Jones TA. Contralesional neural plasticity and functional changes in the less-affected forelimb after large and small cortical infarcts in rats. Exp Neurol 2006; 201: 479-94.

Hsu JE, Jones TA. Time-sensitive enhancement of motor learning with the less-affected forelimb after unilateral sensorimotor cortex lesions in rats. The European journal of neuroscience 2005; 22: 2069-80.

Huang J, Upadhyay UM, Tamargo RJ. Inflammation in stroke and focal cerebral ischemia. Surgical Neurology 2006; 66: 232-45.

Hudson AE, Gollnick C, Gourdine J, Prinz AA. Degradation of extracellular chondroitin sulfate delays recovery of network activity after perturbation. Journal of neurophysiology 2015; 114: 1346-52.

Hum PD, Subramanian S, Parker SM, Afentoulis ME, Kaler LJ, Vandenbark AA, et al. T- and B-cell-deficient mice with experimental stroke have reduced lesion size and inflammation. Journal of Cerebral Blood Flow & Metabolism 2007; 27: 1798-805.

Huybrechts KF, Caro JJ, Xenakis JJ, Vemmos KN. The Prognostic Value of the Modified Rankin Scale Score for Long-Term Survival after First-Ever Stroke. Cerebrovascular Diseases 2008; 26: 381-7.

Hyung Soo Han, Midori A Yenari. Cellular targets of brain inflammation in stroke. Current opinion in investigational drugs (London, England : 2000) 2003; 4: 522-9.

Iizuka H, Sakatani K, Young W. Corticofugal axonal degeneration in rats after middle cerebral

artery occlusion. Stroke 1989; 20: 1396-402.

Ito D, Tanaka K, Suzuki S, Dembo T, Fukuuchi Y. Enhanced Expression of Iba1, Ionized Calcium-Binding Adapter Molecule 1, After Transient Focal Cerebral Ischemia In Rat Brain. Stroke 2001; 32: 1208-15.

Iwasawa H, Nomura M, Sakitani N, Watanabe K, Watanabe D, Moriyama H. Stretching After Heat But Not After Cold Decreases Contractures After Spinal Cord Injury in Rats. Clinical Orthopaedics and Related Research® 2016; 474: 2692-701.

Jacobs BL, Martín-Cora FJ, Fornal CA. Activity of medullary serotonergic neurons in freely moving animals. Brain Res Rev 2002; 40: 45-52.

Jin L, Jianghai C, Juan L, Hao K. Pleiotrophin and peripheral nerve injury. Neurosurgical review 2009; 32: 387-93.

Jin R, Liu L, Zhang S, Nanda A, Li G. Role of Inflammation and Its Mediators in Acute Ischemic Stroke. J of Cardiovasc Trans Res 2013; 6: 834-51.

Johnson AC, Mcnabb AR, Rossiter RJ. Chemistry of wallerian degeneration; a review of recent studies. Archives of neurology and psychiatry 1950; 64: 105.

Jones TA, Adkins DL. Motor System Reorganization After Stroke: Stimulating and Training Toward Perfection. Physiology 2015; 30: 358-70.

Joshva Baskar Jesudasan S, Todd KG, Winship IR. Reduced Inflammatory Phenotype in Microglia Derived from Neonatal Rat Spinal Cord versus Brain. PLoS One 2014; 9.

Julkunen L, Tenovuo O, Jääskeläinen SK, Hämäläinen H. Recovery of somatosensory deficits in acute stroke. Acta Neurol Scand 2005; 111: 366-72.

Karimi-Abdolrezaee S, Schut D, Wang J, Fehlings MG. Chondroitinase and growth factors enhance activation and oligodendrocyte differentiation of endogenous neural precursor cells after spinal cord injury. PloS one 2012; 7: e37589.

Karumbaiah L, Anand S, Thazhath R, Zhong Y, Mckeon RJ, Bellamkonda RV. Targeted downregulation of N-acetylgalactosamine 4-sulfate 6-O-sulfotransferase significantly mitigates chondroitin sulfate proteoglycan-mediated inhibition. Glia 2011; 59: 981-96.

Katsman D, Zheng J, Spinelli K, Carmichael ST. Tissue Microenvironments within Functional Cortical Subdivisions Adjacent to Focal Stroke. Journal of Cerebral Blood Flow & Metabolism 2003; 23: 997-1009.

Kerzoncuf M, Bensoussan L, Viton JM, Delarque A, Durand CR. Plastic changes in spinal synaptic transmission following botulinum toxin A in post-stroke spastic patients. Annals of Physical and Rehabilitation Medicine 2016; 59: e142.

Kessner SS, Bingel U, Thomalla G. Somatosensory deficits after stroke: a scoping review. Topics in Stroke Rehabilitation 2016; 23: 136-46.

Kigerl KA, de Rivero Vaccari, Juan Pablo, Dietrich WD, Popovich PG, Keane RW. Pattern recognition receptors and central nervous system repair. Experimental neurology 2014; 258: 5-16.

Kilpelaeinen I, Kaksonen M, Kinnunen T, Avikainen H, Fath M, Linhardt RJ, et al. Heparin-binding Growth-associated Molecule Contains Two Heparin-binding beta -Sheet Domains That Are Homologous to the Thrombospondin Type I Repeat. Journal of Biological Chemistry 2000; 275: 13564-70.

Kim SY, Allred RP, Adkins DL, Tennant KA, Donlan NA, Kleim JA, et al. Experience with the "good" limb induces aberrant synaptic plasticity in the perilesion cortex after stroke. The Journal of neuroscience : the official journal of the Society for Neuroscience 2015; 35: 8604.

Kinnunen T, Raulo E, Nolo R, Maccarana M, Ulf Lindahl, Heikki Rauvala. Neurite Outgrowth in Brain Neurons Induced by Heparin-binding Growth-associated Molecule (HB-GAM) Depends on the Specific Interaction of HB-GAM with Heparan Sulfate at the Cell Surface. Journal of Biological Chemistry 1996; 271: 2243-8.

Kinnunen A, Kinnunen T, Kaksonen M, Nolo R, Panula P, Rauvala H. N-syndecan and HB-GAM (heparin-binding growth-associated molecule) associate with early axonal tracts in the rat brain. The European journal of neuroscience 1998; 10: 635-48.

Kosofsky BE, Molliver ME. The serotoninergic innervation of cerebral cortex: different classes of axon terminals arise from dorsal and median raphe nuclei. Synapse (New York, N.Y.) 1987; 1: 153-68.

Krakauer JW, Carmichael ST, Corbett D, Wittenberg GF. Getting Neurorehabilitation Right: What Can Be Learned From Animal Models? Neurorehabilitation and Neural Repair 2012; 26: 923-31.

Kroner A, David S. Repertoire of microglial and macrophage responses after spinal cord injury. Nature Reviews Neuroscience 2011; 12: 388-99.

Kubo T, Yamaguchi A, Iwata N, Yamashita T. The therapeutic effects of Rho-ROCK inhibitors on CNS disorders. Therapeutics and clinical risk management 2008; 4: 605-15.

Kuzu Y, Inoue T, Kanbara Y, Nishimoto H, Fujiwara S, Ogasawara K, et al. Prediction of Motor

Function Outcome after Intracerebral Hemorrhage Using Fractional Anisotropy Calculated from Diffusion Tensor Imaging. Cerebrovascular Diseases 2012; 33: 566-73.

Kwak SY, Yeo SS, Choi BY, Chang CH, Jang SH. Corticospinal Tract Change in the Unaffected Hemisphere at the Early Stage of Intracerebral Hemorrhage: A Diffusion Tensor Tractography Study. European Neurology 2010; 63: 149-53.

Kwakkel G, Kollen B, Lindeman E. Understanding the pattern of functional recovery after stroke: facts and theories. Restorative neurology and neuroscience 2004; 22: 281.

Kwok JCF, Dick G, Wang D, Fawcett JW. Extracellular matrix and perineuronal nets in CNS repair. Developmental Neurobiology 2011; 71: 1073-89.

Lai AY, Todd KG. Differential regulation of trophic and proinflammatory microglial effectors is dependent on severity of neuronal injury. Glia 2008; 56: 259-70.

Lampert PW, Cressman MR. Fine-structural changes of myelin sheaths after axonal degeneration in the spinal cord of rats. The American journal of pathology 1966; 49: 1139.

Lang KC, Thompson PA, Wolf SL. The EXCITE Trial: Reacquiring Upper-Extremity Task Performance With Early Versus Late Delivery of Constraint Therapy. Neurorehabilitation and Neural Repair 2013; 27: 654-63.

Langhorne P, Stott D, Knight A, Bernhardt J, Barer D, Watkins C. Very Early Rehabilitation or Intensive Telemetry after Stroke: A Pilot Randomised Trial. Cerebrovasc Dis 2010; 29: 352-60.

Lee H, McKeon RJ, Bellamkonda RV, Langer R. Sustained Delivery of Thermostabilized chABC Enhances Axonal Sprouting and Functional Recovery after Spinal Cord Injury. Proceedings of the National Academy of Sciences of the United States of America 2010; 107:

3340-5.

Lee J, Kim J, Sivula M, Strittmatter SM. Nogo Receptor Antagonism Promotes Stroke Recovery by Enhancing Axonal Plasticity. Journal of Neuroscience 2004; 24: 6209-17.

Lehnardt S, Lehmann S, Kaul D, Tschimmel K, Hoffmann O, Cho S, et al. Toll-like receptor 2 mediates CNS injury in focal cerebral ischemia. J Neuroimmunol 2007a; 190: 28-33.

Leszczyńska AN, Majczyński H, Wilczyński GM, Sławińska U, Cabaj AM. Thoracic Hemisection in Rats Results in Initial Recovery Followed by a Late Decrement in Locomotor Movements, with Changes in Coordination Correlated with Serotonergic Innervation of the Ventral Horn. PLoS ONE 2015; 10: e0143602.

Lexa, F. J., Grossman, R. I., & Rosenquist, A. C. MR of wallerian degeneration in the feline visual system: Characterization by magnetization transfer rate with histopathologic correlation. American Journal of Neuroradiology 1994; 15: 201-12.

Li S, Liu BP, Budel S, Li M, Ji B, Walus L, et al. Blockade of Nogo-66, Myelin-Associated Glycoprotein, and Oligodendrocyte Myelin Glycoprotein by Soluble Nogo-66 Receptor Promotes Axonal Sprouting and Recovery after Spinal Injury. Journal of Neuroscience 2004; 24: 10511-20.

Li S, Overman JJ, Katsman D, Kozlov SV, Donnelly CJ, Twiss JL, et al. An age-related sprouting transcriptome provides molecular control of axonal sprouting after stroke. Nat Neurosci 2010; 13: 1496-504.

Li S, Nie EH, Yin Y, Benowitz LI, Tung S, Vinters HV, et al. GDF10 is a signal for axonal sprouting and functional recovery after stroke. Nature neuroscience 2015; 18: 1737.

Li Y, Raisman G. Sprouts from Cut Corticospinal Axons Persist in the Presence of Astrocytic Scarring in Long-Term Lesions of the Adult Rat Spinal Cord. Exp Neurol 1995; 134: 102-11.

Liu JYW. The severity and associated factors of participation restriction among community-dwelling frail older people: an application of the International Classification of Functioning, Disability and Health (WHO-ICF). BMC Geriatrics 2017; 17.

Liebeskind DS. Wallerian degeneration of the corticospinal tracts. Neurology 2004; 62: 828.

Lin B, Xu Y, Zhang B, He Y, Yan Y, He M. MEK inhibition reduces glial scar formation and promotes the recovery of sensorimotor function in rats following spinal cord injury. Experimental and Therapeutic Medicine 2014; 7: 66-72.

Lindau NT, Bänninger BJ, Gullo M, Good NA, Bachmann LC, Starkey ML, et al. Rewiring of the corticospinal tract in the adult rat after unilateral stroke and anti-Nogo-A therapy. Brain : a journal of neurology 2014; 137: 739-56.

Liu B, Liao M, Mielke JG, Ning K, Chen Y, Li L, et al. Ischemic Insults Direct Glutamate Receptor Subunit 2-Lacking AMPA Receptors to Synaptic Sites. Journal of Neuroscience 2006; 26: 5309-19.

Liu Z, Chopp M. Astrocytes, therapeutic targets for neuroprotection and neurorestoration in ischemic stroke. Progress in neurobiology 2016; 144: 103-20.

Liu Z, Li Y, Cui Y, Roberts C, Lu M, Wilhelmsson U, et al. Beneficial effects of gfap/vimentin reactive astrocytes for axonal remodeling and motor behavioral recovery in mice after stroke. Glia 2014; 62: 2022-33.

Logun MT, Bisel NS, Tanasse EA, Zhao W, Gunasekera B, Mao L, et al. Glioma cell invasion is

significantly enhanced in composite hydrogel matrices composed of chondroitin 4- and 4,6-sulfated glycosaminoglycans. J. Mater. Chem. B 2016; 4: 6052-64.

Lowry F. Stroke rehabilitation services inadequate, experts say. Can Med Assoc J 2010; 182: E284.

Ma C, Liu A, Li Z, Zhou X, Zhou S. Longitudinal study of diffusion tensor imaging properties of affected cortical spinal tracts in acute and chronic hemorrhagic stroke. Journal of clinical neuroscience : official journal of the Neurosurgical Society of Australasia 2014; 21: 1388-92.

Maeda N. Structural variation of chondroitin sulfate and its roles in the central nervous system. Central nervous system agents in medicinal chemistry 2010; 10: 22.

Maier IC, Schwab ME. Sprouting, regeneration and circuit formation in the injured spinal cord: factors and activity. Philos Trans R Soc Lond B Biol Sci 2006; 361: 1611-34.

Mantovani A, Sozzani S, Locati M, Allavena P, Sica A. Macrophage polarization: tumor-associated macrophages as a paradigm for polarized M2 mononuclear phagocytes. Trends in Immunology 2002; 23: 549-55.

Mantovani A, Sica A, Sozzani S, Allavena P, Vecchi A, Locati M. The chemokine system in diverse forms of macrophage activation and polarization. Trends in Immunology 2004; 25: 677-86.

Martinez FO, Sica A, Mantovani A, Locati M. Macrophage activation and polarization. Frontiers in Bioscience 2008; 13: 453-61.

Martín-de-Saavedra MD, del Barrio L, Cañas N, Egea J, Lorrio S, Montell E, et al. Chondroitin sulfate reduces cell death of rat hippocampal slices subjected to oxygen and glucose deprivation

by inhibiting p38, NFκB and iNOS. Neurochem Int 2011; 58: 676-83.

Matsusue E, Sugihara S, Fujii S, Kinoshita T, Ohama E, Ogawa T. Wallerian Degeneration of the Corticospinal Tracts: Postmortem MR-Pathologic Correlations. Acta Radiologica 2007; 48: 690-4.

Melgar-Lesmes P, Garcia-Polite F, Del-Rey-Puech P, Rosas E, Dreyfuss JL, Montell E, et al. Treatment with chondroitin sulfate to modulate inflammation and atherogenesis in obesity. Atherosclerosis 2016; 245: 82-7.

Merenmies J, Rauvala H. Molecular cloning of the 18-kDa growth-associated protein of developing brain. Journal of Biological Chemistry 1990; 265: 16721.

Mi R, Chen W, Höke A. Pleiotrophin is a neurotrophic factor for spinal motor neurons. Proceedings of the National Academy of Sciences 2007; 104: 4664-9.

Miao J, Ding M, Zhang A, Xiao Z, Qi W, Luo N, et al. Pleiotrophin promotes microglia proliferation and secretion of neurotrophic factors by activating extracellular signal-regulated kinase 1/2 pathway. Neurosci Res 2012; 74: 269-76.

Miller GM, Hsieh-Wilson LC. Sugar-dependent modulation of neuronal development, regeneration, and plasticity by chondroitin sulfate proteoglycans. Exp Neurol 2015; 274, Part B: 115-25.

Milner PG, Li Y, Hoffman RM, Kodner CM, Siegel NR, Deuel TF. A novel 17 kD heparin-binding growth factor (HBGF-8) in bovine uterus: Purification and N-terminal amino acid sequence. Biochemical and Biophysical Research Communications 1989; 165: 1096-103.

Mitsiadis TA, Salmivirta M, Muramatsu T, Muramatsu H, Rauvala H, Lehtonen E. Expression of

the heparin-binding cytokines, midkine (MK) and HB-GAM (pleiotrophin) is associated with epithelial-mesenchymal interactions during fetal development and organogenesis. Development 1995; 121: 37.

Miyamoto N, Maki T, Shindo A, Liang AC, Maeda M, Egawa N, et al. Astrocytes Promote Oligodendrogenesis after White Matter Damage via Brain-Derived Neurotrophic Factor. The Journal of neuroscience : the official journal of the Society for Neuroscience 2015; 35: 14002.

Monnier PP, Sierra A, Schwab JM, Henke-Fahle S, Mueller BK. The Rho/ROCK pathway mediates neurite growth-inhibitory activity associated with the chondroitin sulfate proteoglycans of the CNS glial scar. Molecular and Cellular Neuroscience 2003; 22: 319-30.

Montoya CP, Campbell-Hope LJ, Pemberton KD, Dunnett SB. The "staircase test": a measure of independent forelimb reaching and grasping abilities in rats. J Neurosci Methods 1991; 36: 219-28.

Moon LDF, Asher RA, Rhodes KE, Fawcett JW. Regeneration of CNS axons back to their target following treatment of adult rat brain with chondroitinase ABC. Nat Neurosci 2001; 4: 465-6.

Moon LDF, Asher RA, Rhodes KE, Fawcett JW. Relationship between sprouting axons, proteoglycans and glial cells following unilateral nigrostriatal axotomy in the adult rat. Neuroscience 2002; 109: 101-17.

Morecraft RJ, Ge J, Stilwell-Morecraft KS, McNeal DW, Hynes SM, Pizzimenti MA, et al. Frontal and frontoparietal injury differentially affect the ipsilateral corticospinal projection from the nonlesioned hemisphere in monkey (Macaca mulatta). Journal of Comparative Neurology 2016; 524: 380-407.

Morganti JM, Riparip L, Rosi S. Call Off the Dog(ma): M1/M2 Polarization Is Concurrent following Traumatic Brain Injury. PloS one 2016; 11: e0148001.

Mourali J, Bénard A, Lourenço FC, Monnet C, Greenland C, Moog-Lutz C, et al. Anaplastic lymphoma kinase is a dependence receptor whose proapoptotic functions are activated by caspase cleavage. Mol Cell Biol 2006; 26: 6209-22.

Mozaffarian D, Benjamin E, Go A, Arnett D, Blaha M, Cushman M, et al. Executive Summary: Heart Disease and Stroke Statistics—2015 Update: A Report From the American Heart Association. Circulation 2015; 131: 434-41.

Müllner A, Gonzenbach RR, Weinmann O, Schnell L, Liebscher T, Schwab ME. Lamina-specific restoration of serotonergic projections after Nogo-A antibody treatment of spinal cord injury in rats. Eur J Neurosci 2008a; 27: 326-33.

Muramatsu T. Midkine and Pleiotrophin: Two Related Proteins Involved in Development, Survival, Inflammation and Tumorigenesis. Journal of Biochemistry 2002; 132: 359-71.

Murphy TH, Corbett D. Plasticity during stroke recovery: from synapse to behaviour. Nat Rev Neurosci 2009a; 10: 861-72.

Nakamura Y, Si QS, Kataoka K. Lipopolysaccharide-induced microglial activation in culture: temporal profiles of morphological change and release of cytokines and nitric oxide. Neurosci Res 1999; 35: 95-100.

Nakanishi K, Tokita Y, Aono S, Ida M, Matsui F, Higashi Y, et al. Neuroglycan C, A Brain-Specific Chondroitin Sulfate Proteoglycan, Interacts with Pleiotrophin, A Heparin-Binding Growth Factor. Neurochem Res 2010; 35: 1131-7.

Nudo RJ, Milliken GW. Reorganization of movement representations in primary motor cortex following focal ischemic infarcts in adult squirrel monkeys. Journal of Neurophysiology 1996; 75: 2144.

Olson JK, Miller SD. Microglia Initiate Central Nervous System Innate and Adaptive Immune Responses through Multiple TLRs. J Immunol 2004; 173: 3916-24.

O'Neill E, Kwok B, Day JS, Connor TJ, Harkin A. Amitriptyline protects against TNF-α-induced atrophy and reduction in synaptic markers via a Trk-dependent mechanism. Pharmacology Research & Perspectives 2016; 4: n/a.

Ooboshi H, Ibayashi S, Shichita T, Kumai Y, Takada J, Ago T, et al. Postischemic Gene Transfer of Interleukin-10 Protects Against Both Focal and Global Brain Ischemia. Circulation 2005; 111: 913-9.

Orita T, Tsurutani T, Izumihara A, Kajiwara K, Matsunaga T. Pyramidal tract Wallerian degeneration and correlated symptoms in stroke. European Journal of Radiology 1994; 18: 26-9.

Ovbiagele B, Goldstein L, Higashida R, Howard V, Johnston S, Khavjou O, et al. Forecasting the Future of Stroke in the United States: A Policy Statement From the American Heart Association and American Stroke Association. Stroke 2013; 44: 2361-75.

Overman JJ, Clarkson AN, Wanner IB, Overman WT, Eckstein I, Maguire JL, et al. A role for ephrin-A5 in axonal sprouting, recovery, and activity-dependent plasticity after stroke. Proceedings of the National Academy of Sciences 2012; 109: E2239.

Overman JJ, Carmichael ST. Plasticity in the Injured Brain. The Neuroscientist 2014; 20: 15-28.

Pannell M, Szulzewsky F, Matyash V, Wolf SA, Kettenmann H. The subpopulation of microglia

sensitive to neurotransmitters/neurohormones is modulated by stimulation with LPS, interferon-γ, and IL-4. Glia 2014; 62: 667-79.

Pariser H, Perez-Pinera P, Ezquerra L, Herradon G, Deuel TF. Pleiotrophin stimulates tyrosine phosphorylation of beta-adducin through inactivation of the transmembrane receptor protein tyrosine phosphatase beta/zeta. Biochemical and biophysical research communications 2005a; 335: 232.

Pariser H, Ezquerra L, Herradon G, Perez-Pinera P, Deuel TF. Fyn is a downstream target of the pleiotrophin/receptor protein tyrosine phosphatase β/ζ-signaling pathway: Regulation of tyrosine phosphorylation of Fyn by pleiotrophin. Biochem Biophys Res Commun 2005b; 332: 664-9.

Patterson SL. Immune dysregulation and cognitive vulnerability in the aging brain: Interactions of microglia, IL-1β, BDNF and synaptic plasticity. Neuropharmacology 2015; 96: 11-8.

Paveliev M, Fenrich KK, Kislin M, Kuja-Panula J, Kulesskiy E, Varjosalo M, et al. HB-GAM (pleiotrophin) reverses inhibition of neural regeneration by the CNS extracellular matrix. Scientific Reports 2016; 6: 33916.

Pavlov I, Võikar V, Kaksonen M, Lauri SE, Hienola A, Taira T, et al. Role of Heparin-Binding Growth-Associated Molecule (HB-GAM) in Hippocampal LTP and Spatial Learning Revealed by Studies on Overexpressing and Knockout Mice. Molecular and Cellular Neuroscience 2002; 20: 330-42.

Pavlov I, Rauvala H, Taira T. Enhanced hippocampal GABAergic inhibition in mice overexpressing heparin-binding growth-associated molecule. Neuroscience 2006; 139: 505-11.

Paxinos G, Charles W. The Rat Brain in Stereotaxic Coordinates (6th edition). SanDeigo, California: Academic Press; 2008.

Pulsipher A, Griffin ME, Stone SE, Brown JM, Hsieh-Wilson LC. Directing neuronal signaling through cell-surface glycan engineering. Journal of the American Chemical Society 2014; 136: 6794.

Pulsipher A, Griffin ME, Stone SE, Hsieh-Wilson LC. Long-Lived Engineering of Glycans to Direct Stem Cell Fate. Angewandte Chemie International Edition 2015; 54: 1466-70.

Ransohoff RM. A polarizing question: do M1 and M2 microglia exist? Nature neuroscience 2016; 19: 987-91.

Raulo E, Tumova S, Pavlov I, Pekkanen M, Hienola A, Klankki E, et al. The Two Thrombospondin Type I Repeat Domains of the Heparin-binding Growth-associated Molecule Bind to Heparin/Heparan Sulfate and Regulate Neurite Extension and Plasticity in Hippocampal Neurons. Journal of Biological Chemistry 2005; 280: 41576-83.

Rauvala H, Peng HB. HB-gam (heparin-binding growth-associated molecule) and heparin-type glycans in the development and plasticity of neuron-target contacts. Progress in Neurobiology 1997; 52: 127-44.

Rolls A, Cahalon L, Bakalash S, Avidan H, Lider O, Schwartz M. A sulfated disaccharide derived from chondroitin sulfate proteoglycan protects against inflammation-associated neurodegeneration. FASEB Journal 2006; 20: 547-9.

Rolls A, Shechter R, London A, Segev Y, Jacob-Hirsch J, Amariglio N, Schwartz M. A. Two Faces of Chondroitin Sulfate Proteoglycan in Spinal Cord Repair: A Role in Microglia/Macrophage Activation. PLOS Medicine 2008; 5: e171.

Ross AM, Hurn P, Perrin N, Wood L, Carlini W, Potempa K. Evidence of the Peripheral

Inflammatory Response in Patients with Transient Ischemic Attack. Journal of Stroke and Cerebrovascular Diseases 2007; 16: 203-7.

Rothwell NJ, Allan SM. Cytokines and acute neurodegeneration. Nature Reviews Neuroscience 2001; 2: 734-44.

Sairanen T, Carpén O, Karjalainen-Lindsberg ML, Paetau A, Turpeinen U, Kaste M, et al. Evolution of cerebral tumor necrosis factor-alpha production during human ischemic stroke. Stroke; a journal of cerebral circulation 2001; 32: 1750.

Sasi M, Vignoli B, Canossa M, Blum R. Neurobiology of local and intercellular BDNF signaling. Pflugers Arch 2017.

Secher NH, Seifert T, Lieshout JJ. Cerebral blood flow and metabolism during exercise: implications for fatigue. Journal of Applied Physiology 2008a; 104: 306-14.

Segura-Ulate I, Yang B, Vargas-Medrano J, Perez RG. FTY720 (Fingolimod) reverses α-synuclein-induced downregulation of brain-derived neurotrophic factor mRNA in OLN-93 oligodendroglial cells. Neuropharmacology 2017; 117: 149-57.

Seo DK, Kim JH, Min J, Yoon HH, Shin E, Kim SW, et al. Enhanced axonal regeneration by transplanted Wnt3a-secreting human mesenchymal stem cells in a rat model of spinal cord injury. Acta Neurochir 2017: 1-11.

Sharma K, Selzer ME, Li S. Scar-mediated inhibition and CSPG receptors in the CNS. Exp Neurol 2012; 237: 370-8.

Shen Y, Tenney AP, Busch SA, Horn KP, Cuascut FX, Liu K, et al. PTPσ Is a Receptor for Chondroitin Sulfate Proteoglycan, an Inhibitor of Neural Regeneration. Science 2009; 326: 592-

6.

Shen K, Cowan CW. Guidance molecules in synapse formation and plasticity. Cold Spring Harbor perspectives in biology 2010; 2: a001842.

Shen F, Guo W, Li G, Lv G, Wang Y, Fan Z, et al. Mdivi-1 Inhibits Astrocyte Activation and Astroglial Scar Formation and Enhances Axonal Regeneration after Spinal Cord Injury in Rats. Frontiers in Cellular Neuroscience 2016; 10.

Shimbo M, Ando S, Sugiura N, Kimata K, Ichijo H. Moderate repulsive effects of E-unit-containing chondroitin sulfate (CSE) on behavior of retinal growth cones. Brain research 2013; 1491: 34-43.

Shinozaki M, Iwanami A, Fujiyoshi K, Tashiro S, Kitamura K, Shibata S, et al. Combined treatment with chondroitinase ABC and treadmill rehabilitation for chronic severe spinal cord injury in adult rats. Neuroscience Research 2016; 113: 37-47.

Sica A, Mantovani A. Macrophage plasticity and polarization: in vivo veritas. The Journal of clinical investigation 2012; 122: 787-95.

Silasi G, Murphy TH. Removing the brakes on post-stroke plasticity drives recovery from the intact hemisphere and spinal cord. Brain 2014; 137: 648-50.

Silver J, Miller JH. Regeneration beyond the glial scar. Nat Rev Neurosci 2004; 5: 146-56.

Sims NR, Yew WP. Reactive astrogliosis in stroke: Contributions of astrocytes to recovery of neurological function. Neurochemistry International 2017.

Sist B, Fouad K, Winship IR. Plasticity beyond peri-infarct cortex: Spinal up regulation of structural plasticity, neurotrophins, and inflammatory cytokines during recovery from cortical

stroke. Exp Neurol 2014; 252: 47-56.

Snow DM, Brown EM, Letourneau PC. Growth cone behavior in the presence of soluble chondroitin sulfate proteoglycan (CSPG), compared to behavior on CSPG bound to laminin or fibronectin. International Journal of Developmental Neuroscience 1996; 14: 331-49.

Sochocka M, Diniz BS, Leszek J. Inflammatory Response in the CNS: Friend or Foe? Molecular Neurobiology 2016.

Soleman S, Yip P, Leasure JL, Moon L. Sustained sensorimotor impairments after endothelin-1 induced focal cerebral ischemia (stroke) in aged rats. Experimental Neurology 2010; 222: 13-24.

Soleman S, Yip PK, Duricki DA, Moon LDF. Delayed treatment with chondroitinase ABC promotes sensorimotor recovery and plasticity after stroke in aged rats. Brain 2012; 135: 1210-23.

Soriano E, Del Río JA. Overcoming Chondroitin Sulphate Proteoglycan Inhibition of Axon Growth in the Injured Brain: Lessons from Chondroitinase ABC. Current Pharmaceutical Design 2007; 13: 2485-92.

Spera PA, Ellison JA, Feuerstein GZ, Barone FC. IL-10 reduces rat brain injury following focal stroke. Neuroscience Letters 1998; 251: 189-92.

Stabler TV, Huang Z, Montell E, Vergés J, Kraus VB. Chondroitin sulphate inhibits NF-κB activity induced by interaction of pathogenic and damage associated molecules. Osteoarthritis and Cartilage 2017; 25: 166-74.

Starkey ML, Bleul C, Zörner B, Lindau NT, Mueggler T, Rudin M, et al. Back seat driving: hindlimb corticospinal neurons assume forelimb control following ischaemic stroke. Brain : a

journal of neurology 2012; 135: 3265-81.

Steinberg BA, Augustine JR. Behavioral, anatomical, and physiological aspects of recovery of motor function following stroke. Brain Res Rev 1997; 25: 125-32.

Stroemer RP, Kent TA, Hulsebosch CE. Neocortical Neural Sprouting, Synaptogenesis, and Behavioral Recovery After Neocortical Infarction in Rats. Stroke 1995; 26: 2135-44.

Sugahara K, Mikami T. Chondroitin/dermatan sulfate in the central nervous system. Current Opinion in Structural Biology 2007; 17: 536-45.

Suh H, Min J, Choi K, Kim S, Kim K, Jeon S. Axonal regeneration effects of Wnt3a-secreting fibroblast transplantation in spinal cord-injured rats. Acta Neurochir 2011; 153: 1003-10.

Szabat E, Rauvala H. Role of HB-GAM (Heparin-Binding Growth-Associated Molecule) in Proliferation Arrest in Cells of the Developing Rat Limb and Its Expression in the Differentiating Neuromuscular System. Developmental Biology 1996; 178: 77-89.

Tan CL, Kwok JCF, Patani R, ffrench-Constant C, Chandran S, Fawcett JW. Integrin Activation Promotes Axon Growth on Inhibitory Chondroitin Sulfate Proteoglycans by Enhancing Integrin Signaling. J Neurosci 2011; 31: 6289-95.

Tan G, Tabata Y. Chondroitin-6-sulfate attenuates inflammatory responses in murine macrophages via suppression of NF-κB nuclear translocation. Acta biomaterialia 2014; 10: 2684-92.

Tang X, Davies JE, Davies SJA. Changes in distribution, cell associations, and protein expression levels of NG2, neurocan, phosphacan, brevican, versican V2, and tenascin-C during acute to chronic maturation of spinal cord scar tissue. J Neurosci Res 2003; 71: 427-44.

Tang Y, Le W. Differential Roles of M1 and M2 Microglia in Neurodegenerative Diseases. Mol Neurobiol 2016; 53: 1181-94.

Taraschenko OD, Nichter C, Pugh JA. Early Wallerian degeneration in a neonate with middle carotid artery stroke. Pediatric neurology 2015; 52: 252-3.

Tarkowski E, Rosengren L, Blomstrand C, Wikkelso C, Jensen C, Ekholm S, et al. Early Intrathecal Production of Interleukin-6 Predicts the Size of Brain Lesion in Stroke. Stroke 1995; 26: 1393-8.

Tennant KA. Thinking outside the brain: Structural plasticity in the spinal cord promotes recovery from cortical stroke. Exp Neurol 2014; 254: 195-9.

Tester NJ, Plaas AH, Howland DR. Effect of body temperature on chondroitinase ABC's ability to cleave chondroitin sulfate glycosaminoglycans. Journal of Neuroscience Research 2007; 85: 1110-8.

Tetzlaff W, Fouad K, Kwon B. Be careful what you train for. Nat Neurosci 2009; 12: 1077-9.

The Heart and Stroke Foundation of Canada; 2016; 2017.

Thomalla G, Glauche V, Koch MA, Beaulieu C, Weiller C, Röther J. Diffusion tensor imaging detects early Wallerian degeneration of the pyramidal tract after ischemic stroke. Neuroimage 2004; 22: 1767-74.

Thomalla G, Glauche V, Weiller C, Röther J. Time course of wallerian degeneration after ischaemic stroke revealed by diffusion tensor imaging. Journal of neurology, neurosurgery, and psychiatry 2005; 76: 266-8.

Tom VJ, Kadakia R, Santi L, Houlé JD. Administration of chondroitinase ABC rostral or caudal

to a spinal cord injury site promotes anatomical but not functional plasticity. Journal of neurotrauma 2009; 26: 2323-33.

Tonchev AB. Brain ischemia, neurogenesis, and neurotrophic receptor expression in primates. Archives italiennes de biologie 2011; 149: 225.

Tsiperson V, Huang Y, Bagayogo I, Song Y, VonDran MW, DiCicco-Bloom E. Brain-Derived Neurotrophic Factor Deficiency Restricts Proliferation of Oligodendrocyte Progenitors Following Cuprizone-Induced Demyelination. ASN Neuro 2015; 7: 175909141456687.

Ueno M, Hayano Y, Nakagawa H, Yamashita T. Intraspinal rewiring of the corticospinal tract requires target-derived brain-derived neurotrophic factor and compensates lost function after brain injury. Brain 2012; 135: 1253-67.

Vallières M, du Souich P. Modulation of inflammation by chondroitin sulfate. Osteoarthritis and Cartilage 2010; 18, Supplement 1: S6.

Van den Brand R, Heutschi J, Barraud Q, DiGiovanna J, Bartholdi K, Huerlimann M, et al. Restoring Voluntary Control of Locomotion after Paralyzing Spinal Cord Injury. Science 2012; 336: 1182-5.

Vavrek R, Girgis J, Tetzlaff W, Hiebert GW, Fouad K. BDNF promotes connections of corticospinal neurons onto spared descending interneurons in spinal cord injured rats. Brain 2006; 129: 1534-45.

Wahl AS, Omlor W, Rubio JC, Chen JL, Zheng H, Schröter A, et al. Neuronal repair. Asynchronous therapy restores motor control by rewiring of the rat corticospinal tract after stroke. Science (New York, N.Y.) 2014; 344: 1250.

Wahl A, Schwab ME. Finding an optimal rehabilitation paradigm after stroke: enhancing fiber growth and training of the brain at the right moment. Frontiers in Human Neuroscience 2014; 8: 381.

Wanaka A, Carroll SL, Milbrandt J. Developmentally regulated expression of pleiotrophin, a novel heparin binding growth factor, in the nervous system of the rat. Developmental Brain Research 1993; 72: 133-44.

Wang Y, Han S, Zhang K, Jin Y, Xu X, Lu P. Upregulation of heparin-binding growth-associated molecule after spinal cord injury in adult rats. Acta Pharmaco Sin 2004; 25: 611-6.

Wang Q, Tang XN, Yenari MA. The inflammatory response in stroke. Journal of Neuroimmunology 2007; 184: 53-68.

Wang S, Hu L, Gao X, Guo H, Fan G. Anti-inflammatory Activity of Salvianolic Acid B in Microglia Contributes to its Neuroprotective Effect. Neurochem Res 2010; 35: 1029-37.

Wang Y, Qiu B, Liu J, Zhu W, Zhu S. Cocaine- and amphetamine-regulated transcript facilitates the neurite outgrowth in cortical neurons after oxygen and glucose deprivation through PTN-dependent pathway. Neuroscience 2014; 277: 103-10.

Ward NS. Functional reorganization of the cerebral motor system after stroke. Current opinion in neurology 2004; 17: 725-30.

Weese G, Neimand D, Finger S. Cortical lesions and somesthesis in rats: Effects of training and overtraining prior to surgery. Exp Brain Res 1973; 16: 542-50.

Weishaupt N, Silasi G, Colbourne F, Fouad K. Secondary damage in the spinal cord after motor cortex injury in rats. Journal of neurotrauma 2010; 27: 1387-97.

Weishaupt N, Li S, Di Pardo A, Sipione S, Fouad K. Synergistic effects of BDNF and rehabilitative training on recovery after cervical spinal cord injury. Behav Brain Res 2013; 239: 31-42.

WHO. WHO. International classification of functioning disability Health ICF. 2001.

Winship IR, Murphy TH. Remapping the Somatosensory Cortex after Stroke: Insight from Imaging the Synapse to Network. Neuroscientist 2009; 15: 507-24.

Wolf SL, Winstein CJ, Miller J. Effect of constraint-induced movement therapy on upper extremity function 3 to 9 months after stroke: The excite randomized clinical trial. JAMA 2006; 296: 2095-104.

Wu Q, Cao Y, Dong C, Wang H, Wang Q, Tong W, et al. Neuromuscular interaction is required for neurotrophins-mediated locomotor recovery following treadmill training in rat spinal cord injury. PeerJ 2016; 4: e2025.

Xerri C, Merzenich MM, Peterson BE, Jenkins W. Plasticity of Primary Somatosensory Cortex Paralleling Sensorimotor Skill Recovery From Stroke in Adult Monkeys. Journal of Neurophysiology 1998; 79: 2119-48.

Xia Z, Dickens M, Raingeaud J, Davis RJ, Greenberg ME. Opposing Effects of ERK and JNK-p38 MAP Kinases on Apoptosis. Science 1995; 270: 1326-31.

Xu C, Zhu S, Wu M, Han W, Yu Y. Functional Receptors and Intracellular Signal Pathways of Midkine (MK) and Pleiotrophin (PTN). Biological and Pharmaceutical Bulletin 2014; 37: 511-20.

Xu B, Park D, Ohtake Y, Li H, Hayat U, Liu J, et al. Role of CSPG receptor LAR phosphatase in

restricting axon regeneration after CNS injury. Neurobiol Dis 2015; 73: 36-48.

Yamagata T, Saitom H, Habuchi O, Suzuki S. Purification and Properties of Bacterial Chondroitinases and Chondrosulfatases. Journal of Biological Chemistry 1968; 243: 1523.

Yanagisawa H, Komuta Y, Kawano H, Toyoda M, Sango K. Pleiotrophin induces neurite outgrowth and up-regulates growth-associated protein (GAP)-43 mRNA through the ALK/GSK3β/β-catenin signaling in developing mouse neurons. Neurosci Res 2010; 66: 111-6.

Yang K1, Perez-Polo JR, Mu XS, Yan HQ, Xue JJ, Iwamoto Y, Liu SJ, Dixon CE, Hayes RL. Increased expression of brain-derived neurotrophic factor but not neurotrophin-3 mRNA in rat brain after cortical impact injury J Neurosci Res. 1996; 15: 157-64.

Yang Z, Zhao T, Zou Y, Zhang JH, Feng H. Hypoxia Induces autophagic cell death through hypoxia-inducible factor 1α in microglia. PloS one 2014; 9: e96509.

Yeh H, He YY, Xu J, Hsu CY, Deuel TF. Upregulation of Pleiotrophin Gene Expression in Developing Microvasculature, Macrophages, and Astrocytes after Acute Ischemic Brain Injury. Journal of Neuroscience 1998; 18: 3699.

Yuan A, Rao MV, Veeranna, Nixon RA. Neurofilaments at a glance. Journal of cell science 2012; 125: 3257-63.

Zai L, Ferrari C, Dice C, Subbaiah S, Havton LA, Coppola G. Inosine augments the effects of a Nogo receptor blocker and of environmental enrichment to restore skilled forelimb use after stroke. The Journal of neuroscience: the official journal of the Society for Neuroscience 2011; 31: 5977-88.

Zhang L, Zhang RL, Zhang ZG, Chopp M. Proliferation and differentiation of progenitor cells in

the cortex and the subventricular zone in the adult rat after focal cerebral ischemia. Neuroscience 2001; 105: 33-41.

Zhang N, Zhong R, Deuel TF. Domain Structure of Pleiotrophin Required for Transformation. Journal of Biological Chemistry 1999; 274: 12959-62.

Zhang N, Zhong R, Perez-Pinera P, Herradon G, Ezquerra L, Wang Z. Identification of the angiogenesis signaling domain in pleiotrophin defines a mechanism of the angiogenic switch. Biochemical and Biophysical Research Communications 2006; 343: 653-8.

Zhao R, Fawcett J. Combination treatment with chondroitinase ABC in spinal cord injury—breaking the barrier. Neurosci Bull 2013; 29: 477-83.

Zhao S, Zhao M, Xiao T, Jolkkonen J, Zhao C. Constraint-Induced Movement Therapy Overcomes the Intrinsic Axonal Growth–Inhibitory Signals in Stroke Rats. Stroke 2013; 44: 1698-705.

Zhou G, Niepel MS, Saretia S, Groth T. Reducing the inflammatory responses of biomaterials by surface modification with glycosaminoglycan multilayers. Journal of Biomedical Materials Research Part A 2016; 104: 493-502.

Ziegler G, Harhausen D, Schepers C, Hoffmann O, Röhr C, Prinz V, et al. TLR2 has a detrimental role in mouse transient focal cerebral ischemia. Biochemical and Biophysical Research Communications 2007; 359: 574-9.

Zuo J, Neubauer D, Dyess K, Ferguson TA, Muir D. Degradation of Chondroitin Sulfate Proteoglycan Enhances the Neurite-Promoting Potential of Spinal Cord Tissue. Experimental Neurology 1998; 154: 654-62.

Zou P, Zou K, Muramatsu H, Ichihara-Tanaka K, Habuchi O, Ohtake S. Glycosaminoglycan structures required for strong binding to midkine, a heparin-binding growth factor. Glycobiology 2003; 13: 35-42.